ISSN 1173-5996

Full-Scale Testing of Fire Suppression Agents on Shielded Fires

BY

Neil Gravestock

Supervised by

Dr Charley Fleischmann

Fire Engineering Research Report 98/3
June 1998

This report was presented as a project report
as part of the M.E. (Fire) degree at the University of Canterbury

School of Engineering
University of Canterbury
Private Bag 4800
Christchurch, New Zealand

Phone 643 364-2250
Fax 643 364-2758

TABLE OF CONTENTS

ABSTRACT

This report examines the relative effectiveness of water mist, water mist with class A foam concentrate added, and class A compressed air foam in the extinguishment of a shielded, post-flashover, compartment fire. This is to assist the New Zealand Fire Service in determining future firefighting tactics and equipment.

Extinguishing agent application used hand lines operated by Fire Service personnel. Application of each of the three agents was for a fixed total period of ten seconds, with a constant flow rate of 2.8 litres/second. The class A solution was a wet foam with an expansion ratio of 1:2, and the compressed air foam was drier with an expansion ratio of 1:5.

Measurement of the water content in the fire exhaust gases indicated peak moisture contents between 10% and 20%. No rise in water content was observed during suppression.

Compartment temperatures peaked at 750°C to 820°C. Cooling to 200°C occurred within around 80 seconds of extinguishment. Cooling rates were similar for all three methods.

The fires achieved peak heat release rates of up to 4500 kW. All three methods gave good initial extinguishment for fires of this size. Subsequent re-ignition occurred in most cases. No significant difference was found in the suppression performance of the three agents expressed in terms of heat release rate reduction, which was measured using oxygen calorimetry.

LIST OF ILLUSTRATIONS

NOMENCLATURE

A	cross sectional area of the duct [m^2]
A_0	area of the vent opening [m^2]
A_t	surface area of the thermocouple bead [m^2]
A_T	total area of the compartment external surfaces [m^2]
b	width of the vent [m]
c_p	heat capacity of the thermocouple [J/kg.K]
C_D	orifice constriction coefficient, (~0.7) [-]
d	characteristic dimension of the probe, its diameter [m]
D	stick thickness [m]
E	heat released per unit mass of O_2 consumed [MJ/kg of O_2]
E_{CO}	heat released per unit mass of O_2 consumed for combustion of CO to CO_2
E_f	expansion ratio of the foam [litres/kg]
E'	heat released per unit moles of O_2 consumed [MJ/kmol of O_2]
E'_{CO}	heat released per unit moles of O_2 consumed, in combustion of CO [MJ/kmol of O_2]
$f(\mathrm{Re})$	Reynolds number correction [-]
g	acceleration due to gravity, (=9.8) [m/s^2]
h_t	height of the top of the vent [m]
h_n	height of the neutral plane [m]
h_b	height of the bottom of the vent, defined as 0 [m]
h_c	height of the crib [m]
h_k	effective heat transfer coefficient [kW/m^2K]
H_0	height of the vent opening [m]
k	thermal conductivity [kW/mK]
k_c	velocity profile shape factor [-]
$\dot{m}_e$	exhaust mass flow rate [kg/s]
$\dot{m}_u$	mass flow out of the compartment [kg/s]
$\dot{m}_d$	mass flow into the compartment [kg/s]

$\dot{m}_f$	mass consumption rate of the fuel [kg/s]
m_0	initial mass of the crib [kg]
m	unburnt mass of the crib [kg]
m_i	mass loss rate of the crib [kg/s]
$\dot{m}_a$	incoming air mass flow rate [kg/s]
M_f	mass of the foam [kg]
M_{O_2}	molecular weight of oxygen [kg/kmol]
M_a	molecular weight of the incoming air [kg/kmol]
M_{dry}	molecular weight of dry air $(\approx 29 \text{ kg / kmol})$
M_{H_2O}	molecular weight of water $(\approx 18 \text{ kg / kmol})$
M^e_{total}	total molecular weight of the exhaust [kg/kmol]
M_{N_2}	molecular weight of nitrogen [kg/kmol]
M_{CO_2}	molecular weight of carbon dioxide [kg/kmol]
M_{CO}	molecular weight of carbon monoxide [kg/kmol]
n	size of the sample
$\dot{n}^e_{total}$	total molar flow rate of the exhaust [kmol/s]
N_i	number of moles in the input gas stream [kmol]
N_e	number of moles in the exhaust gas stream [kmol]
$p_s\{T_a\}$	saturation pressure of water vapor at T_a [Pa]
p_a	air pressure [Pa]
$\dot{q}$	rate of heat release [kW]
$\dot{Q}_{stoich}$	stoichiometric heat release rate [kW]
r	stoichiometric ratio for the fuel [kg of air/kg of fuel]
RH	relative humidity [%]
S	clear space between sticks [m]
t_{Ih}	time to incapacitation [minutes]
t	time [s]
t_L	lag time, which is a characteristic of the system [s]
t_c	characteristic time constant for the system [s]

T_a	air temperature [K]
T	temperature of the fluid [K]
T_y	temperature measured at y [K]
T_∞	ambient air temperature [K]
T_g	hot gas layer temperature [K]
u	velocity [m/s]
V	local velocity [m/s]
V_b	volume of the thermocouple bead [m^3]
V_f	volume of the foam [litres]
$\bar{x}$	sample mean
$X^a_{H_2O}$	mole fraction of water in the incoming air [-]
$X^{A^a}_{CO_2}$	mole fraction of carbon dioxide in the incoming air [-]
$X^{A^a}_{O_2}$	mole fraction of oxygen in the incoming air [-]
$X^{A^e}_{O_2}$	mole fraction of oxygen in the exhaust stream
$X^e_{H_2O}$	mole fraction of water in the exhaust [-]
$X^{A^e}_{CO_2}$	mole fraction of carbon dioxide in the exhaust [-]
$X^{A^e}_{CO}$	mole fraction of carbon monoxide in the exhaust [-]
$X^{A^e}_{N_2}$	mole fraction of nitrogen in the exhaust [-]
X	calculated, corrected value of the oxygen concentration [-]
y	height in the vent, taken with h_b=0 [m]
Y	measured value of the oxygen concentration at a given time [-]
z	z statistic for the sample
α	expansion factor [-]
δ	thickness of the material [m]
Δp	differential pressure across the probe [Pa]
$\Delta H_{propane}$	heat of combustion of propane [kW/kg]
ΔH_{butane}	heat of combustion of butane [kW/kg]
Δt	time step used for the integration of the crib mass lost [s]

ΔT	time interval between oxygen concentration measurements [s]
ϕ	oxygen depletion factor [-]
μ_a	viscosity of air at ambient conditions [kg/ms]
μ_e	viscosity of air at exhaust conditions [kg/ms]
μ_0	hypothesised true value of the mean
v_p	fuel surface regression rate [m/s]
v_c	centreline velocity [m/s]
$\bar{v}_o$	average velocity of gas flowing out of the compartment [m/s]
ρ_e	density of the exhaust gases [kg/m^3]
ρ_a	density of air at ambient conditions [kg/m^3]
ρ_∞	ambient air density [kg/m^3]
ρ	density of the thermocouple [kg/m^3]
τ	time constant for the thermocouple [s]
σ	sample standard deviation

GLOSSARY OF TERMS

Appliance	A Fire Service operational vehicle, in the context of this report it is one which has pumps for firefighting.
Branch	An adjustable nozzle used on the end of a hand held line which can be used to produce a straight flow or a range of mists depending on the design of the branch.
CAFS	Compressed Air Foam System. A mechanically aspirated foam system capable of producing a wide range of foam types.
Class A	Solid combustible materials such as wood and plastics.
Concentrate	The chemical additive from the supplier which is mixed with water to form the foam solution
Drainage Time	The time taken for water to drain out of foam. The 25% drainage time most commonly used.
Expansion Ratio	The ratio of the volume of the foam in its aerated state to the original volume of the non-aerated foam solution.
Foam	The aerated mixed solution, as produced by foam generation devices. Foam is an aggregation of small bubbles produced by entraining air into a foam solution.
HPD	High Pressure Delivery. The standard hand held extinguishment method used by the New Zealand Fire Service. Produces a fine mist of water.
Knock Down	The reduction of the fire intensity to the point where it poses no realistic threat.
Mop Up	The quenching of hot spots and smoldering areas after the fire has been *knocked down.*
Nozzle	A simple straight bore attachment to a hand held line which constricts the flow forcing the water out at high velocity. These are seldom used today as the more versatile branch is usually used.
Solution	The diluted concentrate to which air is added to produce foam.

1. INTRODUCTION

1.1 Context of the Experimental Work

Currently, the New Zealand Fire Service uses plain water delivered through a high pressure delivery (HPD) as its standard method of extinguishing compartment fires. In order to improve firefighting effectiveness and firefighter safety they are assessing the performance of compressed air foam systems (CAFS). Field trials of fire appliances with CAFS capability are being carried out in several locations and the experimental program presented here is performed in parallel with these trials.

1.2 Scope of the Study

The primary focus of the experimental work was to provide a scientifically rigorous measure of the suppression effectiveness of CAFS compared with the standard High Pressure Delivery currently used. In addition the work examined the effectiveness of applying class A foam solution through an otherwise unmodified HPD line. This method is referred to as 'Solution' or 'Class A Solution' in the remainder of this report. This would be of interest as it would be a low capital cost option for the use of class A foams. Each of the three suppression methods were tested on three separate occasions giving a total of nine experiments.

The experimental work is split into two studies and this report is concerned solely with the second study. The studies were identical in all ways except that in the earlier study the fire was unshielded and in this study the fire is shielded.

Fires were within a compartment with a single doorway, the fuel load was a combination of wooden cribs and medium density fibreboard (MDF). A full height partition shielded the majority of the fuel from direct extinguishing attack. Fires were allowed to flashover before extinguishment started. Each extinguishing agent was applied for a fixed time of 10 seconds and a fixed flow rate of 170 litres/minute. Suppression effectiveness for each of the

extinguishing agents was primarily expressed in terms of reduction of heat release rate, measured using oxygen calorimetry techniques.

The research did not consider operational and business issues such as the ease of use, cost effectiveness and effects of differing suppression equipment settings, class A agents, or methods of application. Furthermore, the effects of other plain water suppression enhancing additives, such as alkali salts, was not investigated in this work.

1.3 Three Suppression Methods: HPD, Class A Foam and CAFS

In order to discuss the research work carried out in the area of fire suppression it is useful to have a basic understanding of the three methods being considered in this research (M. Kibblewhite, B. Shields, M. Vincent., pers. comm.).

1.3.1 Current Extinguishment Methods

Most firefighting appliances in the New Zealand Fire Service have two basic means of putting water onto a fire. These are using a Low Pressure Delivery (LPD) or a High Pressure Delivery (HPD).

1.3.1.1 Low Pressure Delivery

The low pressure delivery allows large quantities of water to be put onto the fire and is normally used where mains water supplies are available, although other supplies such as water storage tanks, lakes and rivers can also be used. The appliance then acts as an inline pump for delivering the water. The branches used produce either a solid stream of water or a variable mist which is applied onto the fire some distance away. The main advantages of this method are the ability to apply water from a considerable distance from the fire, and the large flow rates of water that is delivered to the fire either by hand line application or by the boosting on fixed systems such as sprinklers. The main disadvantages are the time taken to setup the water supplies, the cumbersome nature of the large and heavy hoses and the reliance of a external water supply. For large fires there is no practical alternative to this approach.

1.3.1.2 High Pressure Delivery

The high pressure delivery has a much lower flow rate than the low pressure delivery and thus the supplies of water carried on the appliance, typically 1300 litres, are sufficient. The nozzles used produce a fine mist of particles, giving rise to the other name for this extinguishment method of high pressure fog. This mist is used to cool the upper hot layer reducing the radiative feedback and thus facilitating extinguishment. In order to do this HPDs have to be used close to the fire, often from within the building. The nozzles used have adjustable spray patterns ranging from a relatively straight jet to a wide hollow cone which is often used by firefighters to provide shielding from radiative heat. In the New Zealand Fire Service it would be normal in provincial and city areas for there to be two high pressure deliveries on an appliance.

The main advantages of the HPD are that external water supply is not required, they can be used to provide some shielding from radiation for firefighters within a burning building and the hoses are of smaller diameter than the LPD hoses and are much easier to handle. The main disadvantages are that they cannot be used from a distance, the large quantities of steam makes conditions difficult for firefighters in terms of visibility and comfort, pressure waves formed by the expanding steam can move the fire into uninvolved areas, and they are ineffective against large vented fires.

The HPD has the additional advantage over the LPD that when it is used inside buildings it is less likely to become kinked or looped. Because the HPD and LPD are generally used for very different situations and both types of extinguishing function are required they are not compared as part of this research.

The main features of the low pressure delivery and high pressure delivery are contrasted in Table 1-1.

Low Pressure Delivery	High Pressure Delivery
• 700 kPa operating pressure	• 3000 to 3500 kPa operating pressure
• 6 to 19 l/s flow rate	• 1 to 4 l/s flow rate
• 45 or 70 mm hose diameter	• 25 mm hose diameter
• 30 m maximum range	• Approximately 2 m range when in fog pattern
• 200 m maximum pumping length from single appliance	• Line length 60 m
• Water supply from mains supply, tank supply or natural supplies such as lakes, rivers, etc.	• Water supply from tank on appliance
• Used in very large fires, for augmenting fixed protection systems	• Used in smaller fires, for search and rescue within burning buildings.

Table 1-1: Comparison of Low Pressure Delivery and High Pressure Delivery Characteristics

From the New Zealand Fire Service Fire Incident Reporting System (FIRS) database more than 90% (P. Malthus, pers. comm.) of structure fires were extinguished using high pressure deliveries[1]. It can be seen that the HPD is the day to day workhorse of the Fire Service, with the LPD providing high water application rates for larger fires.

1.3.2 New Extinguishment Methods

1.3.2.1 Class A Solution

Class A foam concentrate is a synthetic detergent hydrocarbon surfactant. Class A fires are those involving solid materials such as wood, plastics, etc. Its main effect when in a water solution is to greatly reduce the water surface tension. For example an aqueous solution of 0.3% by volume of class A foam concentrate will have approximately one third the surface tension of plain water[2].

By introducing class A foam solution into the water tank of a firefighting appliance and then discharging this through the HPD a wet foam is produced when the misted solution mixes with the air as it leaves the nozzle. The use of this approach is recognised by the class A foam industry[3] and is viewed as being a good method for dealing with deep seated fires. The type of foam produced is highly dependent on the nature of the nozzle, straight nozzles produces a milky solution with little air content whereas aspirating branches can produces stable foams.

Spraying class A solution through the HPD shares the advantages and disadvantages of the HPD method and has the additional disadvantage of the additional cost of the class A foam chemical. In principle it has the advantage of improved extinguishment performance due to

the wetting properties given by the additive. This method is not being used by the Fire Service at present but it would only require the addition of an inductor to provide controlled addition of foam concentrate.

1.3.2.2 Compressed Air Foam Systems

Compressed Air Foam Systems (CAFS) generally use the same class A foam chemicals mixed with water, but add air mechanically. This enables a range of foam properties to be achieved depending on the operating conditions of the system. The characteristics of various broad foam types categorised by expansion ratio[4] is summarised in Table 1-2.

Expansion Ratio Range	Foam Type	Characteristics	Uses
>20:1	Dry	• Small Bubbles • Long Drain Times • Clings to Vertical Surfaces	Exposure Protection
10:1 to 20:1	Fluid	• Small/Medium Bubbles • Flows Easily	General Use
2:1 to 10:1	Wet	• Watery • Medium/Large Bubbles • Short Drain Times	Deep Seated Fires General Use
2:1<	Solution	• Clear Milky Fluid • Lacks Bubble Structure	Deep Seated Fires

Table 1-2: Foam Characteristics

The use of compressed air foam requires specialised equipment for the introduction of the air into the solution. This equipment operates completely independently of the high pressure delivery system discussed earlier. The equipment being trialed by the Fire Service uses an inductor and proportioning device to add class A concentrate to the water flow and then air is added. The foam is developed by the mixing in the hose line and for this reason a minimum hose length of 60 metres is required in order to produce foam. There are various other methods for producing compressed air foam but discussion of these is outside of the

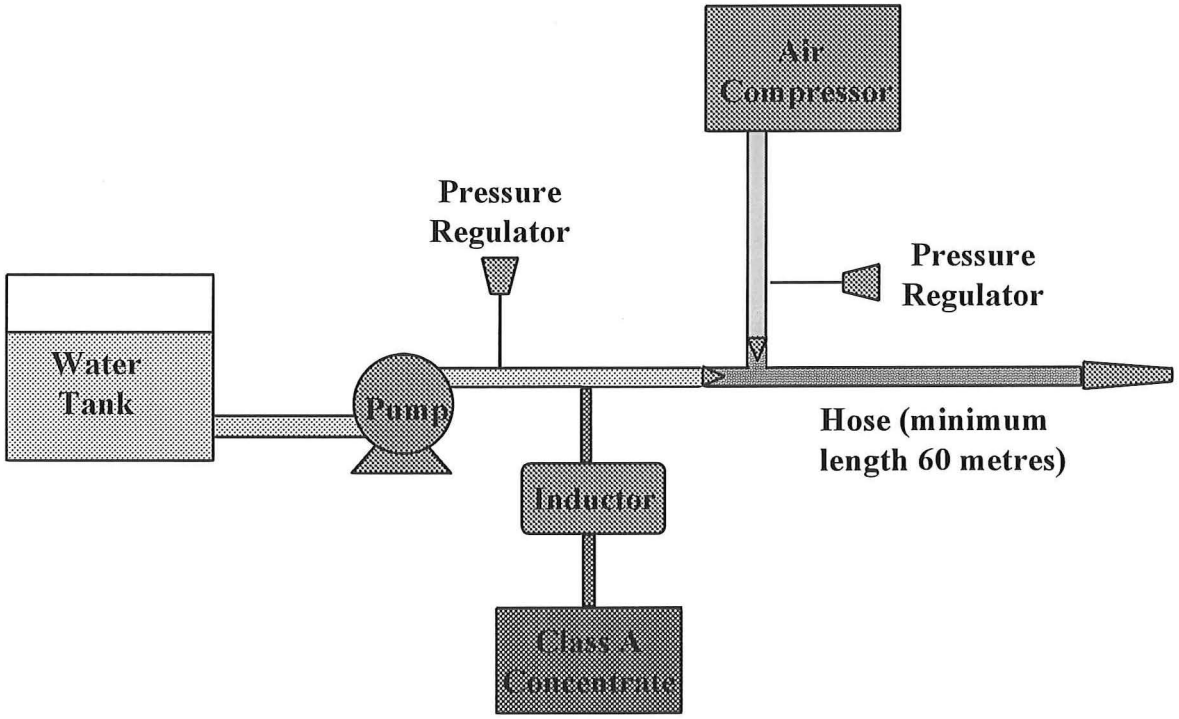

Figure 1-1: Schematic of Compressed Air Foam System

scope of this report. A schematic of the compressed air foam equipment being used in these experiments is shown in Figure 1-1.

The foam is applied through a standard straight bore nozzle and comes out as a solid jet. The main advantages reported for CAFS are: the hoses are light and easy to maneuver, the flexibility of uses; for example the foam can be used for exposure protection, it has a lower water requirement compared to other methods, and it enables extinguishment from some distance away from the fire. The main disadvantages are the requirement for specialised equipment, the added complexity of production and application of foam, the lack of radiation shielding from the spray as compared with HPD, and the potential environmental impact in terms of its low level toxicity to fauna and flora. CAFS is only being used on trial

by the Fire Service at present. The unit used for the research work has the same specification as those units being trialed for operational use.

The main features of the three extinguishment methods being compared in the research are summarised in Table 1-3. The flow rates shown indicate the general working range. For the experiments a fixed flow rate of 2.8 litres/s (170 litres/minute) was used for all methods.

Property	HPD	Class A Solution	CAFS
Operating Pressure [kPa]	3000 to 3500	2500 to 3000	700
Operating Flow rate [l/s]	1 to 4	1 to 4	2 to 4
Hose Diameter [mm]	25	25	41
Discharge Range [m]	2 [fog]	2 [fog]	25
Hose Length [m]	60	60	Up to 1600
Uses	Compartment Fires Small Outside Fires Search and Rescue	As for HPD	Exposure Protection Rural Fires Compartment Fires

Table 1-3: Main Features of Suppression Methods Being Compared

1.4 History of Hand Held Suppression of Class A Compartment Fires

1.4.1 High Pressure Fog

As Grimwood[5] states "Water has been known as an extinguishing agent for as long as fire has been known to humankind. However its capacity to remove heat has never been fully utilised on the fire ground."

Hundreds of years ago there were no methods to apply water to suppress a large fire, the tactics were containment by building fire breaks and soaking neighbouring properties with water.

With the arrival of manual pumps water was able to be put into the fire and thus suppress it. The technique used was to apply water at the base of the flames and the method is known as the direct attack.

During World War II the United States Marine Corps developed a new technique for use in fighting fires in compartments[5], their particular interest being fires in ship's holds. Rather than apply water at the base of the flames they applied the water onto the hot compartment

surfaces. Water applied in this way would rapidly flash to steam. This technique became known as indirect attack and its popularity flourished in the 1950s and 1960s[5]. To provide the necessary water surface area required for rapid evaporation special nozzles producing a mist or fog were produced.

This method came under attack in the US because the steam produced increased the risk of injuring firefighters, its out performance by solid stream for certain types of fires, and the poorer performance in ventilated compartments. This last issue ran counter to the established US practice of venting fires.

In Europe the use of fog attack flourished[5]. The practice of venting fires was rare in Europe and there was greater interest in the use of smaller self contained appliances which could operate more effectively with the lower water requirements of indirect attack methods; such as fog attack.

In New Zealand the use of fog attack has been used since the mid 1960s as the 'front line' suppression method for all but the largest fires where the LPD is used.

1.4.2 Class A Foam

Class A foam concentrates in their current form appeared in the 1980s[6]. They combine the long established surfactant properties of standard detergents but also contain solvent chemicals to improve penetration and other additives to improve the foams mechanical properties. These new foams are also much more concentrated requiring mixture ratios between 0.1% and 1% rather than between 3 and 6% for the older style foam concentrates.

In parallel with the development of class A foam concentrates was the improvement of air foam producing technology[7]. Compressed air foam in a primitive form was first produced for firefighting in 1904. With the appearance of detergents in the 1930s it was taken up by the Naval forces in the UK and US as another means of dealing with fires onboard ships. In the 1940s it stopped being used as it was too complex. It was reintroduced in the late 1970s by the Texas Forest Service and became known as the "Texas Snow Job". It quickly became popular with other forest firefighters as it provided excellent exposure protection and required less water than conventional methods. Use by the forest firefighters led to

continuing improvements in the technology but it was largely ignored as an option for structural firefighting due to the relatively high proportion of concentrates required prior to the arrival of class A foam.

With the coming together of these two strands of technological development there has been a rapid increase in the interest of urban fire brigades in using class A foam concentrate together with compressed air foam systems as a means of tackling structure fires. In the last 10 years it has been used by a growing number of US urban fire departments for structural firefighting[8].

1.5 Suppression Performance

1.5.1 High Pressure Fog

European research has focused on establishing the comparative performance of fog application compared with the traditional solid stream approach. Tests by Kokkala[9] using small compartments and by Salzberg[10] using full scale compartments both indicated the effectiveness of fog compared with solid streams. For the same extinguishment times water application rates were three to four times higher for the solid streams compared with fog.

During the 1980s US interest in indirect attack resurfaced with research in Scandinavia by Giselsson and Rosander[11] indicating that by careful application of the indirect attack technique many of the earlier limitations are overcome. This new method is referred to as offensive fog attack. The fog stream is applied from a low position inside the compartment up at a 45° angle into the hot gas layer.

Tests by Rimen[12] indicated the superiority of high pressure fog systems over low pressure systems in providing penetration and cooling. However, by far the most important factor influencing suppression effectiveness was the method of application.

More recently, there has been a resurgence in fundamental research into the suppression effectiveness of fine water mists. This has been largely driven by the desire to find replacement Halon systems. Notably recent work by Kim and Dlugogorski[13] has compared

the effectiveness of fixed installation water mist and compressed air foam systems. This work is discussed in more detail in the class A foam section.

Mawhinney and Richardson[14] have reviewed the current state of the research into water mist fire suppression. The review mentions the current experimental work of Tuomisaari in modeling the suppression effectiveness of fire hose nozzles, but at the time of writing this report no results from Tuomisaari had been published.

1.5.2 Class A Foam

Much information on the performance of class A foams is anecdotal with there being relatively little rigorous scientific measurement of their performance. Much of the literature promoting the benefits of class A foam comes from individuals or organisations involved in the class A foam industry and the claims made need to be treated with caution.

Based on his qualitative observations of class A foam performance in test burns and real fire incidents Liebson[8] reports on the perceived benefits of class A foam in structural firefighting. He comments on the improvement of firefighter health and safety as well as the improved fire suppression.

Colletti[3] discusses the methods for the generation of various types of class A foam and suggests application tactics and the optimum expansion ratios and drainage times for various fire situations. Again like the work of Liebson[8] these appear to be opinions based upon observation rather than measurement.

Colletti[15] discusses a test comparing water, aspirated foam, and compressed air foam. The fire in a 3.05 metre by 3.35 metre by 2.44 metre compartment was fueled by a mixture of straw and wood pallet. The fire was described by Liebson as "moderate". Compartment temperature measurements were taken from a thermocouple mounted 1.22 metres above the floor. Suppressant flow rates were around 75 litres/minute. The results presented show the time taken to reduce the temperature to 100°C in the compartment. Water is reported as taking 222.9 seconds, aspirated foam 102.9 seconds, and CAFS 38.5 seconds.

Colletti[16] also reports upon results of several other test burns. In one of these burns the performance of unaerated class A foam was compared with mechanically aerated foam in the extinguishment of a pressurised aviation fuel fire. This was unusual in that it was a comparison between different methods of suppression. Most of the information found in trade and firefighting magazines is simply qualitative reports of the performance of CAFS, and is usually expressed in terms of an approximate knockdown time for a described fire scenario. Supporters of CAFS make claims for its improved effectiveness over water. For example Darley[17] states that CAFS is ten times more effective than water, but it is unclear on what basis this is calculated.

A recent article by Thornton[18] advocates the use of class A foam for structural firefighting in Australasia but the arguments appear to be based upon opinion rather than scientific research.

The performance of high expansion foam, generally produced using CAFS equipment, as a exposure protection blanket is well understood, and standards have been established for its performance in a urban and rural fire settings[19]. Phase I of the [American] National Class A Foam Research Project[20] quantified the exposure performance of class A foam.

Madrzykowski[21] reported on the ignition retardant properties of compressed air foam when applied to plywood. It was found that CAFS delayed ignition by twice the time of plain water. Heat fluxes ranged from 15 kW/m^2 to 60 kW/m^2.

This growing interest in the use of class A foam in structural firefighting and the lack of rigorous scientific research into its effectiveness led to the initiation of Phase II of the National Class A Foam Research Project[22]. This research was prepared by Underwriters Laboratory Inc. for the National Fire Protection Research Foundation. The focus of the research was to compare the effectiveness of Water, Class A foam and CAFS in the suppression of an unshielded compartment fire.

This work compared the effectiveness of plain water spray, water plus class A foam concentrate through a spray nozzle and compressed air foam. Two fire types were used:

wood crib fires, and mock upholstered furniture fires constructed using polyether mattresses. A wide variation in peak heat release rates were reported with the wood crib values ranging from 3.3 MW to 4.6 MW, and the mock furniture values ranging from 1.8 MW to 3.7 MW. The fires were contained in a 2.4 metre by 2.4 metre by 3.7 metre enclosure with one doorway opening. Extinguishment commenced 5 seconds after flashover. The heat release rate was measured using an oxygen calorimeter with the suppression effectiveness being expressed in terms of the quantity of agent used and time taken to reduce the fire heat release rate to 500 kW. Expansion ratios for the class A foam varied between around two and seven. Application rates raged from 19 to 38 litres per minute. The work concluded that in general class A foam achieved suppression more rapidly and with less agent than the other methods. The work recommended that further research be carried out to: develop performance criteria for class A foams; further quantify firefighting performance and operational efficiency of class A foams; and determine the optimum tactical approach when using class A foams.

Recently work by Kim and Dlugogorski[13] has compared the fire suppression performance of standard sprinklers, water mist and compressed air foam (using class A and class B foam concentrates) in a fixed installation. While strictly this work is outside of the terms of reference of this research, as it does not consider hand held systems, the comparisons made give some insight into relative performance. Three types of fires were used in the tests: wood crib fires, heptane pool fires, and diesel pool fires. All fires were in a 6.1 metre by 6.1 metre by 3.2 metre compartment with a doorway and a window. The heptane pool fire was allowed to burn for 1 minute before suppression and the wood crib and diesel fires were allowed to burn for 2 minutes. Peak heat release rates were of the order of 500 kW. Measurements of heat release rate were made using an oxygen calorimeter and a CO/CO_2 analyser. The work concluded that compressed air foam performed better than water mist in well ventilated situations and equally as well as water mist for enclosed fires. It was also noted that compressed air foam was more effective than water mist against the wood crib fires.

1.6 Suppression Mechanisms

1.6.1 Water mist

Work by Rasbash et al[23,24,25] examined the interaction of water mist sprays with fires. Several suppression mechanisms were discussed with surface cooling, evolution of diluting steam and the formation of surface froths and emulsions being proposed as contributing mechanisms. In terms of spray characteristics it was found that sprays with finer droplets, higher water flows and higher entrained air velocities were the most effective for suppression.

In their work Jones and Thomas[26] review recent experimental work on water mist suppression. They conclude that there are both macroscopic and microscopic mechanisms occurring in water mist extinguishment.

The macroscopic mechanisms proposed are dilution of flammable vapor by air entrainment, disturbance of the flow of flammable gas or pyrolyzates, the blanketing of the surface with the spray causing surface cooling and blocking of fuel from oxygen. In the case of class A compartment fires the last of these is believed to be the most significant macroscopic mechanism.

The microscopic mechanisms proposed are removal of heat and dilution of the reaction mixture by gas phase evaporation of the droplets, disturbance of flame structure by droplets increasing the flame instability, and the production of water vapor inhibiting the forward combustion reaction.

Kim and Dlugogorski[13] discuss the increased effectiveness of water mist when compartment effects lead to the evaporation of the introduced water droplets. This is contrasted with compressed air foam which does not rely upon compartment effects.

Mawhinney, Dlugogorski, and Kim[27] discuss the extinguishing mechanisms for water mist, reviewing earlier work and presenting a detailed description of extinguishment mechanisms.

The review of Mawhinney and Richardson[14] discusses the current status of research into modeling of water mist fire suppression. This work is focused on the simpler case of a fixed installation rather than hand held application. Work is being carried out into the development of computational fluid dynamics (CFD) models which calculate the interaction between the fire gases and the water spray.

1.6.2 Class A foam

Little quantitative work has been carried out into the suppression mechanisms of class A foam. The reduction in water surface tension due to the surfactants present in class A foam concentrate is well understood and the improved spreading and penetration is often cited as the reason for the improved effectiveness of class A solution, a type of 'wet water', over plain water[2,18]. Apart from this improved spreading and penetration factor there is no change in the extinguishing mechanism over plain water.

With foams, however, the situation is more complex. Foams coat the surface of materials blocking radiative feedback and preventing the mixing of volatile fuels and oxygen in the reaction zone[28]. For the use of foams on liquid fires this behaviour can be modeled as the geometry and chemistry is relatively simple. Generally, neither of these simplifications can be used for solid fuels. The water in the foams behaves much like class A solution. The relative importance of the various mechanisms such as fuel blanketing, fuel cooling, etc, depends amongst other things on the expansion ratio and drainage characteristics of the foam.

1.7 Factors affecting suppression effectiveness

Most work on measuring hand held suppression effectiveness of class A compartment fires has been carried out using wood cribs as the fuel. Most recent work has been carried out with realistic domestic scale compartments. Earlier work focused on the suppression effectiveness with smaller scale apartments often using the Underwriters Laboratory hand held extinguishment test as the measure of suppression effectiveness.

Of the full scale compartment based studies of suppression effectiveness the work of Scheffey and Williams[29] looked at pre-flashover and post-flashover fires, the NFPA study[22]

looked at post flashover fires and the work of Kim and Dlugogorski[13] looked at pre-flashover fires.

The work of Scheffey and Williams[29] included shielding of the fires by the use of full height partitions shielding wooden cribs.

Much qualitative work has been carried out by firefighters in the course of their duties, and for this work a wide variety of different fuel types, configurations and geometry have been encountered. Due to the qualitative nature of these observations and the uncontrolled variation in the factors it is difficult to make any meaningful comparison between results even when they have been roughly quantified as they have in the New Zealand Fire Service FIRS database. However these observations are useful as they provide some insight into behaviour which can be further investigated.

1.8 Measuring Suppression Effectiveness

Suppression effectiveness is measured in various ways. The most common approach is to measure the time taken from the start of suppression until the fire is considered to be suppressed. For much qualitative work this is taken as a visual observation[16] of the fire being out. In recent studies[13,22] the time taken to reduce the heat release rate of the fire to a critical value, either absolute or as a proportion of the peak heat release rate is used. An alternative approach used in the work by Scheffey and Williams[29] and Colletti[16] is to mount a thermocouple above the fuel packages and to use a critical temperature value as the indication of suppression.

Other measurements are also of interest in determining the overall effectiveness. One of these is the quantity of agent used, this is particularly important if a range of application rates are being used. The damage sustained, or degree of burning, within the compartment are another factor in determining the effectiveness of suppression. A further factor with hand held application is the operator's perspective, although this is difficult to quantify it needs to be considered in the overall performance of the suppression agent.

1.9 Environmental and Personal Safety Considerations

The growing use of class A foam has raised concerns about its environmental effects and personal safety issues. NFPA 928[19] sets standards for: foam toxicity; corrosion properties; and eye and skin irritability. Some cases have been reported[30] of skin reaction and eye irritation and of diarrhoea if ingested. As with many chemicals, hyper-allergenic responses can be a problem. Against this risk must be weighed the reported benefits in both firefighter and public safety in using compressed air foam.

Some environmental problems have been reported in the use of class A foams affecting plants, birds and mammals, water birds, fish and invertebrates. Care needs to be taken in interpreting these results as it is often unclear which specific chemical agents have been used and whether the concentrations of agent used were realistic compared with the concentrations hat might be obtained whilst firefighting.

Class A foams break may down the waxy coating on leaves[30]. This can lead to some browning and single year leaf loss. A five year study on Douglas fir showed no long term effects. Another study showed no effects based on biomass accumulation. Research[31] in a mixed grass site in Dakota did indicate changes in growth and more importantly reduced species diversity. Aquatic plants were reported[30] to show no adverse effects.

Birds and mammals may become soaked to the skin and loose body oils which can lead to hypothermia. No reports[30] of toxic reports have been reported. Contamination of water can lead to problems[30] for aquatic birds which rely upon water surface tension in order to float. This observation was based upon on witness data rather than on scientific study.

Fish rely on water surface tension for the correct operation of their gills. Fish will drown if high enough class A chemical concentrations are reached. Larval and young fish are particularly vulnerable[30,31].

Invertebrates such as water boatmen rely on water surface tension and are extremely vulnerable to the effects of class A foam chemicals. Studies[31] show that concentrations as low as 6mg/litre of class A chemicals cause a dramatic reduction in survival.

Scheffey[32] comments on the balance between the actual or potential environmental damage from a fire or potential fire hazard as against the environmental consequences of the use of the firefighting foams. Concerns surrounding the use of chemical foams need to be weighed against the increased environmental damage, Scheffey[32] quotes "In most [fire] situations, the elimination of foam as a suppression agent results in the potential for dramatically increased environmental impact".

2. THEORY

2.1 Duct Mass Flow

The mass flow rate in a duct can be measured using a bi-directional probe. The relationship between the differential pressure across the probe and the centreline velocity is given by McCaffrey and Heskestad[33] as:

$$\Delta p = \frac{1}{2}\rho_e\left[f(\mathrm{Re})v_c\right]^2 \tag{1}$$

For Re>3800, $f(\mathrm{Re})$ is constant. For the duct the centreline velocity obtained using a pitot tube was approximately 13 m/s for ambient conditions. This gives a Reynolds number of:

$$\mathrm{Re} = \frac{\rho_a u d}{\mu_a} = \frac{1.2 \times 13 \times 0.16}{1.95 \times 10^{-5}} = 128{,}000 \text{ [-]} \tag{2}$$

It can be see this is much greater than the value of 3800 above which $f(\mathrm{Re})$ becomes constant. Assuming that the velocity remains approximately the same and that the exhaust gas properties can be estimated by air then the Reynolds number at an exhaust temperature of 1000K is:

$$\mathrm{Re} = \frac{\rho_e u d}{\mu_e} = \frac{0.35 \times 13 \times 0.16}{4.15 \times 10^{-5}} = 17{,}500 \text{ [-]} \tag{3}$$

This is also greatly in excess of 3800 so it is reasonable to assume that the constant value for $f(\mathrm{Re})$ given as 1.08 can be used.

The mass flow rate in the duct is given by:

$$\dot{m}_e = \frac{Ak_c}{f(\mathrm{Re})}\sqrt{2\rho_e \Delta p} \tag{4}$$

The density of the exhaust gases can be approximated by using the ideal gas law which gives:

$$\rho_e \approx \frac{\rho_a T_a}{T_e} \tag{5}$$

Taking the density of ambient air[34] as 1.29 kg/m^3 at a temperature of 273K gives:

$$\rho_e \approx \frac{352}{T_e} \tag{6}$$

Substituting in this value, and the known values for the duct cross sectional area, A, of 0.283 m^2 and the value for the Reynolds number correction, $f(\mathrm{Re})$, of 1.08, gives:

$$\dot{m}_e = 6.95 k_c \sqrt{\frac{\Delta p}{T_e}} \tag{7}$$

The velocity profile shape factor, k_c, is the ratio of the flow rate based upon the centreline velocity and the actual flow rate. For perfect plug flow the shape factor has a value of one.

Measurements of the shape profile for the duct, discussed in Section 4.1, give a k_c value of 0.95. Substituting this in gives:

$$\dot{m}_e = 6.60 \sqrt{\frac{\Delta p}{T_e}} \tag{8}$$

This is the equation used to calculate the mass flow rate in the duct.

2.2 Foam Quality Measurements

The foam is characterised in terms of its 25% drainage time and its expansion ratio. The 25% drainage time is given by the time taken for 25% of the total weight of the sample to be drained. The expansion ratio is given by:

$$E_f = \frac{V_f}{M_f} \tag{9}$$

2.3 Measuring the Rate of Heat Release

For the case where only the oxygen depletion is measured Janssens[54] gives the following equation for the rate of heat release:

$$\dot{q} = E \frac{\phi}{1+\phi(\alpha-1)} \dot{m}_e \frac{M_{O_2}}{M_a} \left(1 - X^a_{H_2O} - X^{A^a}_{CO_2}\right) X^{A^a}_{O_2} \tag{10}$$

The heat release per mass of O_2 consumed was measured by Huggett[35] for a range of materials and for most materials was found to have a value of 13.1 MJ/kg of O_2 ±5%. Tewarson[36] gives values for cellulosic materials of 13.2 MJ/kg for red oak and 12.4 MJ/kg for douglas fir.

For the calibration runs using the propane/butane mixture a weighted value was used. Tewarson gives a value for propane of 12.9 and a value for butane of 12.7. It was assumed that these could be weighted based upon the composition of the fuel. This gives:

$$E_{mixture} = 0.8E_{propane} + 0.2E_{butane} = 0.8 \times 12.9 + 0.2 \times 12.7 = 12.86 \text{ [MJ/kg of } O_2\text{]} \tag{11}$$

Janssens[54] gives the oxygen depletion factor, ϕ, from the following equation:

$$\phi = \frac{X^{A^a}_{O_2} - X^{A^e}_{O_2}}{\left(1 - X^{A^e}_{O_2}\right) X^{A^a}_{O_2}} \tag{12}$$

The expansion factor, α, depends on the stoichiometry of the reaction and in the absence of further information Janssens suggests a value of 1.105.

Tewarson[36] gives the stoichiometric formula for pine as $CH_{1.7}O_{0.83}$ if it is assumed that combustion is complete the reaction is:

$$CH_{1.7}O_{0.83} + 1.01\left(O_2 + 3.76N_2\right) \rightarrow CO_2 + 0.85H_2O + 3.80N_2 \qquad (13)$$

Using the stoichiometric equation an estimate can be made of the expansion factor, α, from the formula:

$$\alpha = \frac{N_e}{N_i} = \frac{5.65}{4.81} = 1.175 \qquad (14)$$

For the volatile wood components Drysdale[37] gives a chemical formula of CH_2O. The stoichiometric equation for the combustion of the wood volatiles is:

$$CH_2O + \left(O_2 + 3.76N_2\right) \rightarrow CO_2 + H_2O + 3.76N_2 \qquad (15)$$

This gives an α value of:

$$\alpha = \frac{5.76}{4.76} = 1.2 \qquad (16)$$

This is close to the value obtained based on the formula for wood, and this value rather than the default value of 1.105 suggested by Janssens[54] will be used in all of the suppression test calculations.

Likewise for the calibration gas of 80% propane and 20% butane the stoichiometric equation is:

$$0.8C_3H_8 + 0.2C_4H_{10} + 5.3\left(O_2 + 3.76N_2\right) \rightarrow 3.2CO_2 + 4.2H_2O + 19.93N_2 \qquad (17)$$

This gives a value for α of :

$$\alpha = \frac{N_e}{N_i} = \frac{27.3}{25.2} = 1.085 \qquad (18)$$

This is the value of α which will be used for the calibration calorimetry calculations.

The fraction of water vapor in the incoming air is a function of the relative humidity, the air temperature and the air pressure. Janssens[54] gives the relationship as:

$$X^0_{H_2O} = \frac{RH}{100}\frac{p_s\{T_a\}}{p_a} \tag{19}$$

The molecular weight of the air needs to be adjusted for the moisture content, Janssens[54] gives the following equation:

$$M_a = M_{dry}\left(1 - X^0_{H_2O}\right) + M_{H_2O}X^0_{H_2O} \tag{20}$$

2.4 Vent Flows

Emmons[38] gives the following equation for the velocity measured with a bi-directional probe:

$$V = 0.07\sqrt{T\Delta p} \tag{21}$$

For the analysis two simplifying assumptions are made: firstly that the velocity is normal to the plane of the vent, and secondly that the temperatures measured by the thermocouples are not corrected for radiation effects.

Using the calculated velocities the mass flow into and out of the compartment can be found by integrating the flow below and above the neutral plane. The neutral plane is estimated by interpolation of the position where the velocity is zero. Emmons[38] gives the following equations for calculating the mass flow into and out of the compartment:

$$\dot{m}_u = 16.79\int_{h_n}^{h_t} b\sqrt{\frac{\Delta p}{T_V}}\cdot dy \tag{22}$$

$$\dot{m}_d = 16.79\int_{h_b}^{h_n} b\sqrt{\frac{\Delta p}{T_V}}\cdot dy \tag{23}$$

Rockett[39] gives the following semi-empirical equations for predicting the mass flow rate out of a horizontal vent.

$$\dot{m}_u = \frac{2}{3} C_D b \rho_\infty \left[2g \frac{T_\infty}{T_g} \left(1 - \frac{T_\infty}{T_g} \right) \right]^{1/2} \left(h_t - h_n \right)^{3/2} \tag{24}$$

For fires approaching flashover and post flashover fires Rockett[39] has shown that the temperature dependency is small and the flow into the compartment can be approximated by:

$$\dot{m}_u = 0.5 A_0 \sqrt{H_0} \tag{25}$$

2.5 Heat Release Rates and Flashover

Heat release rates in compartment fire and the prediction of flashover have been the subject of considerable attention. The first part of this section will consider ventilation limited fires and the second part will consider the predicted mass loss rates of the fuels themselves.

From equation (25) the mass flow rate of air entering the compartment can be estimated. Knowing the heat release rate as a function of the air consumption rate allows an approximation the stoichiometric heat release rate to be calculated. For most fuels the heat released per mass of air consumed is 3000 kJ/kg. So the equation for stoichiometric heat release is given by:

$$\dot{Q}_{stoich} \approx 3000 \times 0.5 A_0 \sqrt{H_0} = 1500 A_0 \sqrt{H_0} \tag{26}$$

There are two contrary effects which affect this heat release value. Firstly in practice combustion is not complete. Kawagoe[40] reports a combustion efficiency of 0.65 for wood in fully involved compartment fires. Secondly combustion will take place outside of the compartment. Babrauskas[41] gives the following equation for the ventilation limited heat release rate for wood cribs:

$$\dot{m}_f = 0.12 A_0 \sqrt{H_0} \tag{27}$$

The stoichiometric fuel consumption rate is given by:

$$\dot{m}_f = \frac{0.5}{r} A_0 \sqrt{H_0} \tag{28}$$

For wood the stoichiometric ratio is approximately 5.7, substituting this value into equation (28) gives:

$$\dot{m}_f \approx \frac{0.5}{5.7} A_0 \sqrt{H_0} = 0.088 A_0 \sqrt{H_0} \tag{29}$$

Comparing equations (27) and (29) it can be seen that the Babrauskas[41] equation gives a value which is 1.36 times higher than the value predicted by the stoichiometric relationship. This excess fuel burns outside of the compartment.

Babrauskas[41] recommends that a heat release rate of 12 MJ/kg be used for wood when using equation (27) to calculate the heat release rate. Comparing this with the more usual value[42] used for wood of 16 MJ/kg to 20 MJ/kg, implies a combustion efficiency of between 0.6 and 0.75, this is in agreement with the 0.65 value given by Kawagoe[40].

Combining the two effects of combustion efficiency and burning outside of the compartment gives a modified version of equation (26):

$$\dot{Q} = 0.65 \times 1.36 \times 1500 A_0 \sqrt{H_0} = 1330 A_0 \sqrt{H_0} \tag{30}$$

The compartment is shielded in such a way that it can be regarded as two separate compartments. A rear compartment with a 0.7 metre by 2.4 metre opening between itself and the front compartment which itself has a 1.2 metre by 2.0 metre opening to the outside.

For the rear compartment equation (30) gives a ventilation limit of:

$$\dot{Q} = 1330 \times 0.7 \times 2.4 \times \sqrt{2.4} = 3460 \text{ [kW]} \tag{31}$$

For the front compartment equation (30) gives a ventilation limit of:

$$\dot{Q} = 1330 \times 1.2 \times 2.0 \times \sqrt{2.0} = 4510 \text{ [kW]} \tag{32}$$

For burning of cribs Babrauskas[41] gives the following relationships in addition to the one already given in equation (27):

$$\dot{m}_f = \frac{4}{D} m_0 v_p \left(\frac{m}{m_0}\right)^{1/2} \tag{33a}$$

with

$$m = m_0 - \sum_i^t m_i(t_i)\Delta t \tag{33b}$$

$$\dot{m}_f = 4.4 \times 10^{-4} \left(\frac{S}{h_c}\right)\left(\frac{m}{D}\right) \tag{34}$$

The three equations represent different controlling mechanisms on the burning rate. Equation (27) represents room ventilation control, equation (33) represents fuel surface control, and equation (34) represents crib porosity control.

At any time it is whichever of the three equations, (27), (33) or (34), with the lowest $\dot{m}_f$ which dominates. It is possible that the controlling mechanism will vary during the lifetime of the burning crib.

The equations were solved in a spreadsheet. The results are presented in Table 2-1.

Time [s]	Crib Mass [kg]	Mass Loss Rates [kg/s]			Heat Release Rate [kW]
		Ventilation Controlled	Crib Porosity Controlled	Surface area Controlled	
0	202.5	0.407	0.119	0.215	1.43
15	200.7	0.407	0.118	0.214	1.41
30	199.0	0.407	0.117	0.213	1.40
45	197.2	0.407	0.116	0.212	1.39
60	195.5	0.407	0.115	0.211	1.38
120	188.6	0.407	0.111	0.208	1.33
180	181.9	0.407	0.107	0.204	1.28
240	175.5	0.407	0.103	0.200	1.24
300	169.4	0.407	0.099	0.197	1.19
360	163.4	0.407	0.096	0.193	1.15
420	157.6	0.407	0.092	0.190	1.11
480	152.1	0.407	0.089	0.186	1.07
540	146.7	0.407	0.086	0.183	1.03
600	141.6	0.407	0.083	0.180	1.00

Table 2-1: Crib Heat Release Rate Calculations

In addition the MDF has an area of approximately 11.5 m^2. Barnett in the Fire Engineering Design Guide[42] gives a burning rate for flat wood of 0.0061 kg/sm^2. Giving a mass loss rate of 0.07 kg/s.

The total peak heat release rate is therefore 1.43 + 1.2 = 2.63 MW

The heat release rate required for flashover can be predicted using the expression given by McCaffrey, Quintiere, and Harkleroad[43]:

$$\dot{Q} = 610\left(h_k A_T A_0 \sqrt{H_0}\right)^{1/2} \tag{35}$$

This expression assumes a temperature difference between the hot gas layer and ambient of 500°C as discussed by Walton and Thomas[44].

h_k can be estimated as k/δ where k is the thermal conductivity and δ is the thickness of the material. For the gypsum plasterboard[42] k is 0.2 x 10^{-3} [W/mK] and taking the thickness as 0.016 [m] to account for the additional insulation of the plywood gives:

$$h_k = \frac{k}{\delta} = \frac{0.2 \times 10^{-3}}{0.016} = 0.0125 \text{ [kW/m}^2\text{K]} \quad (36)$$

A_T is the total area of the walls plus the floor and ceiling minus the area of any openings, this gives:

$$A_T = A_{floor} + A_{ceiling} + A_{walls} - A_{openings} = 4 \times 2.4 \times 3.6 + 2 \times 2.4 \times 2.4 - 2 \times 1.2 = 43.7 \text{ [m}^2\text{]}$$

Substituting values into equation (35) gives:

$$\dot{Q} = 610\left(h_k A_T A_0 \sqrt{H_0}\right)^{1/2} = 610\left(0.0125 \times 43.7 \times 2.4 \times \sqrt{1.2}\right)^{1/2} = 730 \text{ [kW]}$$

2.6 Tenability Conditions

Purser[45] gives the following relationship between the temperature and the time to incapacitation:

$$t_{Ih} = \exp[5.1849 - 0.0273T] \quad (37)$$

Custer[46] recommends using a layer temperature of <80°C for tenability. This equates to an exposure time of 20 minutes using Purser's relationship. This is for direct exposure to the hot gas layer and would normally be applied with a layer height of 1.5 metres above floor level. For radiative exposure Buchanan[42] recommends a limiting layer temperature of 200°C.

2.7 Confidence Intervals

Where a mean value has been calculated from a set of data the confidence in the value of the mean being the 'true' mean can be calculated using:

$$z = \sqrt{n}\left(\bar{x} - \mu_0\right) / \sigma \quad (38)$$

For a 95% confidence interval the two sided z statistic is ±1.96. Substituting this into equation (38) and rearranging gives:

$$\mu_0 = \bar{x} \pm \frac{1.96\sigma}{\sqrt{n}} \tag{39}$$

This is the value of the true mean within a confidence interval of 95%.

3. METHODOLOGY

ASTM E603 Standard Guide for Fire Experiments[47] was used to as the basis for planning for the experimental program. Further general guidance was taken from the Nordtest method for upholstered furniture[48] and the ISO 9705[49] standard.

All apparatus was located at the Woolston Training Centre, Christchurch. This is a New Zealand Fire Service site which houses a large training building with smoke production and removal facilities. The smoke extraction system of the training building was used to provide the smoke capture and exhaust system for the experiments. Purpose built duct work was connected into the building smoke extract shaft. This duct work connected to a smoke hood located outside of the building. Gas analysis equipment and data capture equipment was located inside the building, these are discussed in detail in Section 0. Figure 3-1 shows a schematic site plan.

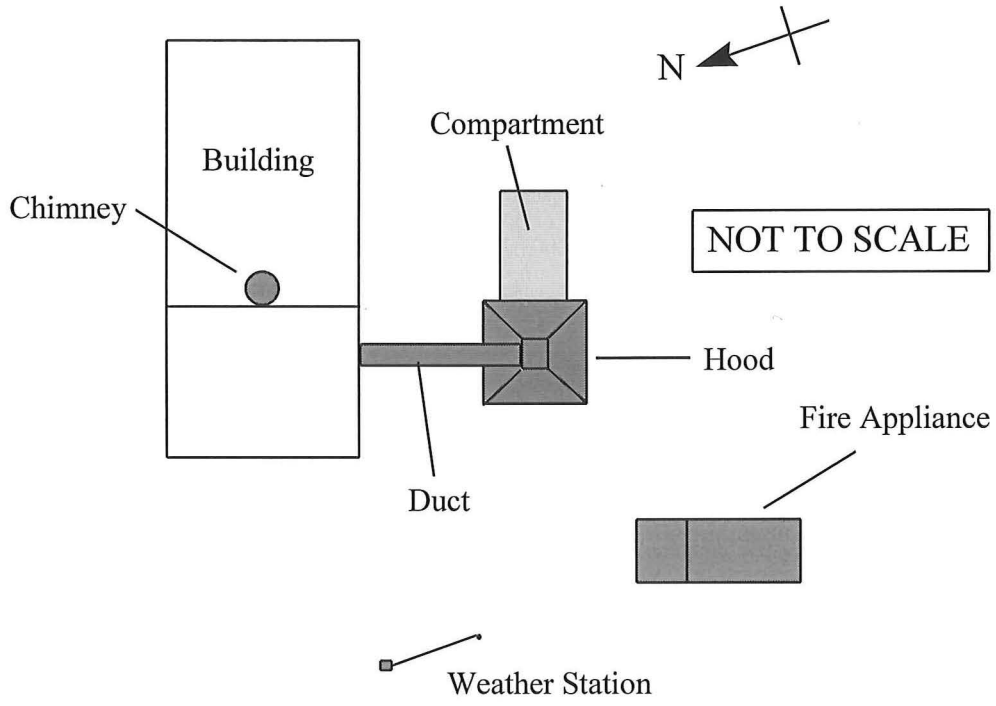

Figure 3-1: Schematic Site Plan

3.1 Description of Apparatus

3.1.1 Fire Room

The fire room dimensions were in accordance with ISO 9705[49], 2.4 metres wide, 2.4 metres high and 3.6 metres long. The external frame construction was box section steel lined with plywood mounted on steel studs. The compartment had a single doorway opening 1.2 metres wide by 2.0 metres high centrally located on one of the 2.4 metre by 2.4 metre walls. There were no other openings in the compartment. Note that this doorway dimension differs from ISO 9705[49] which stipulates a 0.8 metre wide doorway. The doorway was widened primarily for firefighter safety. The dimensions of the compartment are shown in Figure 3-2.

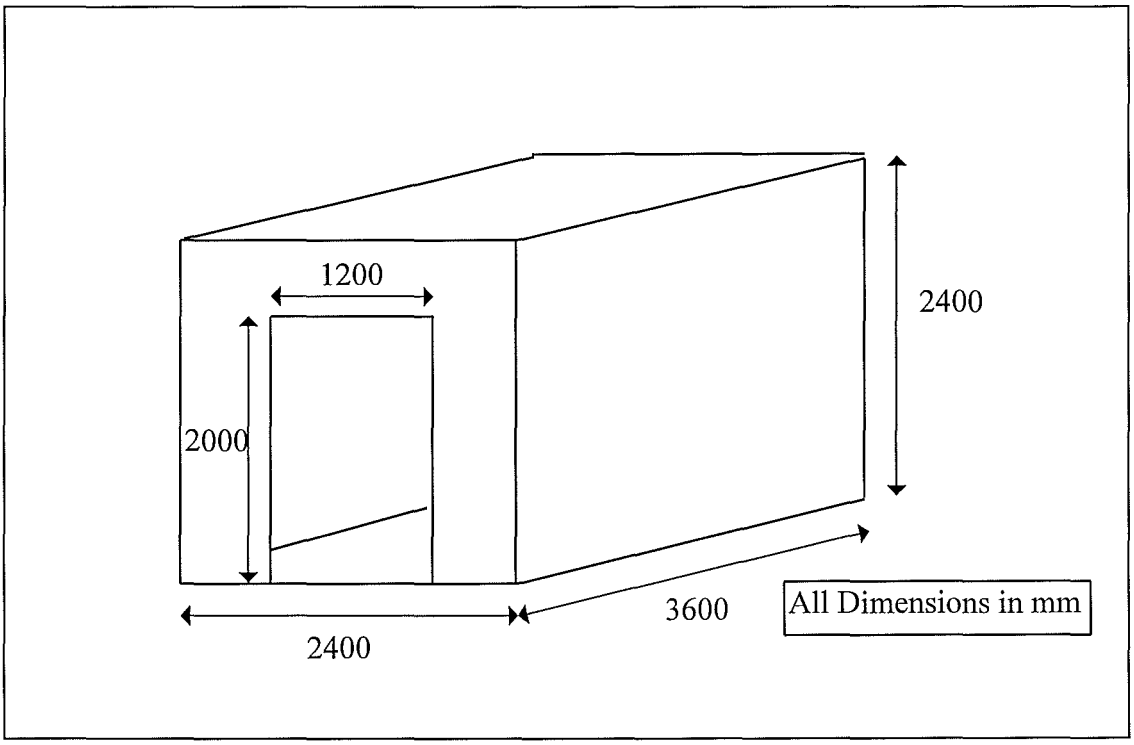

Figure 3-2: Room Dimensions

For the purposes of description of the compartment and objects within it all directions will be from the viewpoint of someone outside of compartment facing towards the compartment doorway. The front of the compartment is that part near the doorway end, the rear is towards the closed end, left is towards the (3.6 metre by 2.4 metre) wall on the viewer's left hand side, right is towards the (3.6 metre by 2.4 metre) wall on the viewer's right hand side. All heights unless otherwise stated are relative to the compartment floor.

The inside of the compartment was completely lined with 12.5 mm thick gypsum board. This was nailed into place on top of the plywood and the seams stopped. The aim of the gypsum lining was to protect the plywood so that the compartments could be used for multiple tests. It also has the benefit that it is a common wall lining in New Zealand homes and thus gives realistic thermal behaviour for the compartment. The exterior wall of the compartment around the doorway was lined with fire rated gypsum board to protect the plywood from the flames issuing from the doorway.

A full height partition wall was within the compartment extending 1.7 metres across the compartment leaving a 0.7 metre gap. The wall was parallel to the rear (2.4 metres by 2.4 metres) wall and was placed 1.2 metres away from it. It was joined with no gaps to the floor, ceiling and left hand (3.6 metres by 2.4 metres) wall. The partition was gypsum board over a steel stud frame. Figure 3-3 illustrates the position of the partition.

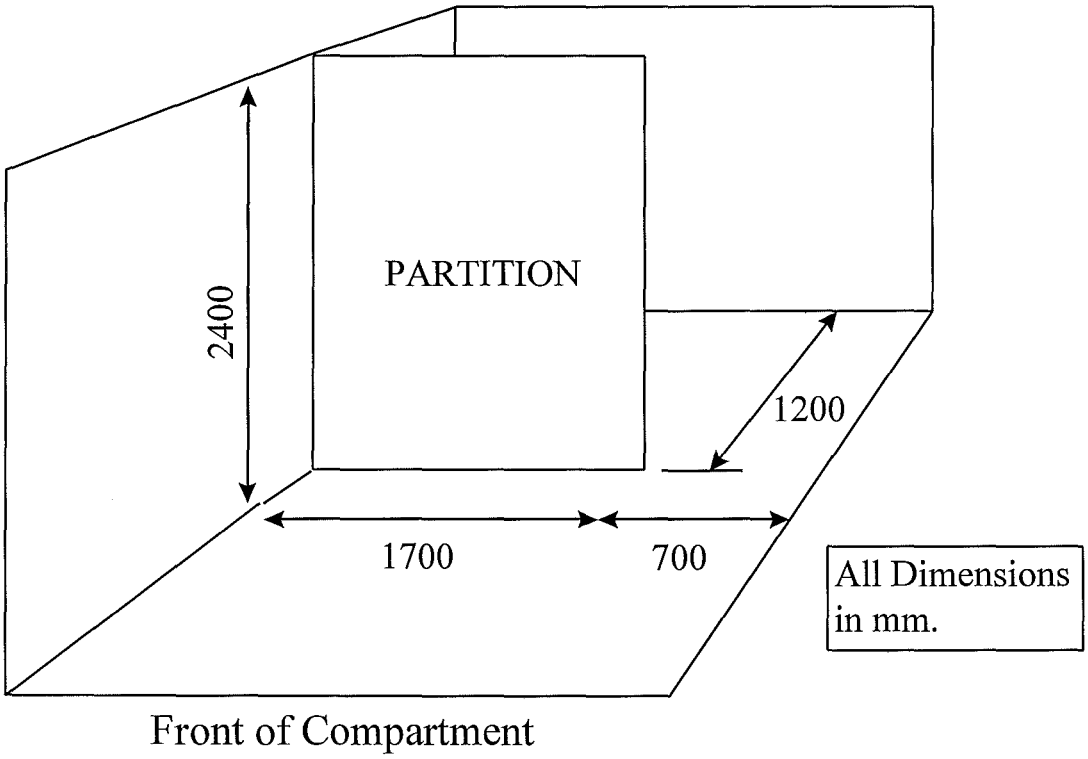

Figure 3-3: Location and Dimensions of the Partition

Four identical compartments were built. This allowed multiple burns on the same day as each compartment requires a three day recommissioning period. Wheels were mounted under the compartments to allow them to be easily moved. The wheels and their supporting posts raised the compartment floor approximately 0.5 metres off the ground.

3.1.2 Fire Load

The fire load consisted of three wooden cribs constructed using kiln dried pine timber, this load was augmented by sheets of medium density fibreboard (MDF).

The cribs had dimensions of 600 mm wide by 600 mm deep by 750 mm high. The cribs contained six sticks per layer arranged in eight alternating layers per crib. The sticks were 50 mm by 50 mm by 600 mm and the horizontal spacing between the sticks was 50 mm. A schematic of a typical crib construction is shown in Figure 3-4.

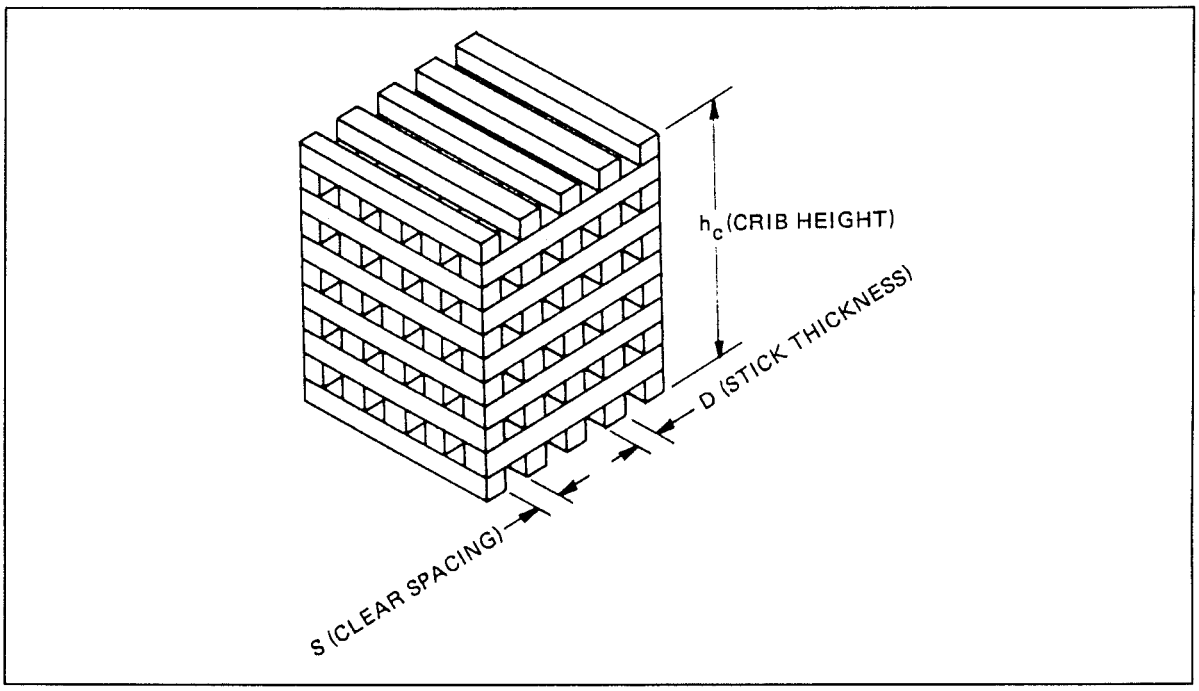

Figure 3-4: Typical Crib Construction (From: Babrauskas, V., *Burning Rates*, SFPE Handbook of Fire Protection Engineering, 2nd Ed. 1995. p 3-3.)

Two of the cribs were located behind the partition wall. One in the rear corner, 50 mm from the rear and left hand walls, the other on the centre line of the compartment again 50 mm from the rear wall. The third crib was located in front of the partition, 50 mm from the left hand compartment wall and the partition wall.

The MDF was in approximately 2.4 metres by 1.2 metres sheets of 3 mm thickness. Eight sheets were nailed to the walls in four double sheets. Figure 3-5 illustrates the location of the fuel packages.

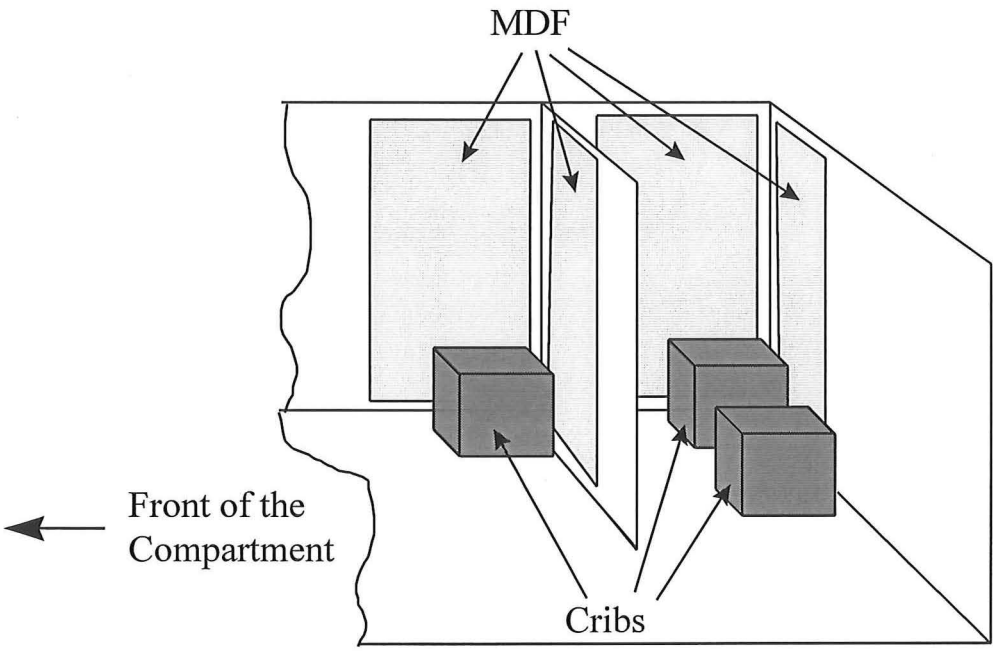

Figure 3-5: Location of the Fuel Load in the Compartment

Ignition was by means of a metal tray containing 200 ml of diesel placed under each of the cribs. Liquid pool fires were used as ignition sources because of the reproducibility of their heat release rates.

3.1.3 Thermocouple Arrays within the Compartments

All thermocouples used in the compartment were of type K chromel-alumel 0.5mm gauge with an approximate bead size of 1 mm. The thermocouples were held in place using 6 mm diameter steel tubes, with approximately 10 mm of the thermocouple tip protruding from the protective steel tubing which extended approximately 0.3 metres from the wall.

Fixed thermocouples were located in the centre of each of the cribs. Care was taken to ensure that the tips were exposed to air and were not pressed against the wood.

An array of twelve thermocouples were located in the front left corner of the compartment starting at a height of 0.1 metres and then spaced at 0.2 metre intervals to a height of 2.3 metres. This is in excess of the seven thermocouples given as a guide by ISO 9705[49]. The location of the thermocouples 0.3 metres from the front and side walls is in accordance with ISO 9705[49]. A strip of gypsum was used to help shield the thermocouples from water spray during the fire suppression. This strip was 300 mm wide and went from floor to

ceiling about 300 mm in front of the thermocouples. Figure 3-6 shows a schematic of the thermocouple tree locations within the compartment.

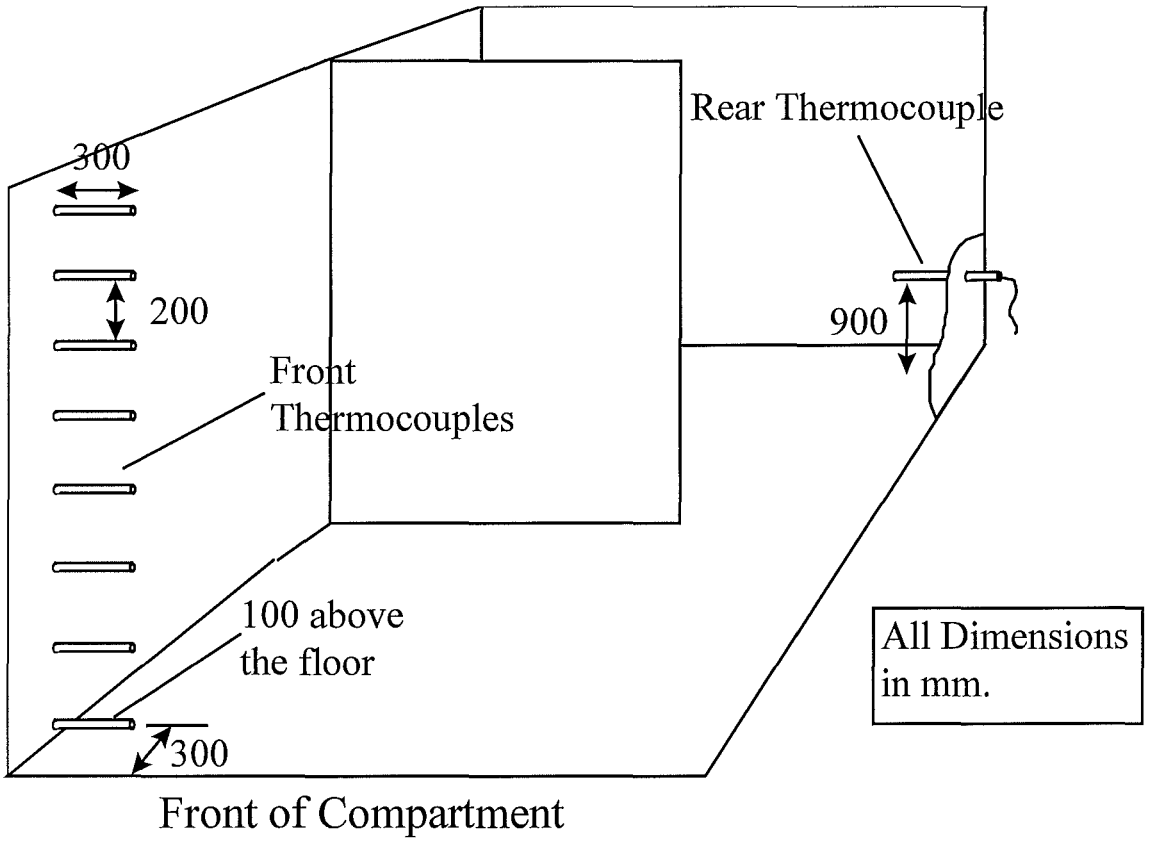

Figure 3-6: Location of Thermocouple Trees within the Compartment

A further thermocouple was placed in the rear right corner of the room at a height of 0.9 metres, unlike the front thermocouples this thermocouple was not protected by gypsum shielding.

3.1.4 Compartment Doorway Measurement

Measurements were taken of temperatures and velocity at a range of heights on the doorway centreline. Eight type K chromel-alumel enclosed thermocouples were used to measure temperatures and eight bi-directional probes to measure flow rates.

These instruments were mounted on a wheeled trolley which could be pulled clear of the doorway prior to the suppression of the fire. Figure 3-7 shows a schematic of the trolley.

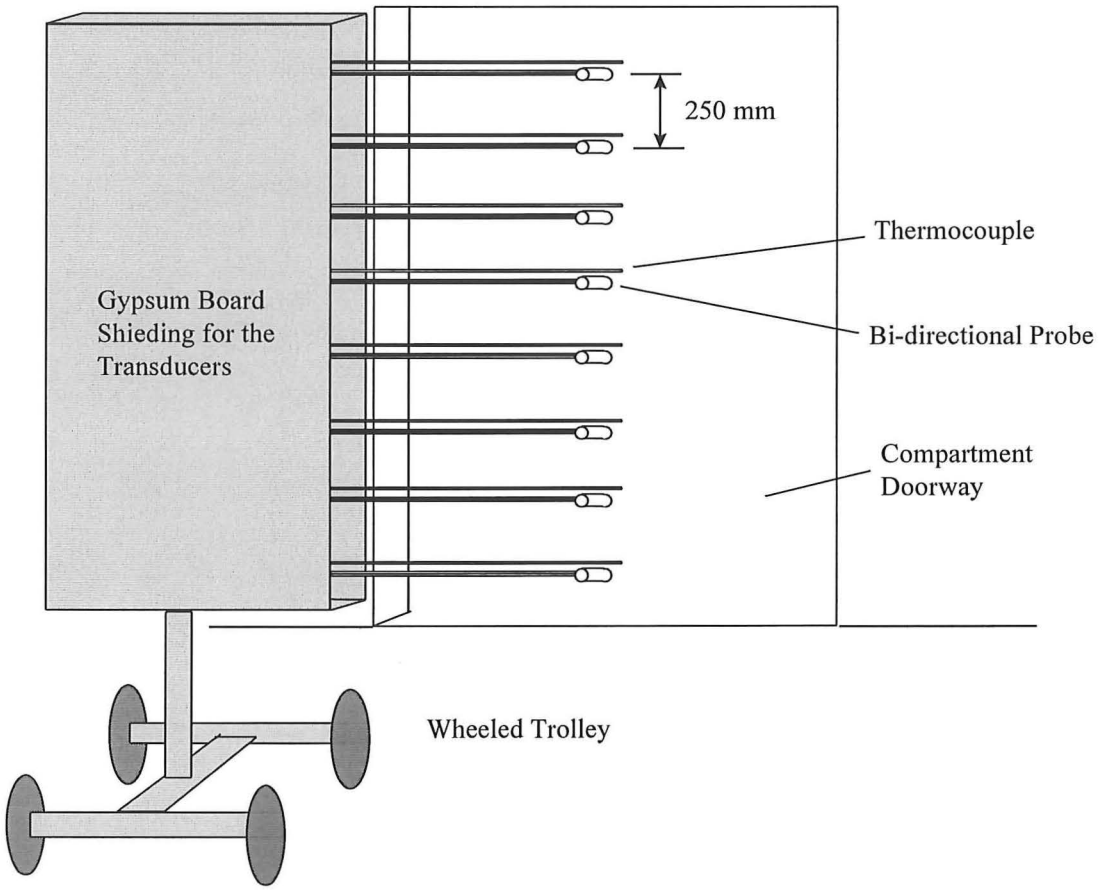

Figure 3-7: Schematic of the Thermocouple and Bi-directional Probe Trolley Placed in the Compartment Doorway

The trolley was aligned so that the tips of the thermocouples and the bi-directional probes were aligned with centreline of the doorway. The height of the trolley was adjusted so that the bottom thermocouple and bi-directional probe were 0.125 metres above the level of the floor of the compartment, the vertical spacing between each measurement point is 0.25 metres. A schematic of the bi-directional probes is shown in Figure 3-8.

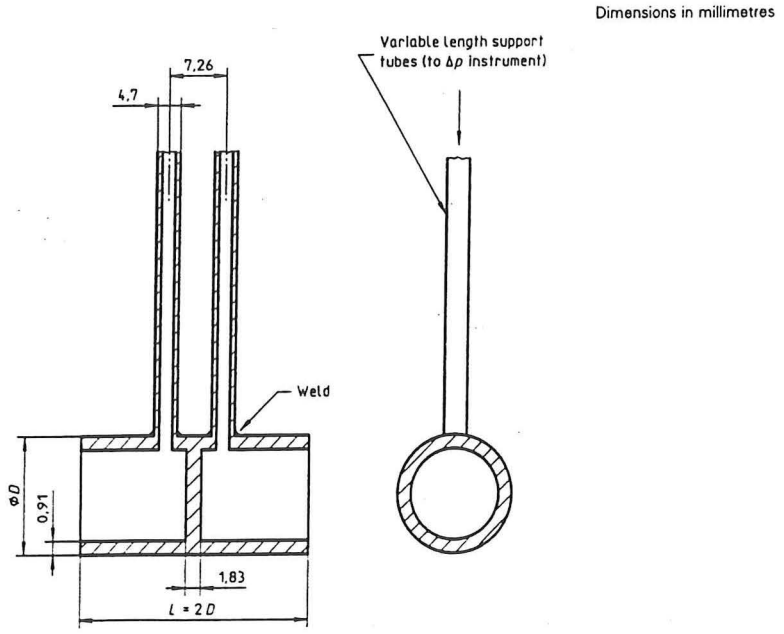

Figure 3-8: Detail of Bi-directional Probe (Taken from ISO 9705[49])

3.1.5 Fire Effluent Collection

Fire effluent is collected in a smoke hood and then drawn through duct work by a turboaxial fan and discharged to atmosphere. A schematic of the apparatus is shown in Figure 3-9.

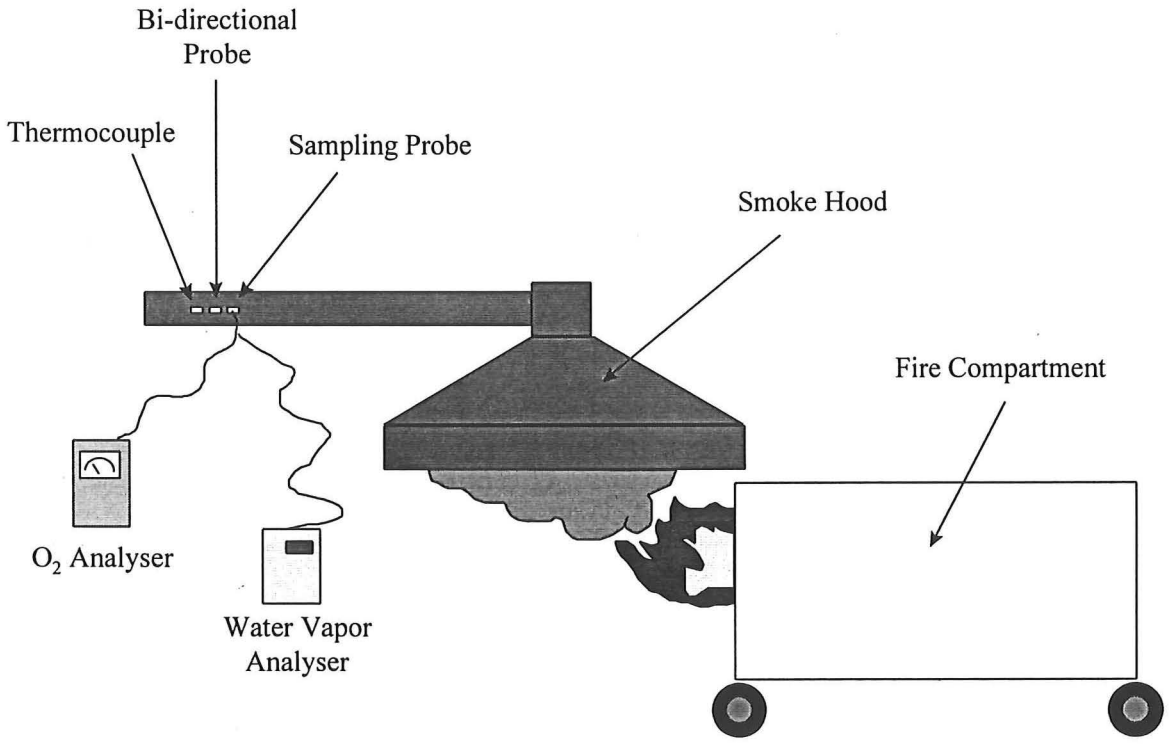

Figure 3-9: Schematic of the Smoke Collection System

Duct measurements are taken of centreline gas temperature using a type K chromel alumel thermocouple with the same dimensions as those that were used in the compartment. A bi-directional probe in the at the centreline of the duct measured the duct flow rate. These two instrument are located close to the gas sample probe.

Figure 3-10: Compartment, Hood and Ductwork

The smoke hood is 3.5 metres by 3.5 metres and is made from mild steel. It is surrounded by a skirt which is 0.4 metres deep. These dimensions are larger than 3 metre by 3 metre hood given in ISO 9705. A larger hood was used in order to assist fire effluent collection. The distance between the top of the compartment and the bottom of the hood skirt is approximately 0.1 metres. Heat resistant cloth was hung in this gap to minimise the loss of smoke between the compartment and the hood.

Gypsum framing was used to extend the skirt on two sides and build a wall on a third side. This was done to minimise the effects of wind. The compartment was placed on the side with no additional skirting. A schematic of the shielding is shown in Figure 3-11.

The duct work was mild steel, 0.6 metres in diameter. This ran horizontally for 6 metres to the point where the sampling probe and duct instruments were mounted. This is in accordance with the guidance given in ASTM E603[47] that the instrumentation should be 10 diameters from the start of the duct. This is enable the flow pattern to become established. The duct ran for a further 6 metres beyond the instruments where it joined a large, 1.2 metres by 1.2 metres square vertical duct. This duct then feeds into a 1 metre diameter circular duct which housed the turbo axial fan. Guide vanes as described in ISO 9705 were used, one set was located at the entrance to the circular duct from the smoke hood and another set were placed immediately downstream of the sampling point. Baffles were not used at the top of the hood in order to achieve the required volumetric flow through the duct.

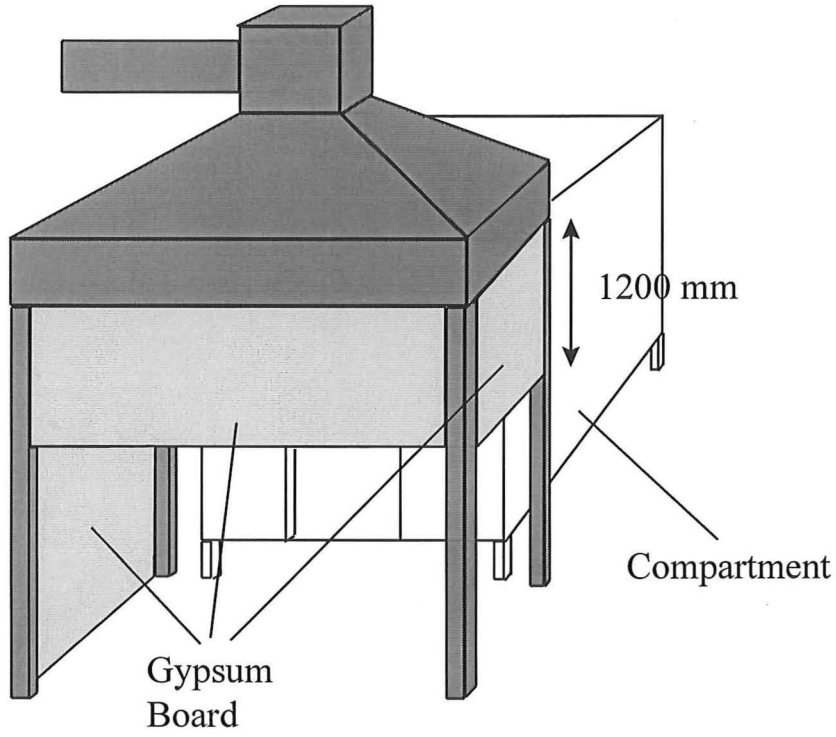

Figure 3-11: Schematic of Shielding

The fan was a 0.96 metre diameter aero-foil axial flow model with a design flow of approximately 11 m^3/s. This design flow was based on much larger flow openings than the 0.6 metre diameter duct and in practice flow rates around 4 m^3/s were achieved.

The fan was only rated at 120°C for intermittent operation so fine mist water sprays were used to cool the effluent stream before it reached the fan. Five water sprays lines were used, two of these were tipped with high flow rate (2.6 litres/min), fine droplet commercial spraying nozzles, the remainder were tipped with standard commercial orifice plate nozzles. Three of the nozzles were introduced into the horizontal circular duct downstream of the measuring instruments, two of the nozzles were in the square vertical duct.

Thermocouples were used to monitor the temperature in the circular duct at a position before the water sprays and in the square vertical duct at a position after the water sprays. This enabled the effectiveness of the water spray system to be monitored.

3.1.6 Oxygen Calorimetry Equipment

A gas sample was drawn from the duct and fed to an oxygen analyser after being cooled and dried and the CO_2 absorbed. A schematic of the oxygen sample line is shown in Figure 3-12.

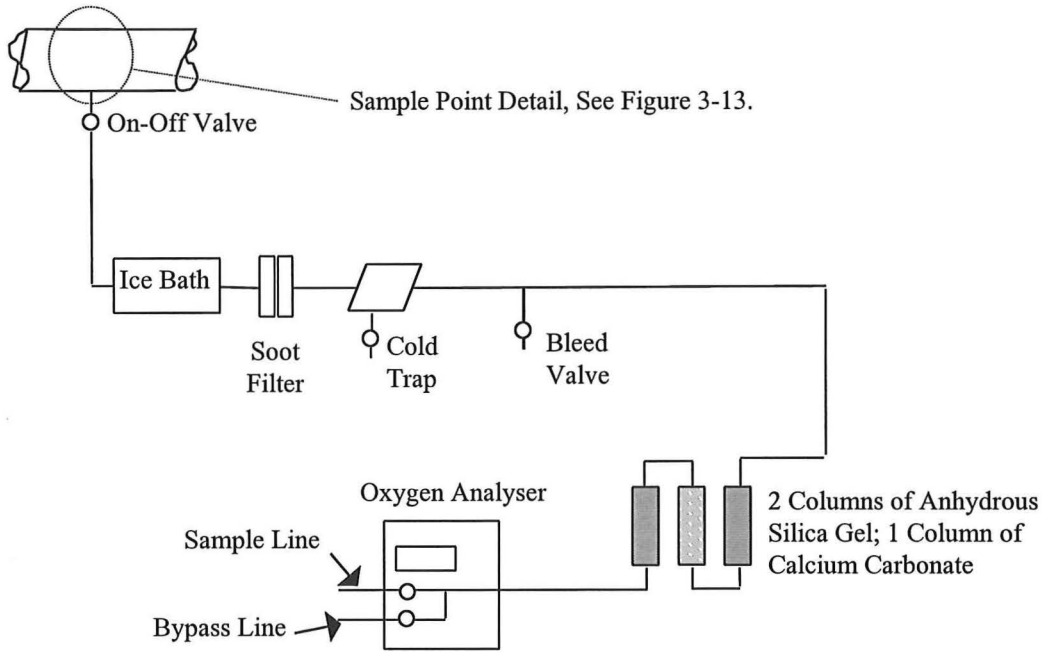

Figure 3-12: Schematic of Oxygen Analyser Sampling Line (Adapted from Dunn[50])

The sample probe consists of a steel tube of 10 mm diameter with holes drilled along its length. A schematic of the sampling probe is shown in Figure 3-13.

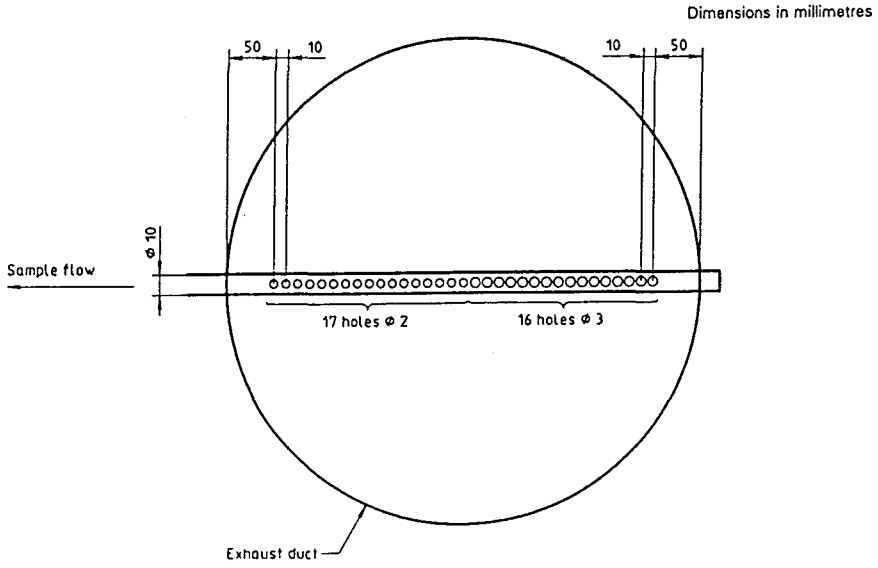

Figure 3-13: Sampling Probe (Taken from ISO 9705[49])

This tube is inserted across the diameter of the exhaust duct and a sample drawn. This sample is passed through a copper coil immersed in an ice bath and then through a soot filter. A cold trap is used to further cool the gas stream down to between 0°C and 4°C. A clear vessel with a drain valve mounted below the cold trap is used to collect and remove and liquid water. The majority of the flow is then bled to atmosphere through an open line controlled by a needle valve with the remaining portion being passed through a tube containing anhydrous silica gel to remove water vapor, then a tube containing soda lime to absorb CO_2 and then another tube containing anhydrous silica gel to further dry the sample. The clean, dry sample is then passed to the line to the oxygen analyser which itself has a bypass valve. The total pipe length between the sample probe and the oxygen analyser is approximately 8 metres, all of this pipe work apart from fittings and joints being 6 mm diameter copper tubing.

A Servomex 540A oxygen analyser was used. Oxygen concentrations are measured from changes in paramagnetic effect[51]. A concentration range of 0% to 25% was used with a quoted accuracy of 0.25%. Quoted 90% response time was 8 seconds.

3.1.7 Water Vapor Analysing Equipment

A sample is taken from the duct using the same sampling probe as for the oxygen sample. A schematic of the sampling line is shown in Figure 3-14.

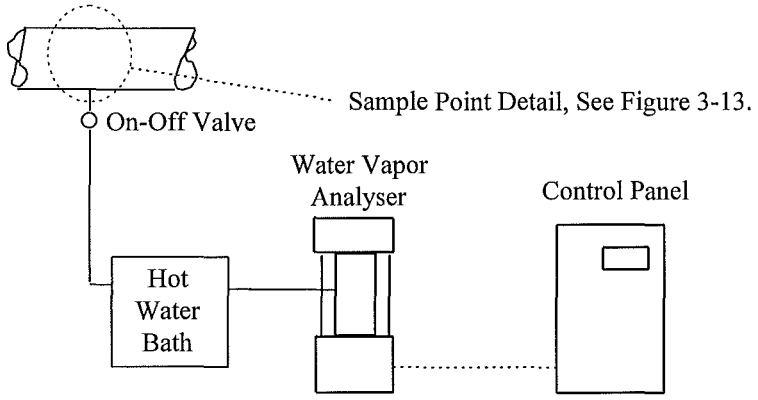

Figure 3-14: Schematic of the Water Vapor Analyser Line

The sample is passed through a hot water bath at 90°C to 100°C and then onto the water vapor analyser.

A Servomex PSA402 infra red water vapor analyser was used. Water vapor concentrations were measured from changes in the ratio of infra red radiation absorption at two wavelengths[52]. A concentration range of 0% to 50% was used with a quoted accuracy of 0.5%. Quoted 90% electrical response time was 5 seconds.

3.1.8 Foam Quality Measuring Equipment

The equipment and procedure for the foam quality measurements is as specified in UL 162[53].

The foam sample is sprayed onto a collection plate or foam slider which funnels it into a collection container. A schematic of the foam slider is shown in Figure 3-15. Three

collection containers were used a 2600 ml container used for the expansion ratio measurement, a 1600 ml container with a drain pipe for collecting the sample for which the drainage time is measured and a 2 litre container used to collect the drained liquid from the drainage time container. A beam scale with a range of 0 to 2600 grams and an accuracy of 0.1 gram was used to measure the sample masses.

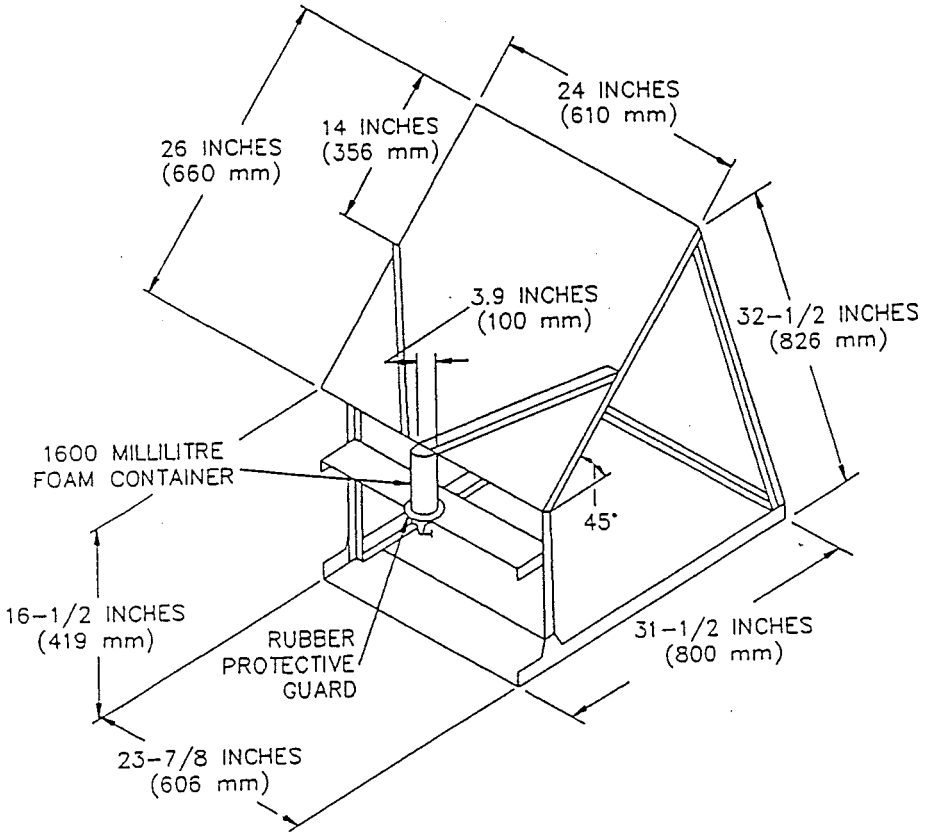

Figure 3-15: Foam Slider

3.1.9 Suppression Equipment

Two New Zealand Fire Service appliances were used one with standard high pressure delivery hose reels and the other with a compressed air foam unit. Class A concentrate was used at a concentration of 0.3% in water with no other additives. Standard variable fog pattern branches were used with the high pressure delivery and a straight bore 25 mm nozzle was used with the compressed air foam. Hose diameters were 25mm for the high pressure delivery and 40mm for the compressed air foam.

3.1.10 Weather Station

The weather station consisted of a wind direction indicator and a wind speed indicator. These were linked into the data acquisition system to give continuous readings. Values of temperature and relative humidity were taken using a hand held device.

A plan of the experimental site (Figure 3-1) shows the location of the weather station relative to the compartment.

3.1.11 Video Equipment

Two video cameras were used to provide views of the front and the side of the area just in front of the compartment. A third camera was used on one days runs to provide views of the development of the fire in the cribs in the rear of the compartment behind the shield. The compartments were modified to include a small heat resistant glass glazed window to allow this to be seen.

The videos were also used to record interviews with the fire crews and to obtain a visual record of the degree of water and fire damage sustained by the compartment.

3.1.12 Data Collection Equipment

This consisted of a analogue to digital converter (ADC) interfaced to the 50 fixed thermocouple ports 36 loose thermocouple ports and 16 voltage ports. The ADC was connected to a Pentium PC running Windows 95 and custom made data logging software. Appendix 1 summarises the data collection channels for the device. Data on all channels was captured 5 times per second and then averaged over 5 readings to give one averaged value each second.

3.2 Experimental Procedure

Experiments were carried out on three days; 27/11/97, 2/12/97, and 12/12/97. On each of these days three experiments were carried out, one for each suppression method. The order of the suppressants used varied for each experimental run. The experiments that were performed are summarised in Table 3-1.

Date	Experiment Number	Suppression Method
27/11/97	1	CAFS
27/11/97	2	Solution
27/11/97	3	HPD
2/12/97	1	HPD
2/12/97	2	CAFS
2/12/97	3	Solution
12/12/97	1	Solution
12/12/97	2	CAFS[†]
12/12/97	3	HPD

Table 3-1: Summary of Experiments

[†] Order planned to be HPD then CAFS but this had to be changed for Fire Service operational reasons.

3.2.1 Foam Quality Tests

Foam quality measurements were carried out according to UL162[53]. Foam was collected onto the foam collection plate. A foam sample of known volume was collected in a cylinder placed under the collection plate and weighed on a beam scale. This weighed sample of known volume was used to calculate the expansion ratio of the foam.

A second sample was then collected in the drainage time container. Once the container was full a stopwatch was started and the clip sealing the drainage tube opened. The liquid draining out of the tube was collected in a separate container and its weight was measured on the beam balance as a function of time.

These tests were carried out prior to each of the Solution and CAFS runs. Operating conditions for the foam producing equipment were selected to be the same as those for the actual fire extinguishment. Foam was lofted as gently as possible from the hose onto the collection plate. This was done in order to minimise the mechanical work done on the foam which could cause breakdown of the foam structure.

3.2.2 Fuel Moisture Content Measuring Equipment

The wooden crib moisture content was measured prior to each run. Three readings were taken from each crib.

3.2.3 Suppression Tests

Due to the complexity of the tests a checklist approach was used. An example of the checklist is provided in Appendix 2. A large part of this covers the setup and calibration process discussed in Chapter 4.

Prior to the experiments using Solution, concentrate would be added to the water tank of the appliance and the appliance driven around to thoroughly mix it.

Prior to the experiments using Solution or CAFS foam quality tests would be carried out as described in Section 3.2.1.

Instrumentation would be calibrated and stabilised prior to the experiments. Data collection would start and a three minute baseline period run. During this baseline final checks would be made that the fire crew was ready for suppression. Measurements would be taken of the temperature and relative humidity.

Video cameras were started two minutes into the baseline (one minute prior to ignition). Time synchronisation between the videos and the data acquisition system was obtained using a lamp mounted in view of the video cameras which flashed on each whole minute.

At three minutes the diesel under the rear corner crib would be ignited. This was achieved by playing a blowtorch over the diesel for ten seconds. Then the diesel under the rear centre crib was ignited the blowtorch being applied for fifteen seconds to compensate to some extent for its later lighting. Finally the diesel under the unshielded crib was ignited the blowtorch being applied for twenty seconds, again the increased time being used to compensate for the later ignition of the crib.

The water misting system to protect the fan was turned on once the duct thermocouple was registering above 50°C. The trolley holding the doorway thermocouples and bi-directional probes was pulled back clear of the door way once the paper surface of the gypsum plasterboard on the floor began to ignite. When the burning of the compartment floor reached the front of the compartment the firefighter was signaled to start the attack. The firefighter would apply the agent for a continuous ten seconds and then stop the attack and stop any further flow of the agent. The volume of agent used was noted and if further agent was required for mopping up this volume was recorded separately. A fixed application period was used to give consistency between the runs, the figure of 10 seconds being arrived at from trial burns carried out before the main experimental program.

After the initial suppression the compartment would be left to see if re-ignition occurred. If it did its location and extent was recorded and the fire crew would then extinguish the re-ignition, often by climbing into the compartment to directly apply the agent.

Figure 3-16: Growing Fire in the Compartment

At the end of the suppression a note would be made of the volume of agent used for the initial attack. Any water used for mopping up or for suppressing any re-ignition would be recorded separately.

The videos would be left running for 3 minutes after suppression and the data logging would continue until at least 3 minutes after temperatures in the compartment had fallen to near ambient.

Video recordings would be made of the compartment interior and an interview would be taken with the branch man and at the end of all three runs with the pump operator.

4. CALIBRATION OF APPARATUS

4.1 Calibration of the Duct Mass Flow Rate

The duct mass flow rate is measured by a bi-directional probe placed in the centre of the duct just before the sample point. In order to calculate the mass flow rate from this point measurement it is necessary to know the form of the velocity profile.

The velocity profile form was obtained by spanning a bi-directional probe across the diameter of the duct and measuring the pressure difference at regular intervals. Due to the erratic nature of the flow the probe was left at each position on the diameter for 5 minutes and the sampled values (themselves 1 second averaged values of 0.2 second interval measurements) were averaged over this time period with the first 20 seconds of data discarded as the probe was moving into position during this time.

The duct velocity profile was determined in order to calculate the correction factor for the mass flow rate equation. The normalised form of the profile is shown in Figure 4-1. For the

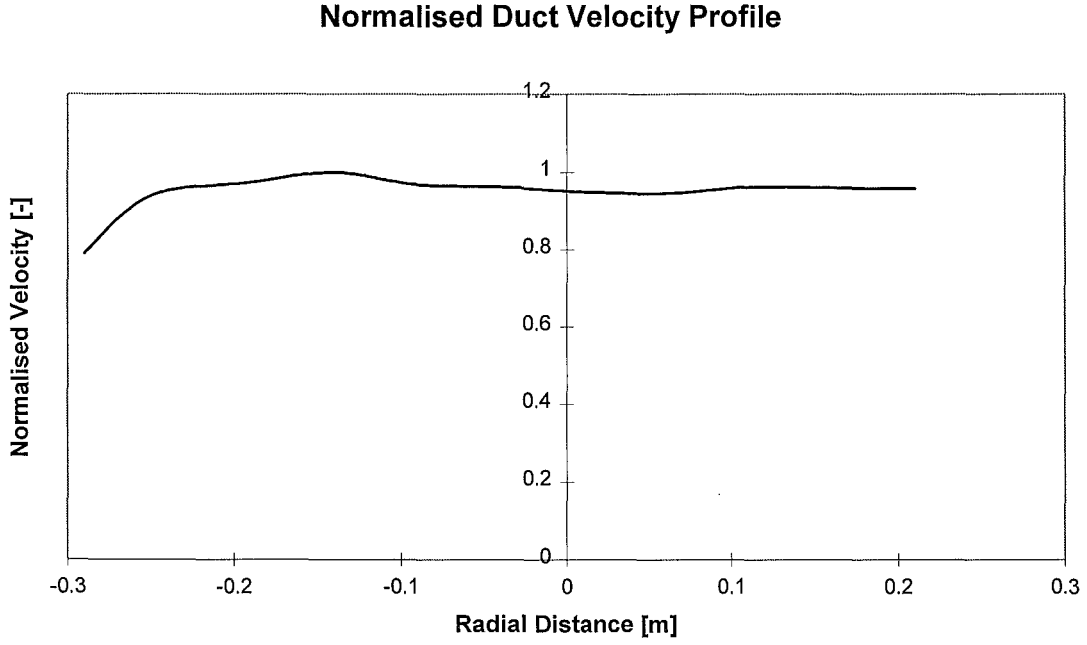

Figure 4-1: Duct Velocity Profile

calculation of the shape factor it was assumed that the velocity profile in radial distance range of +0.2 metres to +0.3 metres, which could not be measured due to limitations in the equipment, has the same form as the velocity profile as in the range -0.3 metres to -0.2 metres.

Calculation of the velocity profile shape factor, k_c [-], was calculated by numerically integrating the duct velocity profile to obtain a flow rate and then dividing this by the flow rate obtained based on the maximum velocity. This gives a k_c value of 0.95.

4.2 Zeroing and Spanning of the Oxygen Calorimeter

The instrument was zeroed by passing through a stream a pure nitrogen for at least 10 minutes and then zeroing against the input voltage into the ADC. The instrument was spanned by passing a stream of dry air through it for at least 10 minutes before spanning to a value of 20.95% oxygen as output by the ADC.

4.3 Heat Release Rate Calibration of the Oxygen Calorimeter

The heat release rate for the fires was calculated based upon a number of measured parameters and assumed constants, these are discussed in more detail in the theory section. In order to check the accuracy of the measurements and the validity of the assumed constants calibration runs were carried out.

A mixture of 20% propane, 80% butane by volume was used as the calibration gas. Four gas cylinders were used to give sufficient flow rate and these were mounted on load cells so that as the gas was burnt the mass flow rate of fuel could be determined. The burner consisted of drilled pipes mounted in a 0.6 metre diameter drum filled with stones to help evenly distribute the flow.

The gas flow rate was controlled with a needle valve and an on-off valve, both mounted at the gas cylinder end of the supply line.

For the calibrations all exhaust gas analysis apparatus was set up exactly as for a compartment burn. The needle valve on the gas cylinders would be set to a number of turns

depending on the gas flow rate and hence heat release rate required. A baseline of 3 minutes would be taken before the main on-off valve was opened and the burner lit. The burn duration was 5 minutes and then there would be a further 3 minute baseline with the burner turned off. This gives a heat release square wave. These would be done in sets of three as long as there was no buildup of condensation on the gas bottles due to their cooling as the gas flowed. Each of these square waves is referred to by number with wave #1 being the first square wave of the set, etc.

For the calibration runs the heat release rate from the calibration gas was measured directly from the mass consumption rate of the fuel. This value was then compared with the values obtained using the calorimetry equipment.

The calibration gas was a mixture of 80% propane and 20% butane by volume. The heat release rate was calculated using equation (40):

$$q = \dot{m}_f \left(0.8\Delta H_{propane} + 0.2\Delta H_{butane}\right) \tag{40}$$

Figure 4-2 compares the predicted heat release rate calculated using equation (40) with the

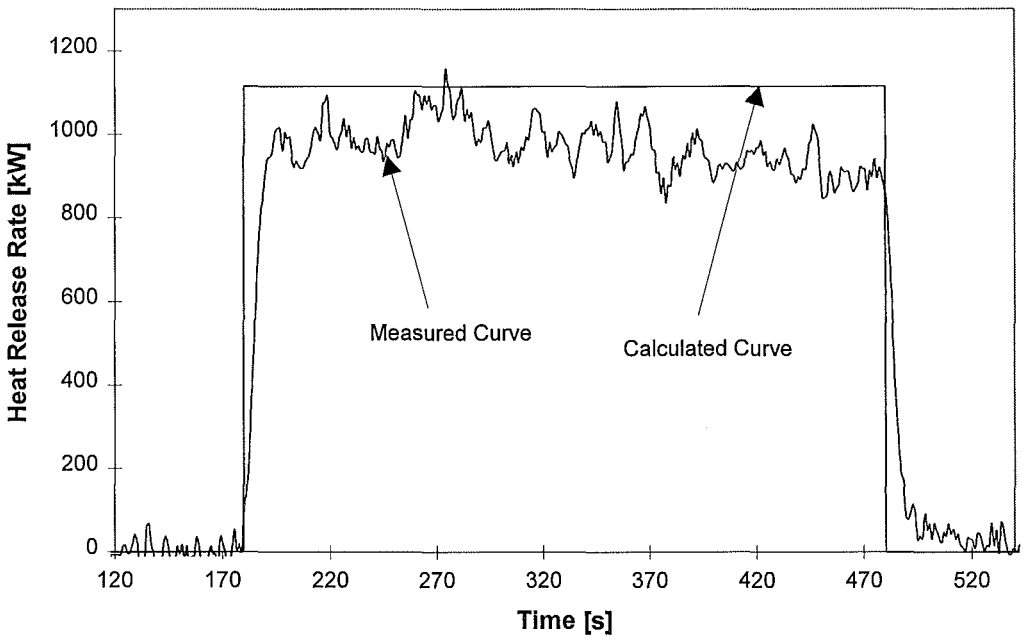

Figure 4-2: Comparison of Calculated and Measured Heat Release Rates

values obtained from the oxygen calorimeter for a typical calibration run. The heat release rate was calculated using the formula of Janssens[54], equation (10). Note the oxygen calorimeter data has been reduced to account for time lags, see Chapter 5 for further information on this process.

Agreement between the measured value and the calculated values is good for the majority of the calibration runs. The ability of the smoke hood to capture all of the fire products was highly dependent on the wind conditions and it was found that successful calibration runs could only be carried out in very still conditions.

5. DATA REDUCTION

The process of data reduction is required to account for the fact that all of the instrument do not respond instantly and fully to changes in the fire compartment. It is necessary to reduce the data captured for each instrument and re-calibrate it to a common time line which has been taken to be the time line with zero time as the moment of starting ignition of the diesel pans in the compartment.

There are two basic types of time lags, transport lags and system response lags. The relative significance of these different lag times depend on the nature of the equipment and how it is used.

5.1 Transport Lags

The experiment is concerned with the properties in the fire compartment and hence by definition any measurements taken remotely from the compartment have an inherent transport lag time. This transport lag time can be broken down into the following components:

- t_1 - time taken for fire effluent to travel from inside to the outside of the compartment (i.e. to the hood).
- t_2 - time taken for fire effluent to travel from the hood to the bi-directional probe, duct thermocouple and the sample point. Due to the close proximity (within 0.5 metres) of these instruments and the high duct velocity (around 14 m/s) any slight variation in the value of t_2 between them is ignored.
- t_3 - time taken for sample to travel from the sampling point to the water vapor analyser.
- t_4 - time taken for sample to travel from the sampling point to the oxygen calorimeter.

The transport lag times for the various measurements is summarised in Table 5-1.

Measurement	Transport Lag Time
Compartment Temperatures	0
Doorway Temperatures	0
Doorway Flow	0
Duct Temperature	$t_1 + t_2$
Duct Flow	$t_1 + t_2$
Water Vapor Concentration	$t_1 + t_2 + t_3$
Oxygen Concentration	$t_1 + t_2 + t_4$

Table 5-1: Transport Lag Times

5.1.1 Compartment to Hood Lag Time, t_1

t_1 can be estimated from the known outwards velocity in the doorway. Obviously this changes with the magnitude of the fire but as an approximation an average value can be taken. The transport lag is then taken relative to the centre of the burning region of the compartment which is located at a distance of approximately 2.4 metres back from the doorway. The fire gases have to travel approximately 1.2 metres from the compartment doorway to the point below the centre of the hood. This gives a total distance of approximately 3.5 metres. The transport lag between the fire and the hood is then given by:

$$t_1 \approx \frac{3.5}{\bar{v}_o} \tag{41}$$

This assumes that the flow in the compartment is channeled towards the doorway opening and the velocities in the compartment are similar to those in the doorway. In practice there would be flow in all directions and the effective velocity in the compartment would be lower than that measured in the doorway. As a very simple analysis, for our compartment the ratio of the width of the compartment to the width of the doorway is 2:1. If the velocities from the fire towards the doorway are uniform across a horizontal layer then the velocity towards the doorway in the compartment is half the value in the doorway. In practice the real flow will be somewhere between the two extremes and hence:

$$\frac{3.5}{\bar{v}_o} < t_1 < \frac{3.5}{0.5\bar{v}_o} \tag{42}$$

Velocities were measured for the upper doorway probes and the averaged values are presented in Table 5-2.

Date	Method	Mean Velocity [m/s]
27/11/97	CAFS	4.0
27/11/97	Solution	3.9
27/11/97	HPD	4.0
2/12/97	HPD	3.8
2/12/97	CAFS	3.2
2/12/97	Solution	3.2
12/12/97	Solution	3.2
12/12/97	CAFS	3.2
12/12/97	HPD	3.2
	Average	**3.5**

Table 5-2: Mean Velocity of Outflow from the Compartment

Using equation (41) this velocity can be used to calculate a lag time. This gives a value for t_1 of approximately 1 second.

t_1 can also be estimated by measuring the comparative response of the thermocouples in the compartment in the duct around the time of extinguishment. As the temperature falls in the compartment a corresponding fall should be seen in the duct temperature at a time $t_1 + t_2$ later, and knowing t_2 it is possible to calculate a value of t_1.

The difference in the response times between the compartment thermocouples and the duct thermocouple gives a measure of $t_1 + t_2$ was measured around the time of extinguishment. The rear thermocouple was used as the front thermocouples are remote from the fuel and would tend to underestimate the time. The results are summarised in Table 5-3. Positive time differences indicate the duct thermocouple response lagging behind the compartment thermocouple, negative time differences indicate the compartment thermocouple response lagging behind the duct thermocouple.

Date	Method	Time Difference [s]
27/11/97	CAFS	+2.2
27/11/97	Solution	-2.0
27/11/97	HPD	-2.0
2/12/97	HPD	+2.1
2/12/97	CAFS	+2.7
2/12/97	Solution	-1.0
12/12/97	Solution	+2.3
12/12/97	CAFS	+2.9
12/12/97	HPD	+4.5

Table 5-3: Time Differences in Compartment and Duct Thermocouple Response

In the cases where a negative time difference was obtained the response of the front thermocouples was examined. The results are given in Table 5-4.

Date	Method	Time Difference [s]
27/11/97	Solution	+1.7
27/11/97	HPD	+1.5
2/12/97	Solution	0.0

Table 5-4: Time Differences Using Front Thermocouples in Compartment

The average time difference will be calculated using the positive values for the Solution and HPD experiments on 27/11/97 and ignoring the values for the Solution experiment on 2/12/97. This gives a mean of 2.5 seconds with a standard deviation of 0.9. Within a 95% confidence interval (Section 2.7) the mean is 2.5 ±0.6 seconds. Given a t_2 value of 1.3 seconds (from Section 5.1.2) this gives t_1 as 1.2 seconds which is agreement with the value estimated using doorway velocities.

5.1.2 Hood to Sample Point Time Lag, t_2

t_2 can be estimated by measuring the initial response time of the duct thermocouple during the burner calibration runs. This assumes that the initial system response time for the thermocouple is small compared with the transport time. A theoretical value can be calculated for t_2 based upon the known volume of the duct work and the volumetric flow rate. A comparison between these two methods is used to increase confidence in the results.

In the first method the transport time lag between the hood and the instruments, t_2, is measured from the initial response time of the duct thermocouple. This gives an upper limit as it does not account for any inherent lag in the thermocouples initial response. The results from this are summarised in Table 5-5 below.

Calibration Date/Number	Wave#1 Lag Time [s]	Wave#2 Lag Time [s]	Wave#3 Lag Time [s]
2/12/97	1.6	2.1	1.1
12/12/97	1.0	0.9	1.0
17/12/97 #1	1.3	1.5	1.3
17/12/97 #2	1.2	1.2	1.1

Table 5-5: Duct Thermocouple Time Lags From Heat Release Calibration Runs

Taking the simple average of these gives t_2 as 1.3 seconds. The standard deviation is 0.32 seconds. Within a confidence interval of 95 % the mean is 1.3 ±0.18 seconds.

The duct length from the hood to the sample point is approximately 6 metres. The duct is 0.6 metres in diameter giving a volume of 1.7 m^3. The hood is 3.5 metres square with a height to its apex of approximately 1.5 metres. The hood volume is approximately that of a pyramid 1.5 metres high with a 3.5 metre square base, that is 6 m^3. Giving a total flow volume of 7.7 m^3. At a volumetric flow rate of 4 m^3/s this gives a transport lag of 1.9 seconds. This is larger that the measured value which is not surprising considering that in practice the flow will tend to 'plug hole' and the effective volume will be lower than 7.7 m^3.

5.1.3 Sample Point to Water Vapor Analyser Time Lag, t_3

t_3 is measured relative to the duct thermocouple by comparing the response of the water vapor analyser to the duct thermocouple.

The differential time lag can be measured by comparing the response of the systems. A heat release square wave is produced by the burner starting at time zero. The response of the both the thermocouple and the water vapor analyser is normalised from zero to 100% based upon the peak value obtained. The time taken for each instrument to reach a certain value, for example 50% of peak, can be measured. Since the square wave of the burner is not perfect this value will vary between calibration runs. More informative is to take the

difference between the times for the thermocouple and the analyser as to some extent this accounts for the variations in the burner behaviour. This time difference can then be used as a relative lag time between the two instruments. The concept is illustrated in Figure 5-1.

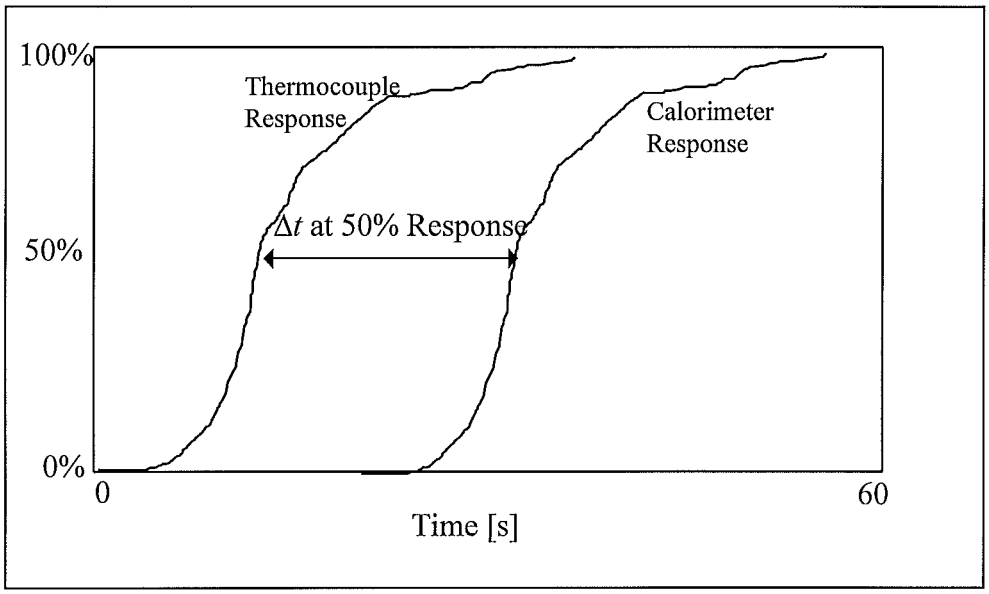

Figure 5-1: Schematic of Normalised Instrument Response

The transport time lag between the sampling point and the water vapor analyser, t_3, was measured by looking at the differential response time between the analyser and the duct thermocouple at 50% and 70% of their normalised values. The results are summarised in Table 5-6.

Calibration Date/ Number	Wave#1 Lag Times [s]		Wave#2 Lag Times [s]		Wave#3 Lag Times [s]	
	50%	70%	50%	70%	50%	70%
12/12/97	6.5	9.9	4.6	6.7	5.1	4.2
17/12/97 #1	5.2	5.6	5.7	3.5	4.8	4.1
17/12/97 #2	12.6	21.5	4.1	4.6	5.8	8.0

Table 5-6: Differential Response Times for the Duct Thermocouple and Water Vapor Analyser

The response times for the first wave in the 17/12/97 #2 run are anomalous. The response of the instrument was very slow and this is believed to be due to an observed problem with the pre-heating apparatus prior to this wave, for this reason these data points will not be considered in the calculation of the means and standard deviations.

The average across the 50% values is 5.2 seconds, and the average across the 70% values is 5.8 seconds. The standard deviation across the 50% values is 0.7 seconds, and across the

70% values is 2.1 seconds. The 50% value mean of 5.2 seconds will be used because of its lower variance. Within a confidence interval of 95% the mean is 5.2 seconds ±0.5 seconds.

5.1.4 Sample Point to Oxygen Analyser Time Lag, t_4

t_4 is measured in two ways. Firstly it is measured using the same method as used for the water vapor analyser. It is also measured directly by introducing a square wave of nitrogen at the sample point and measuring the system response.

The results for the direct measurement from a nitrogen square wave are given in Table 5-7.

Calibration Date/Number	Lag Time [s]
1/12/97 #1	20.0
1/12/97 #2	17.0
1/12/97 #3	18.0
11/12/97 #1	12.5
11/12/97 #2	17.0

Table 5-7: Lag Time of the Oxygen Analyser in Response to a Nitrogen Square Wave

The 11/12/97 #1 run was performed by direct coupling of the nitrogen supply to the sampling point. A higher pressure was set on the nitrogen cylinder for this run than for the 11/12/97 #2 run and it seems reasonable to suggest that the markedly lower lag time noted in the 11/12/97 #1 run is due to the nitrogen flow being forced down the line. For this reason this data point will be ignored. Taking a simple average of the other values gives a t_4 value of 18 seconds.

In the second case the lag time was measured by looking at the differential response time between the calorimeter and the duct thermocouple at 50%, 70% and 90% of their normalised values. The results are summarised in Table 5-8.

Calibration Date/ Number	Wave#1 Lag Times [s]			Wave#2 Lag Times [s]			Wave#3 Lag Times [s]		
	50%	70%	90%	50%	70%	90%	50%	70%	90%
CAL10212	20.6	14.9	18.5	20.5	20.6	11.6	21.1	19.2	19.4
CAL11212	21.9	22.6	7.0	21.6	21.1	6.6	21.7	20.5	3.7
CALB1712	24.6	25.1	22.2	22.9	22.6	25.9	23.0	24.5	22.2
CALC1712	24.4	25.5	21.8	21.6	23.0	21.3	21.6	22.3	24.3
Average	22.9	22.0	17.4	21.6	21.8	16.3	21.9	21.6	17.4

Table 5-8: Differential Response Times for the Duct Thermocouple and Oxygen Analyser

The average across the 50% values is 22.1 seconds, the average across the 70% values is 21.8 seconds, and the average across the 90% values is 17.0 seconds. The standard deviation across the 50% values is 1.3 seconds, across the 70% values is 2.9 seconds, and across the 90% values is 7.7 seconds. The 50% value mean of 22.1 seconds will be used because of its lower variance. Within a 95% confidence interval the mean is 22.1 ±0.7 seconds.

It can be seen that there is a significant difference in the transport lag values given by the two techniques. Which value is to be used will be determined by comparing the effect of the value used on the heat release rate calibration data. This is presented in Section 5.3.

5.1.5 Summary of Transport Lags

Measurement	Transport Lag Time	Lag Value [s]
Compartment Temperatures	0	0
Doorway Temperatures	0	0
Doorway Flow	0	0
Duct Temperature	$t_1 + t_2$	$1 + 1.3 \approx 2$
Duct Flow	$t_1 + t_2$	$1 + 1.3 \approx 2$
Water Vapor Concentration	$t_1 + t_2 + t_3$	$1 + 1.3 + 5.2 \approx 7$
Oxygen Concentration	$t_1 + t_2 + t_4$	$1 + 1.3 + 18 \approx 20$ or $1 + 1.3 + 22.1 \approx 24$

Table 5-9: Summary of Transport Lags

5.2 System Response Lags

As well as transport lag times, the system response lag time need to be estimated. This can be done in two ways.

In the first method given a step input to the system the time taken for it to respond to a certain percentage of the response can be taken. For a perfect linear system, characterised by an exponential response, the theoretical characteristic time is the time taken to reach 63% of the response. In the absence of better information it is assumed that the systems are linear. This time can be measured from the graphs produced for the differential time lag measurements.

In the second method a characteristic differential equation can be assumed for the system and this can be solved algebraically for the system to yield its characteristic response time. This is the basis for the method used by Croce[55] for the characterisation of the oxygen calorimeter which is discussed in Section 5.2.5.

The methods for determining the system response time lags are for various measurements are summarised in Table 5-10.

Measurement	Response Lag
Compartment Temperatures	63% response time
Doorway Temperatures	63% response time
Doorway Flow	63% response time
Duct Temperature	63% response time
Duct Flow	63% response time
Water Vapor Concentration	63% response time
Oxygen Concentration	From Croce method

Table 5-10: System Response Lags

5.2.1 System Response Lag for the Duct Temperature

The system response time for the duct thermocouple is taken as the time taken for the duct thermocouple to reach 63% of its peak value. This measured time is the time constant, τ, given theoretically by:

$$\tau = \frac{\rho c_p V_b}{h_k A_t} \tag{43}$$

Of all of the parameters contributing to the time constant, only one, the heat transfer coefficient, is not a constant property of the thermocouple. Babrauskas and Williamson[56] comment that the time constant is only constant if the flow velocity past the thermocouple is constant. For the duct the assumption that the velocity is constant is reasonable given that the fluctuations in duct velocity are on a smaller time scale than the response of the thermocouple.

The 63% response time is linearly interpolated from the times taken to reach 50% and 70% of the peak value. These times have had the transport lag component t_2 of 1.3 seconds subtracted from them. The results are summarised in Table 5-11.

Calibration Date/ Number	Wave#1 Lag Times [s]			Wave#2 Lag Times [s]			Wave#3 Lag Times [s]		
	50%	70%	**63%**	50%	70%	**63%**	50%	70%	**63%**
2/12/97	3.8	12.2	**9.3**	3.0	4.6	**4.0**	4.5	9.1	**7.5**
12/12/97	1.8	3.8	**3.1**	2.3	4.1	**3.5**	2.2	5.9	**4.6**
17/12/97 #1	2.7	5.2	**4.3**	2.0	5.4	**4.2**	2.8	4.4	**3.8**
17/12/97 #2	2.2	3.1	**2.8**	2.0	3.1	**2.7**	2.6	4.2	**3.6**

Table 5-11: Response Times for the Duct Thermocouple

Conditions during the 2/12/97 calibration run were windy and flame capture was intermittent. The outlying points obtained during this run are suspect due to these conditions and hence will not be used. Taking the average of the remaining points gives a mean value of 3.7 seconds and a standard deviation of 0.61 seconds. Within a 95% confidence interval the mean is 3.7 ±0.4 seconds.

5.2.2 System Response Lag of the Compartment and Trolley Temperatures

The thermocouples in the compartment and trolley are not subject to constant flow conditions and hence even though they are the same specification as the duct thermocouple there is no justification for using the system response lag calculated in Section 5.2.1.

5.2.3 System Response Lag for the Duct and Doorway Flow Rate

No discernible time lag was found in the response of the bi-directional probe. Figure 5-2 shows a typical normalised response of the duct thermocouple, oxygen calorimeter and the bi-directional probe to the square wave heat release of one of the calibration runs. The lags of the calorimeter and thermocouple can be clearly seen but there is no observable delay in the response on the bi-directional probe. This observation was consistent across all of the calibration runs. It will be assumed that the lag in the response of the bi-directional probe is negligible. It will similarly be assumed that the response of the identical bi-directional probes on the trolley also have negligible system response lag.

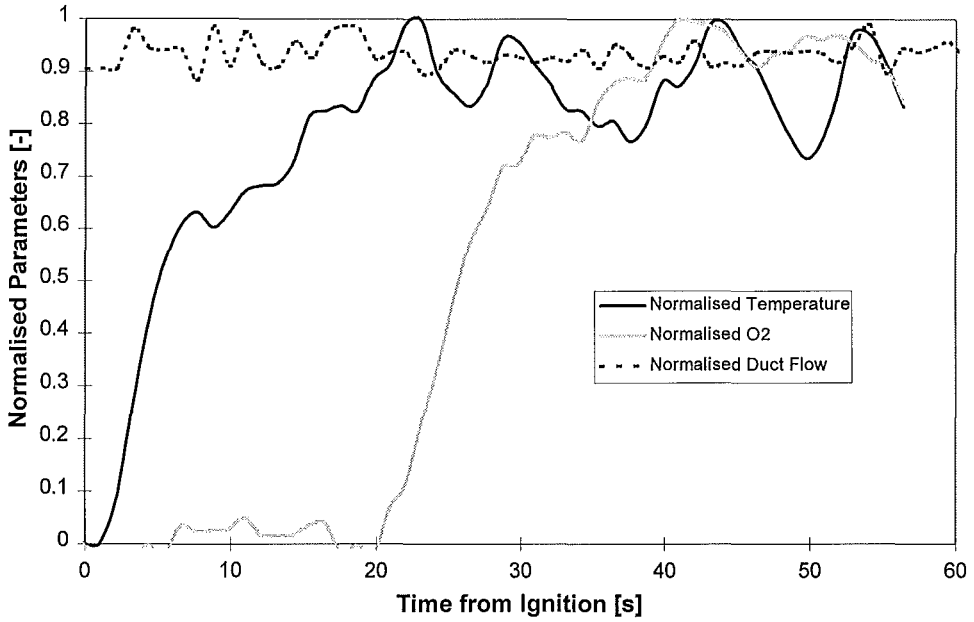

Figure 5-2: System Response Lag of Duct Bi-Directional Probe

5.2.4 System Response Lag of the Water Vapor Analyser

The system response time for the water vapor analyser is taken as the time taken for the analyser to reach 63% of its peak value. This is linearly interpolated from the times taken to reach 50% and 70% of the peak value. These times have had the transport lag component t_2 of 1.3 seconds subtracted from them. The results are summarised in Table 5-12.

Calibration Date/ Number	Wave#1 Lag Times [s]			Wave#2 Lag Times [s]			Wave#3 Lag Times [s]		
	50%	70%	**63%**	50%	70%	**63%**	50%	70%	**63%**
12/12/97	8.3	13.7	**11.8**	6.9	10.8	**9.4**	7.3	10.1	**9.1**
17/12/97 #1	7.9	10.8	**9.8**	7.7	8.8	**8.4**	7.9	12.8	**11.1**
17/12/97 #2	14.8	24.7	**21.2**	6.1	7.7	**7.1**	8.4	12.2	**10.9**

Table 5-12: System Response Lag of the Water Vapor Analyser

The data for the first wave of the 17/12/97 #2 run will be excluded for the reasons previously discussed in Section 5.1.3. Taking the average of the remaining points gives a mean value of 9.7 seconds and a standard deviation of 1.4 seconds. Within a confidence interval of 95% the mean is 9.7 ±0.9 seconds. However this time includes the transport lag time t_3 of 5.2 seconds. So the pure system response lag is $4.5 \approx 5$ seconds.

5.2.5 System Response Lag of the Oxygen Analyser

The sample line leading to the oxygen calorimeter is more than 7 metres long and contains filters, desiccant tubes, cold traps and flow meters. The effect of this is to introduce significant time lags into the system and distortion of the samples profile as compared with the measure at the sampling point. Given the measured output of the analyser the problem is to determine what the corresponding original input at the sampling point would have been.

Similar problems exist in the chemical industry with the characterisation of complex process control loops and reactor bed responses. The approach taken is to assume that the system is linear and therefore that its response behaviour to a particular input form, for example a step function, can be used to predict its response to any other form of input function. The measured response of the system to a known input function can be analysed and characteristic constants for the system obtained. Croce[55] presents three analysis methods; using an approximated differential equation form, using inversion integrals, or use of the Laplace Transform transfer function. Lyon and Abramowitz[57] present a similar analysis of the Laplace Transform approach.

Of these techniques Croce[55] reports that "the differential equation approach is the most straightforward and is well suited for numerical calculations", such as the use of a spreadsheet package. The following section presents the theory behind the differential equation approach.

5.2.5.1 Theory for the Differential Equation Approach

Let $x(t)$ be the input at the sampling port and $y(t)$ the recorded output of the analyser. For a unit step input, the corresponding output $y(t)$ is approximated by:

$$y(t) = \begin{cases} 0, \text{ for } t < t_L \\ 1 - \left[1 + \left(t - t_L\right)/t_c\right] \exp\left[-\left(t - t_L\right)/t_c\right], \text{ for } t \geq t_L \end{cases} \tag{44}$$

Define $t^* = t - t_L$ and substituting in to equation (44), we have:

$$y(t^*) = 1 - [1 + t^*/t_c]\exp[-t^*/t_c], \text{ for } t^* \geq 0 \quad (45)$$

This function satisfies the following differential equation:

$$t_c^2 \frac{d^2 y(t^*)}{dt^{*2}} + 2t_c \frac{dy(t^*)}{dt^*} + y(t^*) = 1, \text{ for } t^* \geq 0 \quad (46)$$

The right hand side of this equation represents the forcing function, in this case a unit step function. Assuming the system characteristics are independent of the form of the forcing function then the general form of equation (46) for a general forcing function $x(t^*)$ becomes:

$$t_c^2 \frac{d^2 y(t^*)}{dt^{*2}} + 2t_c \frac{dy(t^*)}{dt^*} + y(t^*) = x(t^*), \text{ for } t^* \geq 0 \quad (47)$$

Expressed in terms of real output time:

$$t_c^2 \frac{d^2 y(t)}{dt^2} + 2t_c \frac{dy(t)}{dt} + y(t) = x(t - t_L), \text{ for } t \geq t_L \quad (48)$$

Expressed in terms of real input time:

$$x(t) = t_c^2 \frac{d^2 y(t + t_L)}{dt^2} + 2t_c \frac{dy(t + t_L)}{dt} + y(t + t_L), \text{ for } t \geq 0 \quad (49)$$

Using this equation then given a known $x(t)$, for example a square wave, and a known time lag t_L, then the characteristic time constant t_c can be calculated.

For numerical calculations equation (49) can be formulated as:

$$X = t_c^2 \frac{Y|_{T+\Delta T} - 2Y|_T + Y|_{T-\Delta T}}{\Delta T^2} + t_c \frac{Y|_{T+\Delta T} - Y|_{T-\Delta T}}{\Delta T} + Y \quad (50)$$

5.2.5.2 Obtaining the Characteristic Time

Using equation (50) numerically in a spreadsheet corrected values of oxygen concentration can be calculated. The value of t_c to be used was obtained iteratively by increasing t_c until it just started to over predict the resulting oxygen concentration leading to cusps on the square wave. This is illustrated in Figure 5-3.

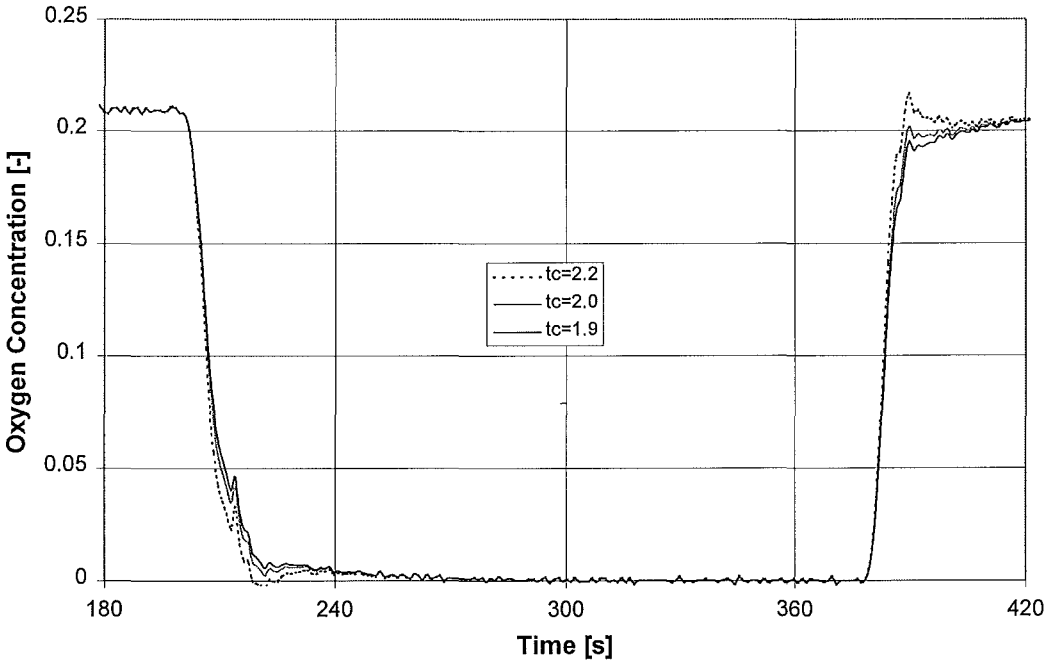

Figure 5-3: Normalised Oxygen Concentration Square Waves with Varying t_c

This technique gave the following t_c values, summarised in Table 5-13.

Calibration Date/Number	t_c [s]
1/12/97 #1	1.9
1/12/97 #2	1.9
1/12/97 #3	1.9
11/12/97 #1	2.2
11/12/97 #2	2.2

Table 5-13: Summary of t_c values

Taking a simple average of these gives a t_c value of 2.0 seconds.

5.2.6 Summary of System Response Lags

Measurement	System Response Lag [s]
Compartment Temperatures	0
Doorway Temperatures	0
Doorway Flow	0
Duct Temperature	4
Duct Flow	0
Water Vapor Concentration	5
Oxygen Concentration	2

Table 5-14: Summary of System Response Lags

5.3 Application of Time Lags to Heat Release Data

Figure 5-4 shows the application of the calculated time lags to the heat release data for a calibration run.

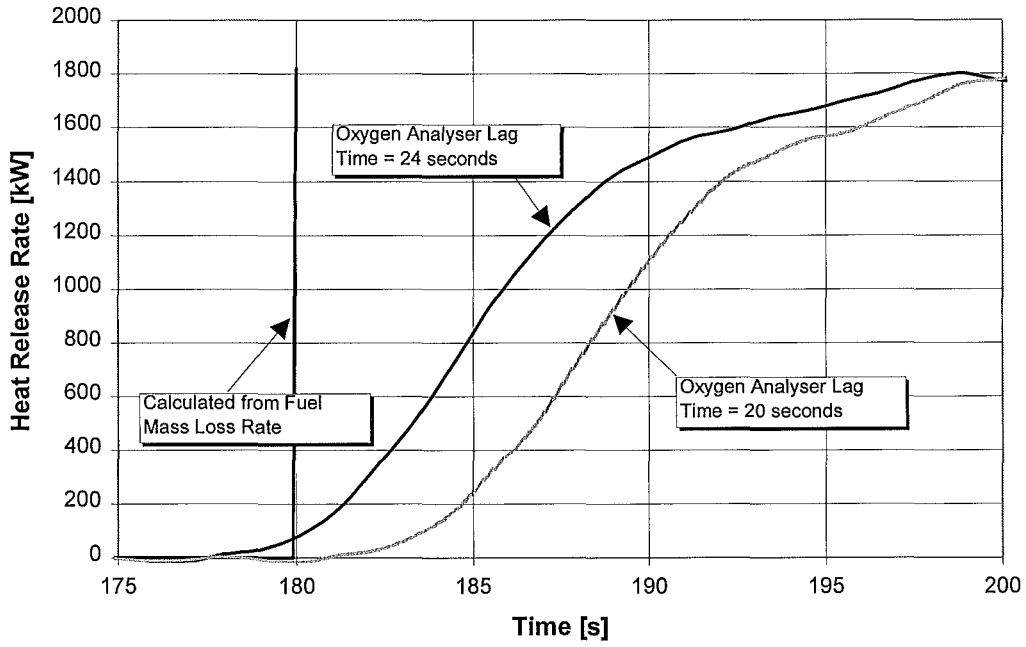

Figure 5-4: Comparison of Heat Release Rate Plots for Two Oxygen Analyser Lag Values

From examination of these plots for all of the calibration runs it was found that using the value of 20 seconds for the transport lag time of the oxygen analyser produced a better fit to the expected heat release rate than using the 24 second transport lag time. All other

transport and system response lags were as discussed above. The total lags, transport plus system response, are summarised in Table 5-15.

Measurement	Transport Lag [s]	Response Lag [s]	Total Lag [s]
Compartment Temperatures	0	0	0
Doorway Temperatures	0	0	0
Doorway Flow	0	0	0
Duct Temperature	2	4	6
Duct Flow	2	0	2
Water Vapor Concentration	8	5	13
Oxygen Concentration	20	2	20[†]

Table 5-15: Summary of Total Lags

[†] The system lag is included implicitly by the application of a correction using the method of Croce to the raw data.

6. CONSIDERATION OF WATER VAPOR

Measurement of water vapor was undertaken for two reasons. Firstly to give an understanding of the quantities of produced and how this varied throughout the fire and suppression process; secondly by using the known water concentration in calorimetry equations it was hoped to be able to improve the accuracy of the heat release rate measurements.

6.1 Introduction and Theory

Dlugogorski, Mawhinney and Duc[58] and Janssens[59] have produced general equations which allow the heat release rate to be calculated where significant (>7%) quantities of water exist in the exhaust gases. The equations developed require the measurement of the carbon dioxide and carbon monoxide in the exhaust gas. These values were not measured in the experiments and therefore assumptions have to be made about the values of these quantities.

The work of Janssens[59] assumes that all of the water vapor is due to chemical combustion or is in the combustion air flow. In contrast in the work of Dlugogorski et al[58] can include water added by suppression or evaporation.

The equations developed by Janssens are:

$$\dot{q} = \left[E\phi - \left(E_{CO} - E\right)\frac{1-\phi}{2}\frac{X_{CO}^{A^e}}{X_{O_2}^{A^e}} \right] \dot{m}_a \frac{M_{O_2}}{M_a}\left(1 - X_{H_2O}^{a}\right)X_{O_2}^{A^a} \tag{51a}$$

with

$$\phi = \frac{X_{O_2}^{A^a}\left(1 - X_{CO_2}^{A^e} - X_{CO}^{A^e}\right) - X_{O_2}^{A^e}\left(1 - X_{CO_2}^{A^a}\right)}{\left(1 - X_{O_2}^{A^e} - X_{CO_2}^{A^e} - X_{CO}^{A^a}\right)X_{O_2}^{A^a}} \tag{51b}$$

and

$$\frac{\dot{m}_a}{M_a} = \frac{\left(1-X^e_{H_2O}\right)\left(1-X^{A^e}_{O_2}-X^{A^e}_{CO_2}-X^{A^e}_{CO}\right)}{\left(1-X^a_{H_2O}\right)\left(1-X^{A^a}_{O_2}-X^{A^a}_{CO_2}\right)} \cdot \frac{\dot{m}_e}{18+4\left(1-X^e_{H_2O}\right)\left(X^{A^e}_{O_2}+4X^e_{CO_2}+2.5\right)} \quad (51c)$$

Tewarson[36] gives the stoichiometric formula for pine as $CH_{1.7}O_{0.83}$. If it is assumed that combustion is complete the reaction is:

$$CH_{1.7}O_{0.83} + 1.01\left(O_2 + 3.76N_2\right) \rightarrow CO_2 + 0.85H_2O + 3.80N_2 \quad (52)$$

The ratio of the production of CO_2 to H_2O is 1.18, i.e. for each mole of water vapor produced 1.18 moles of CO_2 are produced. Note that because water exists in the incoming air this has to be subtracted before the CO2 yield is calculated. This analysis neglects the effects of any water contribution from suppression or evaporation.

$$X^{A_e}_{CO_2} = 1.18\left(X^e_{H_2O} - X^a_{H_2O}\right) + X^{A^a}_{CO_2} \quad (53)$$

Similarly for the burner calibrations a mixture of butane and propane was used. The stoichiometric equation is:

$$0.8C_3H_8 + 0.2C_4H_{10} + 5.3\left(O_2 + 3.76N_2\right) \rightarrow 3.2CO_2 + 4.2H_2O + 19.93N_2 \quad (54)$$

The ratio of CO2 to H2O is 0.76, and the analogous equation to equation (53) is:

$$X^{A_e}_{CO_2} = 0.76\left(X^e_{H_2O} - X^a_{H_2O}\right) + X^{A^a}_{CO_2} \quad (55)$$

This equivalency or that in equation (53) can be used along with equations (51a) to (51c). If it is further assumed that the mass fraction of CO in the exhaust is zero then equations (51a) to (51c) can be simplified to:

$$\dot{q} = E\phi\dot{m}_a \frac{M_{O_2}}{M_a}\left(1-X^a_{H_2O}\right)X^{A^a}_{O_2} \quad (56a)$$

with

$$\phi = \frac{X_{O_2}^{A^a}\left(1 - X_{CO_2}^{A^e}\right) - X_{O_2}^{A^e}\left(1 - X_{CO_2}^{A^a}\right)}{\left(1 - X_{O_2}^{A^e} - X_{CO_2}^{A^e}\right)X_{O_2}^{A^a}} \tag{56b}$$

and

$$\frac{\dot{m}_a}{M_a} = \frac{\left(1 - X_{H_2O}^{e}\right)\left(1 - X_{O_2}^{A^e} - X_{CO_2}^{A^e}\right)}{\left(1 - X_{H_2O}^{a}\right)\left(1 - X_{O_2}^{A^a} - X_{CO_2}^{A^a}\right)} \cdot \frac{\dot{m}_e}{18 + 4\left(1 - X_{H_2O}^{e}\right)\left(X_{O_2}^{A^e} + 4.X_{CO_2}^{A^e} + 2.5\right)} \tag{56c}$$

The equations developed by Dlugogorski et al[58] are:

$$\dot{q} = \dot{n}_{total}^{e}\left(1 - X_{H_2O}^{e}\right)\left[0.5\left(E' - E'_{CO}\right)X_{CO}^{A^e} + E\left(X_{O_2}^{A^a}\frac{1 - X_{O_2}^{A^e} - X_{CO_2}^{A^e} - X_{CO}^{A^e}}{1 - X_{O_2}^{A^a} - X_{CO_2}^{A^a}} - X_{O_2}^{A^e}\right)\right] \tag{57a}$$

with

$$M_{total}^{e} = X_{H_2O}^{e}M_{H_2O} + \left(1 - X_{H_2O}^{e}\right)\left(X_{N_2}^{A^e}M_{N_2} + X_{O_2}^{A^e}M_{O_2} + X_{CO_2}^{A^e}M_{CO_2} + X_{CO}^{A^e}M_{CO}\right) \tag{57b}$$

As above carbon monoxide is assumed zero. The exhaust mass flow rate is known and the molar flow rate can be calculated from this knowing the total molecular weight. Equations (57a) and (57b) then reduce to:

$$\dot{q} = \frac{\dot{m}_e}{M_{total}^{e}}\left(1 - X_{H_2O}^{e}\right)E'\left(X_{O_2}^{A^a}\frac{1 - X_{O_2}^{A^e} - X_{CO_2}^{A^e}}{1 - X_{O_2}^{A^a} - X_{CO_2}^{A^a}} - X_{O_2}^{A^e}\right) \tag{58a}$$

$$M_{total}^{e} = X_{H_2O}^{e}M_{H_2O} + \left(1 - X_{H_2O}^{e}\right)\left(X_{N_2}^{A^e}M_{N_2} + X_{O_2}^{A^e}M_{O_2} + X_{CO_2}^{A^e}M_{CO_2}\right) \tag{58b}$$

These equations are used in conjunction with equation (53) or (55) which give the relationship between water vapor and carbon dioxide concentrations.

Comparison of the predictions of these equations with the burner calibration runs show good agreement. A typical result is shown in .

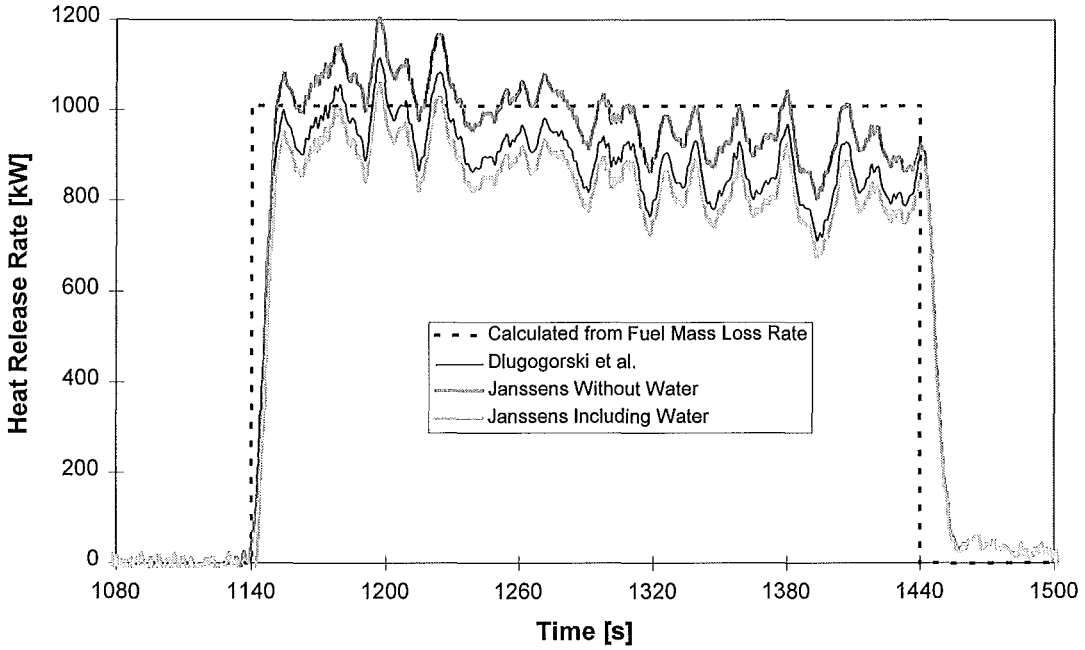

Figure 6-1: Comparison of Heat Release Rates

6.2 Results and Discussion

Figure 6-2 shows a typical water vapor concentration curve for one of the experimental

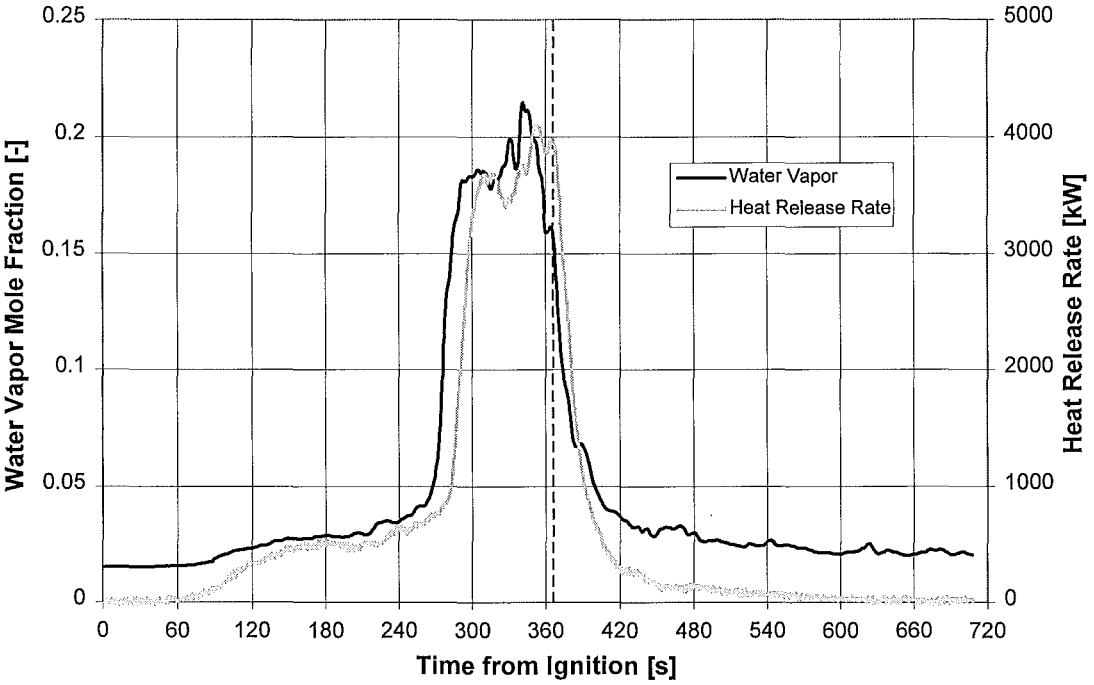

Figure 6-2: Water Vapor and Heat Release Rate Curves, CAFS, 12/12/97

runs. The water vapor profile is similar in form to the heat release rate curve. Peak water vapor concentrations were observed during flashover prior to suppression. Peak water vapor concentrations are summarised in Table 6-1.

Method	Date	Peak Water Vapor Concentration [-]
CAFS	27/11/97	0.14
CAFS	2/12/97	0.20
CAFS	12/12/97	0.21
HPD	27/11/97	0.11
HPD	2/12/97	0.17
HPD	12/12/97	0.21
Solution	27/11/97	0.12
Solution	2/12/97	0.11
Solution	12/12/97	0.21

Table 6-1: Peak Water Vapor Concentrations

Water vapor concentrations were relatively high. Dlugogorski et al regard concentrations >7% as having significant effects on the heat release rate. Suppression itself caused no clear increase in measured water vapor. There was a rapid rise in water release a few

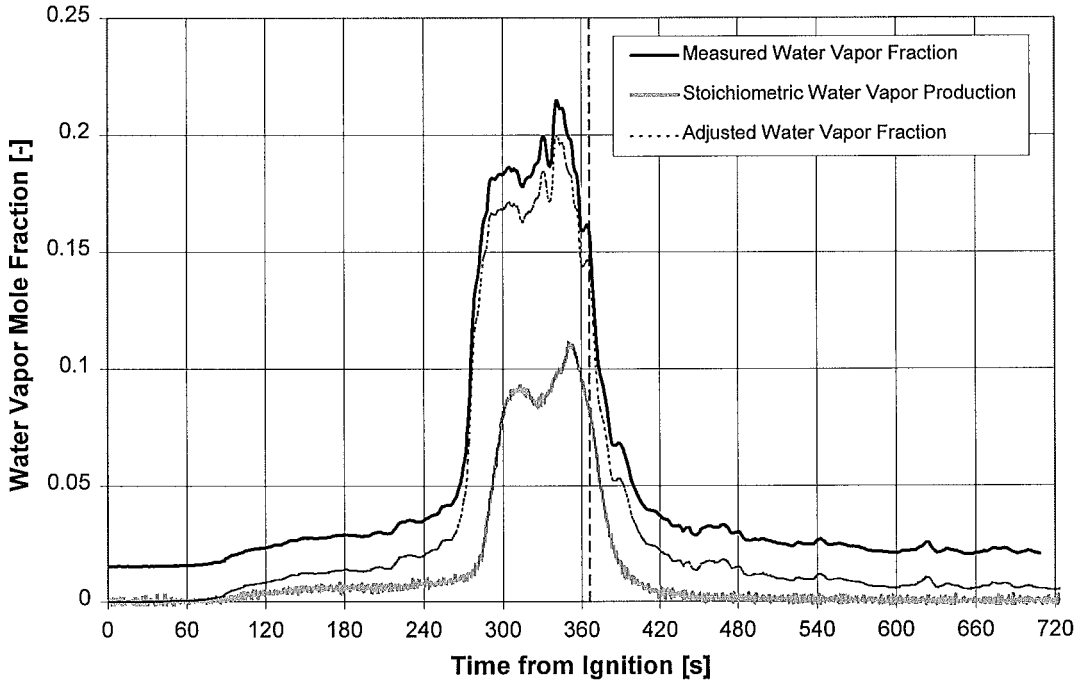

Figure 6-3: Water Vapor Profiles; Measured, Adjusted, and Stoichiometric

seconds prior to a similar rise in the heat release rate. This was observed on other experiments and it is suggested that this is due to water being driven out of the lining materials of the compartment.

Figure 6-3 compares the measured water vapor concentration, with a concentration corrected for ambient water concentration , and a stoichiometric water vapor concentration calculated from the consumed oxygen assuming stoichiometric reaction of the wood. This suggests that combustion water only accounts for a fraction of the observed water. It can be seen that the value of this fraction is not constant but varies throughout the fire. The largest difference between the stoichiometric water vapor and the measured occurs just before flashover.

The measured water vapor concentration is used to predict the CO_2 concentration using equation (53). This linkage between H_2O and CO_2 production assumes that the water produced is due entirely to combustion. The results suggest this is not the case. When the heat release rate is calculated using the equations Janssens or Dlugogorski et al negative heat release rates are obtained around the time just prior to flashover. This is occurring because the large observed water vapor concentration is predicting a large CO_2 concentration which causes a negative value of the oxygen depletion factor, ϕ . Figure 6-4 illustrates the heat release rate curves obtained using the approach of Janssens and

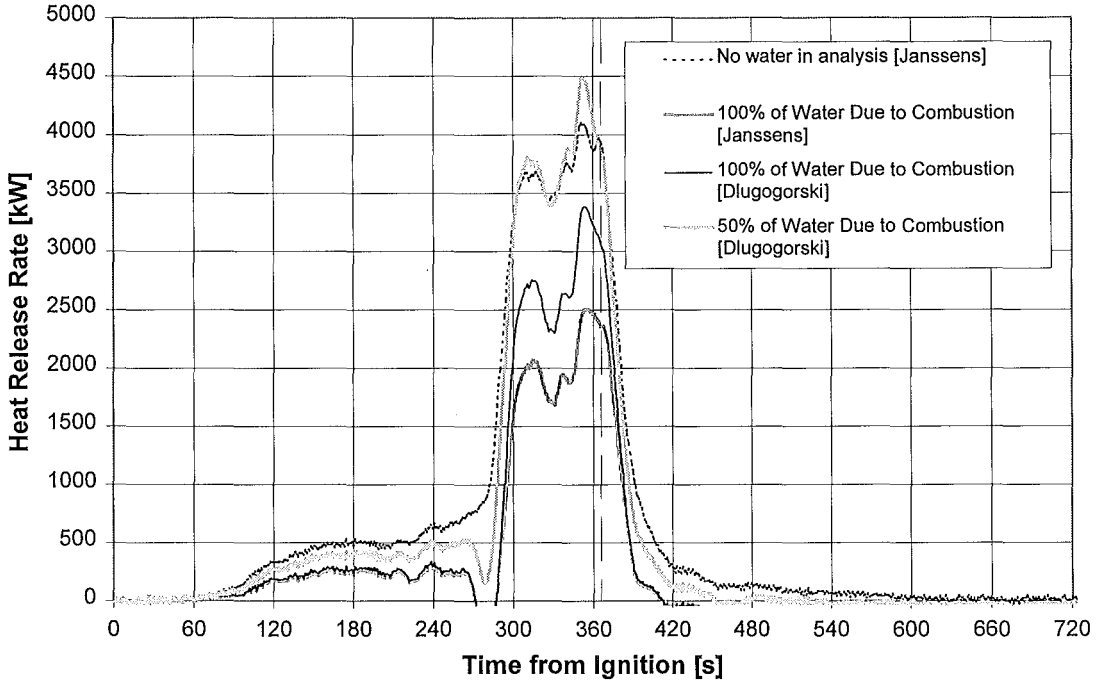

Figure 6-4: Comparison of Heat Release Rates

Dlugogorski et al. These curves are compared with the standard Janssens equation with no water vapor in the analysis.

Figure 6-3 suggests that approximately 50% of the water vapor observed may be due to combustion. Figure 6-4 shows the result using the method of Dlugogorski et al if only 50% of the water is assumed to be from combustion. This is achieved by amending equation (53) to:

$$X_{CO_2}^{A_e} = 0.6\left(X_{H_2O}^{e} - X_{H_2O}^{a}\right) + X_{CO_2}^{A^a} \qquad (59)$$

As would be expected the curve obtained is a closer fit to the standard Janssens curve which takes no account of water vapor. However since a fixed correction was used the curve under predicts in some parts and over predicts in others. Using the ratio of the stoichiometric water vapor fraction to the measured water vapor fraction would give a means of calculating a correction as a function of time. This was considered but it was felt that the uncertainties in the reaction stoichiometry and how this varied throughout the duration of the fire made the accuracy of any result obtained questionable.

6.3 Conclusions

Water vapor concentrations, at around 10% to 20%, are higher than the 7% regarded by Dlugogorski et al[58] as having a significant effect on the heat release rate.

Water vapor concentrations peak during flashover with no obvious increase with the application of water during suppression.

Measured water vapor concentrations are around twice those that would be obtained based upon stoichiometric combustion.

Use of a fixed relationship to predict the quantity of CO_2 based on the quantity of water present leads to unrealistic heat release rate curves.

6.4 Recommendations

1. The standard Janssens method, no water vapor present, for calculating heat release rate be used for the analysis of the heat release rate for the experimental work.
2. In future work a CO_2 /CO analyser should be used along with the water vapor analyser.

7. RESULTS

7.1 Weather

Strictly the weather is not a result of the experiments, rather it is contributing data. It is

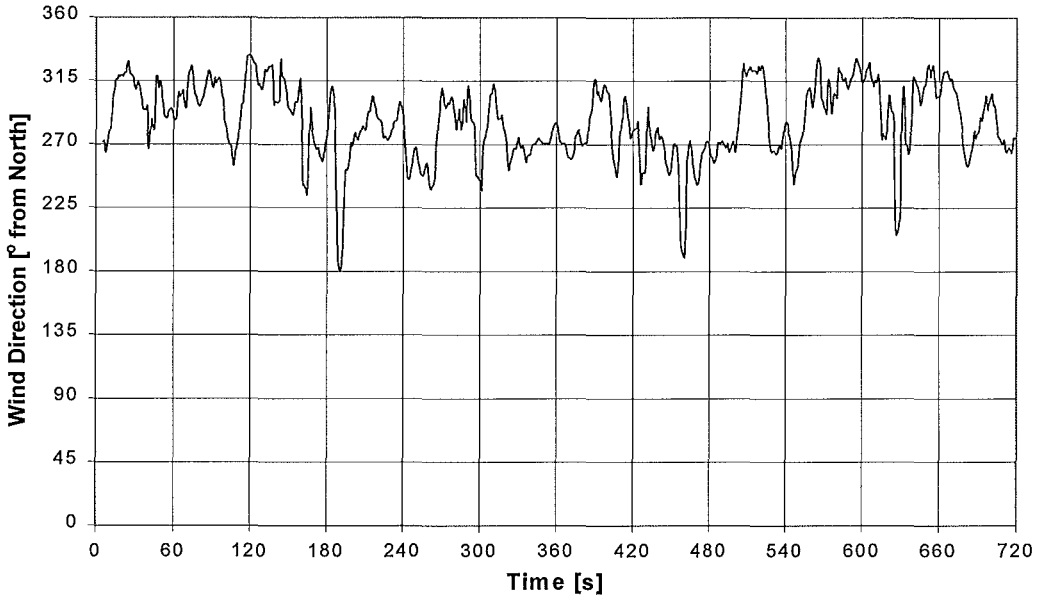

Figure 7-1: Wind Direction, Solution, 12/12/97

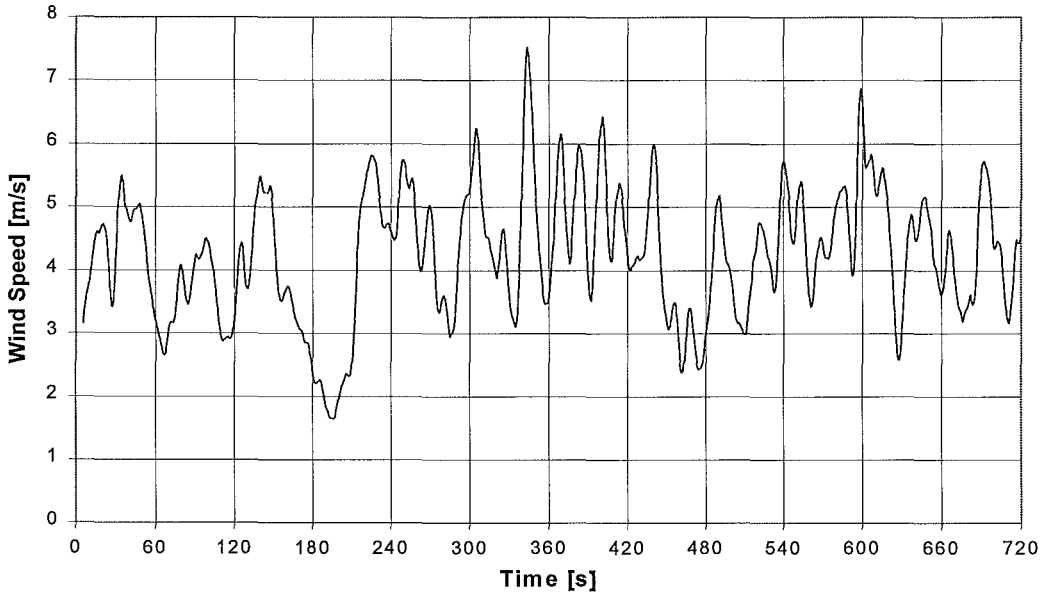

Figure 7-2: Wind Speed, Solution, 12/12/97

presented here to explain the weather measurements taken and the data obtained as these

are important for the interpretation and discussion of experimental results. Four pieces of weather data were collected; the temperature, the relative humidity, the wind speed, and the wind direction. The wind direction and wind speed were collected continuously using a weather station. Figure 7-1 and Figure 7-2 show an example plot of wind direction and wind speed.

Table 7-1 gives a summary of weather conditions for each of the runs. Descriptions of wind directions and wind speed are given as average values, and as qualitative descriptions based on the data.

Detailed weather data is given in Appendix 3.

Method	Date	Temperature [°C]	Relative Humidity [%]	Wind Speed [m/s]	Wind Direction [° from N]
CAFS	27/11/97	26	24	Mean 3.2 Gusting 2 to 5	Mean 280 Steady
CAFS	2/12/97	19	50	Mean 2.1 Gusting 1 to 4	Mean 120 Variable
CAFS	12/12/97	16	46	Mean 2.8 Gusting 1 to 4	Mean 70 Steady
HPD	27/11/97	25	33	Mean 2.2 Gusting 1 to 4	Mean 230 Highly Variable
HPD	2/12/97	19	39	Mean 3.0 Gusting 2 to 4	Mean 50 Steady
HPD	12/12/97	19	42	Mean 4.2 Gusting 2 to 7	Mean 100 Variable
Solution	27/11/97	27	24	Mean 3.3 Gusting 2 to 5	Mean 230 Highly Variable
Solution	2/12/97	19	50	Mean 4.2 Gusting 3 to 7	Mean 290 Variable
Solution	12/12/97	13	64	1.9 Gusting 1 to 4	140 Highly Variable

Table 7-1: Summary of Weather Conditions

7.2 Qualitative Results

During the experiments timings were made of key events and observations made of significant or unusual behaviour. Table 7-2 summarises the timings and observations. All timings are from the time of ignition and are in minutes and seconds.

Method	Date	Flames out of doorway	Floor Burning	Extinguishment Begins	Comments
CAFS	27/11/97	4:20	5:15	5:45	• Smoke loss from hood • Re-ignition of two cribs - light burning • Firefighter close in (<4 metres)
CAFS	2/12/97	4:00	5:15	5:45	• Little observed smoke loss • Re-ignition of one crib and MDF after 2 to 3 minutes
CAFS	12/12/97	4:40	5:35	6:05	• Little observed smoke loss • Re-ignition of two cribs - light burning
HPD	27/11/97	4:15	5:20	5:45	• Smoke loss from hood • Re-ignition of one crib - intense burning
HPD	2/12/97	4:45	5:00	5:50	• Smoke loss from hood • Re-ignition of one crib - intense burning
HPD	12/12/97	4:20	5:15	5:45	• Smoke loss from hood • Re-ignition of one crib - intense burning
Solution	27/11/97	4:00	4:55	5:20	• Smoke loss from hood • Re-ignition of one crib • Thermocouple shield fell down during extinguishment
Solution	2/12/97	4:00	4:35	5:10	• Smoke loss from hood • Re-ignition of rear cribs - intense burning • 12 second application
Solution	12/12/97	4:15	5:00	5:35	• Some slight smoke loss • No re-ignition

Table 7-2: Fire Event Timings and Observations

Certain general observations can be made that are common for all the fires. The fire intensity in the doorway seemed to peak when the paper on the floor was burning. This lasted for around 10 or 15 seconds. The fire then appeared to die back and the front crib, previously obscured by flames in the doorway, became visible again.

Visibility in the fire compartment during extinguishment was much better using CAFS than with the HPD based methods. This observation is supported by the comments of the firefighter (pers. comm. M.Elston).

On some of experiments where CAFS was used there was an observation of flames coming out of the compartment when the CAFS was first applied.
The firefighter was impressed by the ability of CAFS to knockdown the fire and overall rated it as good as if not better than HPD. The pump operator had no significant problems with any of the methods.

7.3 Foam Quality Results

Foam quality measurements were taken for the compressed air foam and the class A solution before each of the experimental runs. The results are summarised in Table 7-3.

Foam Type	Date	Expansion Ratio [l/kg]	25% Drainage Time [s]
CAFS	27/11	4.9	79
CAFS	2/12	5.8	144
CAFS	12/12	4.0	84
Average		**4.9**	**102**
Standard Deviation		0.7	29
Solution	27/11	2.1	34
Solution	2/12	2.0	33
Solution	12/12	1.9	33
Average		**2.0**	**33**
Standard Deviation		0.08	0.5

Table 7-3: Summary of Foam Quality Results

7.4 Suppressant Flow Rates and Volumes

Suppressant flows were measured at the time of 'knock down' and after any subsequent 'mopping up' of re-ignition or hot spots. Flow rate for all experiments was approximately 170 litres/minute, apart from the HPD experiment on 27/11/97 where the flow was 140 litres/minute. Results are summarised in Table 7-4.

Method	Date	Application Period [s]	Total for Knock Down [Litres]	Total for Complete Extinguishment [Litres]
CAFS	27/11/97	10	26	196
CAFS	2/12/97	10	23	76
CAFS	12/12/97	10	25	125
HPD	27/11/97	10	23	272
HPD	2/12/97	10	30	150
HPD	12/12/97	10	28	199
Solution	27/11/97	10	33	108
Solution	2/12/97	12	27	143
Solution	12/12/97	10	30	123

Table 7-4: Suppressant Flows

The means and the 95% probability bounds for each of the methods is summarised in Table 7-5.

Method	Knock Down Flow [Litres]	Extinguishment Flow [Litres]
CAFS	24 ±2	130 ±60
HPD	27 ±3	210 ±60
Solution	30 ±3	125 ±15

Table 7-5: Means and 95% Confidence Intervals for Knock Down and Extinguishment Flows

7.5 Crib Moisture Contents

Average crib moisture contents measured immediately before each experiment are summarised in Table 7-6.

Method	Date	Moisture Content [% dry weight]
CAFS	27/11/97	12.5
CAFS	2/12/97	11.0
CAFS	12/12/97	10.5
HPD	27/11/97	12.0
HPD	2/12/97	11.0
HPD	12/12/97	10.5
Solution	27/11/97	11.5
Solution	2/12/97	11.5
Solution	12/12/97	10.0

Table 7-6: Crib Moisture Content

7.6 Crib Temperature Results

Thermocouples were positioned in the centre of each of the cribs. Figure 7-3 shows a typical temperature profile for the cribs. The temperature spike at around 480 seconds for the front crib corresponded to an observed re-ignition of the front crib. Temperature spikes of this general type were observed on other temperature plots were crib re-ignition occurred.

The vertical dashed line indicates the time of suppression. The fall off in temperatures of the rear cribs prior to suppression, particularly the rear corner crib, was observed in all of the experiments. Temperature reduction due to suppression was noticeable for the front crib. No temperature reduction was observed for the other cribs apart from the rear centre

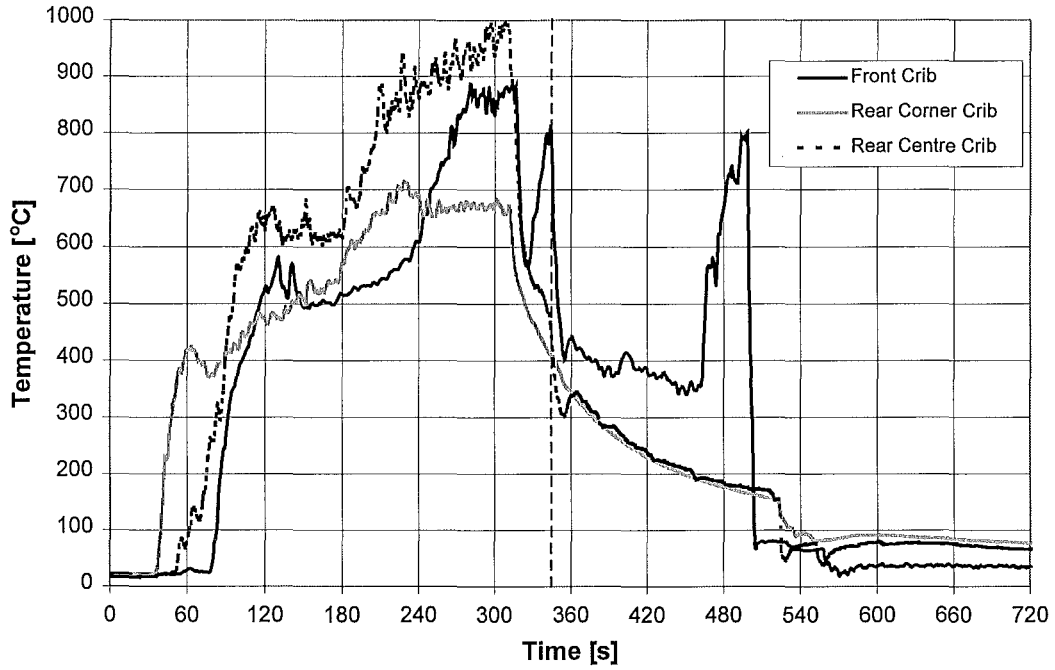

Figure 7-3: Crib Temperature Profiles

crib for the CAFS runs on 27/11/97 and 2/12/97.

Table 7-7 shows a summary of the peak recorded temperature, T_{peak}, and number of clear re-ignitions, N_{re-ign} for each crib in each run. For more detailed results see Appendix 4.

Method	Date	Front Crib		Rear Corner Crib		Rear Centre Crib	
		T_{peak} [°C]	N_{re-ign}	T_{peak} [°C]	N_{re-ign}	T_{peak} [°C]	N_{re-ign}
HPD	27/11/97	920	0	860	1	890	1
HPD	2/12/97	840	0	840	0	670	0
HPD	12/12/97	970	1	920	0	880	0
CAFS	27/11/97	930	2	580	0	780	0
CAFS	2/12/97	890	2	720	0	990	0
CAFS	12/12/97	930	2	900	0	780	0
Solution	27/11/97	670	1	890	0	350	0
Solution	2/12/97	800	0	760	0	720	0
Solution	12/12/97	940	2	900	0	840	0

Table 7-7: Crib Peak Temperatures and Re-Ignitions

7.7 Room Temperature Results

Room temperatures were measured using a fixed array of thermocouples located close to the front of the compartment and a single thermocouple located in the rear of the compartment. Room temperature results are split into three sets depending on the heights of the thermocouples in the compartment; top thermocouples, middle thermocouples, and bottom thermocouples. Typical temperature results from each region of the compartment are given in Figure 7-4, Figure 7-5, and Figure 7-6.

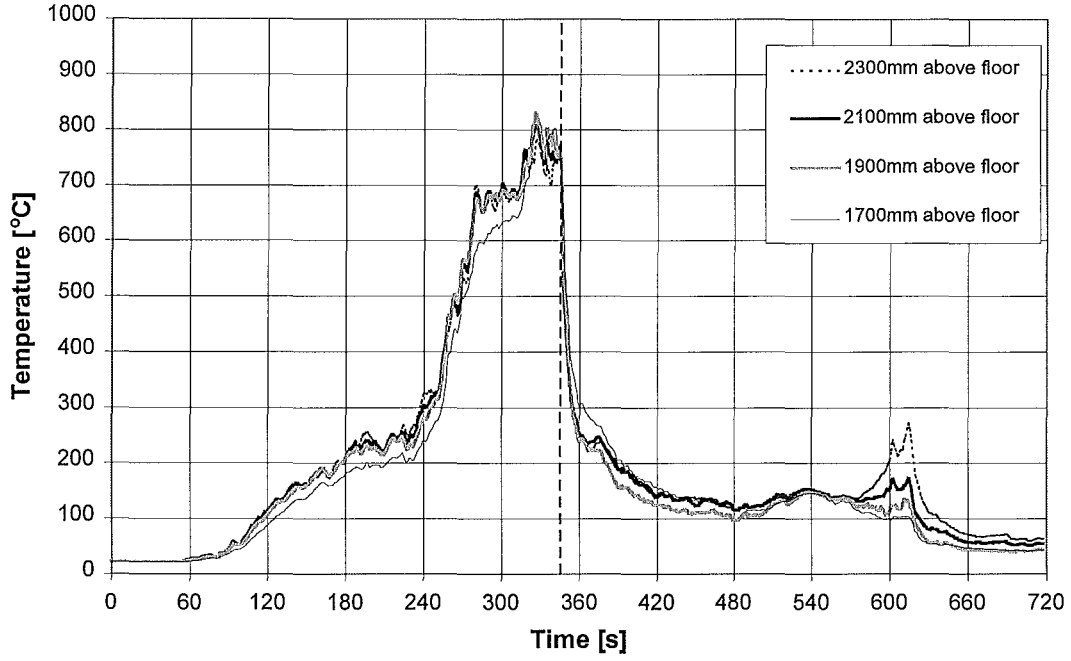

Figure 7-4: Top Thermocouple Temperatures, CAFS 27/11/97

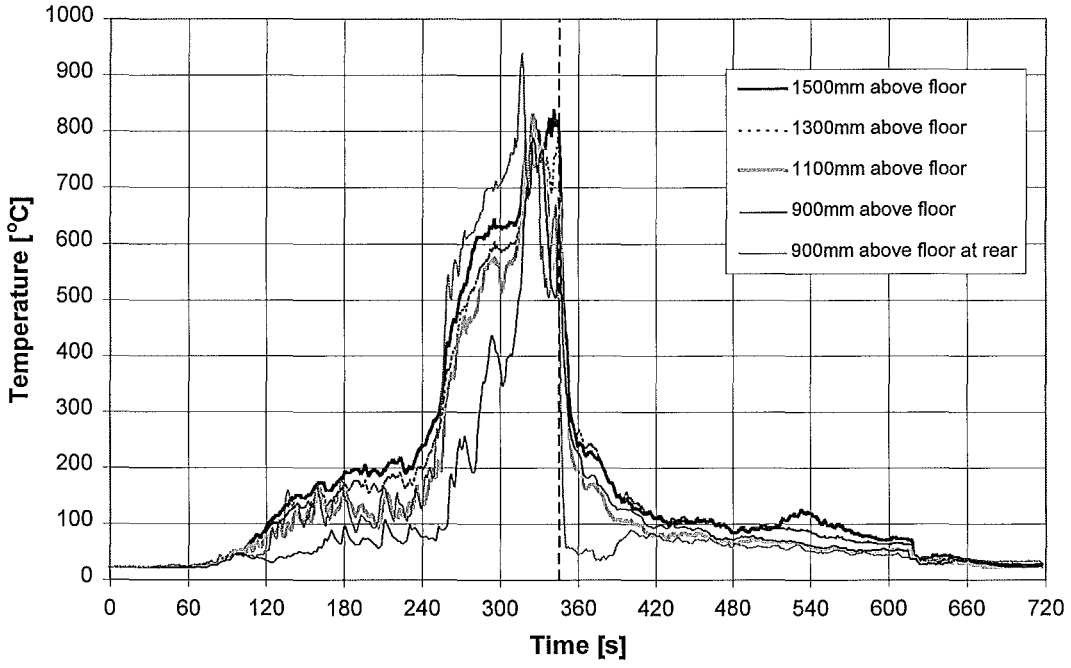

Figure 7-5: Middle Thermocouple Temperatures, CAFS 27/11/97

The vertical dashed line indicates the time of suppression. Peak temperatures in the upper third of the compartment were observed to range between 750°C and 820°C. In some runs

higher temperatures than this were observed by the rear thermocouple which was at a height of 0.9 metres above the compartment floor.

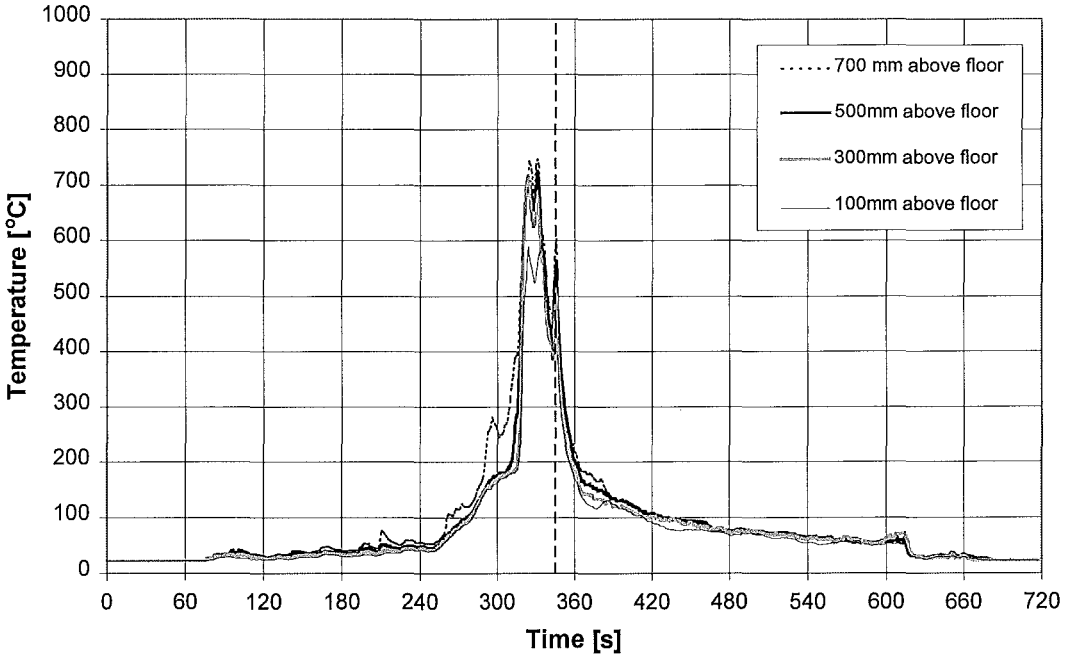

Figure 7-6: Bottom Thermocouple Temperatures, CAFS 27/11/97

Temperatures initially rose most rapidly in the upper part of the compartment, but as the fire develops temperatures in the middle part of the compartment also rise. Temperatures in the bottom part of the compartment are the slowest to rise.

In several of the runs the temperatures on some of the thermocouples dropped suddenly to 100°C during suppression.

Table 7-8 summarises the time taken for the temperature conditions to become untenable after ignition and the time to become tenable again after suppression of the fire. Times are measured relative to ignition in the former case and relative to the start of suppression in the latter case.

Method	Date	T>80°C at 1.5 m		Layer Temperature >200°C	
		Onset Time [s]	Recovery Time [s]	Onset Time [s]	Recovery Time [s]
HPD	27/11	117	184	200	80
HPD	2/12	145	233	189	56
HPD	12/12	97	174	150	96
Average		**120**	**197**	**180**	**77**
95% Confidence		**120 ±19**	**197 ±25**	**180 ±20**	**77 ±15**
CAFS	27/11	117	234	173	49
CAFS	2/12	126	341	183	177
CAFS	12/12	97	320	167	102
Average		**113**	**298**	**174**	**109**
95% Confidence		**113 ±11**	**298 ±43**	**174 ±7**	**89 ±49**
Solution	27/11	113	218	205	97
Solution	2/12	125	170	174	57
Solution	12/12	103	231	152	112
Average		**114**	**206**	**177**	**89**
95% Confidence		**114 ±9**	**206 ±25**	**177 ±21**	**89 ±22**

Table 7-8: Summary of Tenability Times (front thermocouples)

A further measure of temperature reduction is the time taken for the temperature of the rear thermocouple and the duct thermocouple to fall. Table 7-9 summarises the results, times are expressed as the time since the start of suppression.

Method	Date	T<80°C at Rear Thermocouple [s]	T<80°C in Duct [s]
HPD	27/11	N/A[†]	40
HPD	2/12	92	54
HPD	12/12	111	66
Average		**101**	**53**
95% Confidence		**101 ±11**	**53 ±10**
CAFS	27/11	75	48
CAFS	2/12	160	62
CAFS	12/12	107	70
Average		**114**	**60**
95% Confidence		**114 ±33**	**60 ±9**
Solution	27/11	202	56
Solution	2/12	120	51
Solution	12/12	104	17
Average		**142**	**41**
95% Confidence		**142 ±41**	**41 ±16**

Table 7-9: Temperature Reduction Times Measured at the Rear Thermocouple and in the Duct

Detailed Results for compartment temperatures are given in Appendix 4.

[†] Not measurable due to re-ignition of a crib.

7.8 Doorway Temperature Profile

The doorway temperature profile was measured using the array of eight thermocouples mounted on the trolley. Figure 7-7 shows a typical temperature profile in the doorway. For clarity only results from four of the thermocouples are shown. The drop off in temperature after 300 seconds is due to the trolley being pulled away from the doorway prior to the start of suppression. This is decline in temperature is a common feature of all of the doorway temperature results.

Peak temperatures were observed in the range 750°C to 900°C, these being measured in the top 0.375 metres of the doorway. Temperatures at a height of 0.5 metres above the compartment floor ranged from 100°C to 250°C.

Detailed results for doorway temperatures are given in Appendix 5.

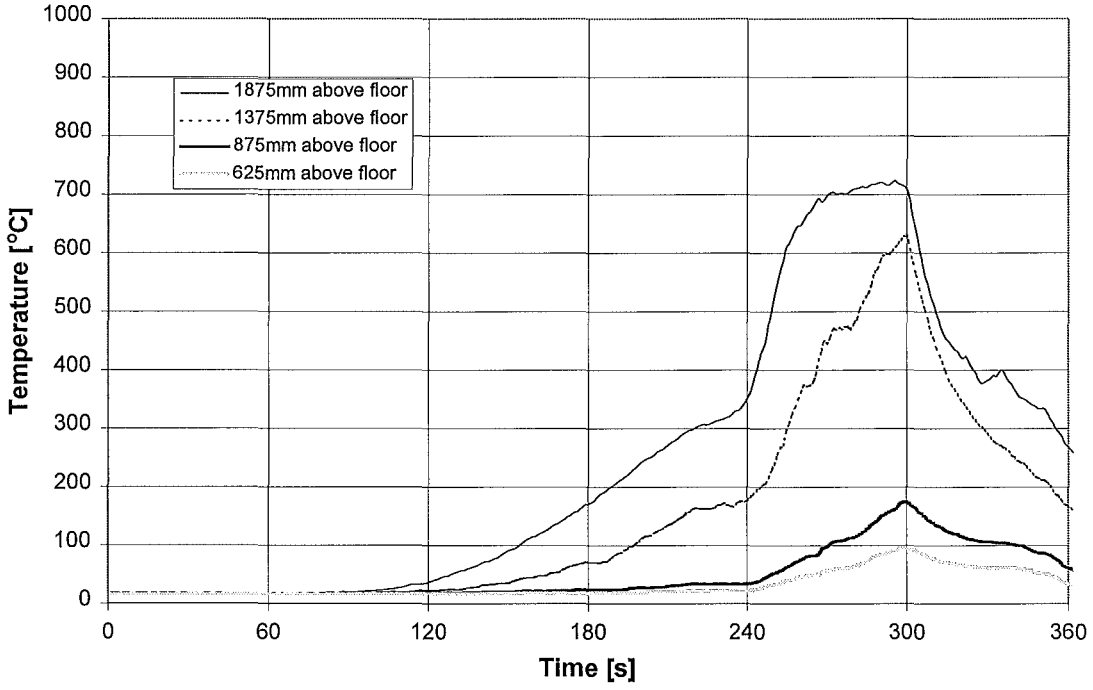

Figure 7-7: Doorway Temperature Profile, HPD 2/12/97

7.9 Doorway Mass Flow

The doorway velocity profile was measured using the array of bi-directional probes mounted on the trolley. Together with the temperature data this allowed the mass flow into

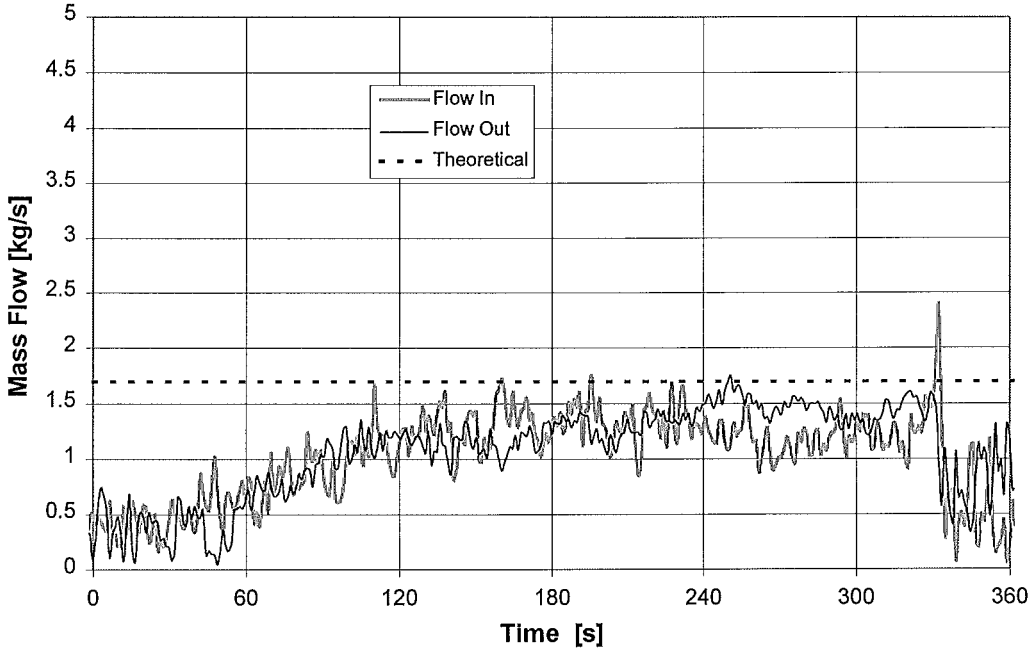

Figure 7-8: Mass Flow Into and Out Of the Compartment, HPD 12/12/97

and out of the compartment to be calculated. Figure 7-8 shows a plot for the mass flows. The dashed horizontal line is the theoretical mass flow given by $0.5A\sqrt{H}$ [equation (25), Section 2.4]. The figure is typical of the measurements taken on the days with calm weather. On windier days mass flow measurements were erratic as shown in Figure 7-9.

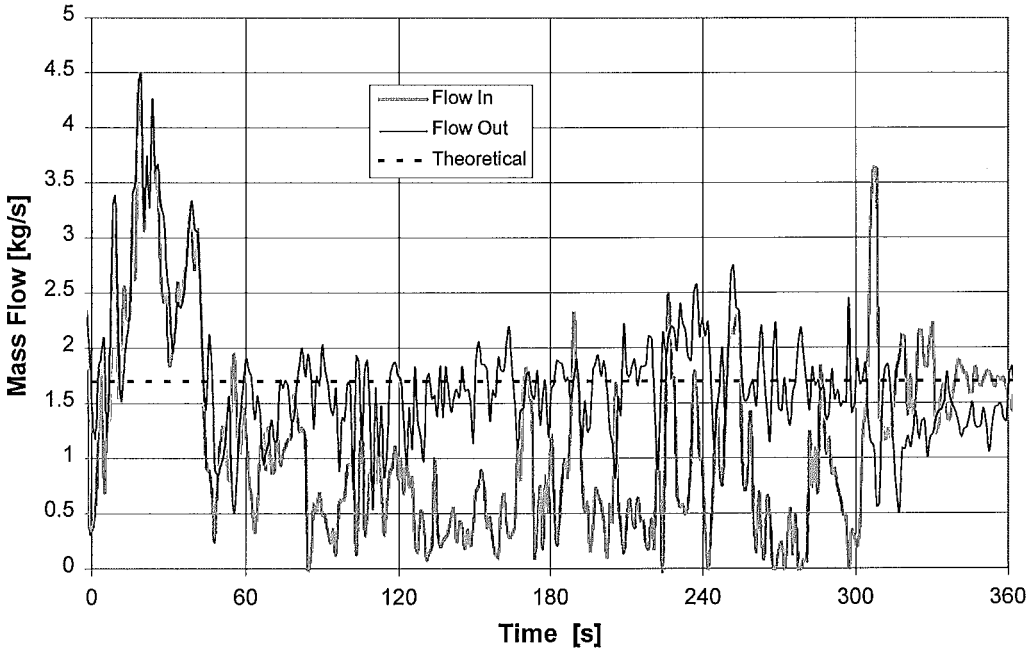

Figure 7-9: Mass Flow Into and Out Of the Compartment, Solution 27/11/97

Detailed results for the doorway mass flows are given in Appendix 6.

7.10 Heat Release Rates

Heat release rates were obtained for each experiment. Figure 7-10 shows an example result. The dashed line indicates the start of suppression. The form of this curve is typical of the other results. Peak heat release rates ranged from 2900 kW to 4600 kW and are summarised in Table 7-10. Detailed results are given in Appendix 7.

Method	Date	Peak Heat Release [kW]
HPD	27/11/97	3000
HPD	2/12/97	3900
HPD	12/12/97	4600
CAFS	27/11/97	3200
CAFS	2/12/97	4400
CAFS	12/12/97	4100
Solution	27/11/97	3000
Solution	2/12/97	2900
Solution	12/12/97	4100

Table 7-10: Summary of Peak Heat Release Rates

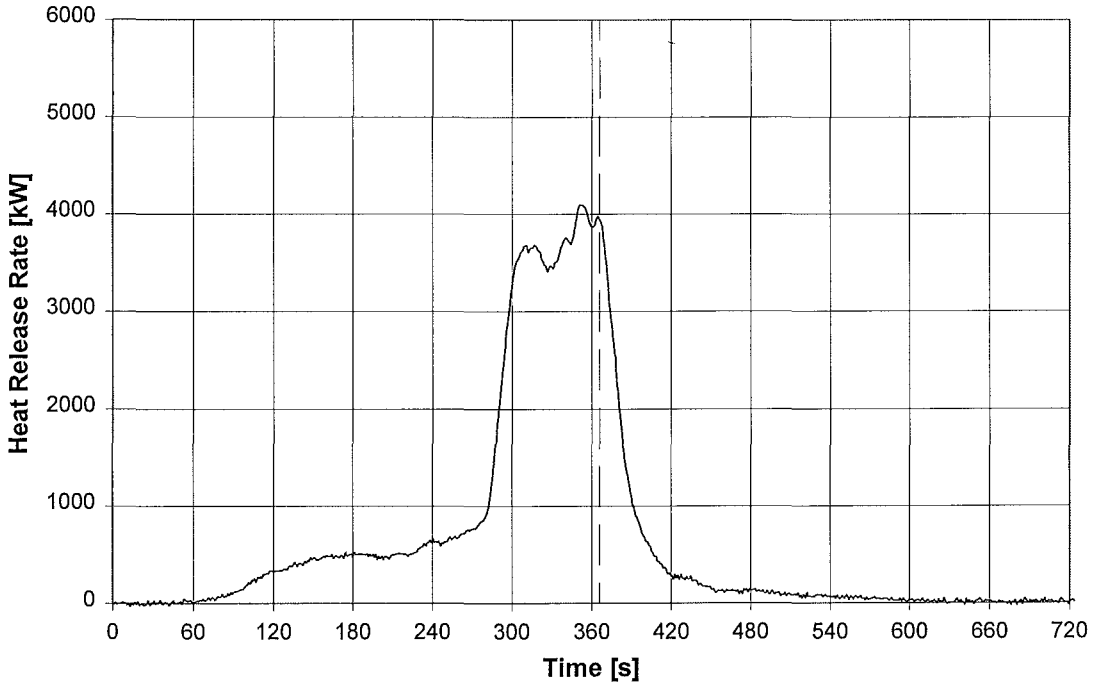

Figure 7-10: Heat Release Rate, CAFS, 12/12/97

A further burn was carried on 17/12/97 to test the effectiveness of a fixed water mist system. The results from this are outside of the scope of this report but the heat release curve (Figure 7-11) is of interest as it was allowed to burn for some time beyond the

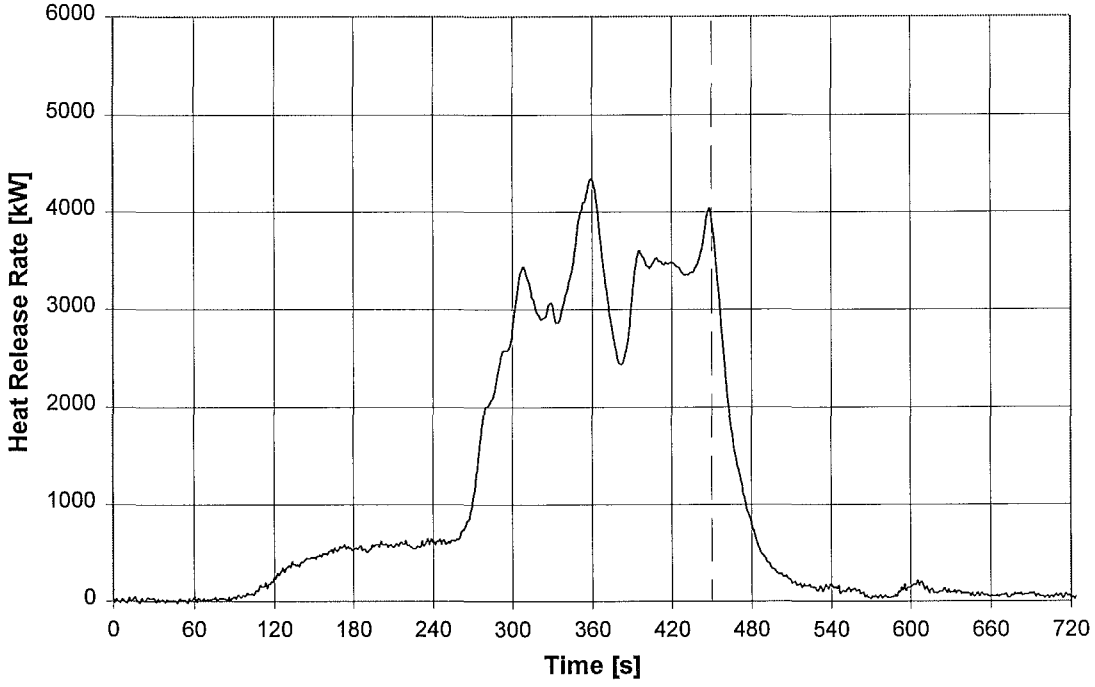

Figure 7-11: Heat Release Rate, Water Mist, 17/12/97

normal suppression time in these experiments and hence gives an indication of the un-suppressed burning behaviour in the compartment.

7.11 Fire Suppression

The suppression of the fire is quantified in several ways. Time taken to reduce the temperature has been presented in Section 7.7. Another measure is the time taken to reduce the heat release rate to a percentage of its pre-suppression value or to a fixed value. Table 7-11 presents data for each approach, percentage reduction and reduction to 500 kW.

Method	Date	Time from Suppression to Reduce Heat Release [s]						
		80%	60%	40%	30%	20%	10%	500 kW
HPD	27/11	6	10	15	19	26	38	28
HPD	2/12	5	8	12	17	24	39	34
HPD	12/12	5	7	15	22	30	46	44
Average		**6**	**8**	**14**	**19**	**27**	**41**	**35**
CAFS	27/11	10	14	20	24	30	41	35
CAFS	2/12	7	11	16	20	25	39	34
CAFS	12/12	7	13	18	23	31	47	41
Average		**8**	**13**	**18**	**22**	**29**	**42**	**37**
Solution	27/11	7	12	17	23	31	46	34
Solution	2/12	5	8	14	17	23	37	22
Solution	12/12	5	9	15	20	29	42	38
Average		**6**	**10**	**15**	**20**	**28**	**42**	**31**

Table 7-11: Suppression Times

8. Discussion

Discussion of equipment calibration and data reduction is found in Chapters 4 and 5.

8.1 Foam Quality

Foam quality was relatively consistent for the class A solution sprayed through the high pressure delivery. Expansion ratios of around 1:2 were typical with the foam type qualitatively described as a wet foam. This compares closely with the expansion ratios used in the National Class A Foam project[22] which were just over 1:2 apart from one run with a higher value of 1:2.85. Drainage times ranged from 33 to 34 seconds and were relatively rapid compared to those for the foam produced by the CAFS unit. These drainage times were more rapid than those measured by the National Class A Foam project[22] which had drainage times of around one minute. The differences in measured drainage times could be due to the different measurement technique for drainage times used in this research, namely UL162, or they could be due to the different nozzle type, or the nature or proportion of the class A concentrate.

Expansion ratios for the CAFS foam ranged from 1:4.0 to 1:5.8 and the foam was visibly drier and stiffer than the foam produced by spraying the class A solution. The range of expansion ratios was lower than the range used in the National Class A Foam project[22] which ranged from 1:5.6 to 1:7.3. Kim and Dlugogorski[13] used expansion ratios ranging from 1:4 to 1:10. Drainage times for the CAFS foam ranged from 79 to 144 seconds. This compares with the reported values from the National Class A Foam project[22] which ranged from 110 to 171 seconds. The differences observed could be for the same reasons as discussed above for the sprayed class A solution.

Care was taken to loft the foam as gently as possible onto the collecting plate. However it was observed that wind conditions did effect the ease with which the foam could be lofted. It is believed that this accounts for some of the variation observed in the characteristics of the compressed air foam. The sprayed class A solution was applied from a short distance away from the collection plate and so no significant wind effect was observed.

Expansion ratios measured for the foam produced by the CAFS unit were lower than the values reported by the manufacturer (D. Heath, pers. comm.), and a 20% increase in the expansion ratio was observed when the flow rate was reduced to 150 litres/minute. Note that this flow was not used for any experimental runs. A more significant factor was the presence of the nozzle, when this was removed and the foam was produced through an open line the expansion ratio increased by 120%. Care needs to be taken in interpreting these results as they are based on a single measurement.

Kim and Dlugogorski[13] measured the effect of CAFS foam expansion ratio on the effectiveness of suppression. Figure 7-3 presents their findings for the case of a single CAFS nozzle suppressing a wood crib fire.

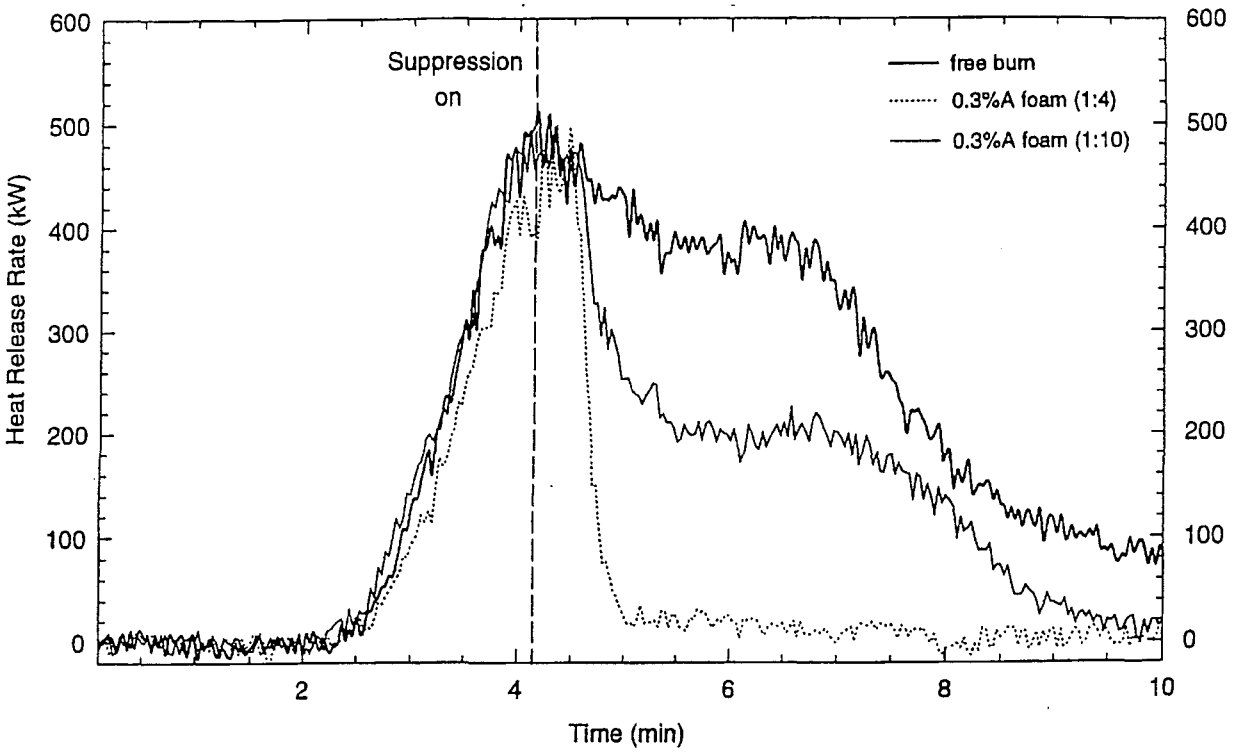

Figure 8-1: Effect of Expansion Ratio on Suppression of a Wood Crib Fire (Taken from Dlugogorski and Kim[13])

Dlugogorski and Kim commented on the effect of expansion ratio "... at the expansion ratio of 1:10, the foam performed less effectively in extinguishing the fire. The foam reduced the fire size, but required more than 5 min[utes] for complete extinguishment. This foam is more viscous than the less expanded foam and, as a result, has a higher resistance

to flow across the solid surface of the fuel. It also contains less water in thin films to drain effectively into the [burning] core of the wood crib."

Although these findings are of interest, care must be taken in their interpretation in the context of operational firefighting. The CAFS was discharged through a fixed nozzle directly above the crib, and the flows used were low, of the order of 1 litre/minute, applied to the top surface of the crib.

8.2 Crib Temperatures

The development of the crib temperatures show considerable variation in the precise form of the temperature-time curves but there were several phenomena which were commonly observed, as described below.

Temperatures in the cribs, particularly the rear corner crib declined as the fire increased in intensity. This is illustrated in Figure 8-2.

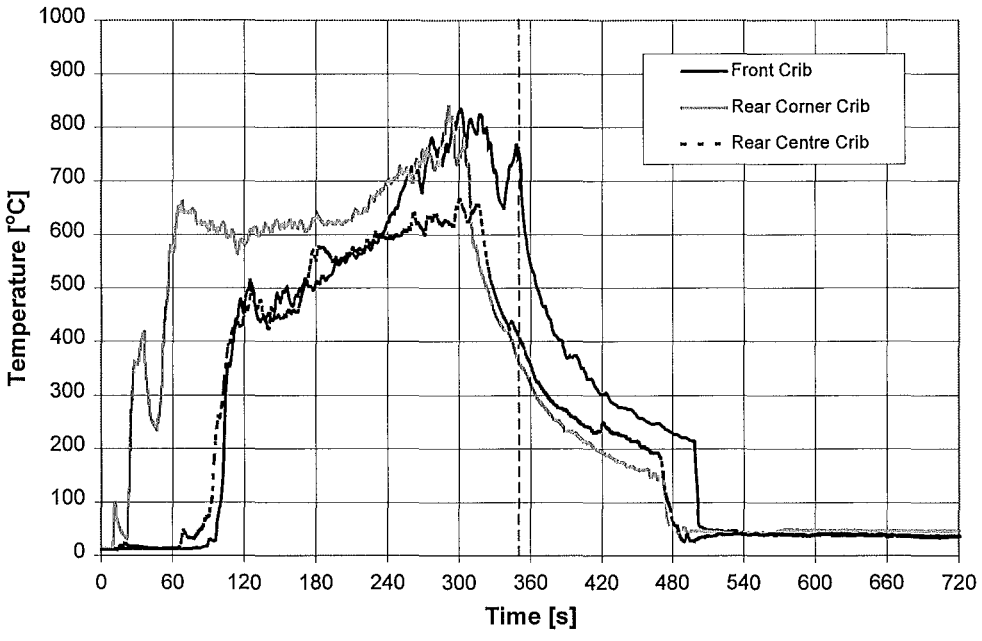

Figure 8-2: Crib Time Temperature Curves

The dashed vertical line indicates the start of extinguishment so it can be seen that the temperature decline in the rear cribs occurs some considerable time before extinguishment. It is believed that this phenomena is due to decreased burning in the crib core due to

oxygen starvation. As the fire develops and approaches flashover, oxygen was consumed further forward in the compartment with large scale burning of the MDF sheets and the paper lining of the gypsum board. The oxygen starvation of the rear cribs was accentuated by the partition which restricted the air flow into the rear of the compartment. This hypothesis is supported by the timing of this crib temperature drop which in all cases is aligned with the period of rapid heat release rate growth.

The application of the suppressant onto the fire caused some immediate reduction in the temperature of the front crib. Reduction in the temperature of the rear cribs was only observed in two of the runs, both of which were using CAFS, where there was some reduction in the temperature of the rear centre crib. The CAFS stream has a much higher momentum than the mist produced by the HPD and this may have allowed the penetration of suppressant to the rear of the compartment and into the core of the crib.

The crib thermocouples also indicated re-ignition of the cribs. The re-ignition of the front crib occurred most commonly and seemed to be a particular problem with the use of CAFS although it did occur with the other suppressants. The time temperature curves indicate that in the cases where re-ignition of the front crib occurred the core crib temperature was not reduced below 400°C, and re-ignition occurred within 2 or 3 minutes.

8.3 Compartment Temperatures

Temperatures in the upper third of the compartment rose steadily for 60 seconds after ignition. At this time ignition of the diesel in the trays under the cribs was complete but burning of the cribs themselves was minimal. Temperatures in the upper layer started to rise rapidly between 180 and 270 seconds after ignition. The most rapid onset was observed when there was a steady wind blowing into the compartment and this may have had some effect on the development of the fire. During this rapid temperature rise phase the temperature generally was observed to rise from around 300°C to 500°C in a matter of a few seconds. Temperatures measured by the four thermocouples in the upper third of the room were relatively close to each other both before and after the rapid temperature rise. Peak temperatures in the upper third of the compartment ranged from 750°C to 820°C, this temperature being recorded in the upper part of the room. This temperature was above the

accepted[44] temperature indicating flashover which was consistent with the observed fire behaviour at this time of rapid flame growth and flaming out of the compartment doorway.

Temperatures in the middle third of the compartment also followed a similar pattern, rising steadily and then rapidly with the approach to flashover. Temperatures after flashover were similar to those seen in the upper third of the room. The thermocouple 900mm above the floor at the rear of the compartment recorded peak temperatures around 900°C on several of the runs which was significantly (100°C) higher than the temperature recorded by the thermocouple at the same height in the front of the compartment . As this thermocouple was not shielded by gypsum board and was close to the fuel packages it is possible that the higher temperature was as a result of direct impingement of flame.

Temperatures in the lower third of the room were slow to rise with typical values of 50°C when temperatures higher in the compartment were around 300°C. This is consistent with this part of the compartment forming the "cold layer". Temperatures in this part of the compartment do not exhibit a rapid rise until some 60 seconds after the temperatures in the upper part of the room have risen. The peak temperatures in this part of the compartment were also slightly lower, ranging from 650°C to 820°C.

The peak temperatures observed were lower than those reported by the National Class A Foam project[22] which ranged from 750°C to 1020°C. This work differed from ours in that synthetic fuels such as polyether foam were included in the fuel load.

Tenability within the compartment in terms of temperature is assessed according to two criteria[42,46]; the upper layer temperature exceeding 200°C and the layer temperature exceeding 80°C at a height of 1.5 metres. The former criteria is exceeded within 100 to 150 seconds after ignition and the latter criteria within 140 to 190 seconds after ignition. The time taken to restore the compartment to tenable conditions after suppression varied widely. Ranging from 200 to 300 seconds to reduce the temperature of the compartment to below 80°C at a height of 1.5 metres, and ranging from 77 to 89 seconds to reduce the upper layer temperature below 200°C.

Some of the thermocouple data exhibited dips down to 100°C or below at the time of suppression and then the temperature rose again. This is illustrated in Figure 8-3. It is believed that this phenomena was caused by water spray on the surface of the thermocouples and that it does not reflect a real change in compartment gas temperatures.

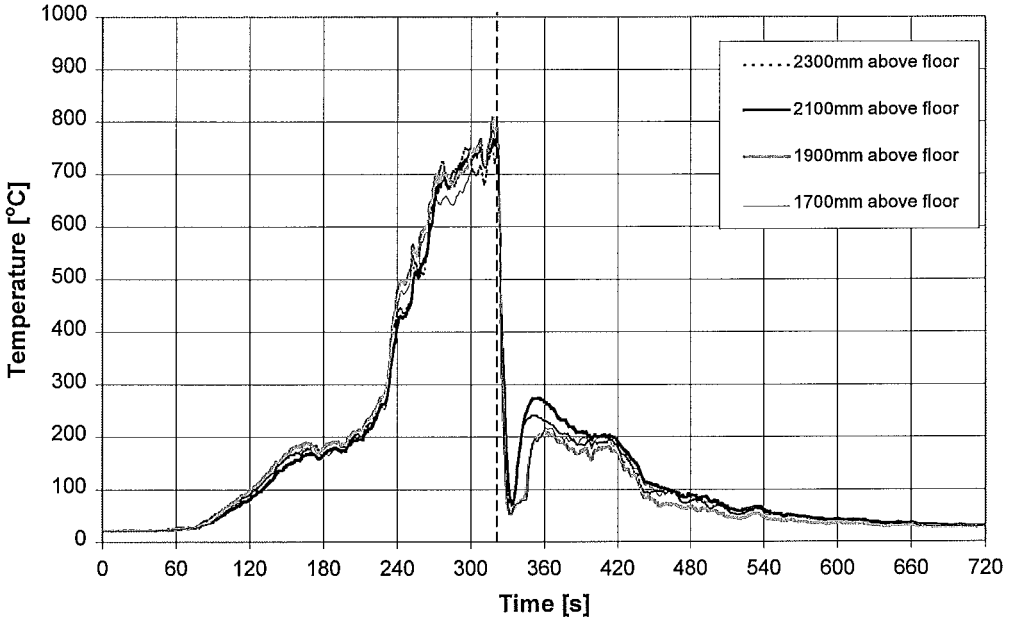

Figure 8-3: Water Spray Cooling of Thermocouples

8.4 Doorway Temperatures

Doorway temperatures reached temperatures comparable with those seen at the same time at the corresponding heights inside the compartment. Peak temperature values were observed near the top of the doorway and these ranged between 750°C and 900°C.

Temperatures at a height that a firefighter in a crouching or lying down stance might face (assumed to be around 0.5 metres) ranged from 100°C to 250°C. The actual temperature at the time of extinguishment is likely to be higher than this as the trolley was moved some time before extinguishment commenced.

8.5 Doorway Flows

Doorway mass flow rate measurements were sensitive to the wind conditions and on several of the runs the measurement was erratic with large swings in the mass flow value which can be matched to the wind behaviour.

On calmer days the measurements show a rising value of the mass flow rate which reaches a value of between 1.0 and 1.5 kg/s as the fire becomes established. This was less than the value predicted by Rockett's equation, which gives a mass flow rate of 1.7 kg/s. But given the relatively small number of thermocouples and bi-directional probes, the approximate nature of Rockett's relationship, and the effects of wind, the agreement is considered to be reasonable.

8.6 Fire Growth

Considerable variation was observed in the form of the fire growth. Initial fire growth was slow and then rises rapidly in a similar manner to the compartment temperatures discussed in Section 7.7. As would be expected comparing the compartment temperatures and the heat release rates indicates that this sudden rise in heat release rate coincides with the sudden rise in compartment temperatures.

A particularly intense period of burning was observed when the paper lining on the gypsum board catches alight. However comparison of the timing of this event with the heat release rate curves shows no correspondence between it and the peak heat release rate.

The equation of McCaffrey, Quintiere and Harkleroad[43] predicts a critical heat release rate for flashover of 730 kW. The heat release rate data shows a range of values for the onset of flashover between 550kW and 900kW. Given the assumptions inherent in the derivation of the predicted value and the effects of wind on the underlying assumptions of the vent flow behaviour the agreement is reasonable.

Peak heat release rates varied between 2900 kW and 4500 kW indicating the variability of the heat release rate despite the attention to the use of consistent fuel configuration and

loading. The wind direction had a significant effect on losses of fire effluent from the hood and the low peak heat release rates correspond with these.

Ventilation limited heat release rates were calculated based on the relationships of Babrauskas[41] for the burning of wood cribs. The value predicted is 4500 kW for the heat release based upon the compartment doorway flow and ignoring the ventilation limiting effect of the compartment partition. This predicted value corresponds to the maximum value obtained for the experimental runs. A value of 2600 kW was calculated for a fuel limited heat release rate based upon the wood crib heat release rate work discussed by Babrauskas[41] and an estimate of the heat release rate from the MDF based upon wood panel burning rates given in the Fire Engineering Design Guide[42]. Measured heat release rates were in excess of this indicating that the heat release rate was ventilation limited. However the estimate is crude as does not model the compartment effects on the mass loss rate of the fuels. Hence it will underestimate heat release rates as the compartment approaches flashover. Given the complicating effect of unknown losses due to wind effects it is difficult to clearly state whether the fires were ventilation limited, fuel limited or whether they moved between the two regimes during the course of the fire. The evidence of the crib temperatures suggests that at least in the rear of the compartment, behind the partition, the burning was limited by the amount of air that could get to the fuel.

The peak heat release rates are comparable with those reported for the National Class A Foam Project[22] which ranged from approximately 3300 kW to 4600 kW for the series I runs which used a wood crib and simulated furniture as the fuel packages. The wood crib fires used by Kim and Dlugogorski[13] were smaller with peak heat release rates of around 500 kW.

The measured water vapor concentrations range between 10% and 20%. This is greater than the 7% threshold suggested by Dlugogorski et al[58] above which the effect of water vapor on the heat release rate may be significant. It was not possible to obtain an accurate heat release curve using the equations developed by Dlugogorski et al[58] since these require measurements of CO_2/CO concentrations. By estimating the CO_2 concentration based upon the stoichiometric equation it is possible to obtain the heat release relative to the standard

method of Janssens[54] which does not account for water. A peak heat release rate of around 85% of the value predicted by Janssens' method is obtained if the conservative assumption is made that all of the water measured is due to combustion, and around 110% of the Janssens method value if only 50% of the measured water is due to combustion. This suggests a maximum variation of around 15% which is large enough to consider the use of a CO_2/CO analyser in future suppression experiments. This would have the additional benefit of providing a confirmation of the suitability of the method of Dlugogorski et al beyond the 7% water vapor concentrations reached in their study. For more detail on water vapor and its effect on heat release rate see Chapter 6.

8.7 Suppression Performance

The most direct quantitative measurement of suppression performance is the time taken to achieve a certain reduction in the heat release rate of the fire. This was the broad approach adopted by earlier scientific studies such as the work of the National Class A Foam Project[22], Kim and Dlugogorski[13], and Scheffey and Williams[29]. The National Class A project[22] measured this in terms of the time taken to reduce the heat release rate to 500 kW. Using a fixed value in this way prejudices the performance of an agent in a fire with a high heat release rate and would only be applicable if a very large number of experiments were carried out such that the fluctuations in peak heat release could be dealt with statistically.

The work of Kim and Dlugogorski[13] and Mawhinney et al[27] used a continuous application of suppression agent and measured the time for the heat release rate to be reduced to near zero. This approach is not suitable for the aim of this study as from a Fire Service operational perspective the time taken for the fire to be completely extinguished is less important than the time taken to control the fire to a level where it is safe to enter the compartment. Due to continued low level smoldering and smoke clearing it can take several minutes for the heat release rate to reach zero. This value is of interest in examining the efficiency of the agent in penetrating into deep seated fires but it is not seen as the primary measure of suppression effectiveness for this study. Scheffey and Williams[29] used a criteria of there being no visible flame for the estimation of the extinguishment time. This approach may be considered a reasonable estimate for very large fires which require a

relatively long period of application and, along with total amount of agent flowed, it is the common measure used in the test burns by Fire Brigades and workers such as Colletti[16].

Given the unsuitability of the above approaches this research measured the time taken to

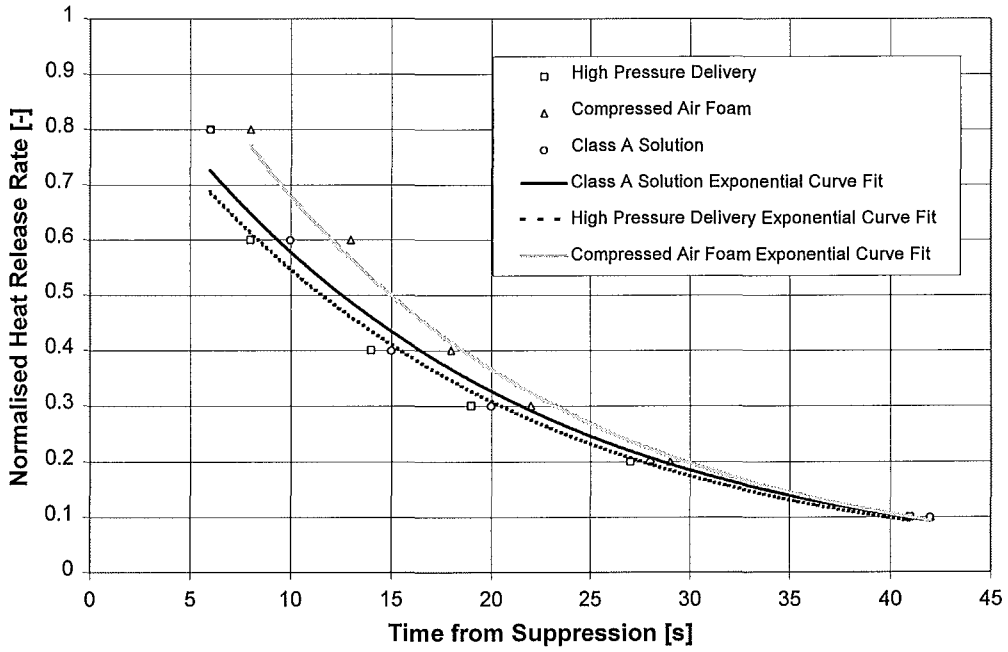

Figure 8-4: Comparison of Normalised Heat Release Rates

reduce the heat release rate of the fire to a percentage of its value immediately prior to suppression. This is summarised in Figure 8-4 which shows the normalised reduction in heat release rate for the three suppression methods averaged across the three days of runs. It can be seen there is little difference in the rate of heat release reduction between the three

Method	Date	Time Reduce Heat Release to 500kW [s]
HPD	27/11	29
HPD	2/12	34
HPD	12/12	45
	Average	**36**
CAFS	27/11	34
CAFS	2/12	34
CAFS	12/12	41
	Average	**36**
Solution	27/11	34
Solution	2/12	21
Solution	12/12	38
	Average	**31**

Table 8-1: Time to Reduce Heat Release Rate to 500 kW

methods. The time taken to reduce the heat release rate to 500 kW is summarised in Table 8-1.

The values reported by the National Class A Foam project[22] ranged from 48 to 60 seconds for direct water application, 27 to 66 seconds for CAFS, and 39 to 45 seconds for direct class A solution application. These values were for the series II fuel package which consisted of mock furniture constructed from polyether foam mattresses, no values are given for the series I fuel package. The peak heat release rates for the relevant series II experiments ranged from 2157 to 2853 kW. These were smaller fires than the ones suppressed in this study but lower, continuous, flow rates were used in the National Class A Foam project[22], 26.5 litres/minute compared to 170 litres/minute in this study. The net result of these countering effects is that the suppression times are similar to those measured in this study.

The temperature reduction in the compartment after suppression shows no discernible differences between the three suppression methods. Table 8-2 summarises the results.

Suppression Method	Time to reduce upper layer Temperature to 200C [s]	Time to reduce upper layer Temperature @1.5 metres to 80C [s]
HPD	**80 ±15**	**200 ±25**
CAFS	**110 ±49**	**300 ±45**
Solution	**90 ±22**	**205 ±25**

Table 8-2: Summary of Temperature Reduction Times

There is a wide spread in the underlying data, indicated by the 95% confidence intervals, for these results so it is difficult to form firm conclusions. The differences in the time taken to reduce the upper layer temperature below 200°C are within the 95% confidence intervals so no conclusion can be made about the longer response time for CAFS. With the time taken to reduce the temperature to 80°C at a height of 1.5 metres the higher CAFS value is outside the 95% confidence interval so the time difference may be of some significance. This higher time value would indicate that the CAFS is less effective at cooling the air within the compartment.

Examination of the temperature drops at the 0.9 metre high rear thermocouple do not indicate such a clear distinction between the methods. Table 8-3 summarises the results.

Suppression Method	Time to reduce upper layer Temperature @0.9 metres to 80°C [s]
HPD	**100 ±10**
CAFS	**115 ±30**
Solution	**140 ±40**

Table 8-3: Time to Reduce Temperatures at Rear of the Compartment

Results indicate that HPD was the most effective at reducing temperatures at the rear of the compartment, CAFS was slightly less effective, and Solution was the least effective. The difference in times between HDP and Solution is surprising and may be explained in part by the low flow rate, 140 litres/minute as opposed to 170 litres/minute, observed on the 27/11/97. If this result is not included then the time for Solution drops to around 110 seconds. In this case the results for all three methods are very similar.

From these observations it is difficult to draw any firm conclusions, especially when there are complicating events such as re-ignition. There appears to be little difference between the methods in the cooling observed at the rear of the compartment however there is a slight improvement in upper layer cooling when using HPD or Solution, at least when cooling down to lower temperatures. These observations are in marked contrast to Colletti[16] who reports that to drop the temperature to 100°C at a height of 1.2 metres took 38.5 seconds for CAFS, 102.9 seconds for foam solution, and 222.9 seconds for water.

This latter observation is supported by Kim and Dlugogorski[13] who comment "Unlike water mist, there seems to be no compartment [gas layer cooling] effect with a CAF system" and by Mawhinney et al[27] who discuss the effectiveness of water mist in cooling the hot gas layer in compartment fires. It needs to be remembered that this statement does not imply that using CAFS does not result in cooling of the upper gas layer, rather that it does not rely upon the upper gas layer cooling as an extinguishment mechanism.

Mawhinney et al[27] comment that "[using water mist] it is easier to extinguish 'large' fires than 'small' fires" in a compartment. This is explained in the increased effectiveness of the

oxygen displacement mechanism of water mist in fully involved compartment fires. This observation together with the observation of Kim and Dlugogorski[13] that CAFS performs equally well inside or outside of a compartment indicates that a fully involved compartment fire shows the performance of water mist (including class A solution mist) in the best possible light relative to CAFS.

The ease with which the fires are extinguished by all the methods suggests that the size and nature of the fires was relatively unchallenging. This can be dealt with in two basic ways, increase the size of the fire, or handicap the suppression method, usually by decreasing the suppressant flow rate. Use of lower flow rates increases the challenge but it is unclear how results from low flow rate experiments can be scaled up to realistic firefighting flows, or whether scaling effects differ between methods leading to bias in the results. Increasing the size of the fire is expensive and it would require the use of enclosures larger than the ISO standard making the results less easily comparable.

A qualitative performance measure of interest to the Fire Service is the ease of use of the suppression medium. It was observed for the CAFS experiment visibility in the compartment was relatively good whereas for HPD and Solution experiments large quantities of steam (Figure 8-5) were generated with consequent poor visibility in the compartment. With CAFS it was observed that as the suppressant was first applied a brief pulse of flame would issue 2 or 3 metres out from the compartment. It is believed this occurs because the momentum of the CAFS jet carries the water to the rear of the compartment where it turns to steam and as there is no other vent in the compartment the expanding steam 'pushes' the fire forward out of the compartment doorway.

Figure 8-5: Steam Production During Suppression

The compartments were examined after each of the runs to ascertain the degree of burning and whether there was any water damage in the compartment. No significant differences were found between the degree of water damage of the three mechanisms.

There was a significant human factor in the suppression. Use of a firefighter rather than a mechanical method to apply the suppressant gave realism to the study which after all was concerned with practical firefighting effectiveness. It also introduced a degree of uncertainty and variability which was countered to some extent by the use of multiple tests and the use of standard operating procedures and application times. The uncertainty could be further reduced by detailed analysis of the operating method and rigorous definition of

a ‘standard’ method including position relative to compartment, direction and movement of application.

9. CONCLUSIONS

Little difference was found in the suppression effectiveness of the three methods measured in terms of time taken to reduce the heat release rate. A fully involved compartment fire gives maximum benefit to the extinguishment mechanisms employed by the water mist based methods, HPD and Solution. Therefore, as CAFS performs equally as well in a situation which would be expected to favour HPD and Solution, it is an indirect positive result for CAFS.

Rate of temperatures reduction in the compartment was also similar for the three methods. This was in contrast to the findings of Colletti[16] who reported markedly better performance for CAFS.

Flow rates used by previous researchers in comparing CAFS with other methods used lower flow rates. These low flow rates are not realistic for firefighting. The use of realistic flows makes distinction between the methods difficult since the fire is relatively unchallenging. Use of lower flow rates increases the challenge but it is unclear how results from low flow rate experiments can be scaled up to realistic firefighting flows, or whether scaling effects differ between methods leads to bias in the results. Increasing the size of the fire is expensive and it would require the use of enclosures larger than the ISO standard making the results less comparable.

A further observed benefit of CAFS was the relatively good visibility in the compartment during suppression compared with HPD and Solution. Less steam was produced by CAFS and the firefighter was at a distance from the doorway and so was not enveloped in the clouds of steam that are produced.

Wind effects are significant with losses of fire effluent leading to under-prediction of heat release rate. The disturbance of the air flow around the compartment doorway complicates any interpretation of the fire behaviour.

Water vapor concentrations, at around 10% to 20%, were higher than the 7% regarded by Dlugogorski et al[58] as having a significant effect on the heat release rate. Water vapor concentrations reached a peak during flashover with no measured increase in water vapor concentration when the water was applied to extinguish the fires.

Measured water vapor concentrations were around twice those that would be obtained based upon stoichiometric combustion. Use of a fixed relationship to predict the quantity of CO_2 based on the quantity of water and the stoichiometric equation for wood combustion leads to unrealistic (negative) heat release rate curves. It was estimated that, for the fires studied, ignoring the water in the exhaust stream results in a maximum of a 15% over prediction in the peak heat release rate.

10. RECOMMENDATIONS

1. CAFS is worthy of further investigation and continued interest. It performs as well as HPD or Class A Solution in a fire situation which would be expected to favour them.

2. Any future work comparing the fire suppression performance needs to consider the use of larger fires. House burns could provide the scale but would not provide the necessary repeatability.

3. More fundamental research into the suppression mechanisms of class A foam and investigation of small scale tests for comparing suppression effectiveness.

4. Ensuring any similar experiments are carried out inside a large building or wind sheltered area is recommended in order to minimise the loss of fire effluent due to wind effects.

5. Method of application by the firefighter would benefit from detailed definition to improve the consistency between experiments.

6. Measurement of water vapor indicates that the water vapor concentrations are significant (>7%) and should be measured to correct the heat release rate. Estimation of the CO_2 content from the water content based on reaction stoichiometry is not a viable technique in fires under suppression or where there is significant moisture in the fuel or surroundings. It is recommended that a CO_2/CO analyser be used for any further work.

7. The method of Dlugogorski et al[58] and Janssens[59] for calculating heat release rate where O_2, CO_2, CO and H_2O are measured need to be ratified for situations where water vapor concentrations exceed the 7% level studied in the work of Dlugogorski et al[58].

11. REFERENCES

[1] New Zealand Fire Service (NZFS) (1997) *Emergency Incident Statistics 1993-1996.* NZFS, Wellington.

[2] Colletti, D.J. (1992) Class A Foam for Structure Firefighting. *Fire Engineering*, July, p 23.

[3] Colletti, D.J. (1994) Class A Foam: An Emerging Technology. *Fire Engineering*, March, p 61.

[4] National Wildfire Coordinating Group (1992) *Foam vs Fire: Primer*, October 1992.

[5] Grimwood, P.T. (1992) Fog Attack, FMJ International Publications, Redhill, Surrey.

[6] National Wildfire Coordinating Group (1993) *Foam vs Fire: Class A Foam for Wildland Fires*, 2nd ed. October 1993.

[7] Rochna, R. (1991) Compressed Air Foam: What It Is!, *American Fire Journal*, August, p 21.

[8] Liebson, J. (1991) *Introduction to Class A Foams and Compressed Air Foam Systems for the Structural Fire Service.* International Society of Fire Service Instructors, Ashland, MA.

[9] Kokkala, M.A. (1986) Extinguishment of Compartment Fires Using Portable Chemical Extinguishers and Water. *Fire Safety Journal*, **11**, pp 201-209

[10] Salzberg, F., Vodvarka, F.J. and Maatman, G.C. (1970) Minimum Water Requirements for the Suppression of Room Fires, *Fire Technology*, **6**, p 22

[11] Giselsson, K. and Rosander, M. (1984) Making the Best Use of Water for Extinguishing Purposes, *Fire Journal (GB),* October.

[12] Rimen, J.G. (1990) The Use of High Pressure and Low Pressure Pumps with Hose-reel Systems, *Home Office (FEU) Research Report No. 36*, Home Office, London.

[13] Kim, A.K., and Dlugogorski, B.Z. (1997) Multipurpose Overhead Compressed Air Foam System and its Fire Suppression Performance, *J. of Fire Prot. Engr.*, 8(**3**), pp 133-150.

[14] Mawhinney, J.R. and Richardson, J.K. (1997) A Review of Water Mist Fire Suppression Research and Development, 1996. *Fire Technology*. First Quarter, **33**, pp 54-90.

[15] Colletti, D.J. (1993) *Quantifying the Effects of Class A Foam in Structure Firefighting.* Fire Engineering, February 1993, pp 41-44.

[16] Colletti, D.J. (1994) Testing CAFS in Live Burns. *Fire Engineering*. March, p 74.

[17] National Wildfire Coordinating Group (1995) The Use of Class A Foam and Compressed Air Foam Systems (CAFS) in Firefighting, *Foam Applications for Wildland & Urban Fire Management*. 7(2), September, p 15.

[18] Thornton, T. (1997) Class A Foam: Use for Wildfire and Structure Fire Control in Australia. *Fire Australia*. May, p 14.

[19] NFPA 298 (1994): *Fire Fighting Foam Chemicals for Class A Fuels in Rural, Suburban, and Vegetated Areas*. National Fire Protection Association, Quincy, MA.

[20] Carey, W.M. (1993) *National Class A Foam Research Project Technical Report*. National Fire Protection Research Foundation, Quincy, MA.

[21] Madrzykowski, D. (1988) *Study of the Ignition Inhibiting Properties of Compressed Air Foam*. NISTIR-88/3880, National Institute of Science and Technology, Gaithersburg, MD.

[22] Carey, W.M. (1994) *National Class A Foam Research Project Technical Report, Phase II*. National Fire Protection Research Foundation, Quincy, MA.

[23] Rasbash, D.J., Rogowski, Z.W., and Stark, G.W.V. (1960) Mechanism of Extinction of Liquid Fires Using Water Sprays, *Combustion and Flame*. **4**, p 223.

[24] Rasbash, D.J., and Rogowski, Z.W. (1957) Extinction of Fires in Liquids by Cooling with Water Sprays, *Combustion and Flame*. **1**, p 453.

[25] Rasbash, D.J., Rogowski, Z.W., and Stark, G.W.V. (1956) Properties of Fires on Liquids, *Fuel*, **35**, p 94.

[26] Jones, A. and Thomas, G.O. (1993) The Actions of Water Sprays on Fires and Explosions: A Review of Experimental Work, *Trans IChemE*, **71**, February, pp 41-49.

[27] Mawhinney, J.R., Dlugogorski, B.Z. and Kim, A.K. (1994) A Closer Look at the Fire Extinguishing Properties of Water Mist, *Proceedings of the 4th International Symposium on Fire Safety Science*, 1994, pp 47-60.

[28] Scheffey, J.L. (1995) 'Foam Agents and AFFF System Design Considerations', Section 4/Chapter 4, In: *The SFPE Handbook of Fire Protection Engineering*. Eds: P.J. DiNenno. 2nd Ed., National Fire Protection Association, Quincy, MA. p 3-145.

[29] Scheffey, J.L. and Williams, F.W. (1991) The Extinguishment of Fires Using Low Flow Water Hose Streams - Part II. *Fire Technology*, **27**(4), pp 291-320.

[30] Personal Safety and Environmental Concerns, National Class A Foam Technology Workshop, CFA Training College, Fiskville, November 1995.

[31] Finger, S. (1995) Environmental Implications of Firefighting Chemicals, *Foam Applications for Wildland & Urban Fire Management*, **7**(1), National Wildfire Coordinating Group.

[32] Scheffey J.L. (1995) 'Foam Agents and AFFF System Design Considerations', Section 4/Chapter 4, In: *The SFPE Handbook of Fire Protection Engineering*. Eds: P.J. DiNenno. 2nd Ed., National Fire Protection Association, Quincy, MA.

[33] McCaffrey, B.J. and Heskestad, G. (1976) *Combustion and Flame*, **26**, 125.

[34] SFPE (1995) Property Data, Appendix B, *The SFPE Handbook of Fire Protection Engineering*, 2nd Ed., A-26, National Fire Protection Association, Quincy, MA.

[35] Hugget, C. (1980) Estimation of Rate of Heat Release by Means of Oxygen Consumption Methods, *Fire and Materials*, **4**, 61-65.

[36] Tewarson, A. (1995) 'Generation of Heat and Chemical Compounds in Fires', Section 3/Chapter 4, In: *The SFPE Handbook of Fire Protection Engineering*. Eds: P.J. DiNenno. 2nd Ed., National Fire Protection Association, Quincy, MA.

[37] Drysdale, D D. (1985) An Introduction to Fire Dynamics, John Wiley and Sons, Chichester.

[38] Emmons, H.W. (1995) Vent Flows, Section 2/Chapter 5, The SFPE Handbook of Fire Protection Engineering, 2nd Ed., 3-145, National Fire Protection Association, Quincy, MA.

[39] Rockett, J.A. (1976) Fire Induced Gas Flow in an Enclosure, *Combustion Science and Technology*, **12**, 165-175.

[40] Kawagoe, K. (1958) Fire Behaviour in Rooms, Report No. 27, Building research Institute, Tokyo.

[41] Babrauskas, V. (1995) 'Burning Rates', Section 3/Chapter 1, In: *The SFPE Handbook of Fire Protection Engineering*. Eds: P.J. DiNenno. 2nd Ed., National Fire Protection Association, Quincy, MA.

[42] Buchanan, A.H. (1994) Fire Engineering Design Guide

[43] McCaffrey, B.J., Quintiere, J.G., and Harkelroad, M.F. (1981) Estimating Room Fire Temperatures and the Likelihood of Flashover Using Fire Test Data Correlations, *Fire Technology*, **17**(2), 98-119

[44] Walton, W.D. and Thomas, P.H. (1995) 'Estimating Temperatures in Compartment Fires', Section 3/Chapter 6, In: *The SFPE Handbook of Fire Protection Engineering*. Eds: P.J. DiNenno. 2nd Ed., National Fire Protection Association, Quincy, MA.

[45] Purser, D.A. (1995) 'Toxicity Assessment of Combustion Products', Section 2/Chapter 8, In: *The SFPE Handbook of Fire Protection Engineering*. Eds: P.J. DiNenno. 2nd Ed., National Fire Protection Association, Quincy, MA.

[46] Custer, R.L.P. and Meacham, B.J. (1997) *Introduction to Performance Based Fire Safety*. National Fire Protection Association, Quincy, MA

[47] ASTM E603 - 94 (1994) *Standard Guide for Room Fire Experiments*, American Society for Testing and Materials, Philadelphia, PA. September 1994.

[48] NT FIRE 032 (1991) *Upholstered Furniture: Burning Behaviour - Full Scale Test*, NORDTEST, Esbo, Finland. May 1991.

[49] ISO 9705 (1993) *Full Scale Room Test for Surface Products*, International Standards Organisation, Geneva, Switzerland.

[50] Dunn, M (1998) Full Scale Testing of Fire Suppression Agents on Unshielded Fires, MEFE thesis, University of Canterbury, Christchurch, New Zealand.

[51] Servomex (1994) 540A Oxygen Analyser: Instruction Manual, Servomex plc., Crowborough, East Sussex.

[52] Servomex (1985) PSA402 Instruction Manual, Servomex plc., Crowborough, East Sussex.

[53] UL162 (1993) *Standard for Foam Equipment and Liquid Concentrates*, Underwrites Laboratory Inc,. Northbrook, IL. July 1993.

[54] Janssens, M.L. (1991) Measuring Rate of Heat Release by Oxygen Consumption, *Fire Technology*. **27**, pp 234-249.

[55] Croce, P.A. (1976) *Combustion Science and Technology*. **14**, pp 221-228.

[56] Babrauskas, V. and Williamson, R.B. (1978) Fire Technology, **14**, pp 226-238.

[57] Lyon, R.E. and Abramowitz, A. (1995) Effect of Instrument Response Time on Heat Release Rate Measurements, *Fire and Materials*. **19**, pp 11-17.

[58] Dlugogorski, B.Z., Mawhinney, J.R. and Duc, V.H., (1994) The Measurement of Heat Release Rates in Fires Under Suppression, *Proceedings of the 4th International Symposium on Fire Safety Science*. pp 877-888.

[59] Janssens, M.L. (1995) 'Calorimetry', Section 3/Chapter 2, In: *The SFPE Handbook of Fire Protection Engineering*. Eds: P.J. DiNenno. 2nd Ed., National Fire Protection Association, Quincy, MA.

Appendix 1 Data Collection Channels

Logical #	Physical #	Description	Units	Range
1	Calculated	O_2 Mole Fraction	[-]	
2	CH01	O_2 Concentration	V	0/+1 [+0.8379]
3	Calculated	Duct Pressure Difference	[Pa]	
4	CH02	Duct Pressure Transducer	V	
5	Calculated	Scale Mass	[kg]	
6	CH03	Scale	V	0/+1
7	Unused			
8	CH04	H_2O Concentration	V	0/+10
9	L01	Duct Thermocouple	K	Over Ambient
10	L02	Fan Thermocouple	K	Over Ambient
11	L03	Cold Trap Thermocouple	K	Over Ambient
12	Unused			
13	Unused			
14	Calculated	Mass Flow	[kg/s]	
15	Calculated	Heat Release Rate	[kW]	
16	Calculated	Oxygen Mole Percentage	[%]	
17	CH05	Trolley Pressure Transducer #1 (top)	V	0/+5 [+2.5]
18	CH06	Trolley Pressure Transducer #2	V	0/+5 [+2.5]
19	CH07	Trolley Pressure Transducer #3	V	0/+5 [+2.5]
20	CH08	Trolley Pressure Transducer #4	V	0/+5 [+2.5]
21	CH09	Trolley Pressure Transducer #5	V	0/+5 [+2.5]
22	CH10	Trolley Pressure Transducer #6	V	0/+5 [+2.5]
23	CH11	Trolley Pressure Transducer #7	V	0/+5 [+2.5]
24	CH12	Trolley Pressure Transducer #8 (bottom)	V	0/+5 [+2.5]
25	F01	Front Thermocouple Tree2.3 m	K	Over Ambient
26	F02	Front Thermocouple Tree2.1 m	K	Over Ambient
27	F03	Front Thermocouple Tree1.9 m	K	Over Ambient
28	F04	Front Thermocouple Tree 1.7 m	K	Over Ambient
29	F05	Front Thermocouple Tree 1.5 m	K	Over Ambient
30	F06	Front Thermocouple Tree 1.3 m	K	Over Ambient
31	F07	Front Thermocouple Tree 1.1 m	K	Over Ambient
32	F08	Front Thermocouple Tree 0.9 m	K	Over Ambient
33	F09	Front Thermocouple Tree 0.7 m	K	Over Ambient
34	F10	Front Thermocouple Tree 0.5 m	K	Over Ambient
35	F11	Front Thermocouple Tree 0.3 m	K	Over Ambient
36	F12	Front Thermocouple Tree 0.1 m	K	Over Ambient
37	F13	Front Crib Thermocouple	K	Over Ambient
38	F14	Back Corner Crib Thermocouple	K	Over Ambient
39	F15	Back Centre Crib Thermocouple	K	Over Ambient
40	F16	Back Thermocouple Tree 0.9 m	K	Over Ambient
41	F17	Trolley Thermocouple #1 (Top)	K	Over Ambient
42	F18	Trolley Thermocouple #2	K	Over Ambient
43	F19	Trolley Thermocouple #3	K	Over Ambient
44	F20	Trolley Thermocouple #4	K	Over Ambient
45	F21	Trolley Thermocouple #5	K	Over Ambient
46	F22	Trolley Thermocouple #6	K	Over Ambient
47	F23	Trolley Thermocouple #7	K	Over Ambient
48	F24	Trolley Thermocouple #8	K	Over Ambient
49	F25	Ambient	K	
50	F26	Heating Water for H_2O Analyser	K	Over Ambient
51	CH13	Wind Speed	V	0/+5
52	CH14	Wind Direction	V	0/+5

Appendix 2 Checklist

Date :
Run Order :
Experimenter :

❑ *Calorimeter Start Up and Calibration Procedure*

- ❑ Wire up O2 calorimeter, duct bi-directional and scale to data acquisition system.
- ❑ Wire up thermocouple from cold trap air stream to digital thermometer.
- ❑ Turn on water to cold trap - only a slow flow required.
- ❑ Turn on power to cold trap, takes 10 minutes to warm up. Yellow lead to outside socket on control panel.
- ❑ Check load cell OK. If it has been reset then at first unload platform and power cycle and then retest. If OK reload platform and continue.
- ❑ Power up computer install CAFs software, set preferences:
    - ❑ Set acquisition rate to 5/s.
    - ❑ Averaging over 5 samples, averaging on, and store average only.
    - ❑ Standard Graph 1:
        - ❑ Unipolar, Voltages, V, range 0 to 5, horizontal range 5 minutes
        - ❑ Channels 1,2,3,14,6.
    - ❑ Standard Graph 2:
        - ❑ Unipolar, Temperatures, deg K, range 400, horizontal range 5 minutes
        - ❑ Channels 9,10, 25, 26, 37.
- ❑ Check state of crystals and soot filter. Replace filter at start of test day. Replace pink anhydrous copper sulphate with blue, recycle by heating in oven. Check that don't have tubes back to front. Replace CO absorber, cannot be recycled. If time is short these steps can be carried out during the zeroing of the calorimeter.
- ❑ Turn on pump. Check cold trap temperature, can use voltmeter or digital thermometer. It is the yellow plug with fine prongs. Temperature should be in the range 0 to 4°C. Value °C. Turn off pump.

❑ *Vacuum Testing of the Sample Line*

- ❑ Turn off sample point valve at the duct.
- ❑ Turn on pump it should read -90 to -95 kPa on the pressure gauge.
- ❑ Turn vacuum test valve to test position.
- ❑ Turn off pump. Start stopwatch.
- ❑ Time how long it takes for the line pressure to drop to -70 kPa. Should not be less than 1 minute.
- ❑ Re-open sample valve on the duct.
- ❑ Turn vacuum test valve to normal position.
- ❑ Turn pump back on. Should be reading -15 to -20 kPa on the gauge.
- ❑ Turn off the pump.

❑ *Zeroing O_2 Analyser*

- ❑ Switch the valve from sample to zero on the calorimeter.
- ❑ Close the sample line, ensure bypass line is open.
- ❑ Open N_2 regulator and set pressure to 120 kPa. Should see flow on bypass flow meter.
- ❑ On O_2 analyser panel set scale dial from 25 to 1.
- ❑ Use the left hand knob to zero the setting. Takes 10 minutes to stabilise.
- ❑ Turn off N_2 and allow line to purge.
- ❑ On O_2 analyser panel set scale dial back to 25.
- ❑ Close the sample line.
- ❑ Switch the valve from zero to sample on the calorimeter.

❑ *Spanning O_2 Analyser - Repeat as Necessary Between Runs*

- ❑ Turn on the pump.
- ❑ Set flow through the analyser using the sample knob.
- ❑ Check pressures in the sample line are OK.
- ❑ Leave 10 minutes to reach equilibrium.
- ❑ Adjust till reading 20.95% O_2.
- ❑ Turn off pump.

❑ *Testing the Duct Flow*

- ❑ Turn on the duct fan.
- ❑ Check pressure difference is greater than around 130 Pa.
- ❑ Check the mass flow in the duct is around 4 kg/s. Value [kg/s]
- ❑ If low flow or pressure then check duct covers are intact and well sealed.

❑ *Weather Station Set up*

- ❑ Fill water buckets for the weather station.
- ❑ Erect weather station without instruments, need to align cross arm N-S.
- ❑ Leave for 20-30 minutes to check that it is stable.
- ❑ Put on instruments and wire back.

❑ *Heat Release Rate Calibration*

- ❑ Turn on water at the hose reel for the water misting system.
- ❑ Move burner into position.
- ❑ Turn on gas at cylinders and set needle valve at 1 full turn.
- ❑ Record relative humidity and temperature. [RH %; Temperature °C.]
- ❑ Record mass on scale. Mass [kg.]
- ❑ Set up calibration file `CAL#ddmm.CSV`. Filename : [ ]
- ❑ **Ensure duct fan and sample pump are on and OK.**
- ❑ Start baseline. Can change display to show Q in kW, range 0-1200.
- ❑ Typical timings would be:
- ❑ 0 - 3 minutes, baseline
- ❑ 3 - 8 minutes, burning gas set at 1 full turn
- ❑ 8 - 11 minutes, baseline
- ❑ 11 - 16 minutes, burning gas set at 1½ full turns
- ❑ 16 - 19 minutes, baseline

Record Actual

- ❑ Watch the square duct temperature (channel 10) and turn on water spray if it exceeds 400K.
- ❑ Record the scale weight after each burn period. Masses : [kg]
- ❑ When completed close needle valve and each cylinder valve.
- ❑ Move burner back out of the way.

❑ *Wiring Up of Instrumentation*

- ❑ Wire up computer end thermocouples. Channels 1-16 for the room thermocouples. Channels 17-24 for the tree thermocouples. Wire up pressure transducers and duct thermocouples and ambient thermocouple.

❑ *Checking the Trolley*

- ❑ Scan through each of the pressure transducer channels, should have a reading of +2.5V.
- ❑ Check each of the trolley thermocouples.

❑ *Foam Quality Set up*

- ❑ Put collection plate on wagon.

❑ Gather measuring cylinders and the scales to a nearby sheltered location.

❑ *Crib Moisture Content*

Compartment	Moisture Content Readings

For each burn run

❑❑❑ *Set up the Compartment*

❑ ❑ ❑ Move it into position.
❑ ❑ ❑ Connect up thermocouples.
❑ ❑ ❑ Test the thermocouples.
❑ ❑ ❑ Nail on run name.
❑ ❑ ❑ Put trays with 200ml of diesel under each crib.
❑ ❑ ❑ Put trolley into position.
❑ ❑ ❑ Put video cameras into position.

❑❑ *Foam Quality Measurements (Class A, and CAFS)*

❑ ❑ Get sample of foam from collection plate in 2000ml beaker.
❑ ❑ Get sample in draining container and measure drainage time.
❑ ❑ Collect foam sample in labeled jar.

❑❑❑ *Prior to Baseline*

❑ ❑ ❑ Video run name board on each camera, finalise shots.
❑ ❑ ❑ Check crew are ready to go.
❑ ❑ ❑ **Check water mist is operating OK.**
❑ ❑ ❑ **Check duct fan is on and OK.**
❑ ❑ ❑ **Check sample pump is on, that there is sample flow through calorimeter and the pressure is OK.**
❑ ❑ ❑ Set up run file name, `RUN#ddmm.CSV`.
❑ ❑ ❑ Record Relative Humidity and Temperature.

Run	RH [%]	Temperature [°C]

❑❑❑ *From Baseline to Extinguishment*

❑ ❑ ❑ Warn everyone baseline is about to start, check all is OK.
❑ ❑ ❑ Start baseline.
❑ ❑ ❑ At 2 minutes start video cameras.
❑ ❑ ❑ Show time synchronisation board at 2:30.
❑ ❑ ❑ Ignite fuel from 3:00.
❑ ❑ ❑ Pull out trolley before flashover.
❑ ❑ ❑ Give crew signal to extinguish when floor is ignited right to front of compartment.
❑ ❑ ❑ Crew call fire out.
❑ ❑ ❑ Keep all videos going until end baseline of 5 minutes after fire out call is completed.
❑ ❑ ❑ Turn off water mist.

❑ ❑ ❑ Turn off sample pump.
❑ ❑ ❑ Turn off duct flow.

❑❑❑ *Post Extinguishment Data Collection*

❑ ❑ ❑ Video firefighter to collect comments. For last run of the day also video comments of the pump operator.
❑ ❑ ❑ Video inside of the container.
❑ ❑ ❑ Collect pump settings and timings from the pump operator.

❑❑❑ *Clear Out Ready for Next Run*

❑ ❑ ❑ Remove thermocouple trunk connections from the compartment. Tow back and empty out cribs, make sure to keep bricks and trays.
❑ ❑ ❑ Move wheels onto next container.
❑ ❑ ❑ Copy data file onto floppy disk.

❑ *Final Tidy Up*

❑ ❑ ❑ Take down weather station.
❑ ❑ ❑ Move all tools, video cameras, etc, into the container.
❑ ❑ ❑ Power down equipment apart from scale and O_2 analyser.
❑ ❑ ❑ Disconnect thermocouple trunks.
❑ ❑ ❑ Turn off water to cold trap.
❑ ❑ ❑ Turn off water to misting system.

Foam Quality Measurements

Date of runs :
Foam Type [delete appropriate] : Class A/CAFS

Foam Expansion

Container mass : g

Container plus foam mass : g

Mass of foam : g

Volume of foam : ml

Expansion ratio = volume/mass =

Drainage Time

Container mass : g

Time [s]							
Mass [g]							
Time [s]							
Mass [g]							
Time [s]							
Mass [g]							

Final mass of container plus foam : g
Total mass of foam : g

Time to drain 25% of the foam : s

Appendix 3 Weather

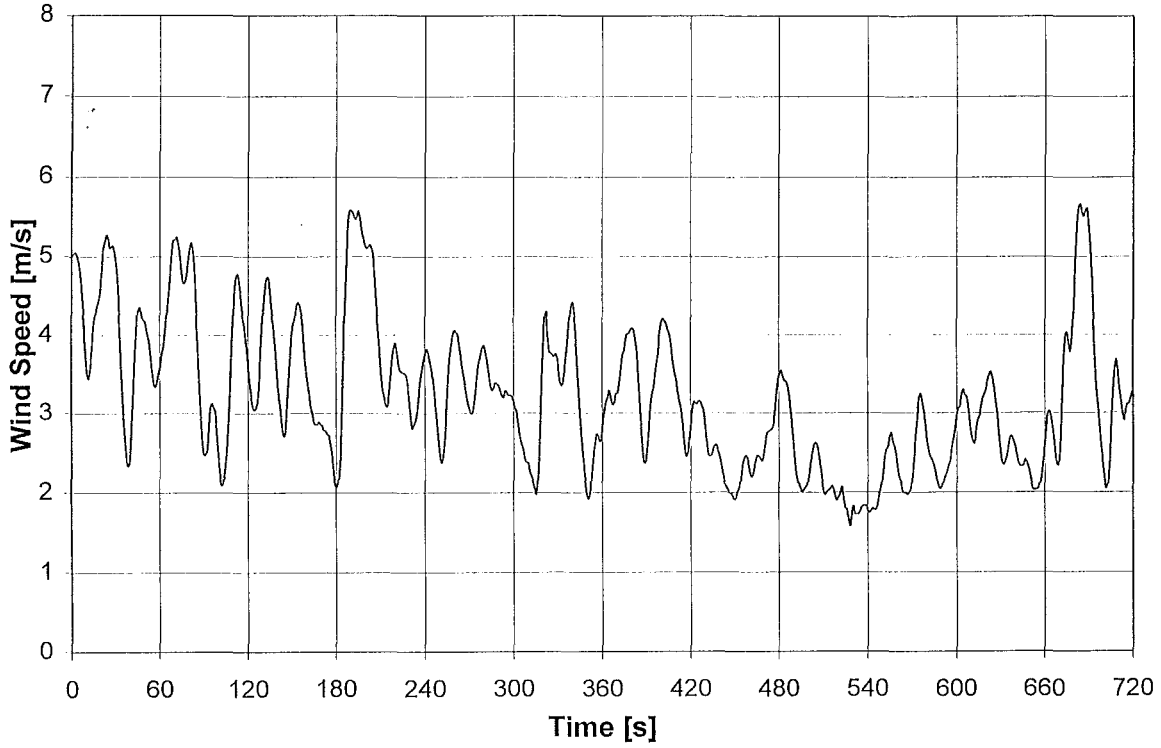

Wind Speed, CAFS, 27/11/97

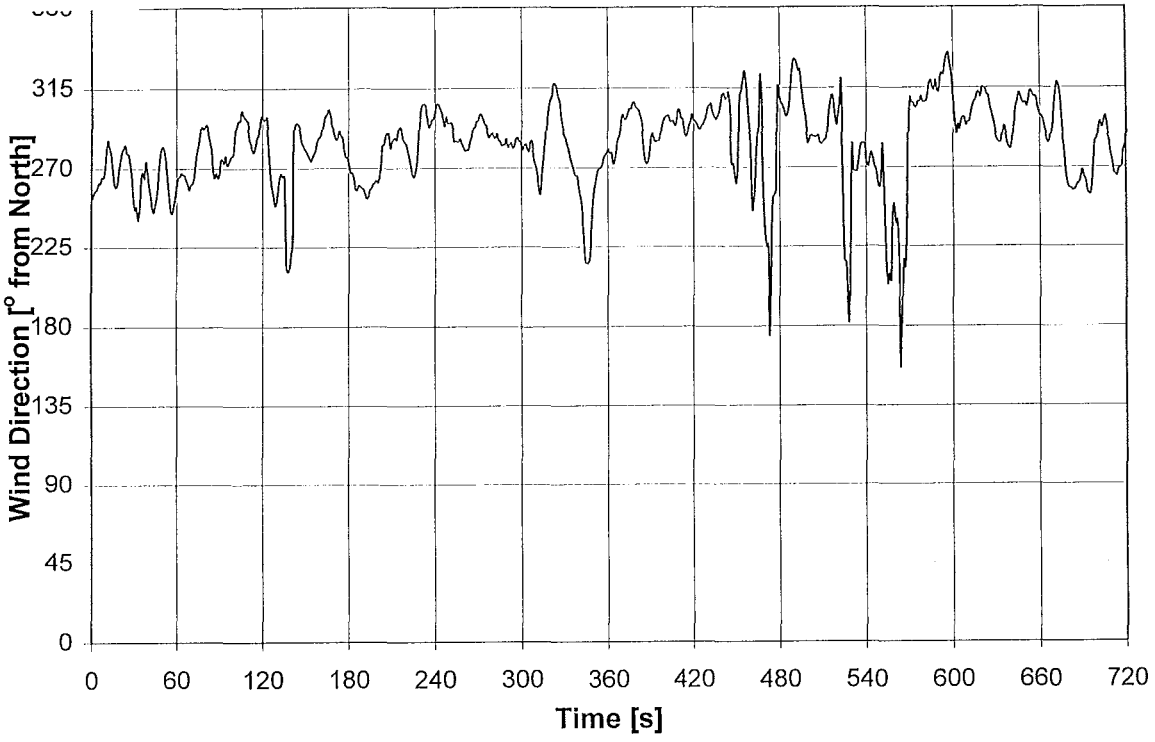

Wind Direction, CAFS, 27/11/97

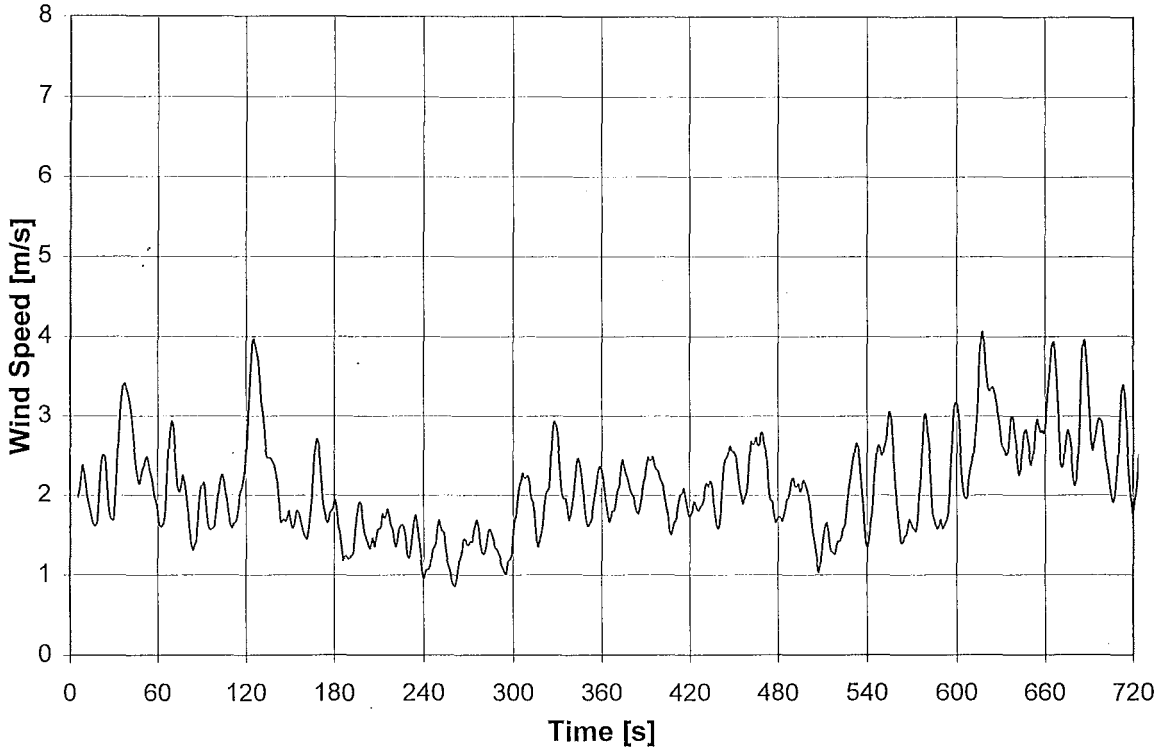

Wind Speed, CAFS, 2/12/97

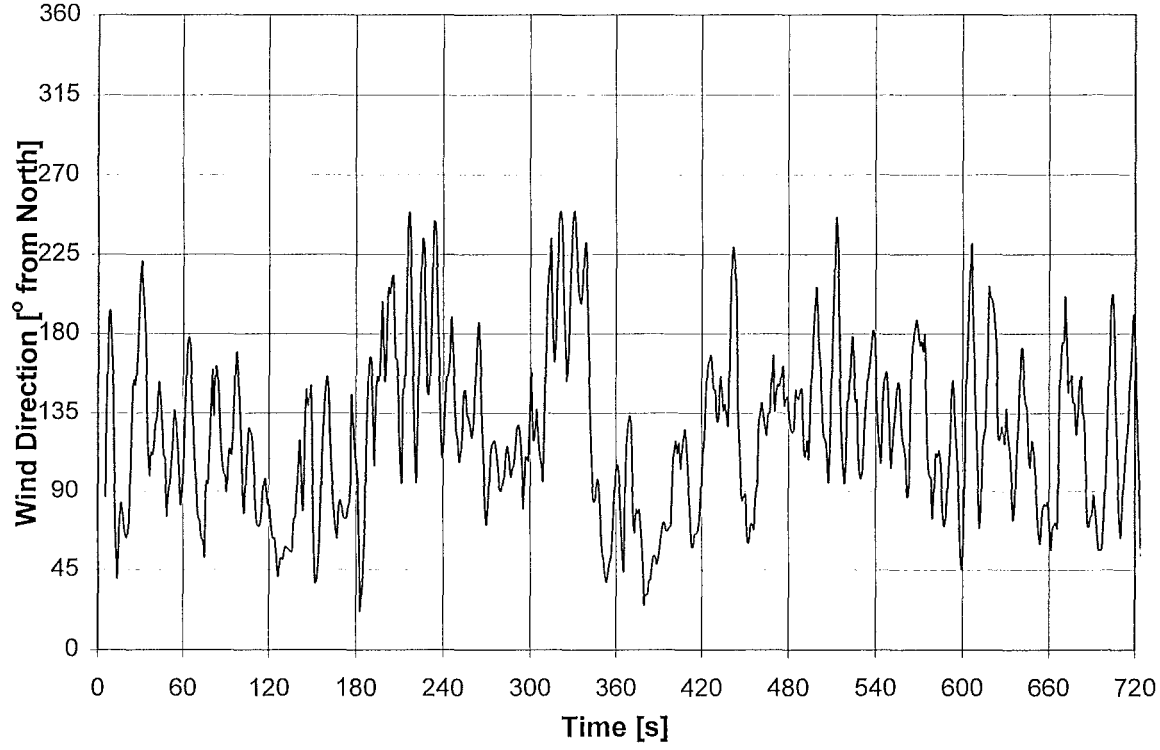

Wind Direction, CAFS, 2/12/97

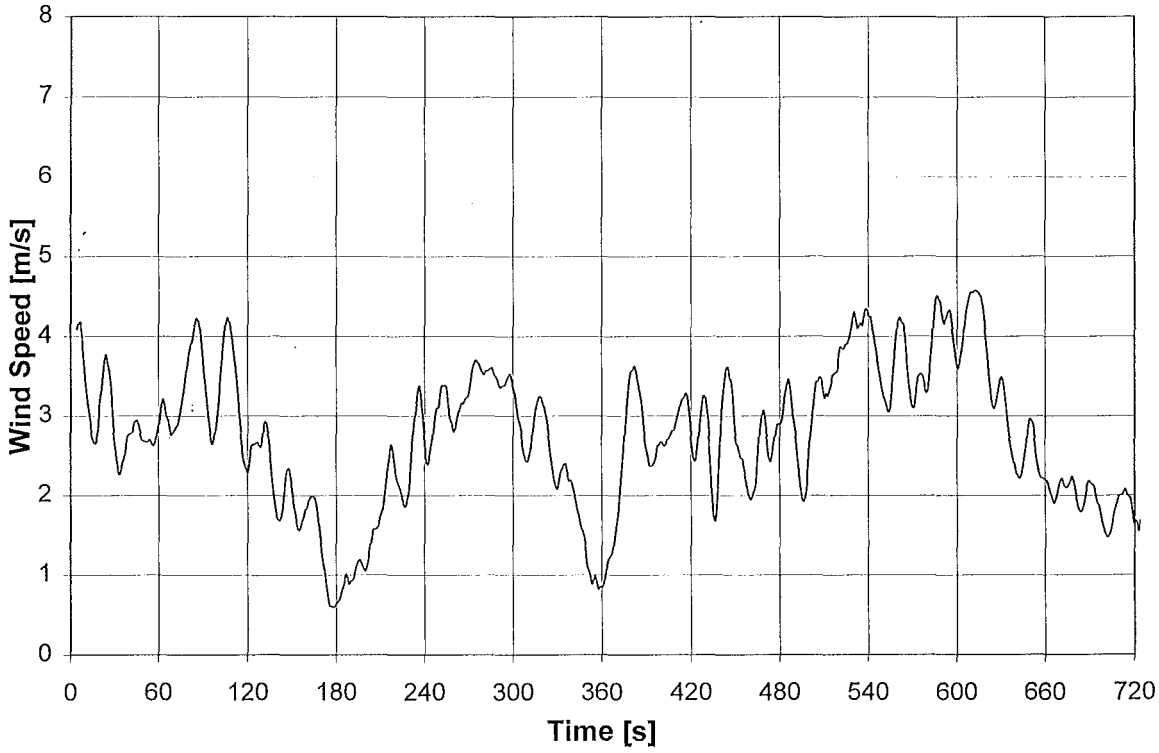

Wind Speed, CAFS, 12/12/97

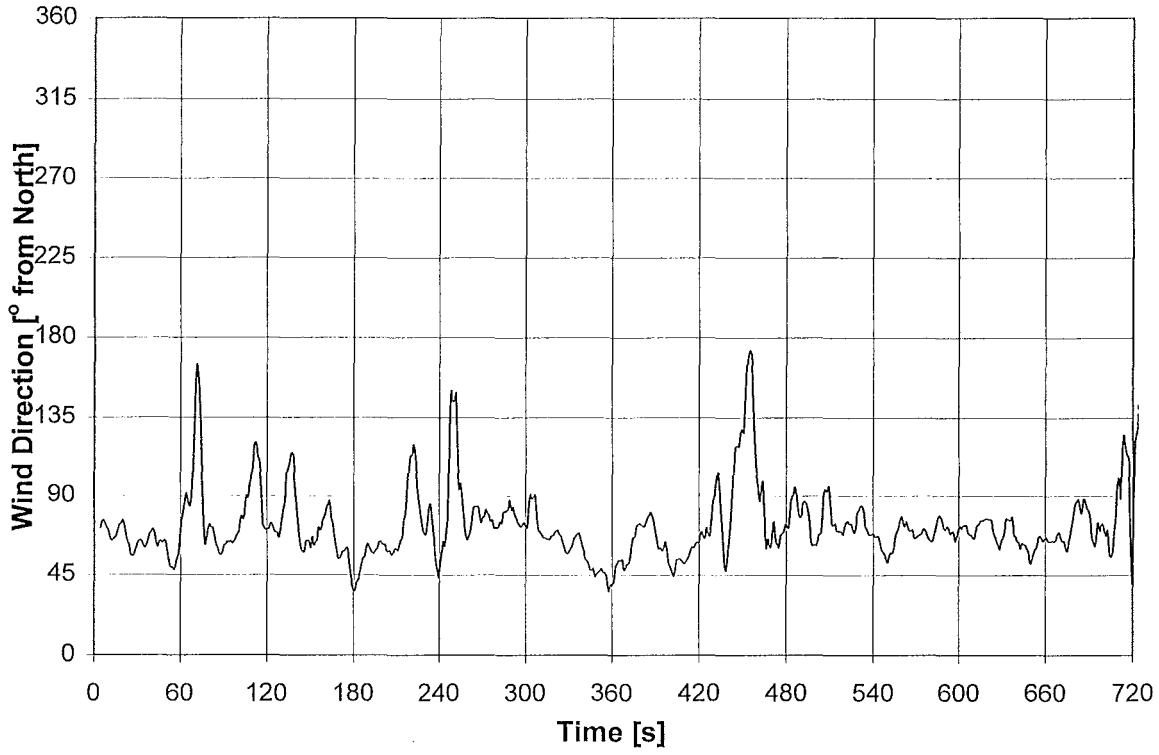

Wind Direction, CAFS, 12/12/97

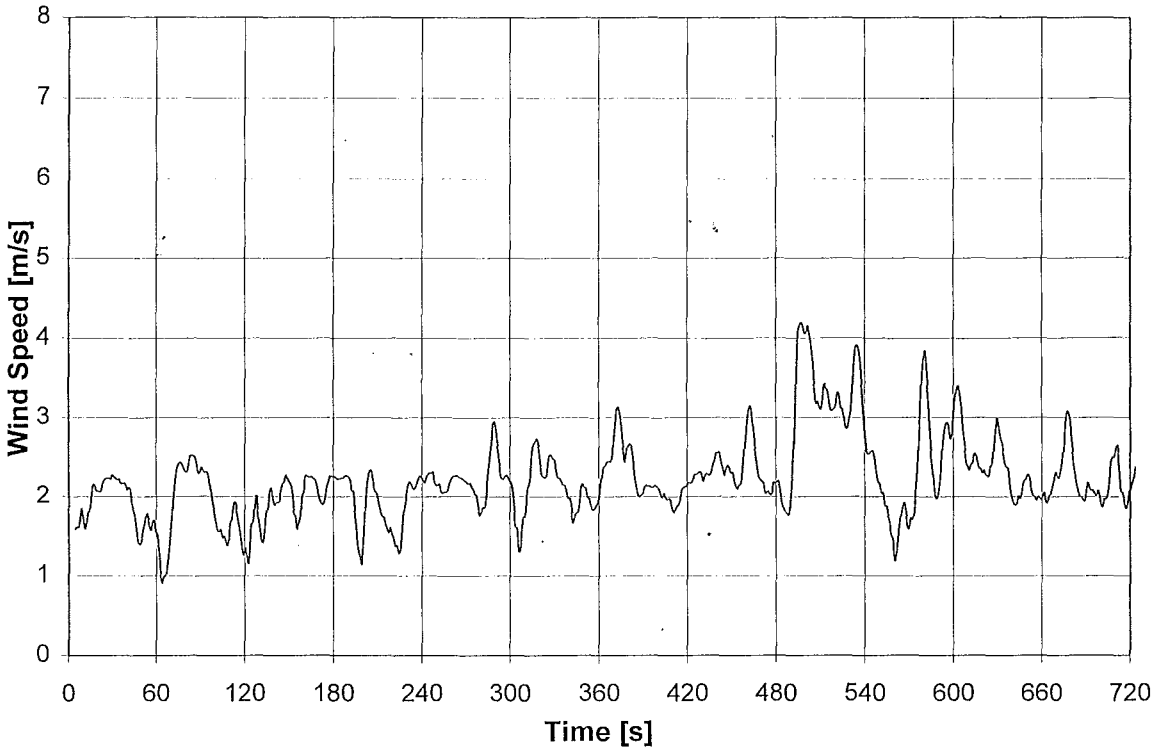

Wind Speed, HPD, 27/11/97

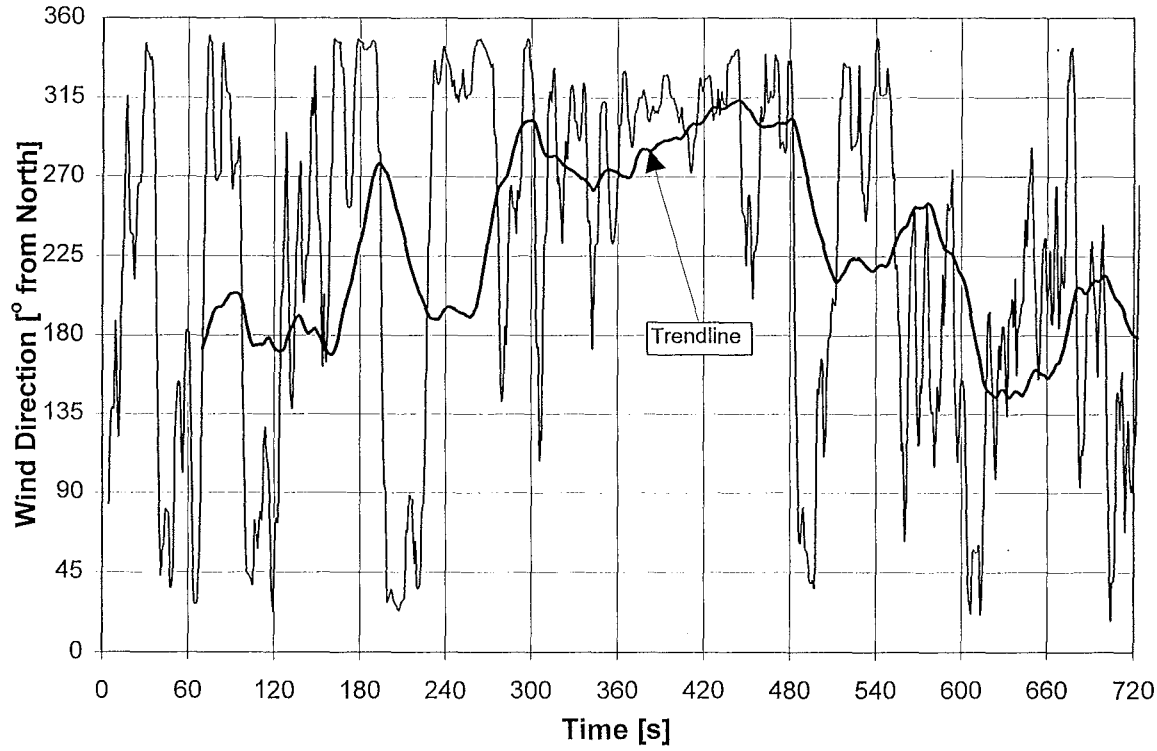

Wind Direction, HPD, 27/11/97

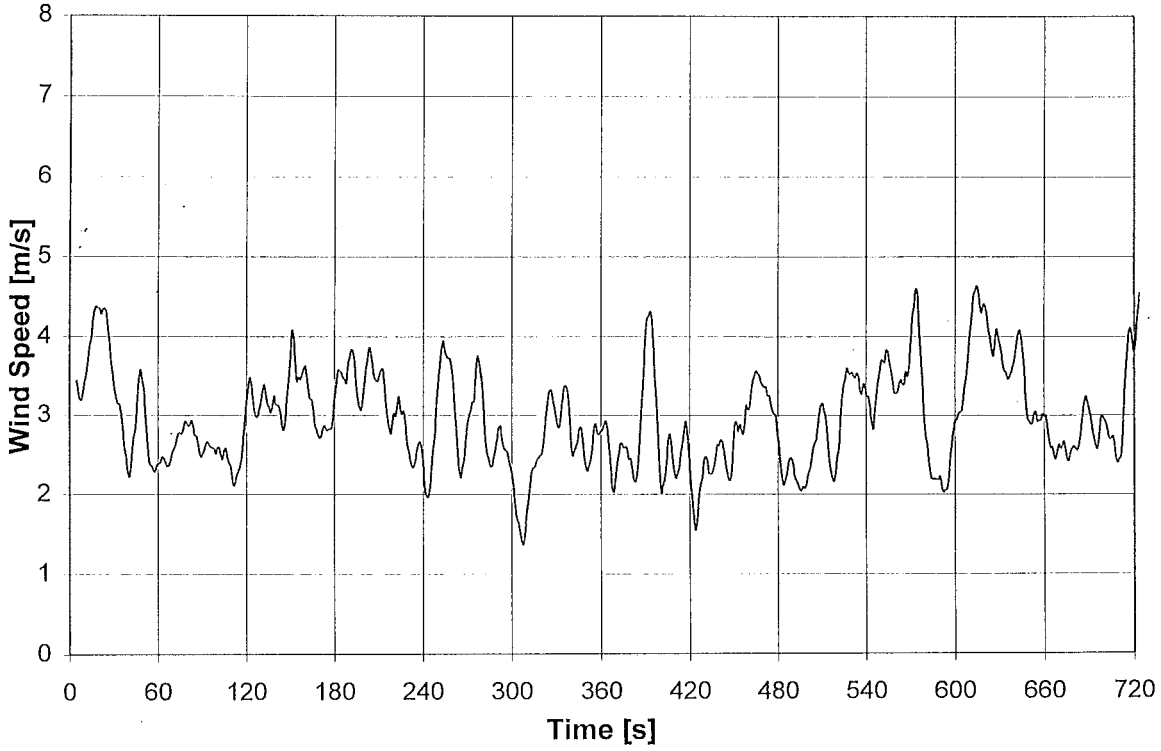

Wind Speed, HPD, 2/12/97

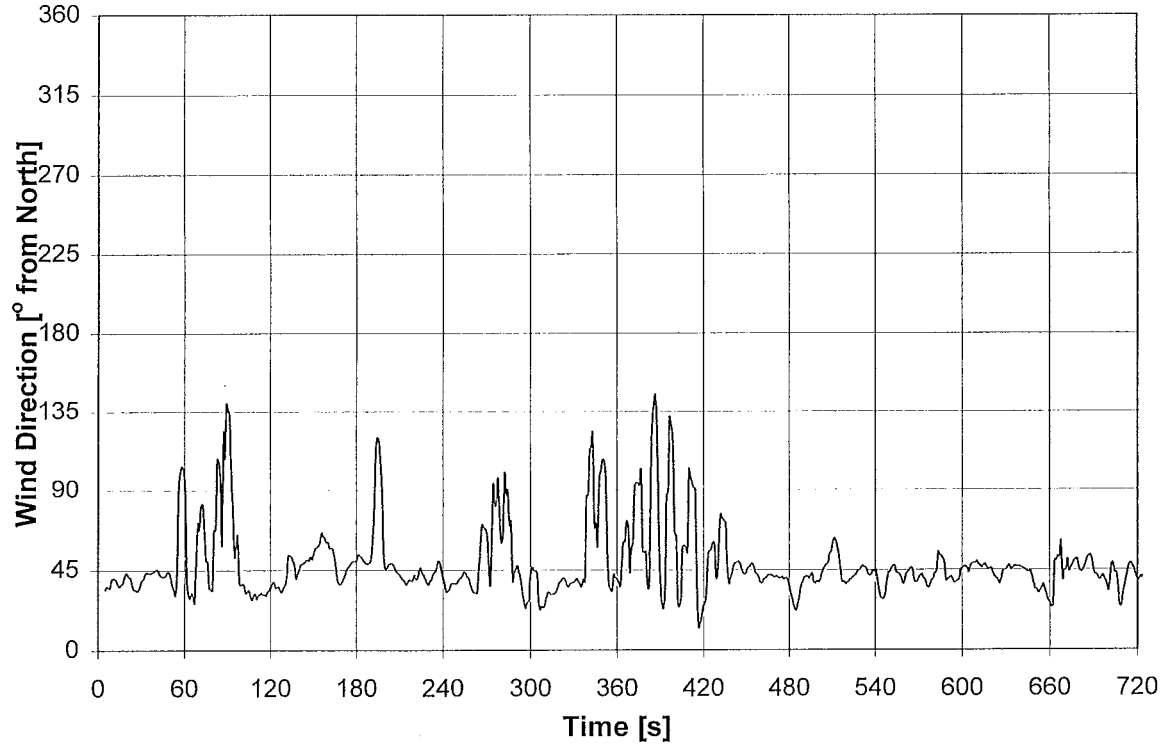

Wind Direction, HPD, 2/12/97

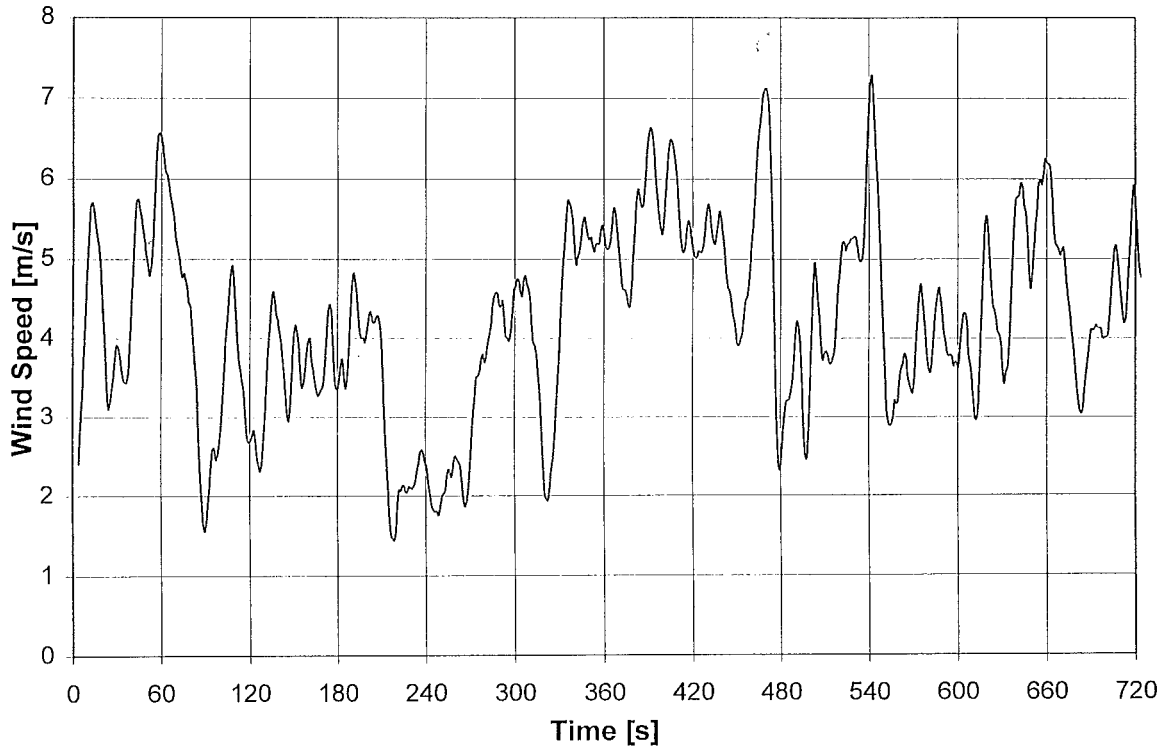

Wind Speed, HPD, 12/12/97

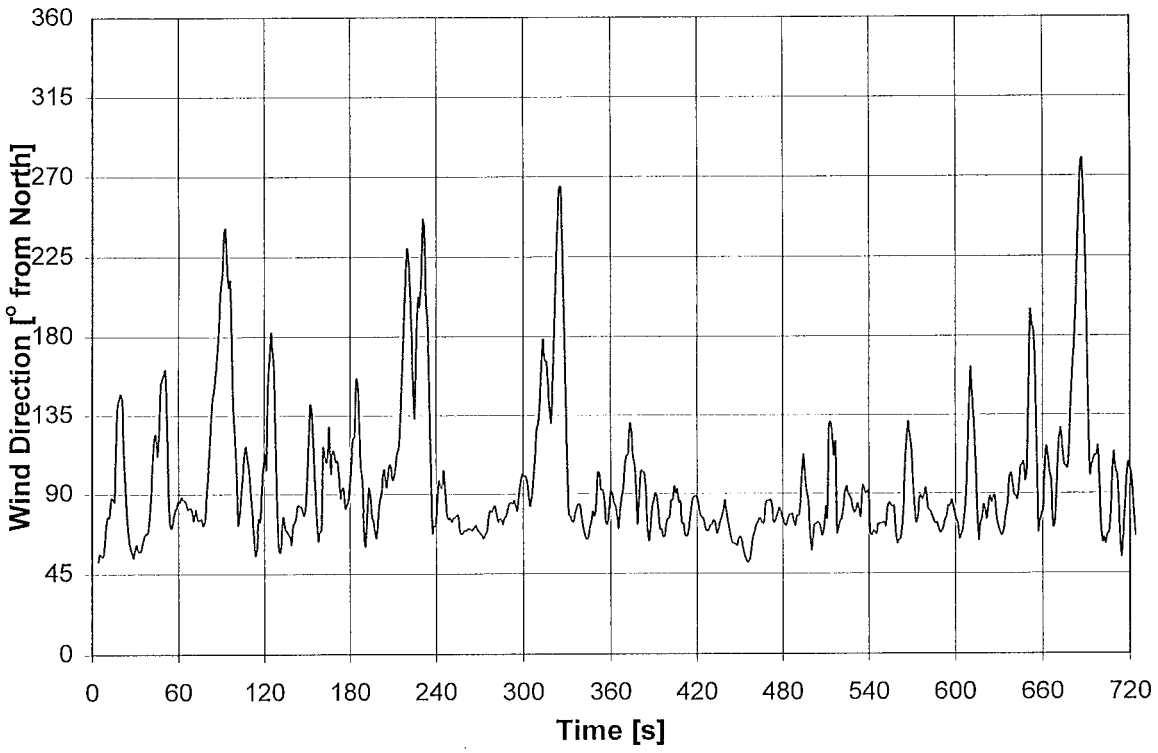

Wind Direction, HPD, 12/12/97

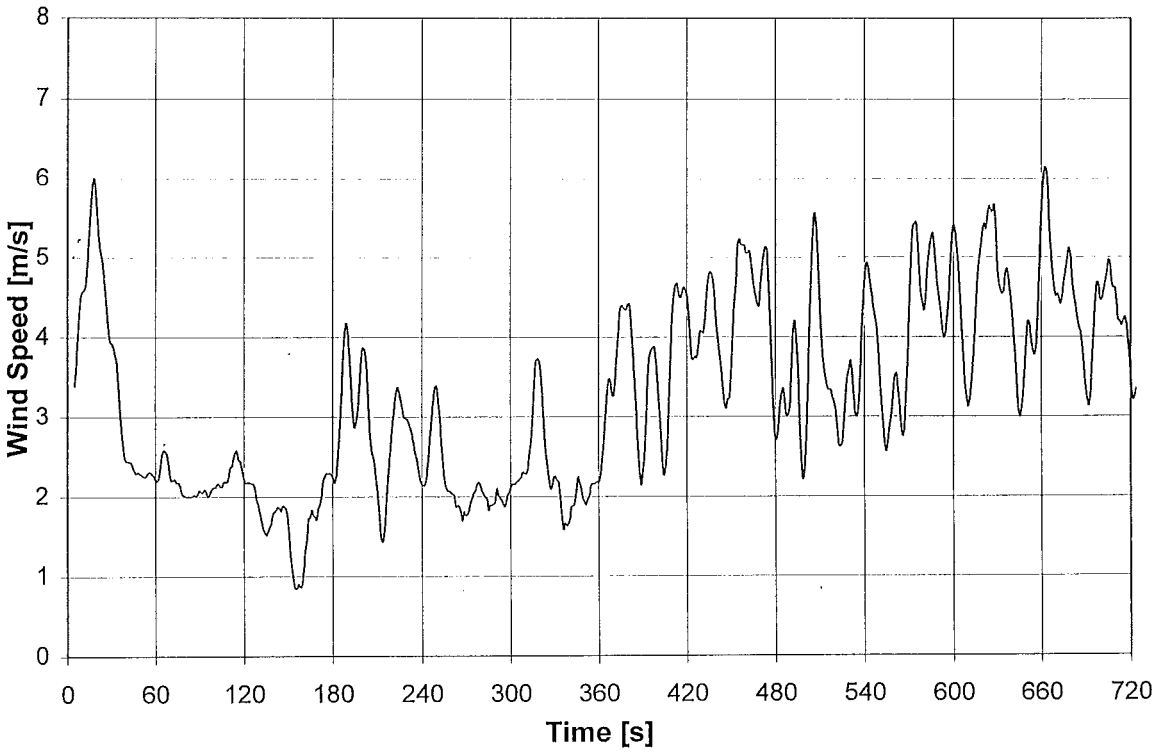

Wind Speed, Solution, 27/11/97

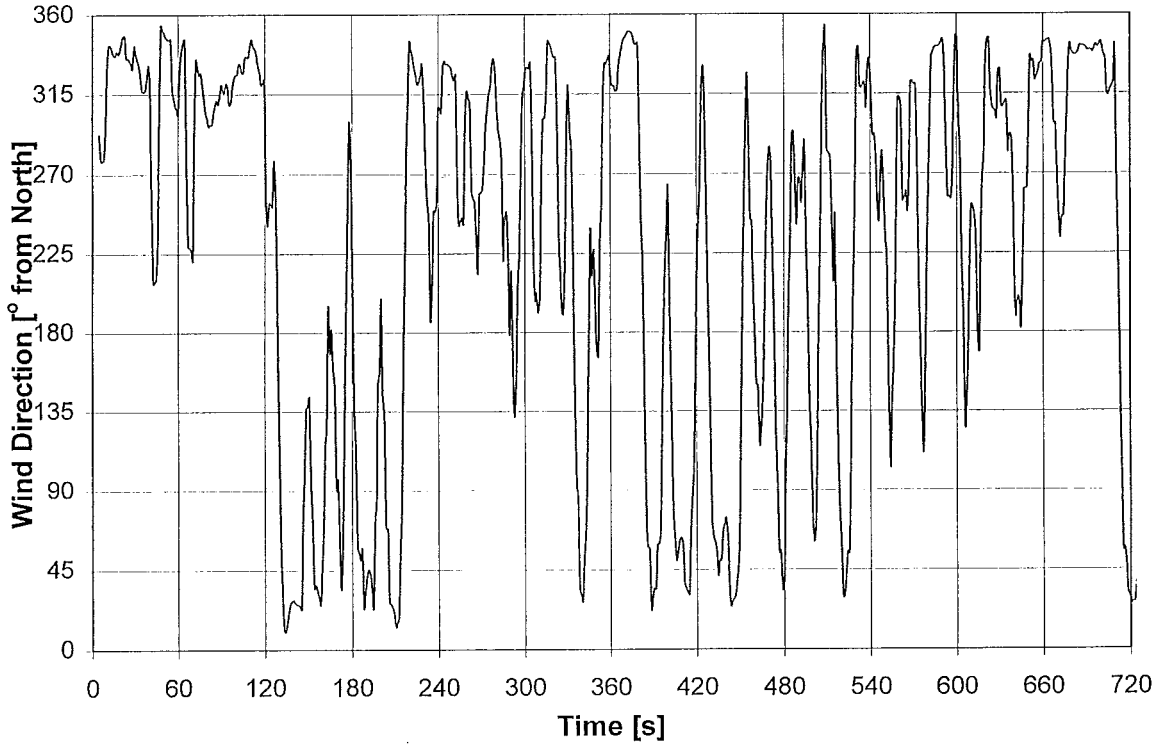

Wind Direction, Solution, 27/11/97

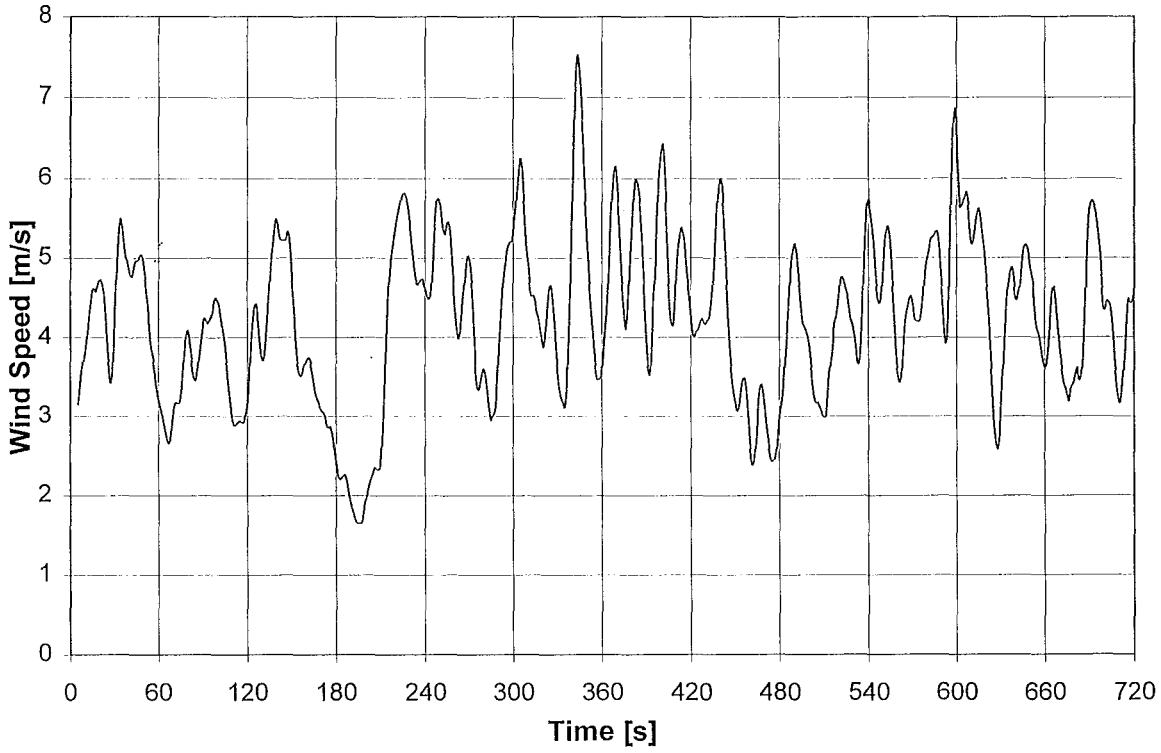

Wind Speed, Solution, 2/12/97

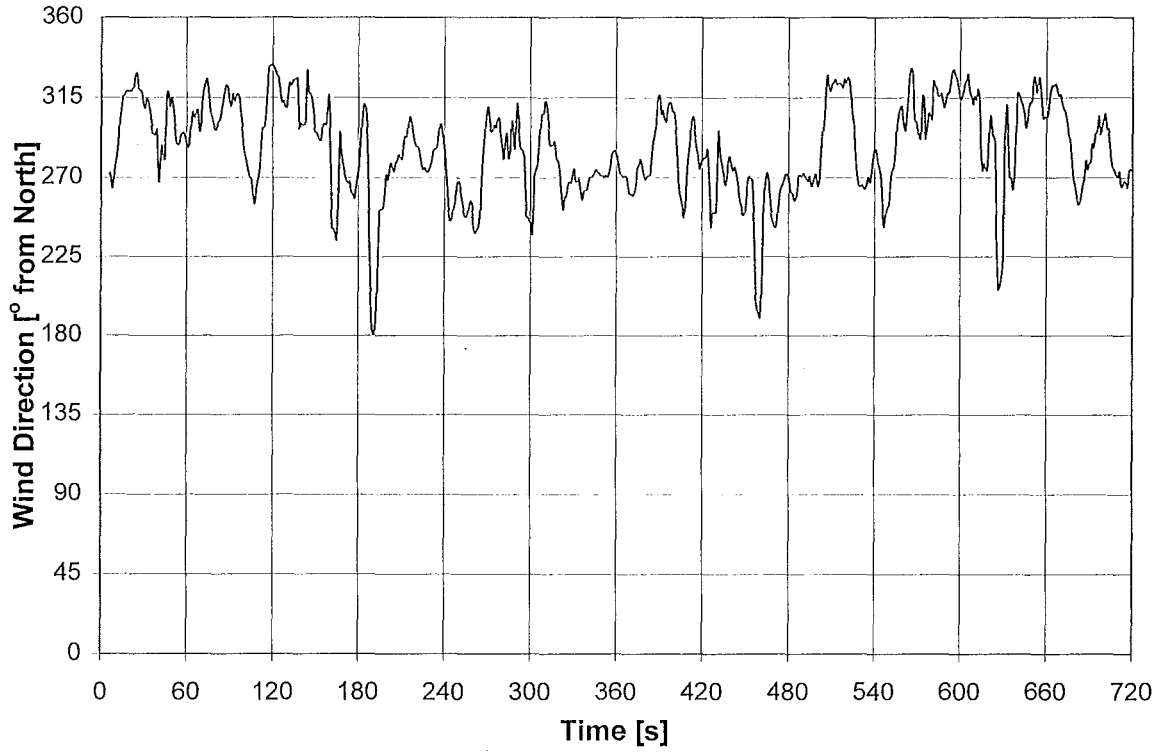

Wind Direction, Solution, 2/12/97

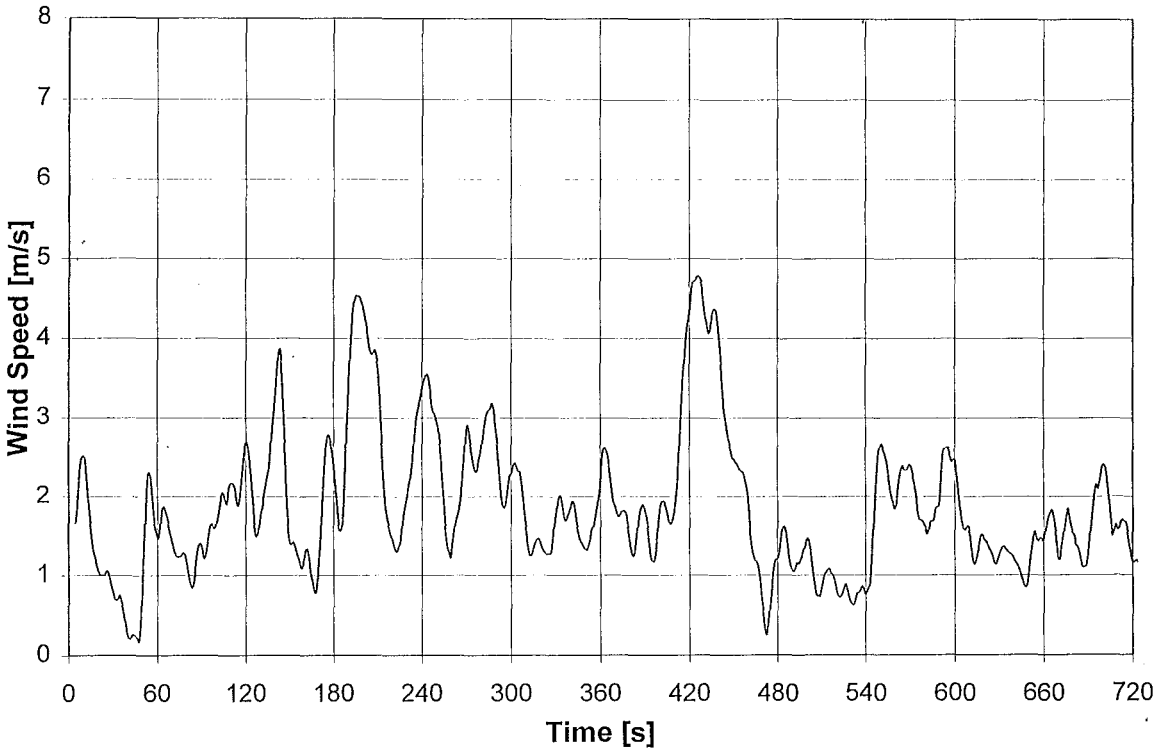

Wind Speed, Solution, 12/12/97

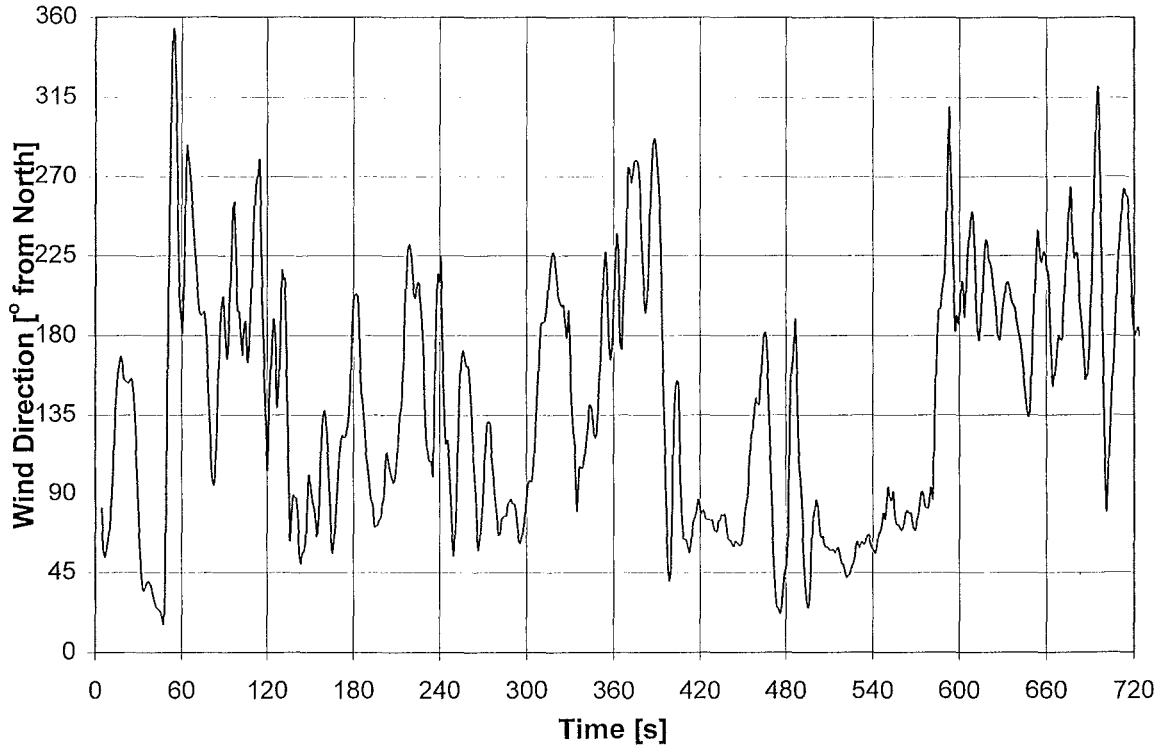

Wind Direction, Solution, 12/12/97

Appendix 4 Crib and Compartment Temperatures

(Start Overleaf)

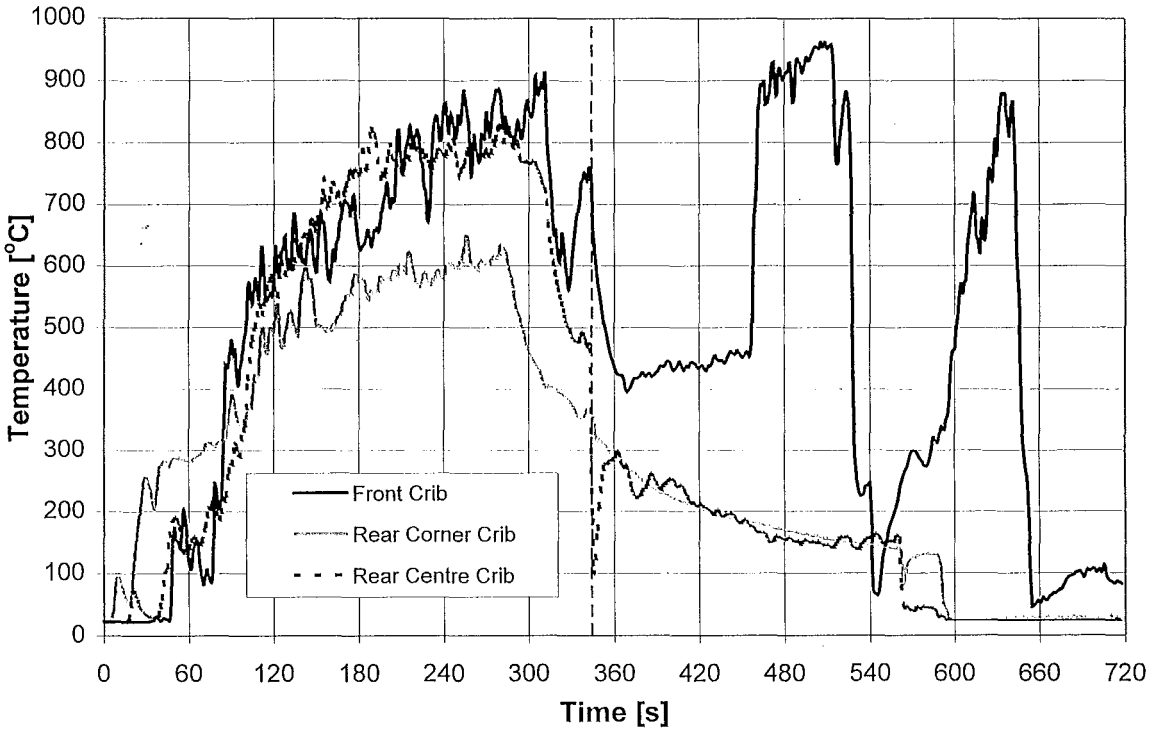

Crib Temperatures, CAFS, 27/11/97

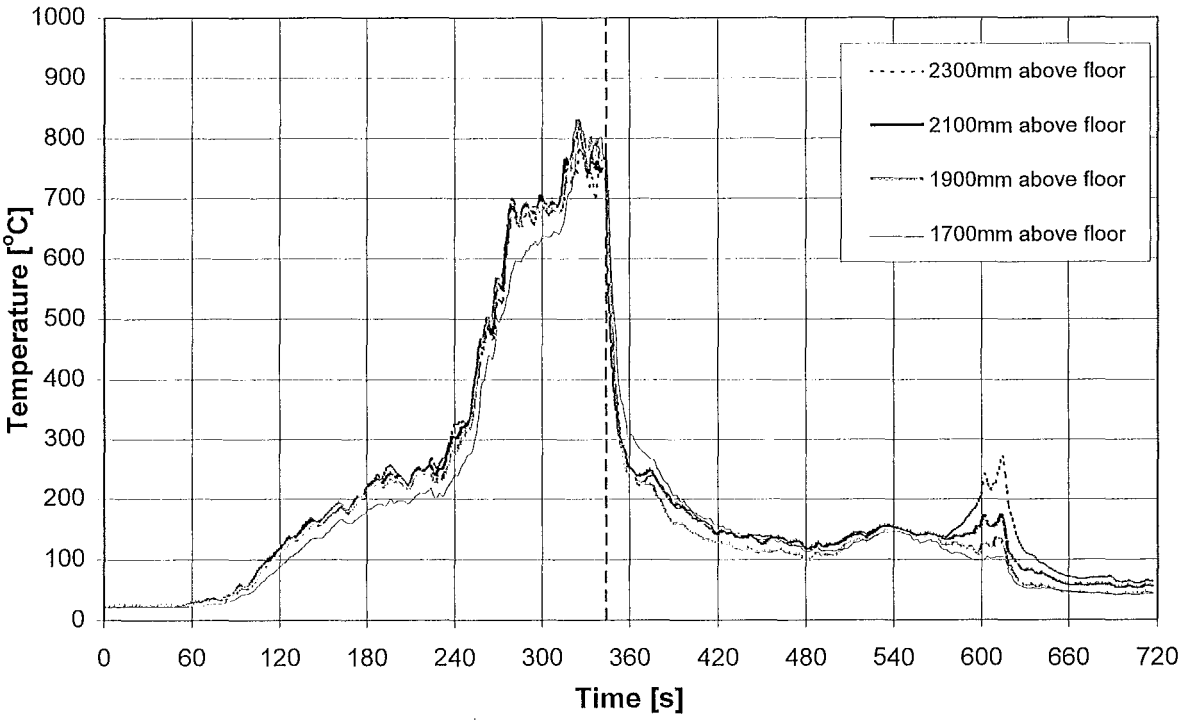

Thermocouple Tree, CAFS, 27/11/97

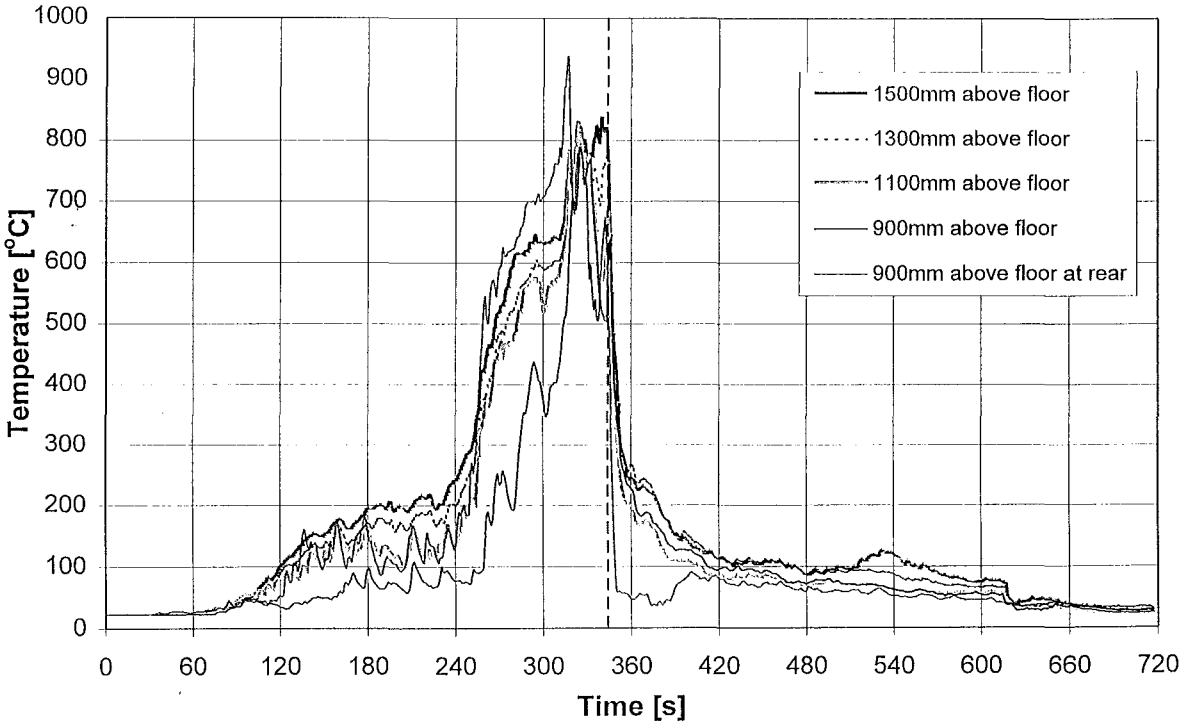

Thermocouple Tree, CAFS, 27/11/97

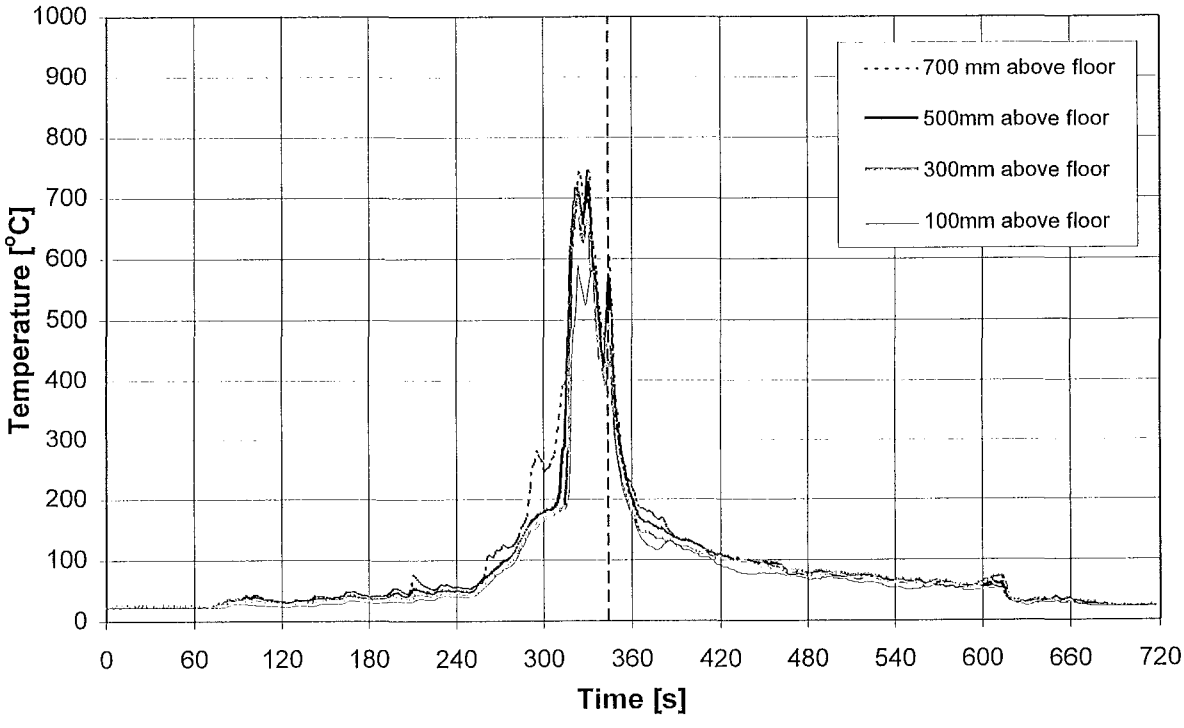

Thermocouple Tree, CAFS, 27/11/97

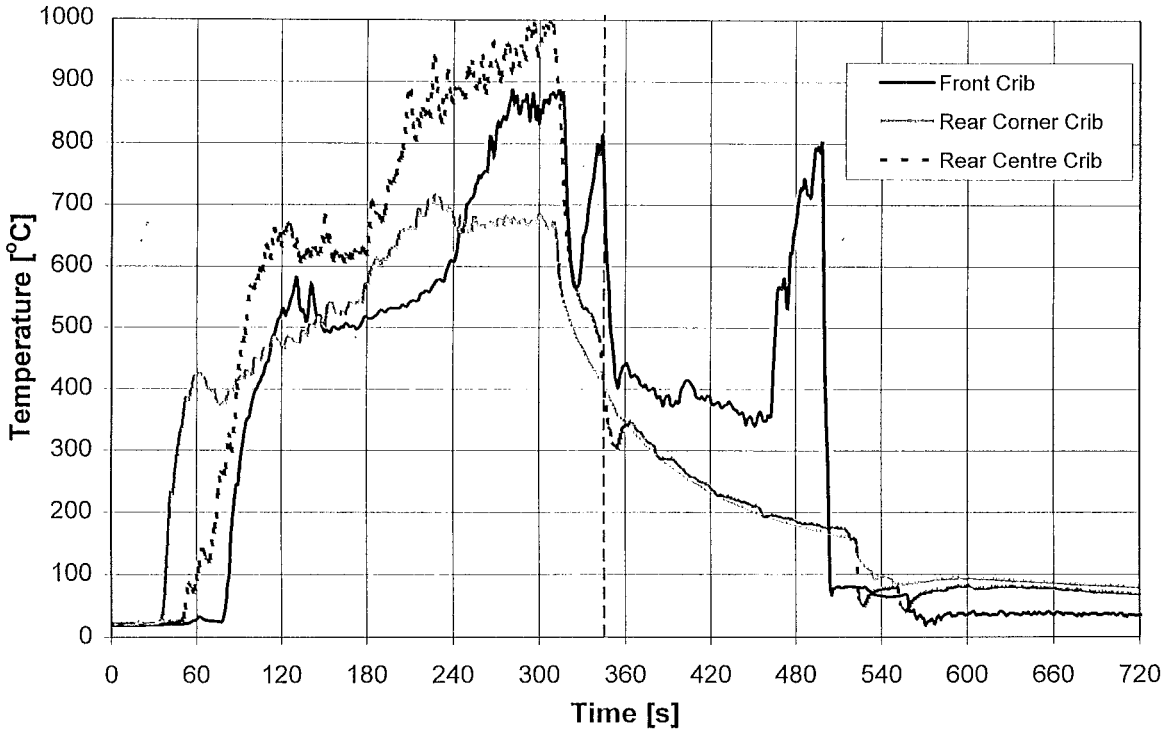

Crib Temperatures, CAFS, 2/12/97

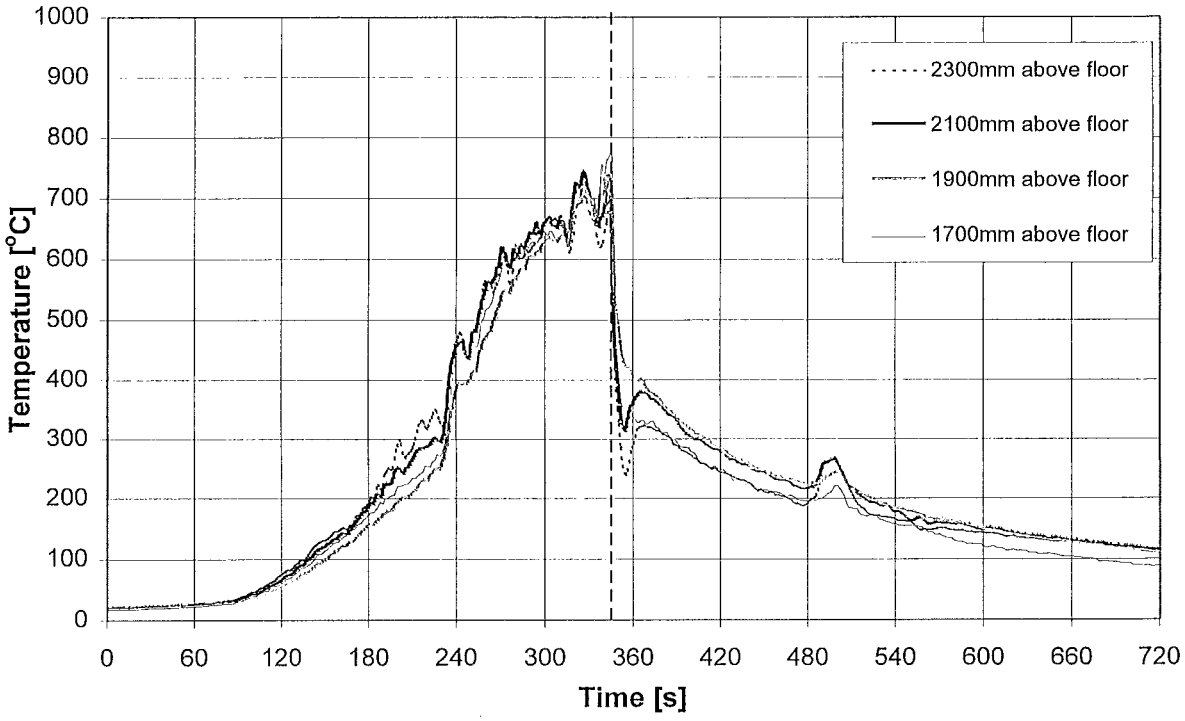

Thermocouple Tree, CAFS, 2/12/97

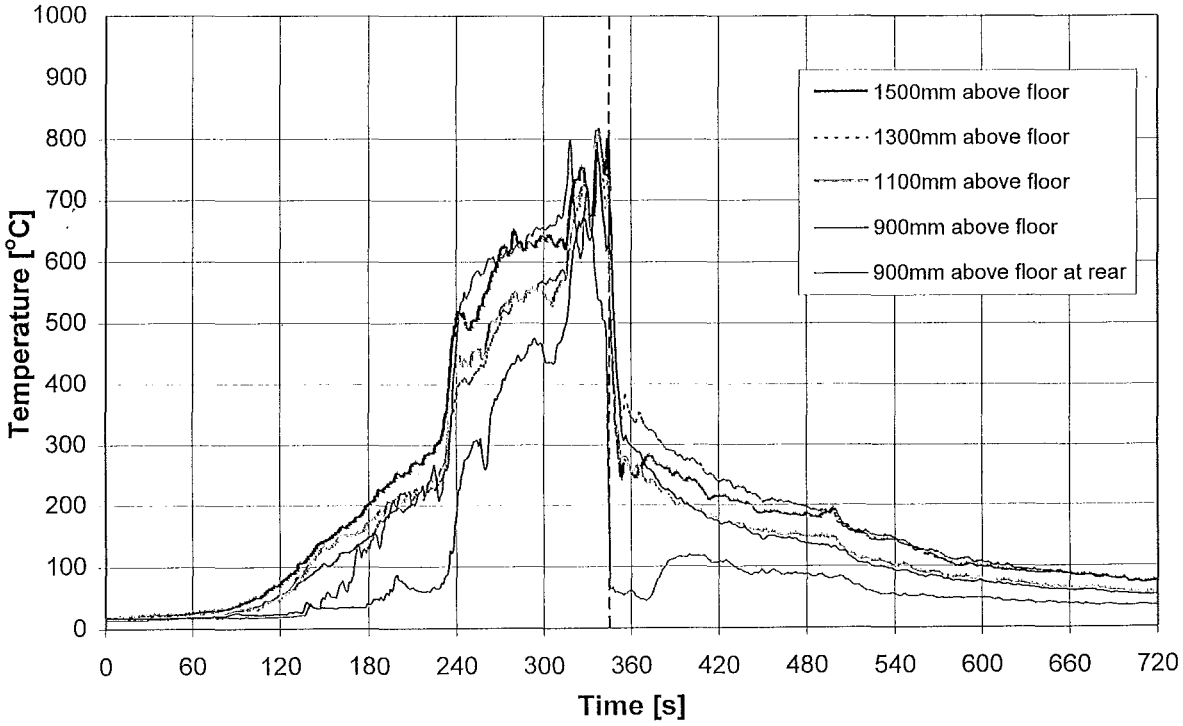

Thermocouple Tree, CAFS, 2/12/97

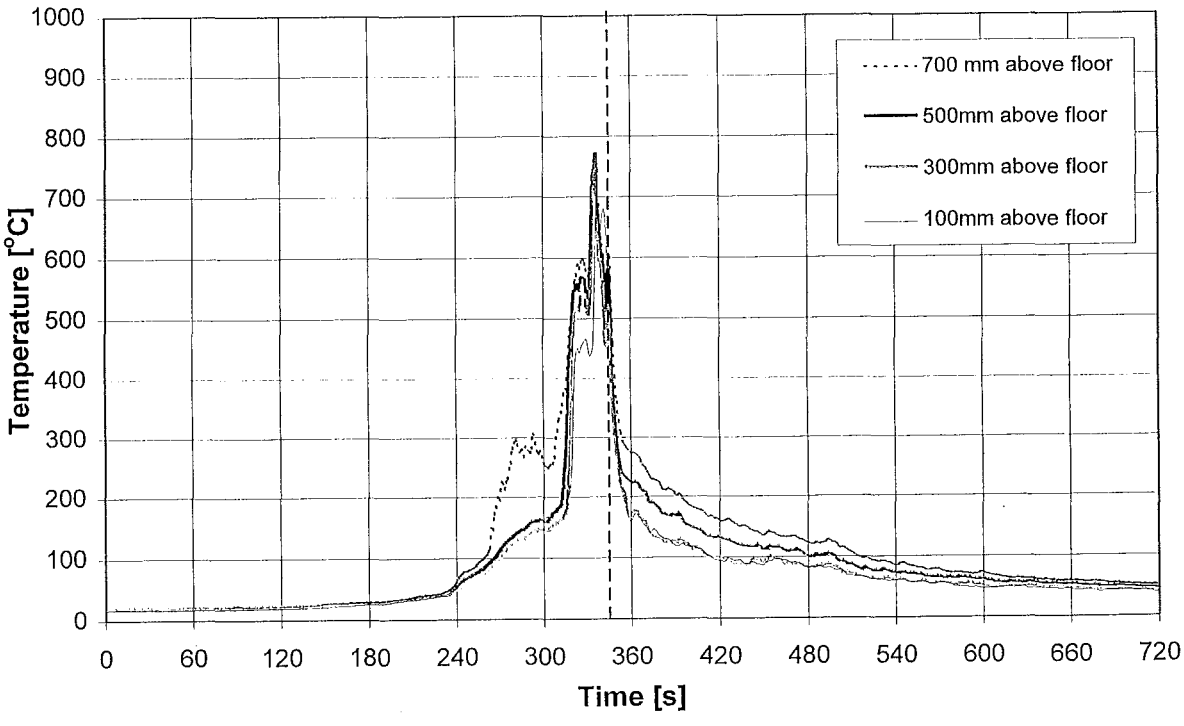

Thermocouple Tree, CAFS, 2/12/97

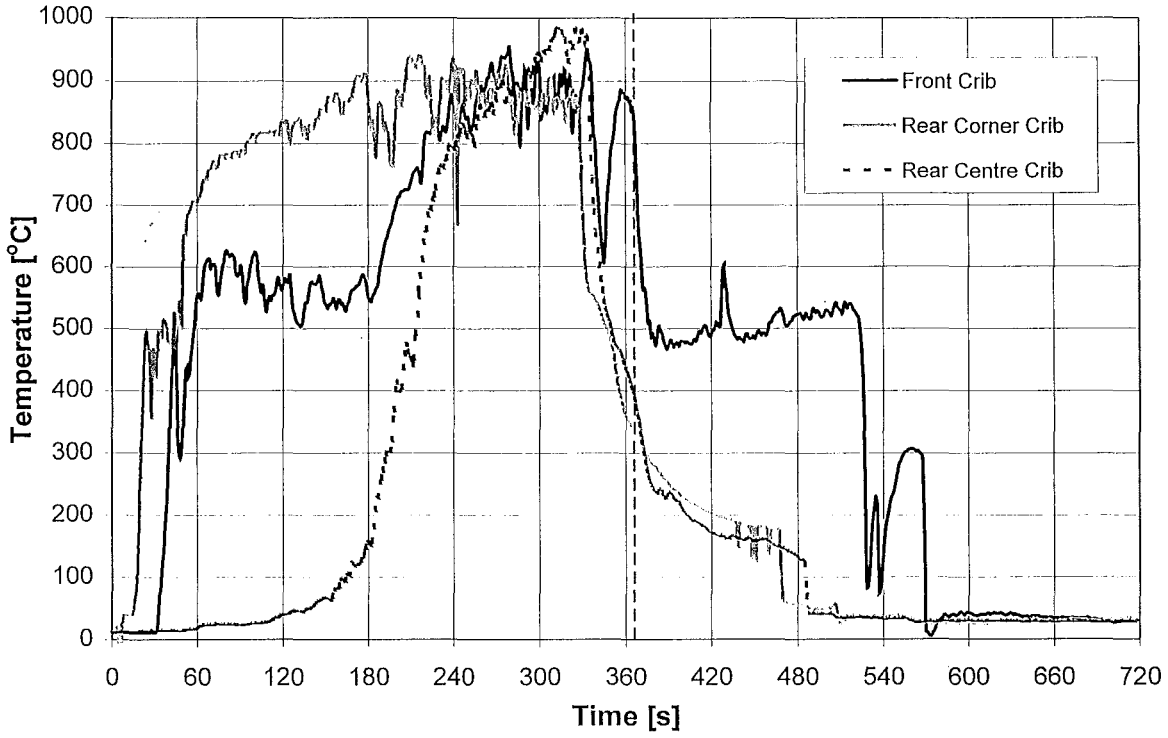

Crib Temperatures, CAFS, 12/12/97

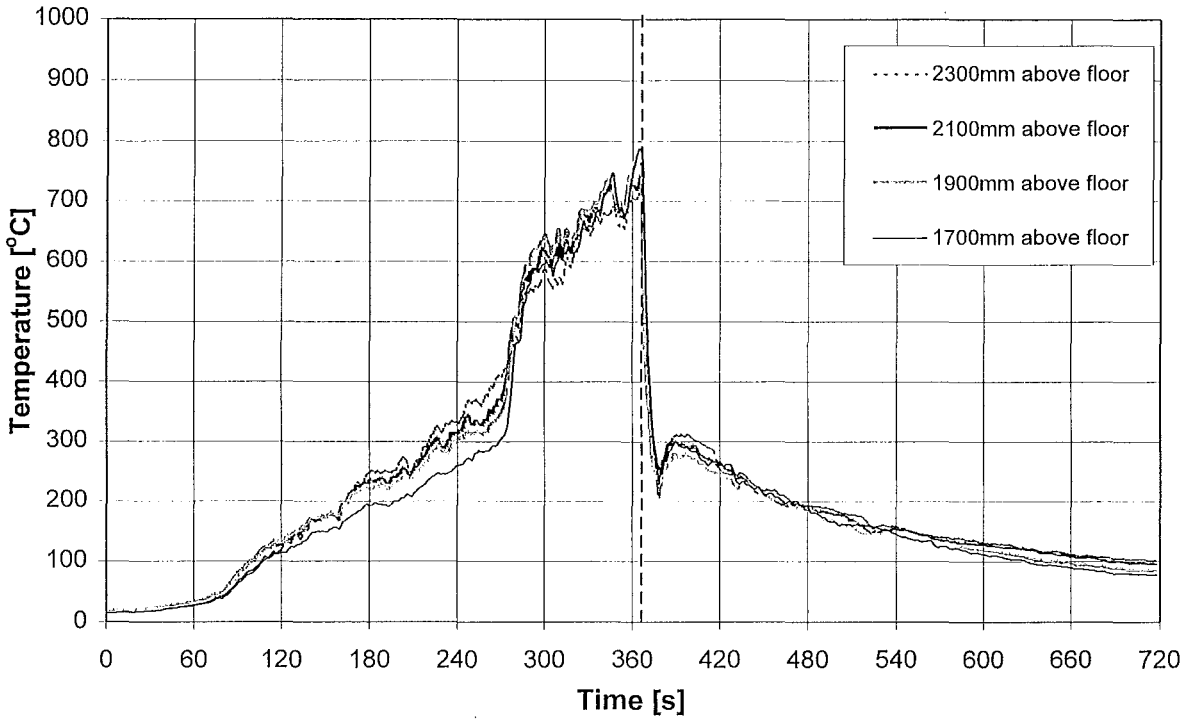

Thermocouple Tree, CAFS, 12/12/97

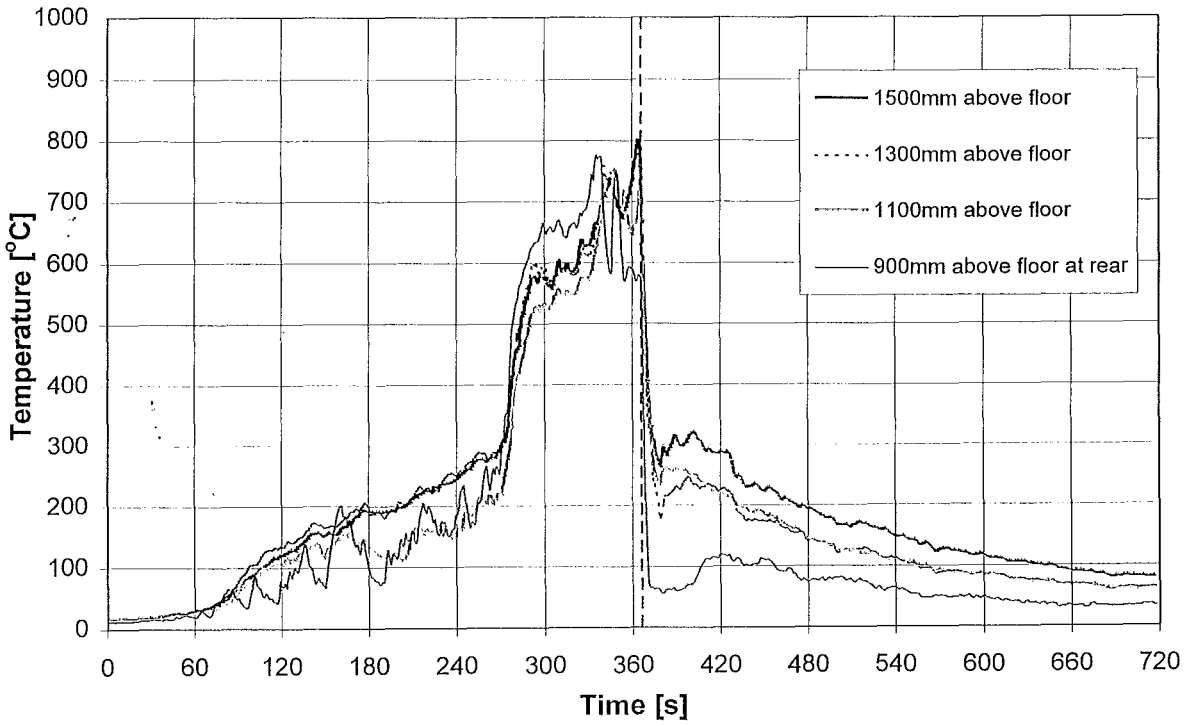

Thermocouple Tree, CAFS, 12/12/97

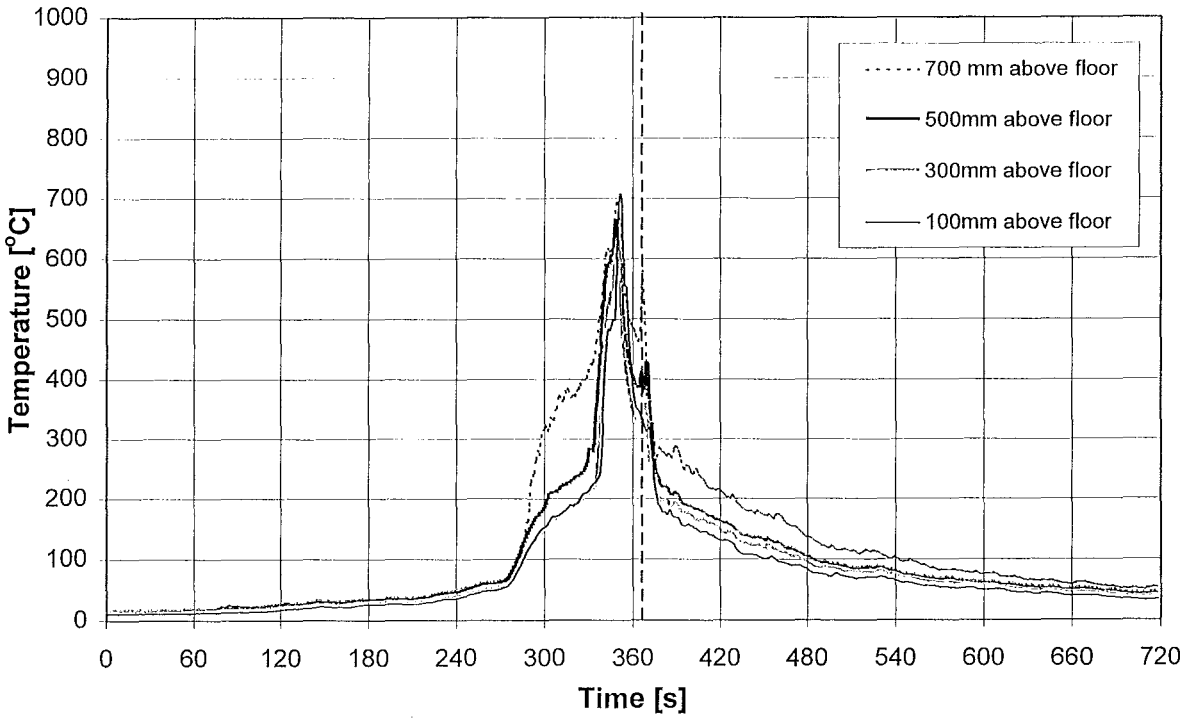

Thermocouple Tree, CAFS, 12/12/97

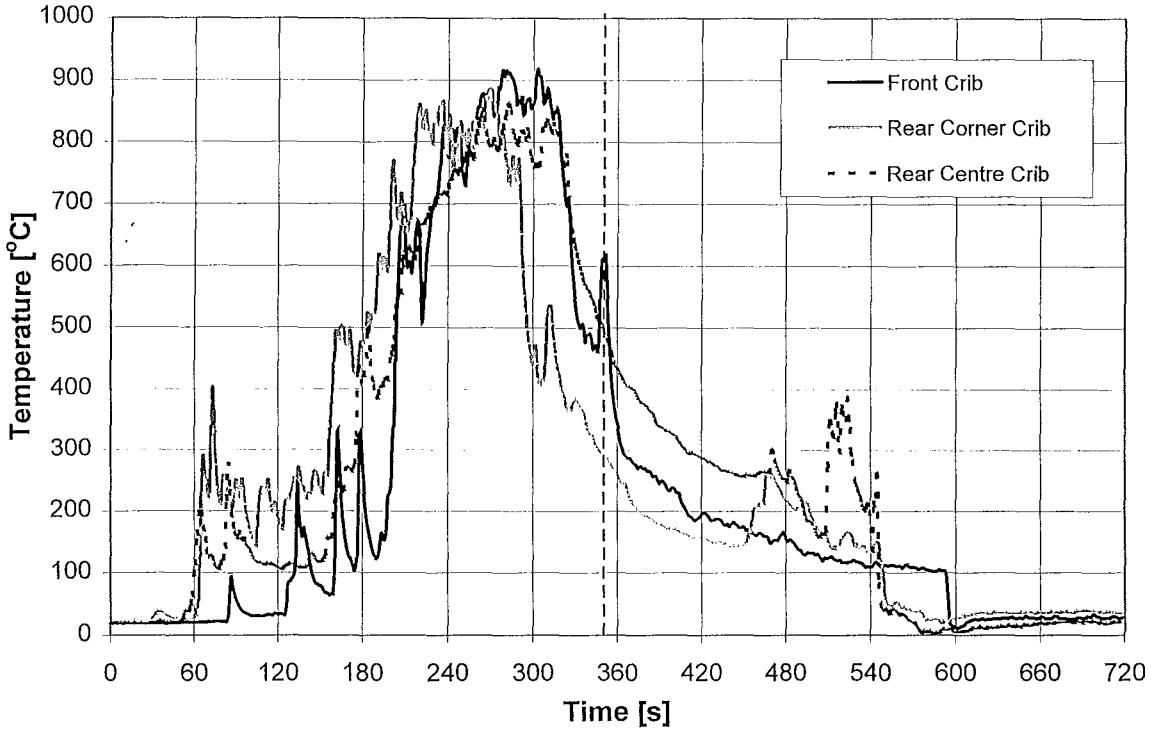

Crib Temperatures, HPD, 27/11/97

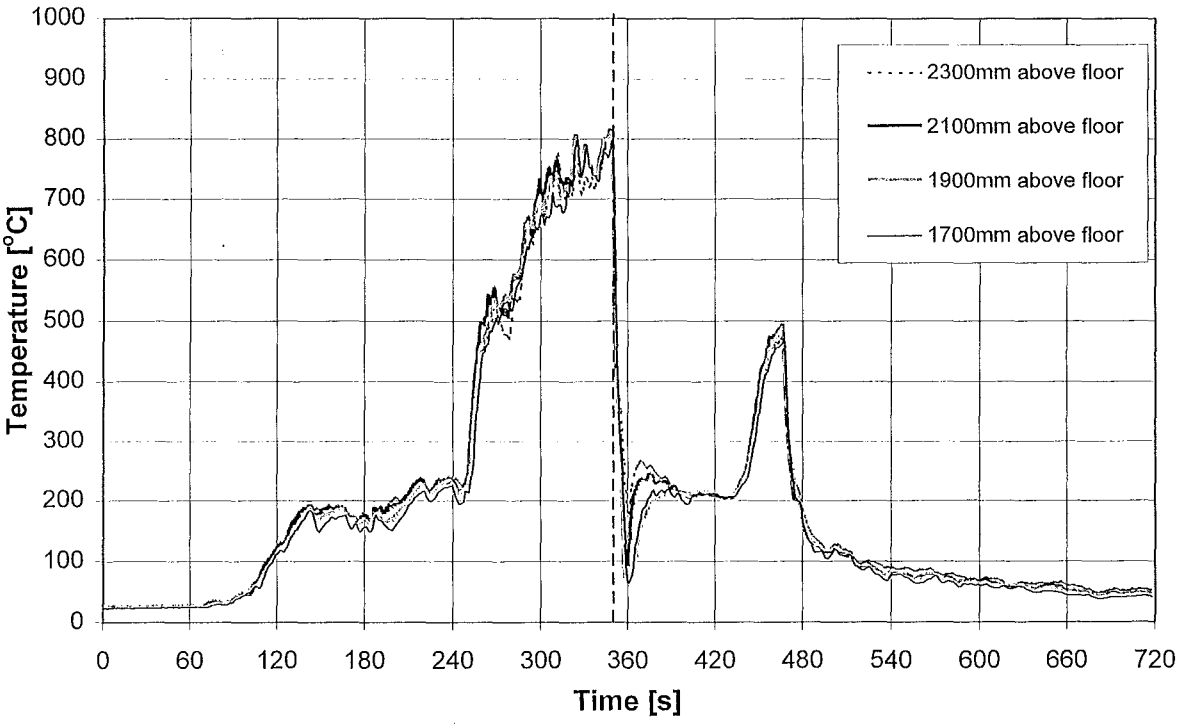

Thermocouple Tree, HPD, 27/11/97

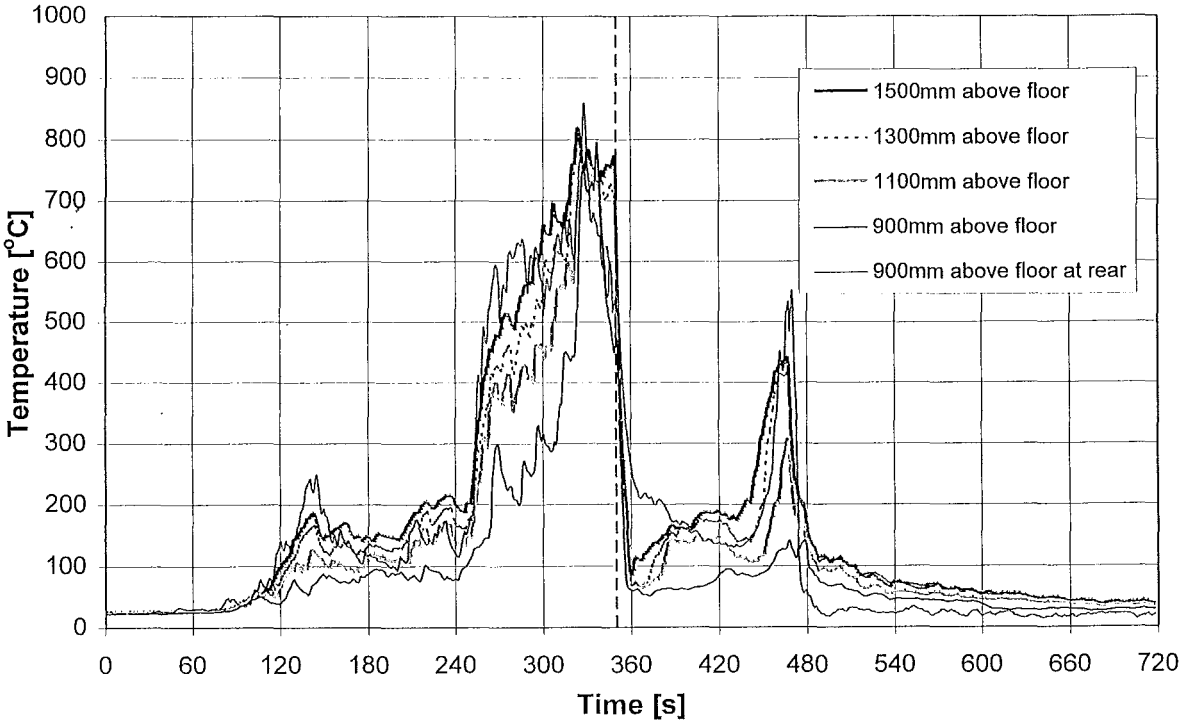

Thermocouple Tree, HPD, 27/11/97

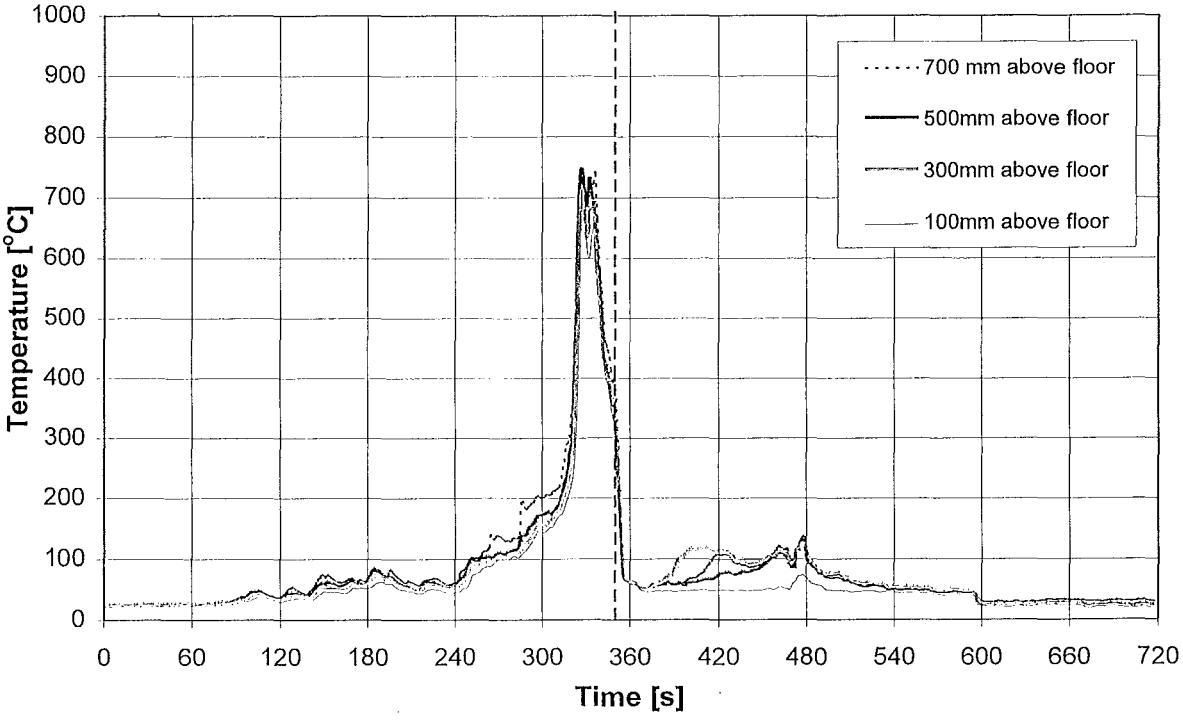

Thermocouple Tree, HPD, 27/11/97

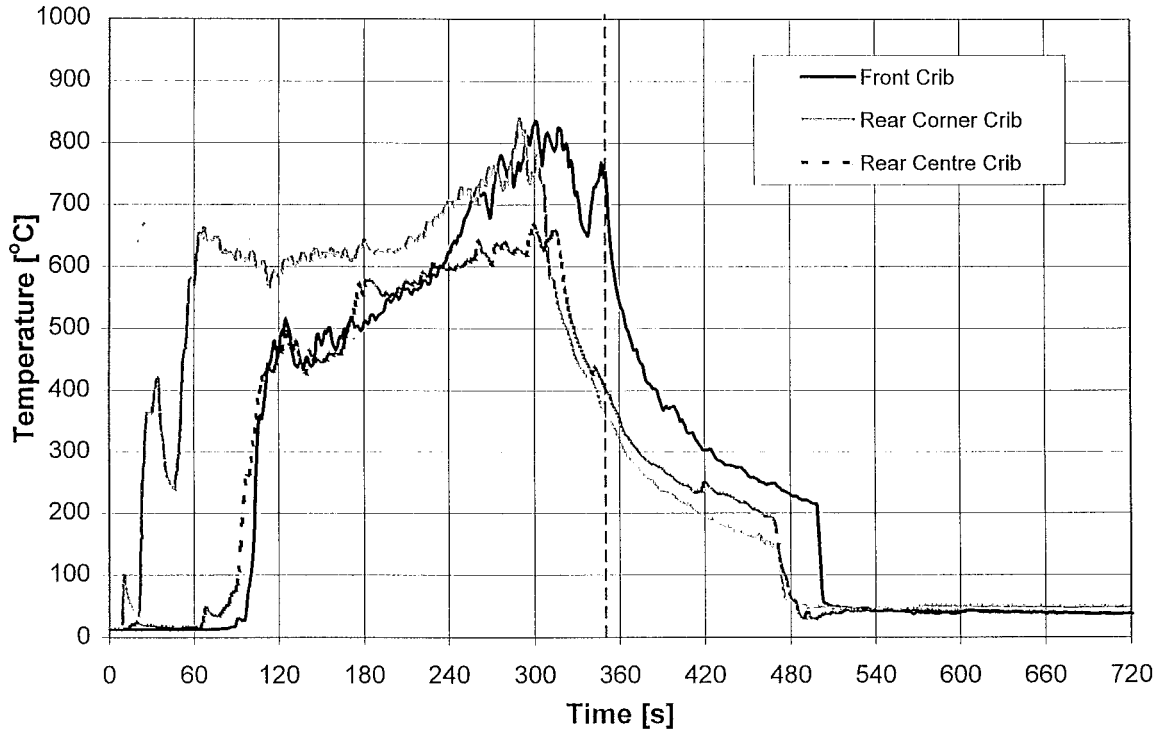

Crib Temperatures, HPD, 2/12/97

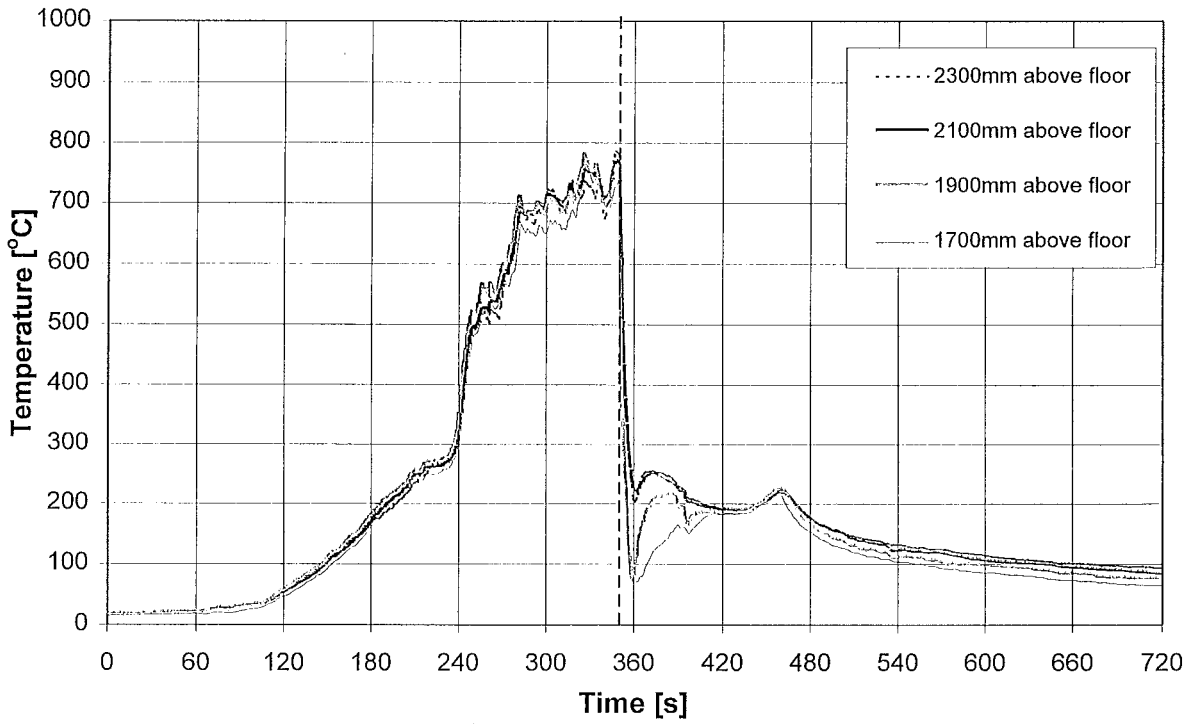

Thermocouple Tree, HPD, 2/12/97

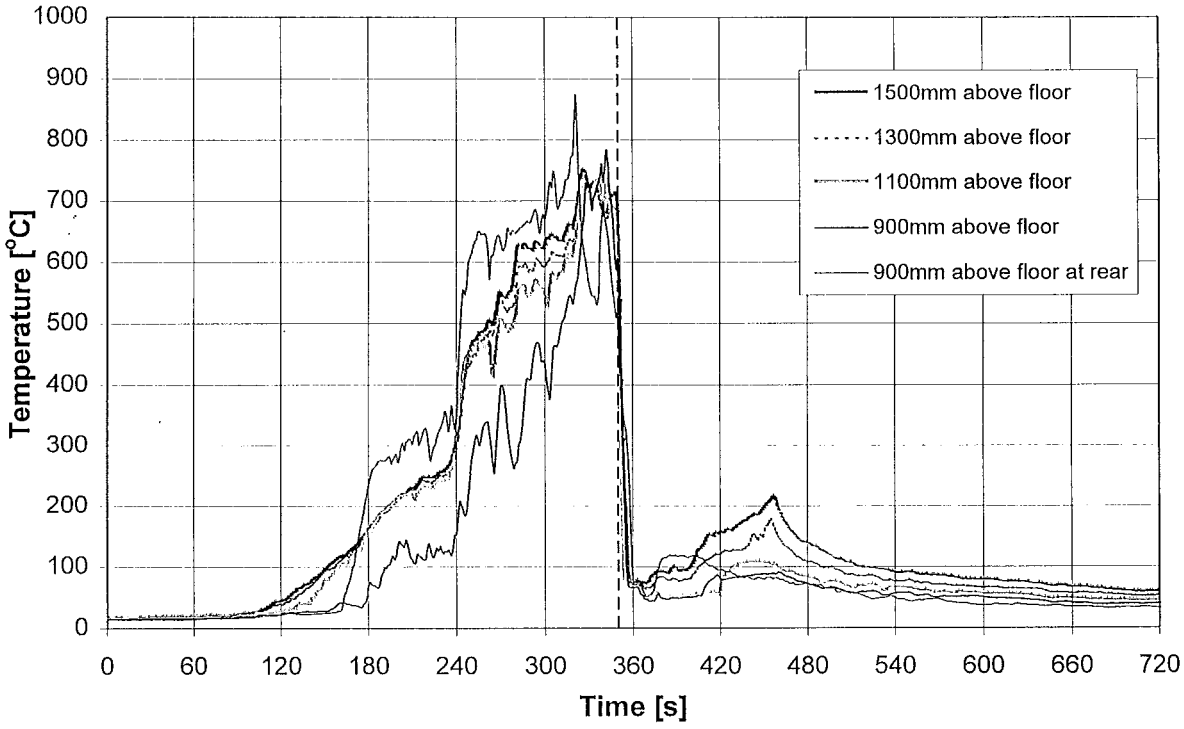

Thermocouple Tree, HPD, 2/12/97

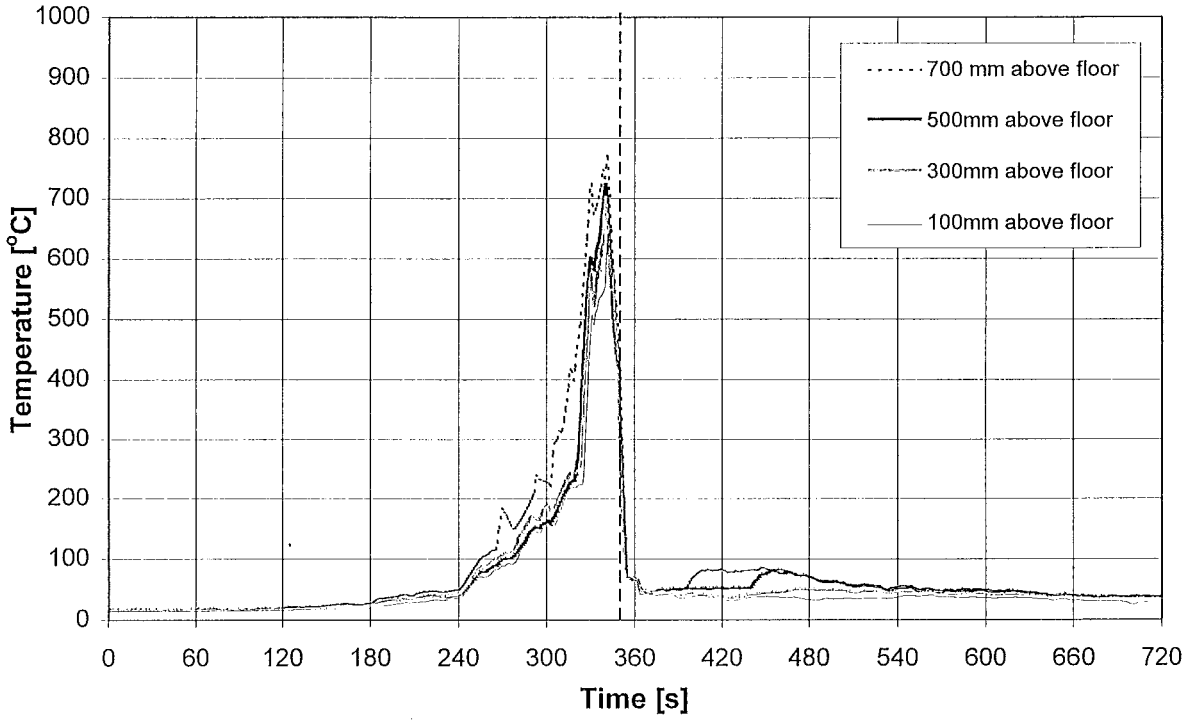

Thermocouple Tree, HPD, 2/12/97

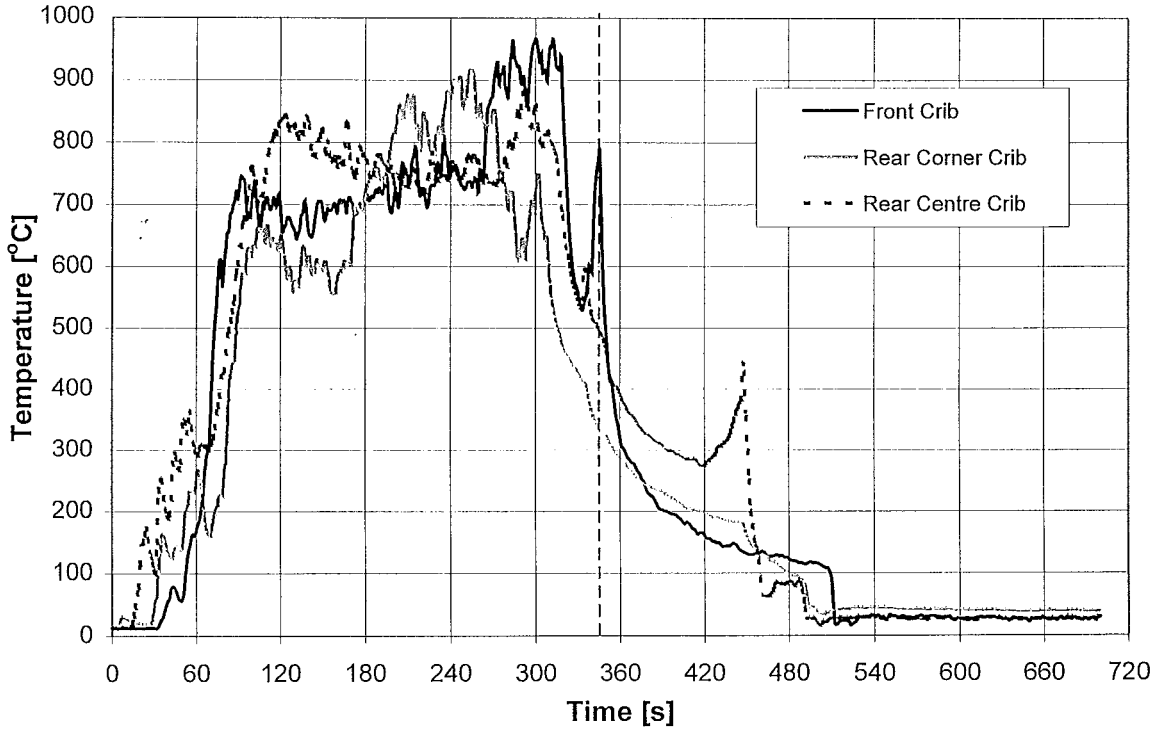

Crib Temperatures, HPD, 12/12/97

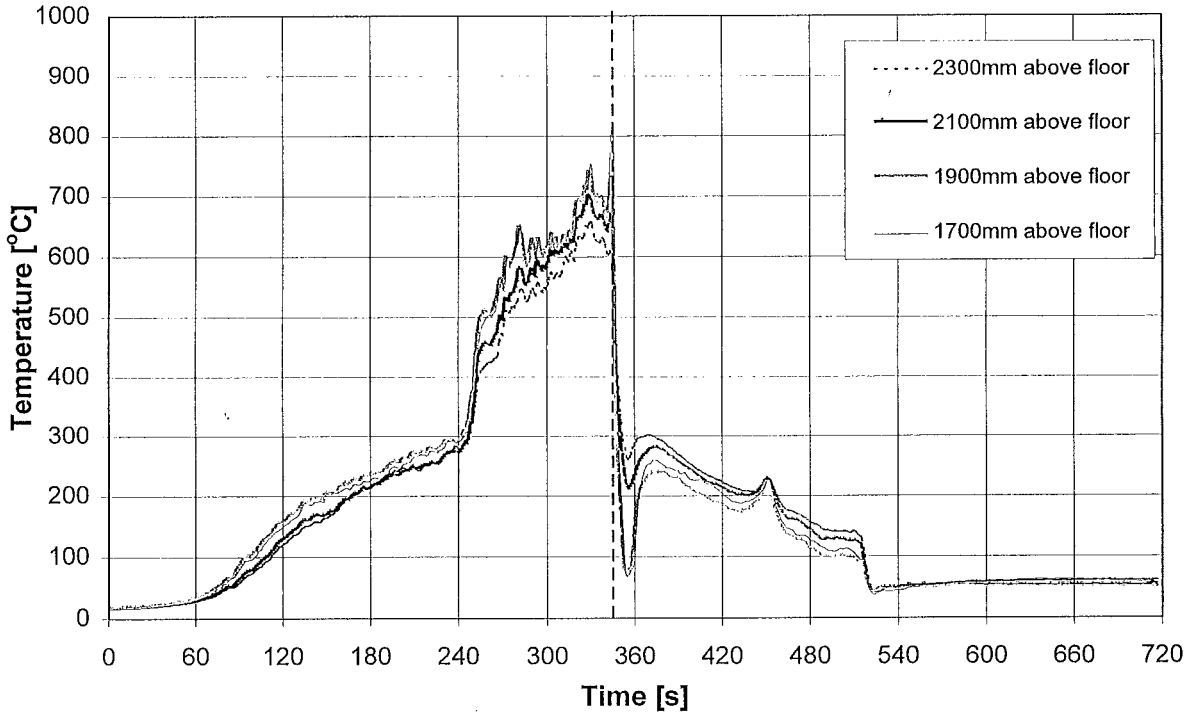

Thermocouple Tree, HPD, 12/12/97

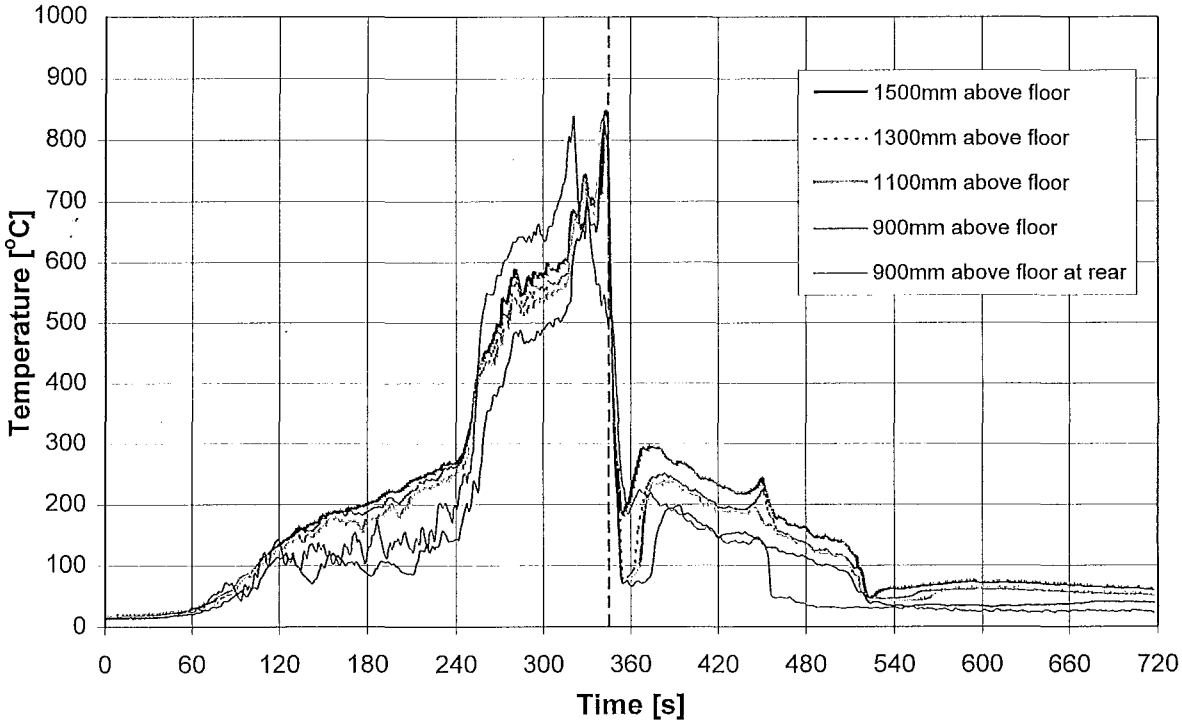

Thermocouple Tree, HPD, 12/12/97

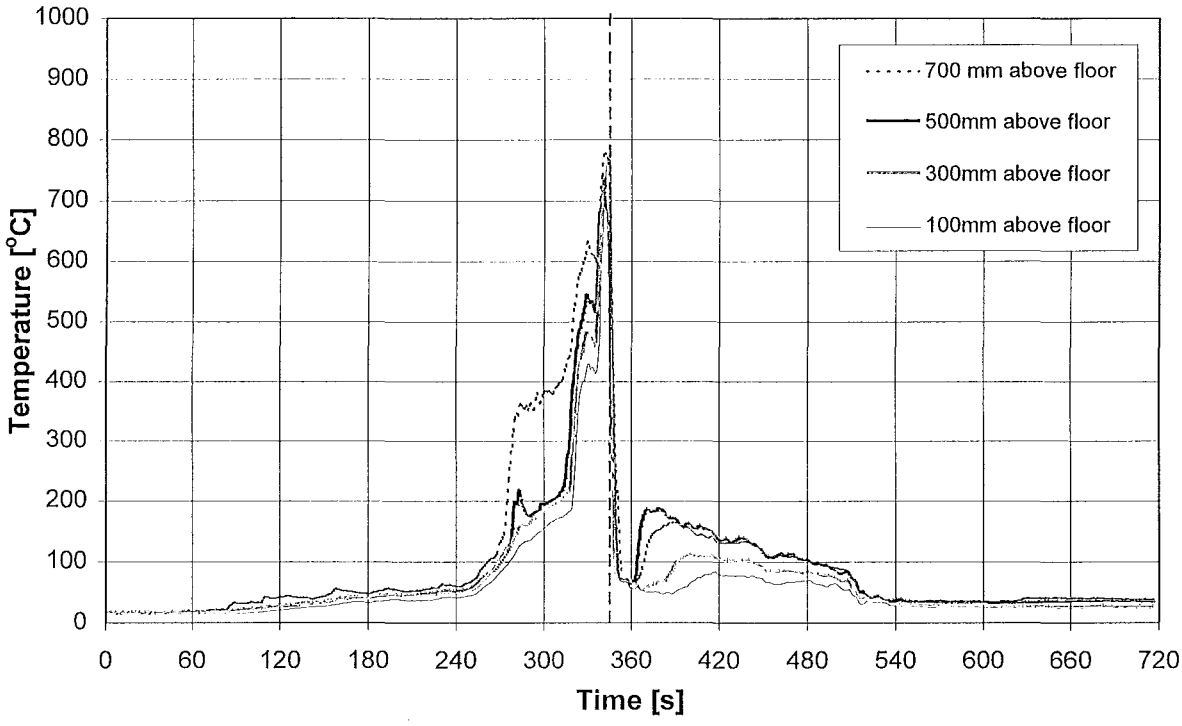

Thermocouple Tree, HPD, 12/12/97

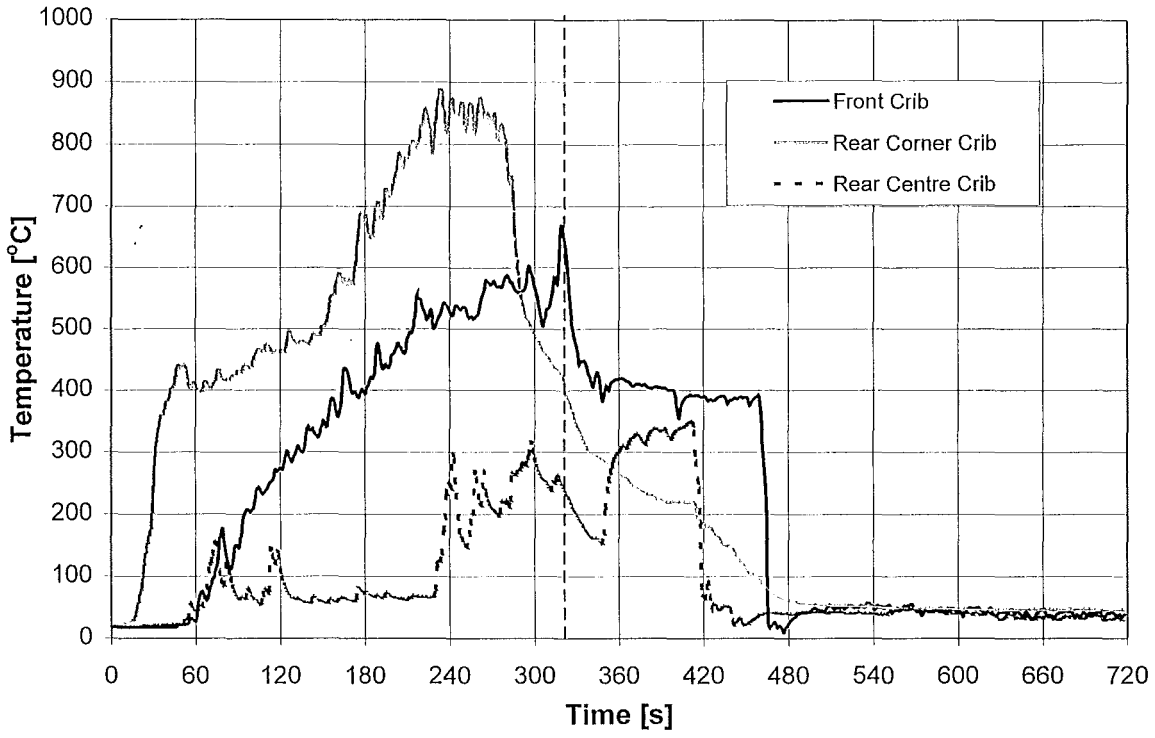

Crib Temperatures, Solution, 27/11/97

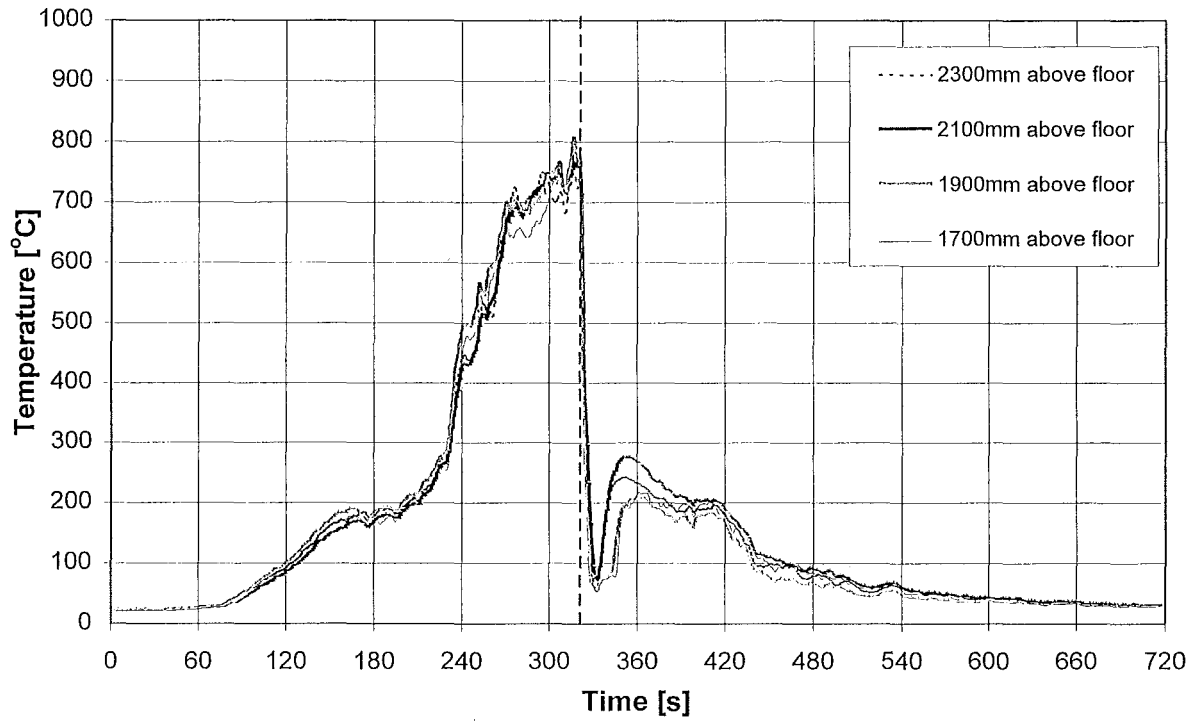

Thermocouple Tree, Solution, 27/11/97

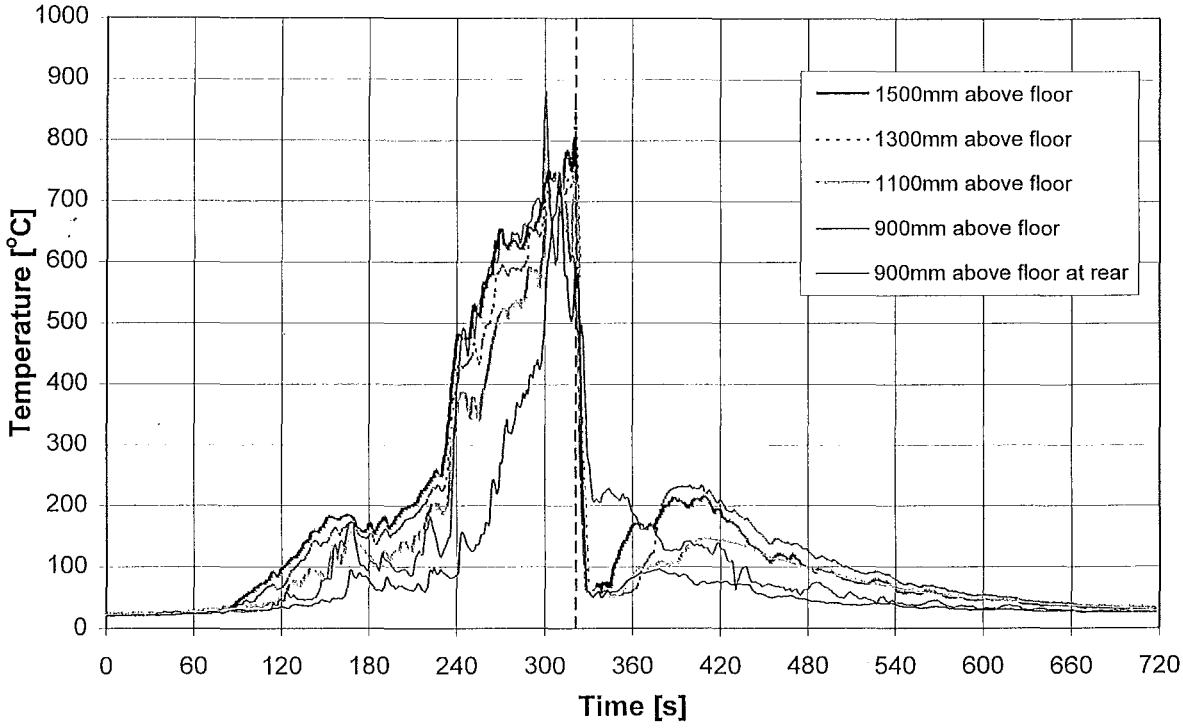

Thermocouple Tree, Solution, 27/11/97

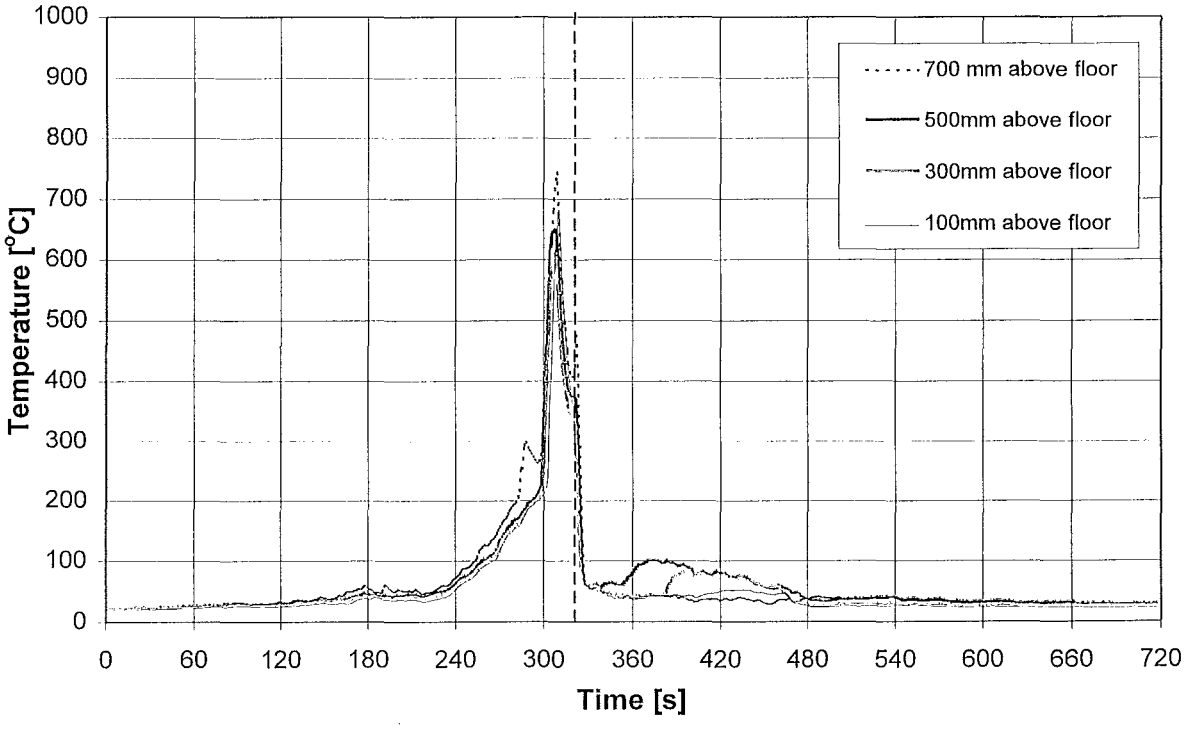

Thermocouple Tree, Solution, 27/11/97

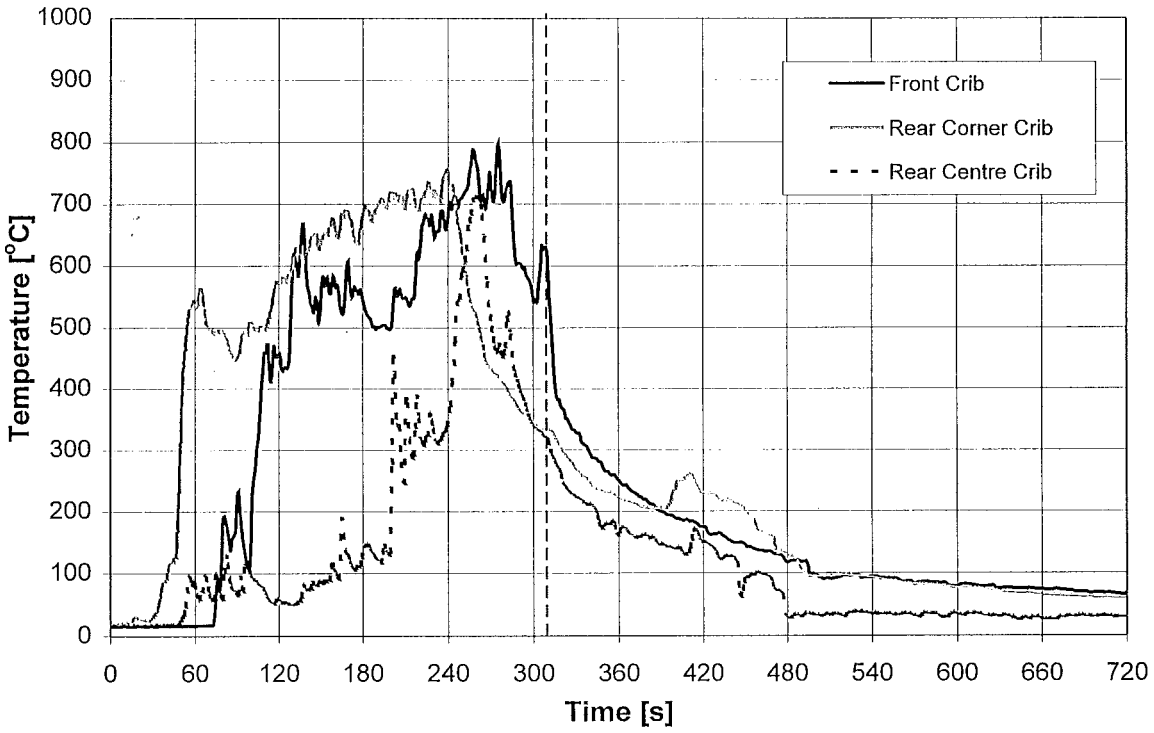

Crib Temperatures, Solution, 2/12/97

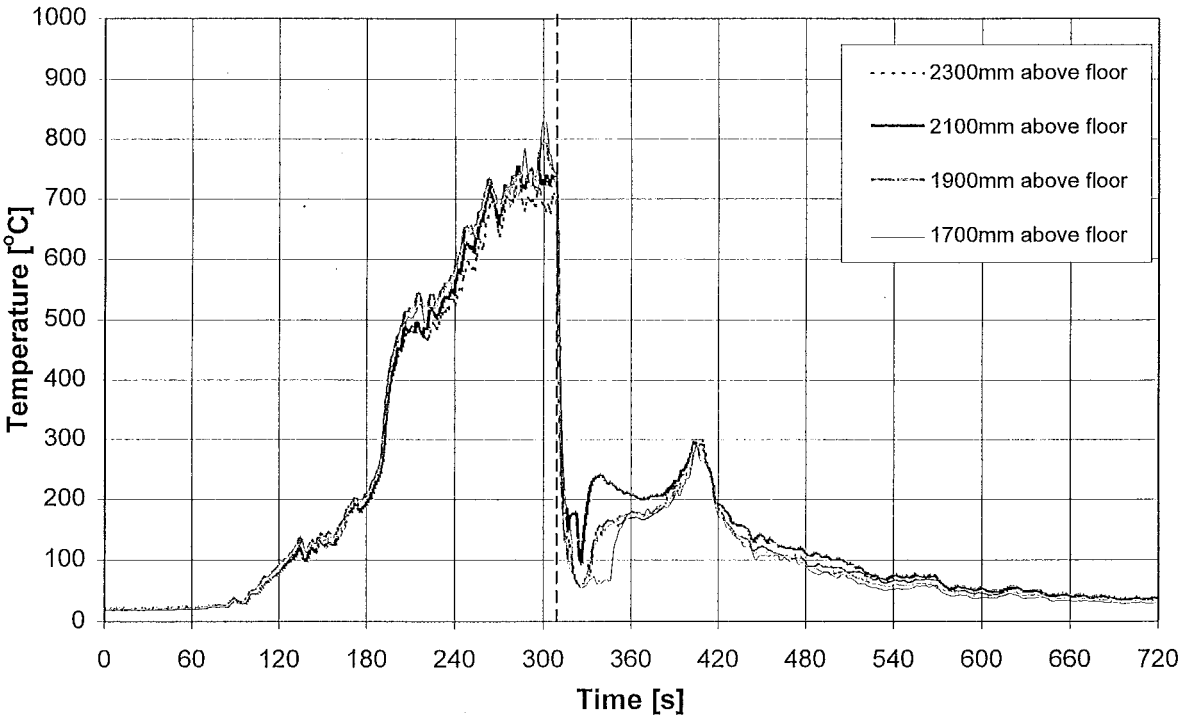

Thermocouple Tree, Solution, 2/12/97

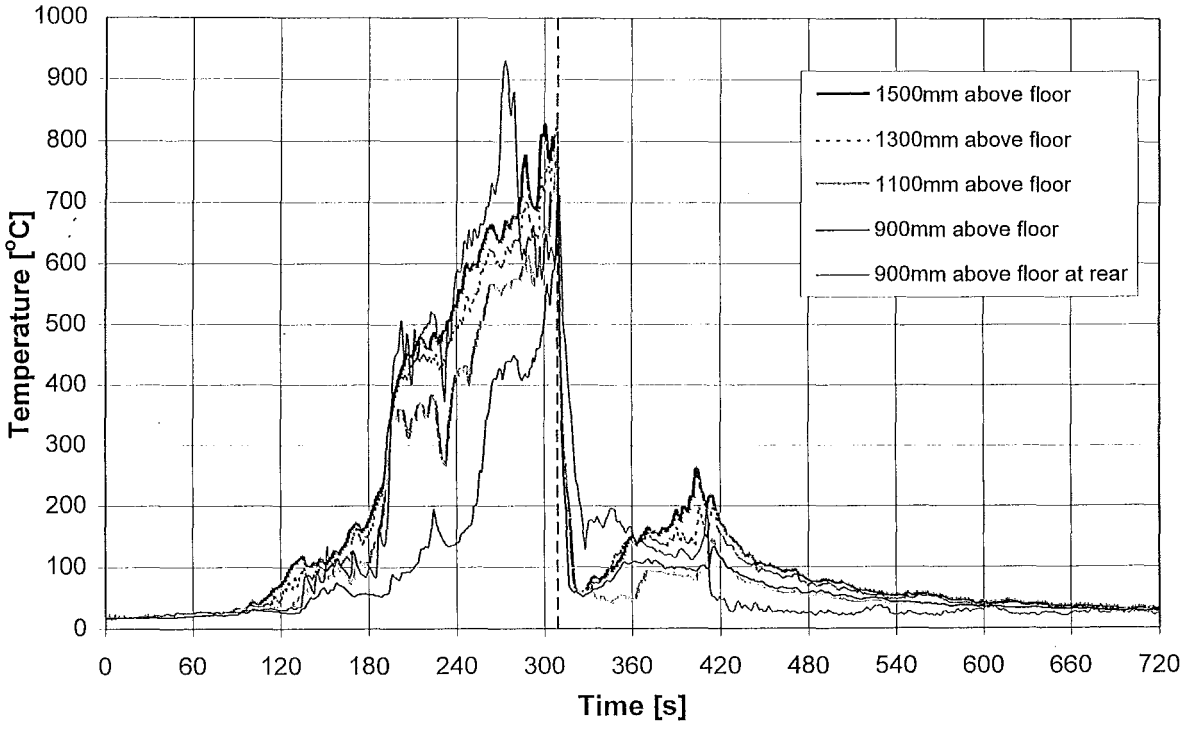

Thermocouple Tree, Solution, 2/12/97

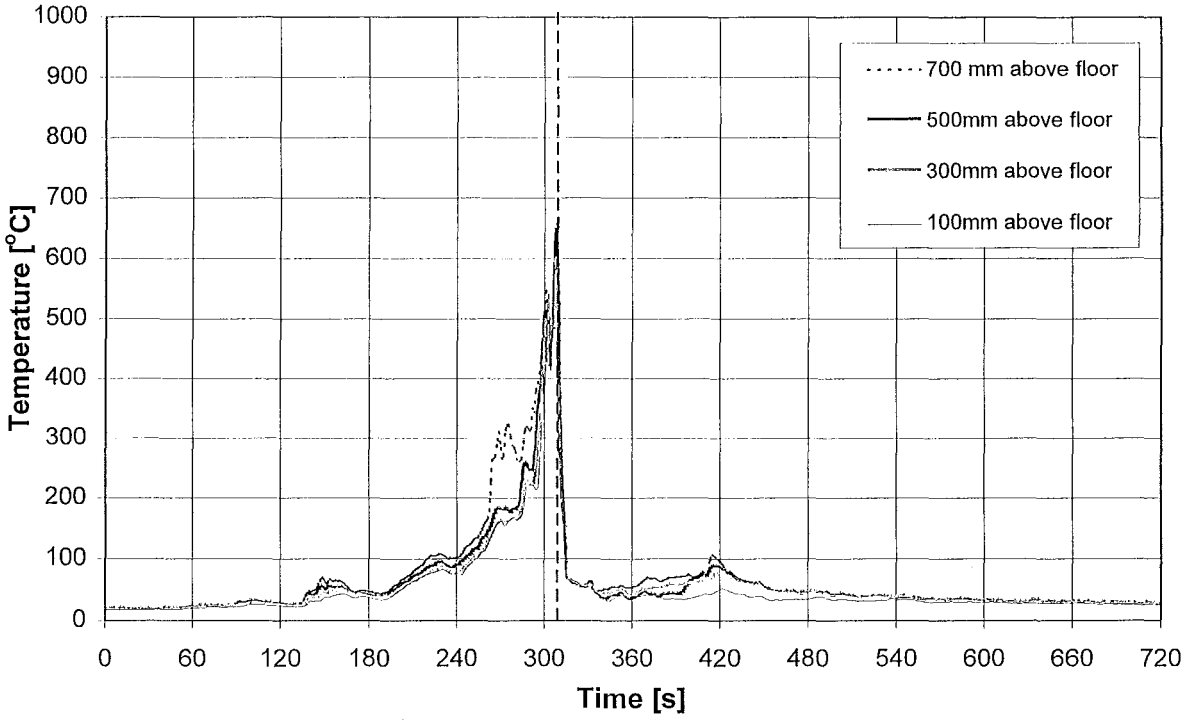

Thermocouple Tree, Solution, 2/12/97

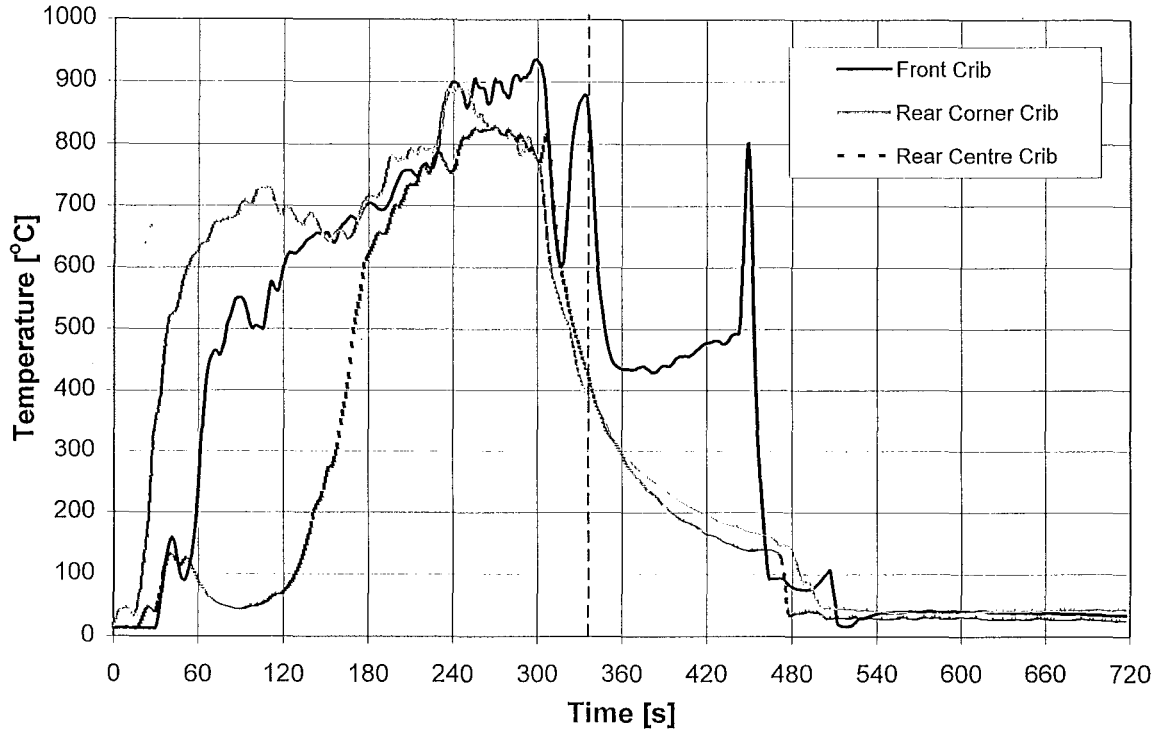

Crib Temperatures, Solution, 12/12/97

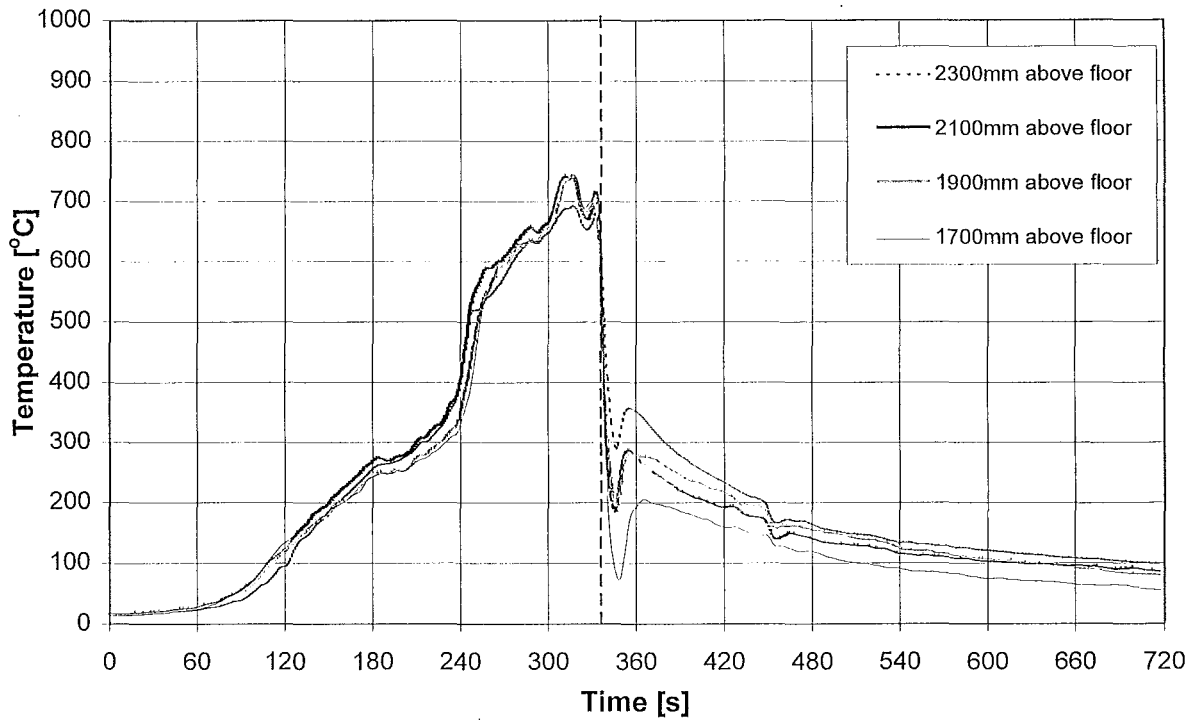

Thermocouple Tree, Solution, 12/12/97

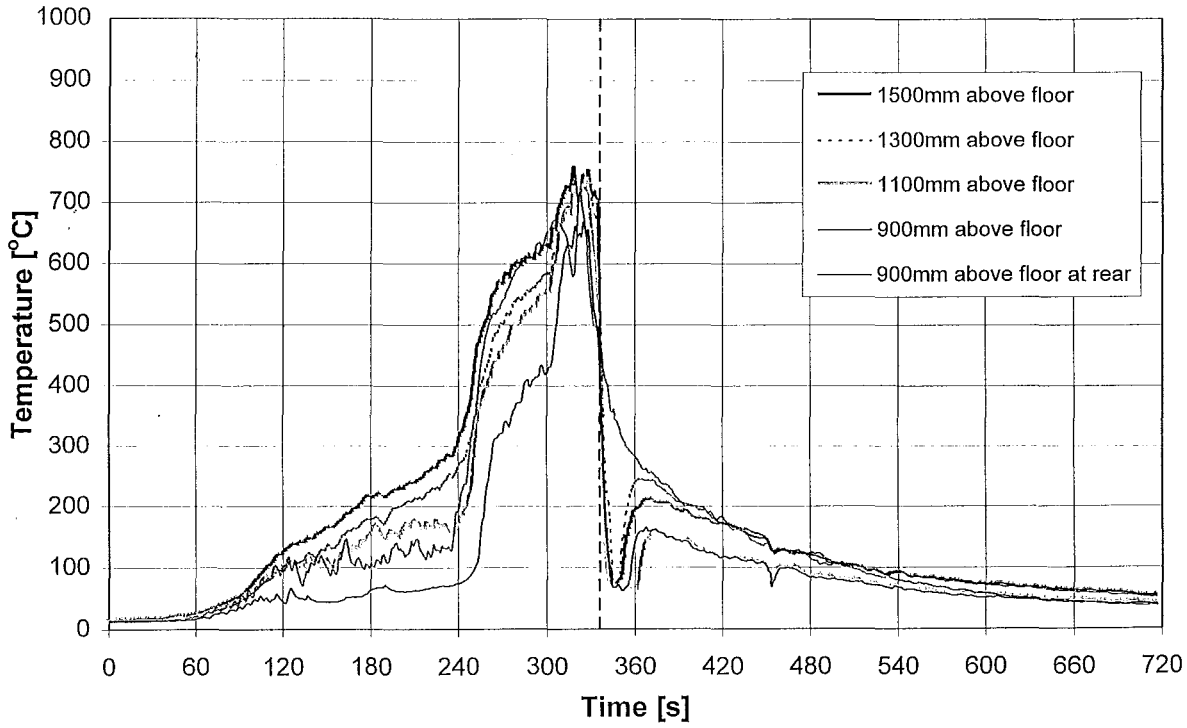

Thermocouple Tree, Solution, 12/12/97

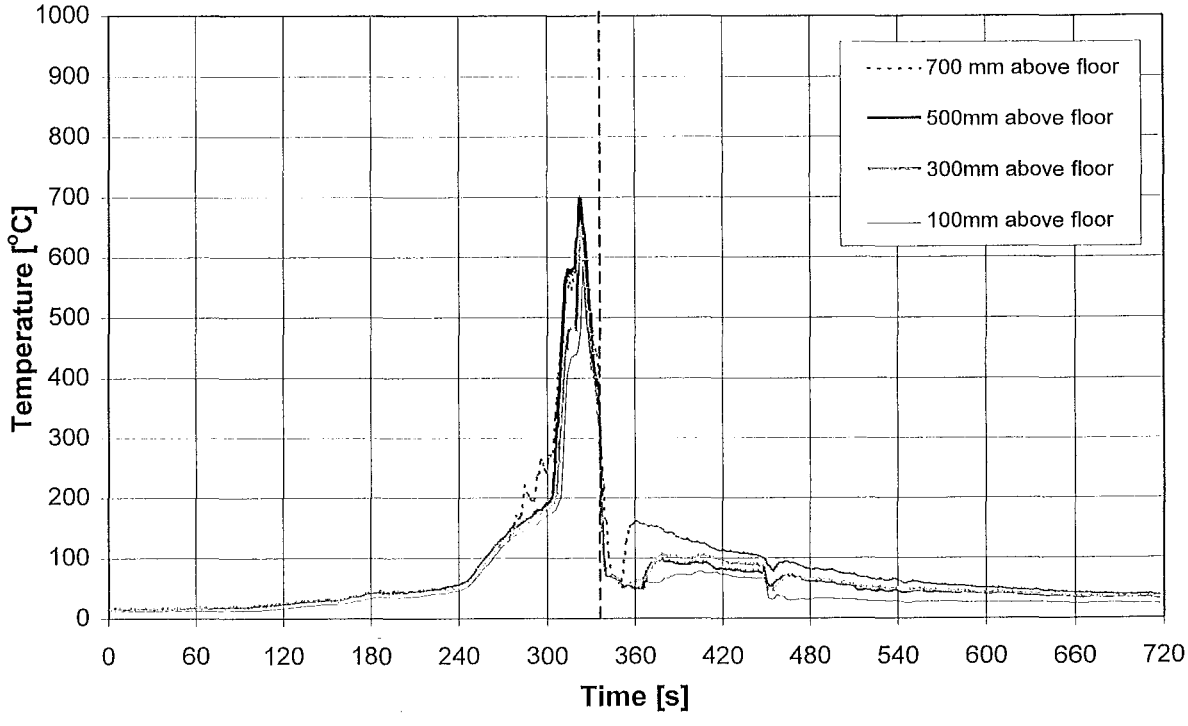

Thermocouple Tree, Solution, 12/12/97

Appendix 5 Doorway Temperatures

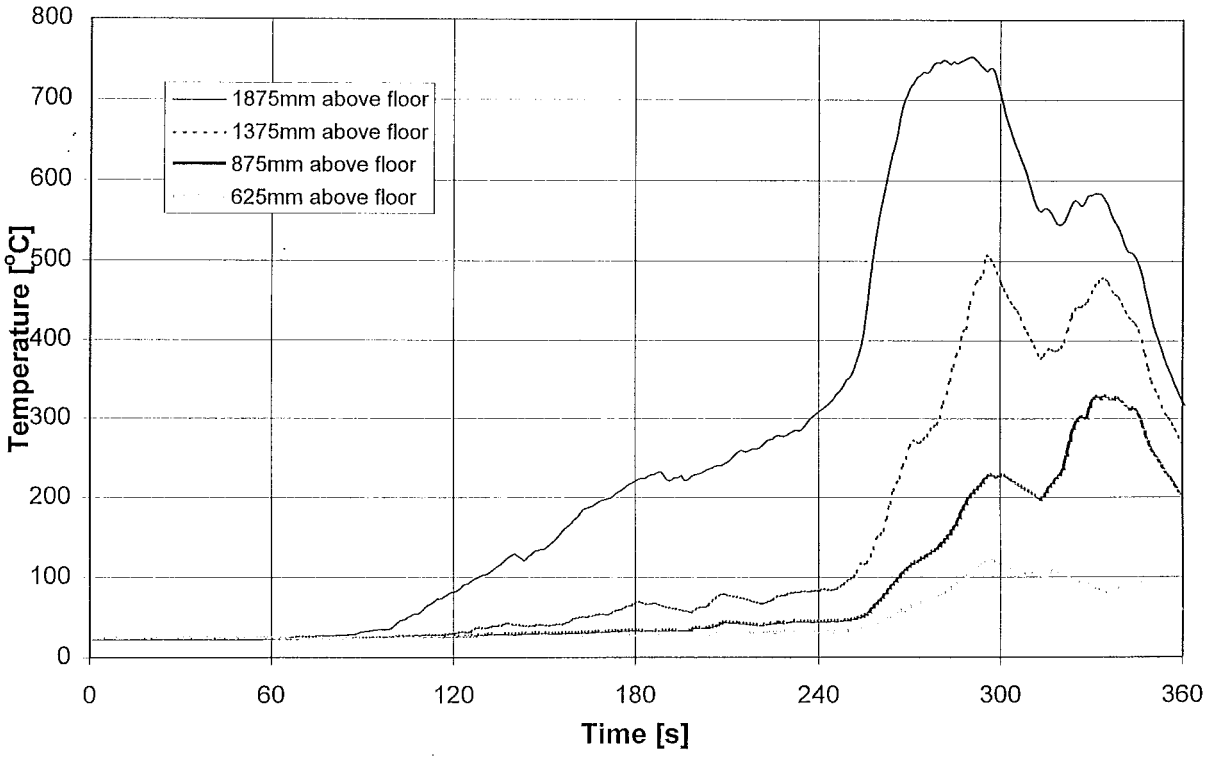

Doorway Temperatures, CAFS, 27/11/97

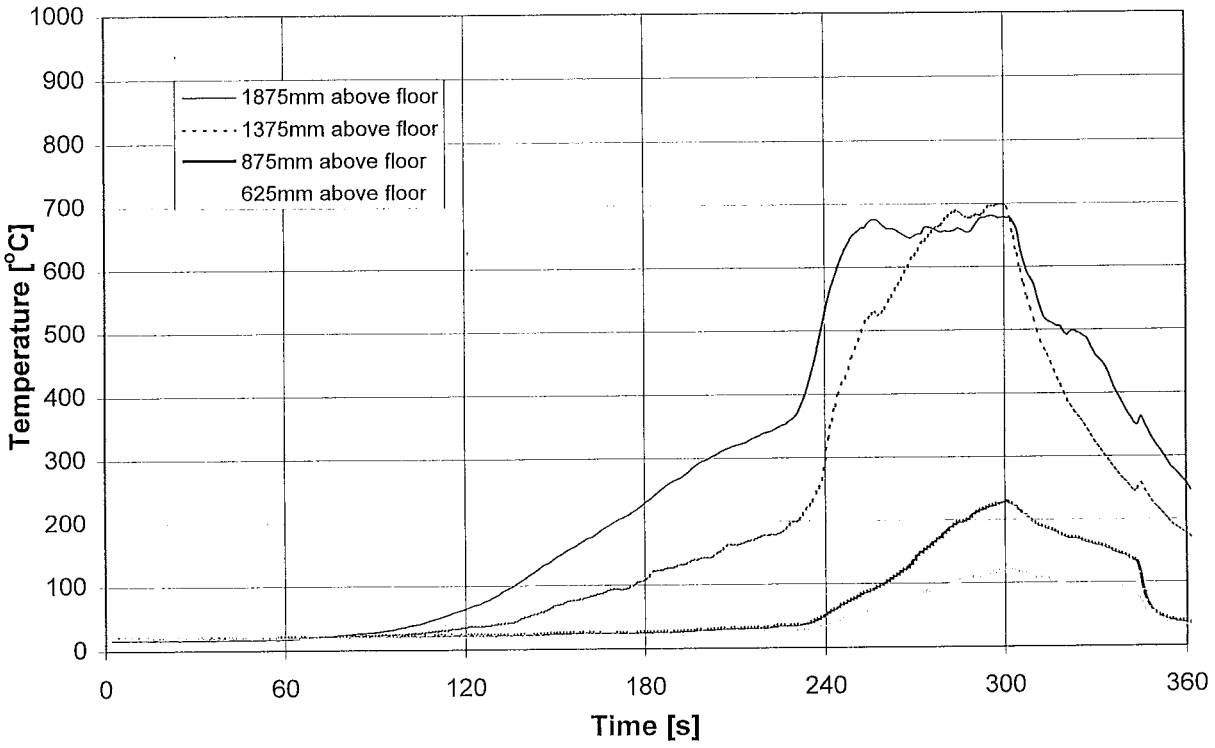

Doorway Temperatures, CAFS, 2/12/97

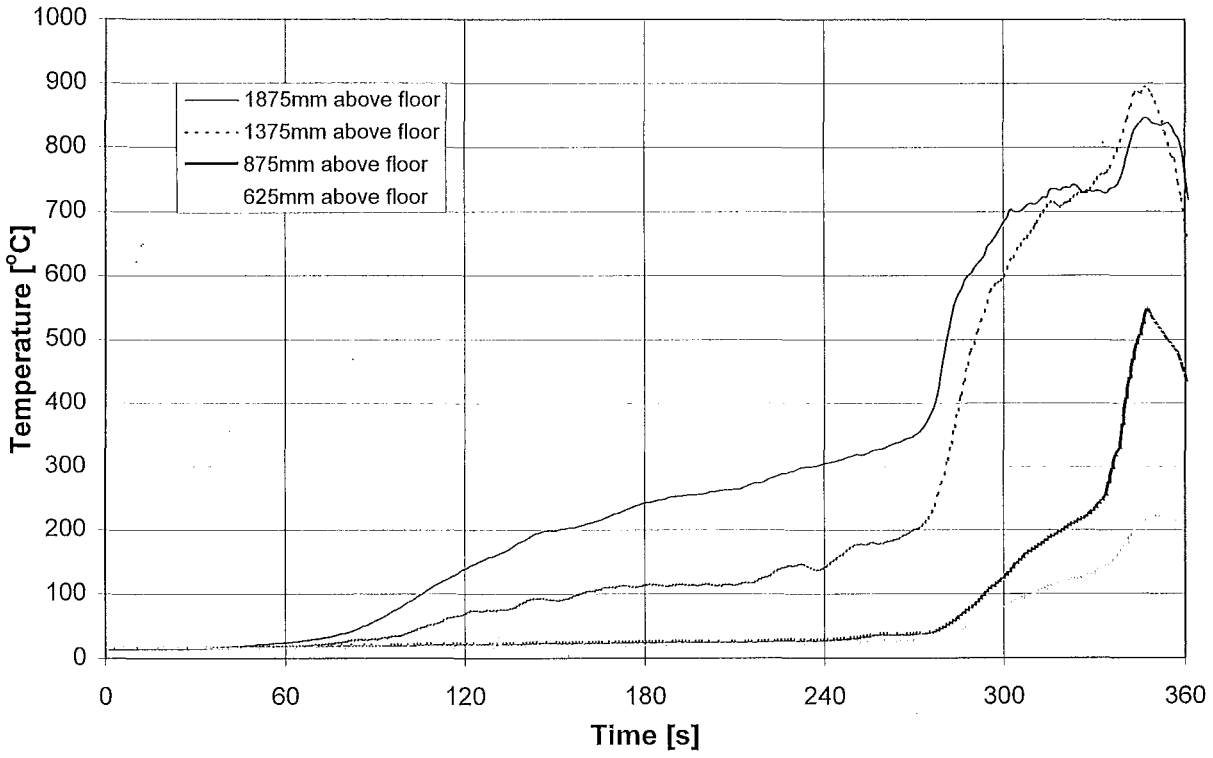

Doorway Temperatures, CAFS, 12/12/97

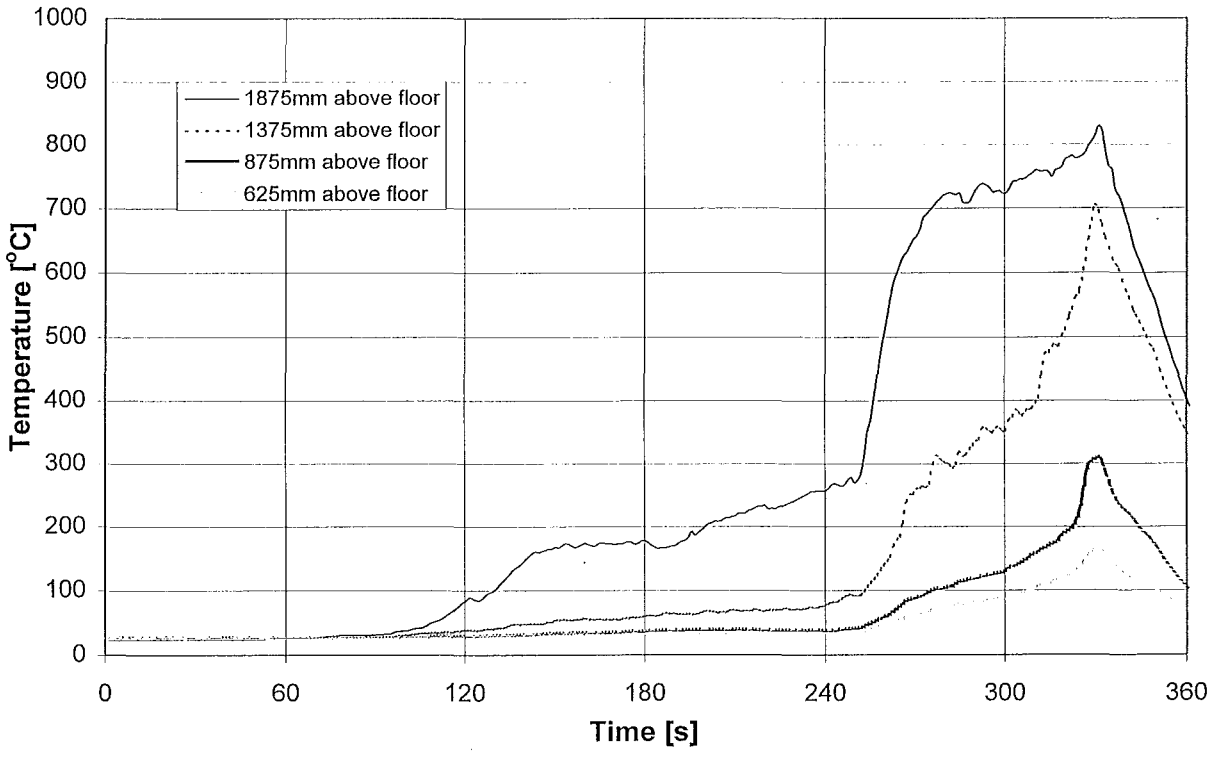

Doorway Temperatures, HPD, 27/11/97

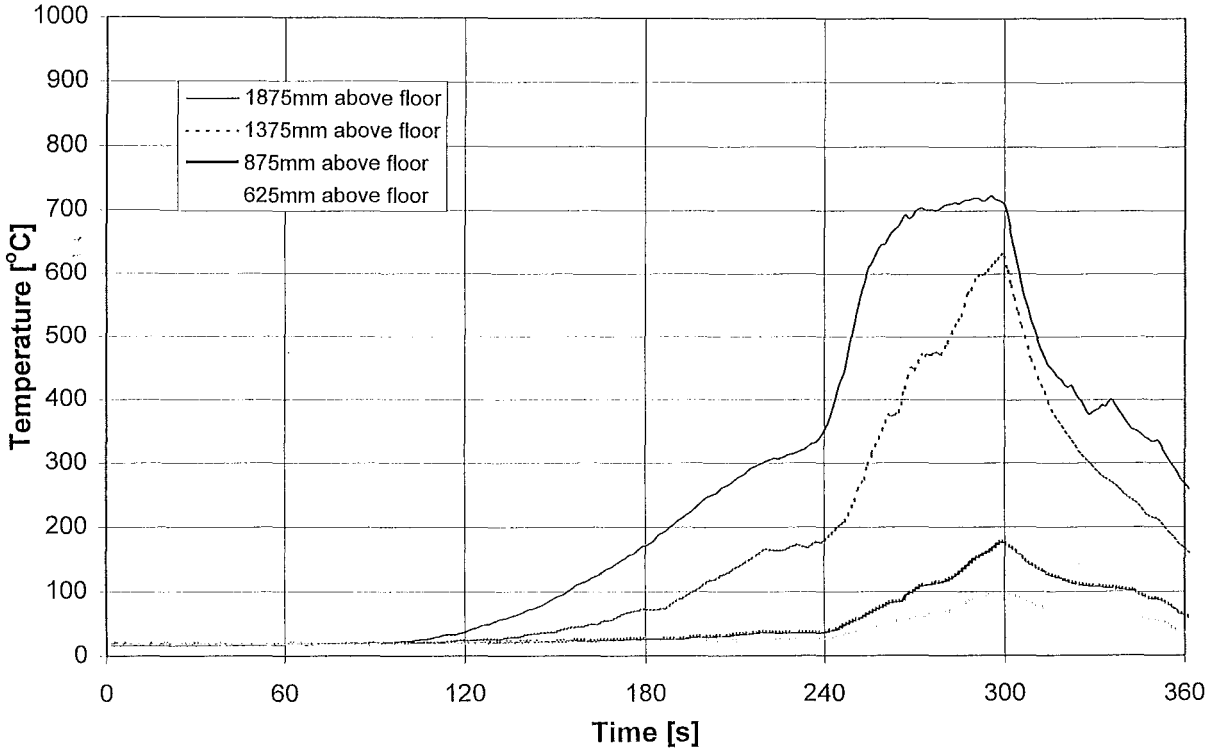

Doorway Temperatures, HPD, 2/12/97

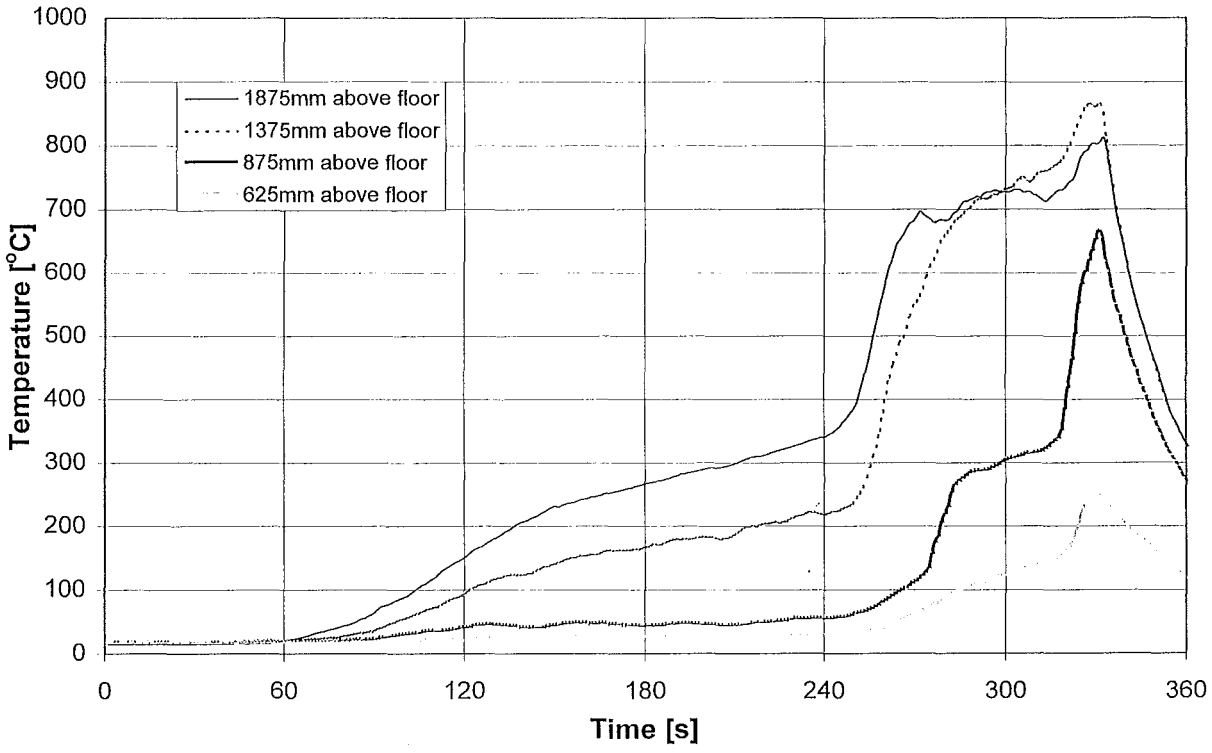

Doorway Temperatures, HPD, 12/12/97

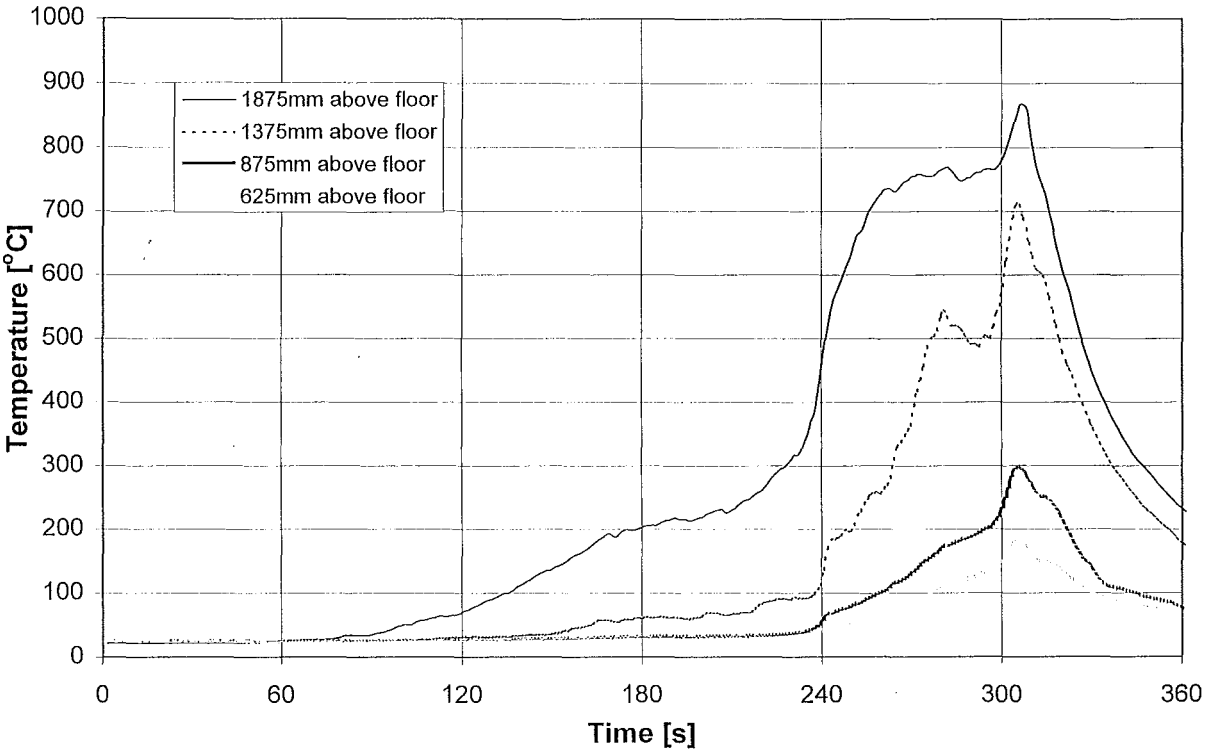

Doorway Temperatures, Solution, 27/11/97

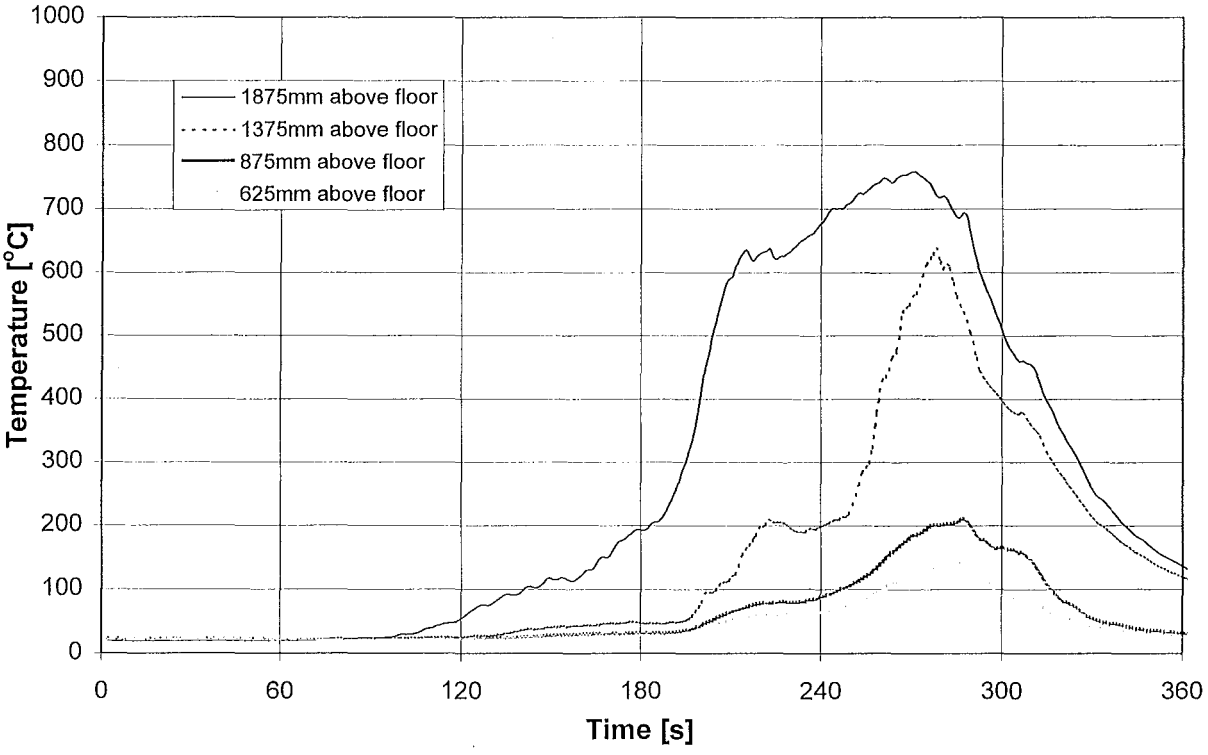

Doorway Temperatures, Solution, 2/12/97

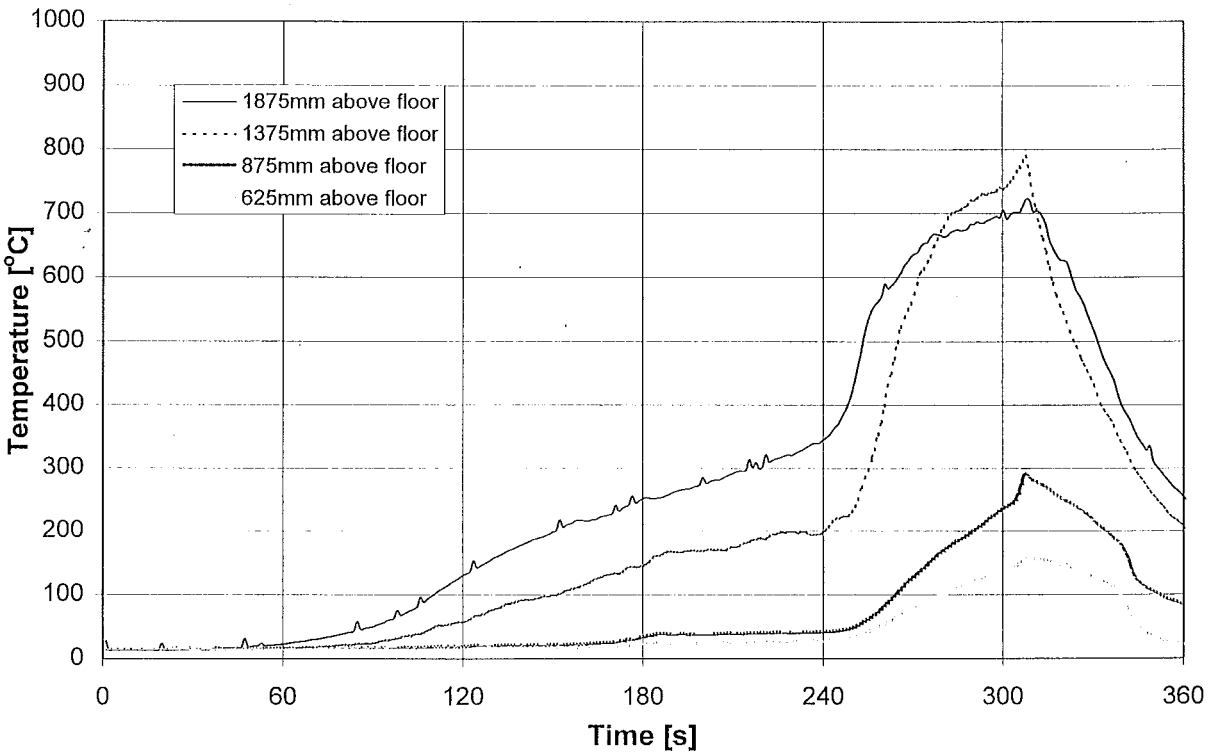

Doorway Temperatures, Solution, 12/12/97

Appendix 6 Doorway Mass Flows

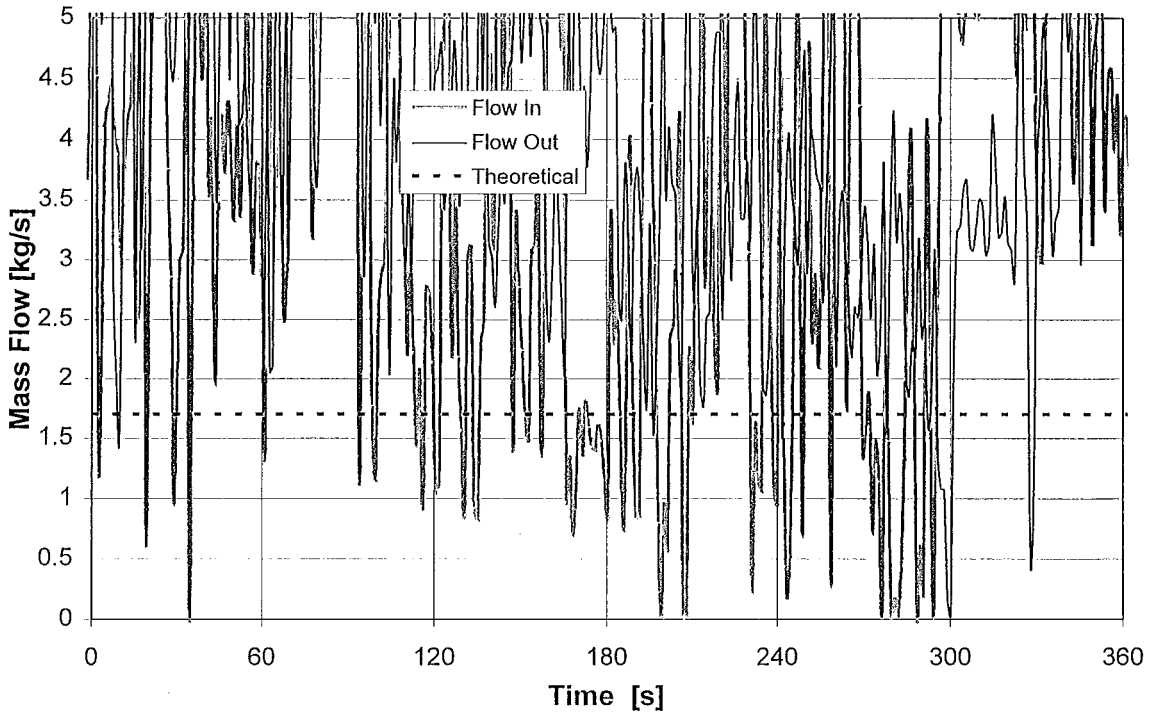

Doorway Mass Flow, CAFS, 27/11/97

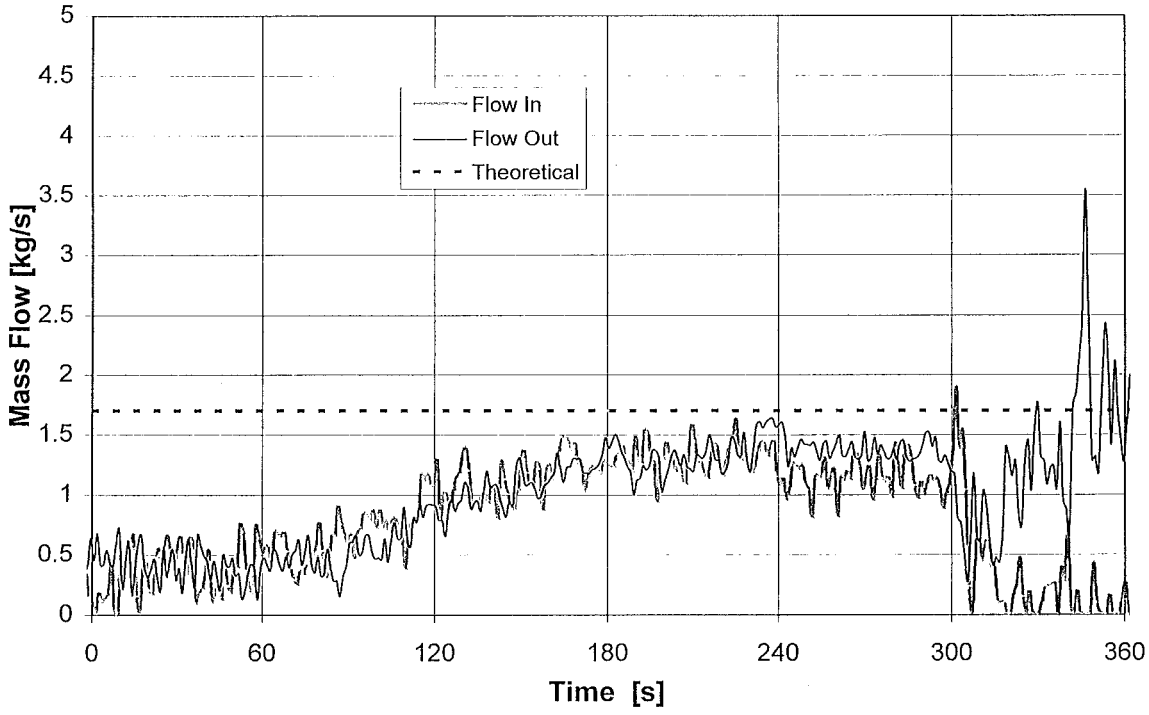

Doorway Mass Flow, CAFS, 2/12/97

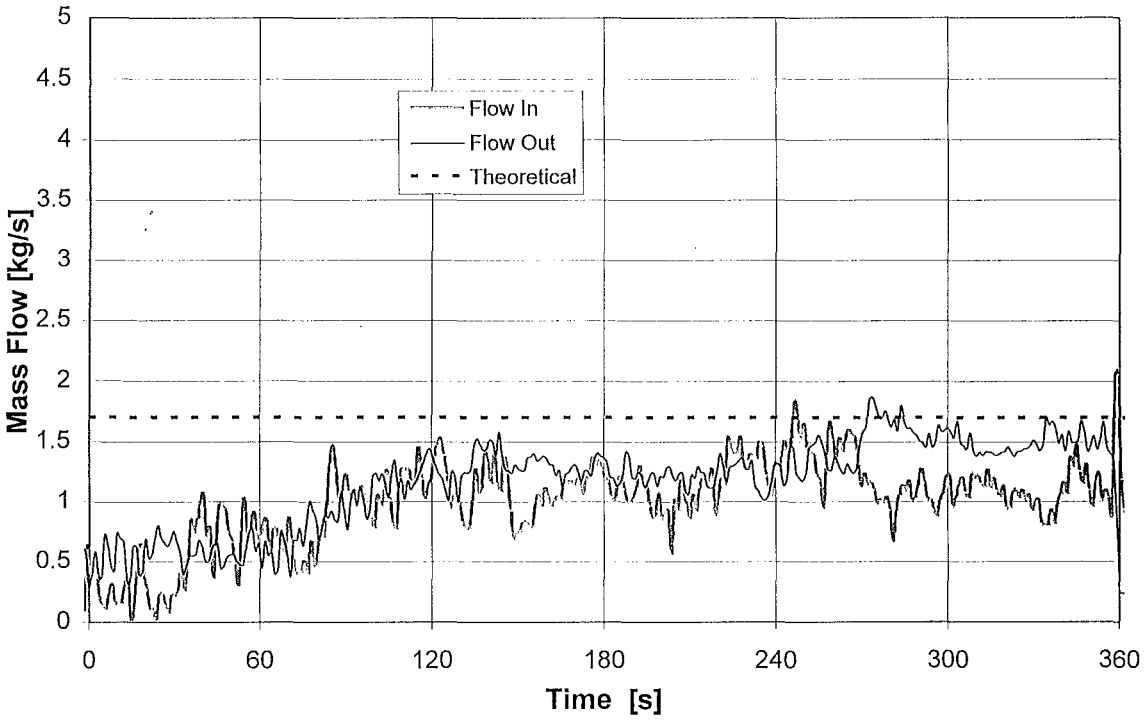

Doorway Mass Flow, CAFS, 12/12/97

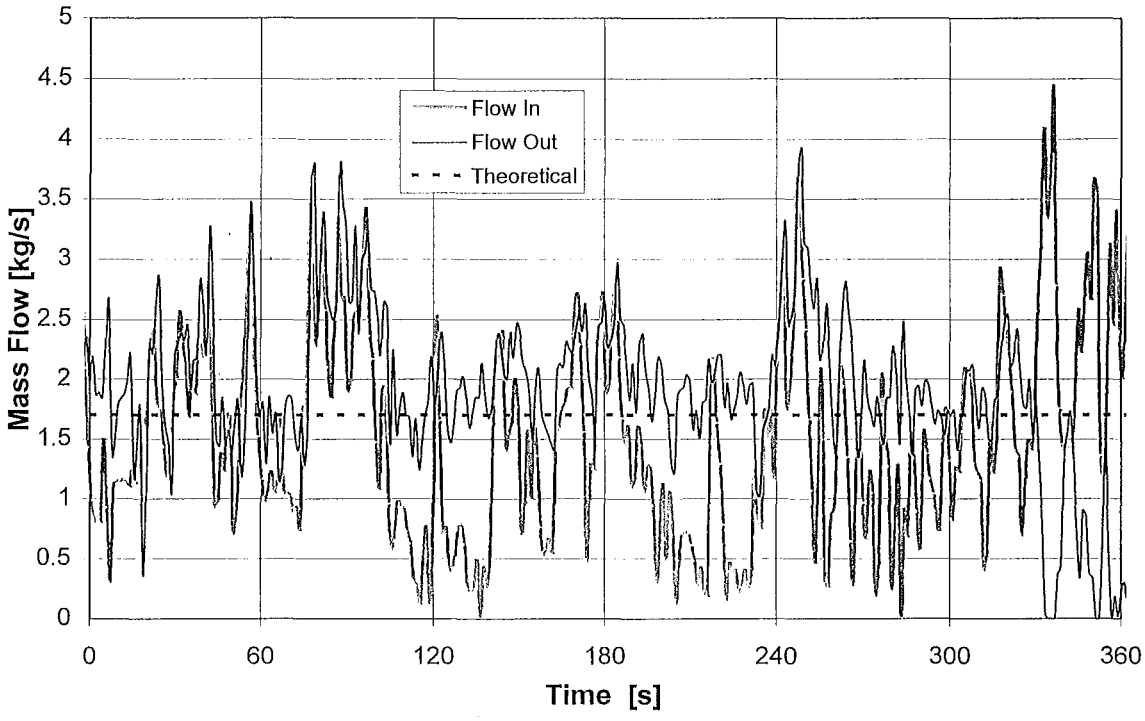

Doorway Mass Flow, HPD, 27/11/97

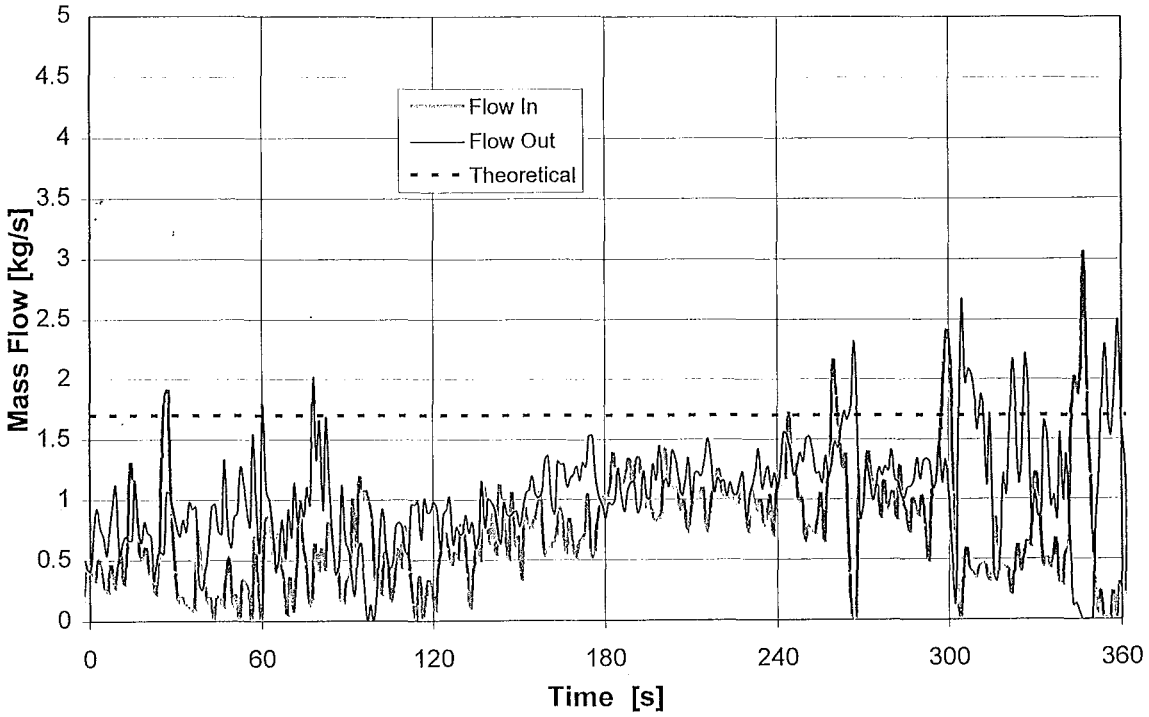

Doorway Mass Flow, HPD, 2/12/97

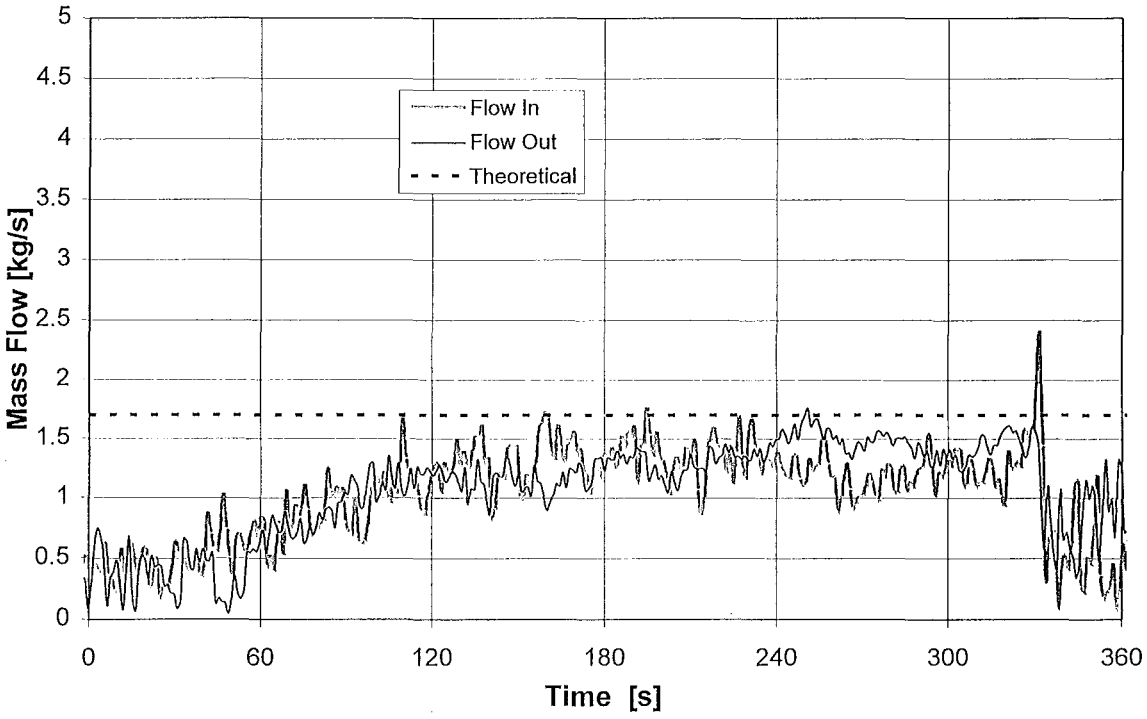

Doorway Mass Flow, HPD, 12/12/97

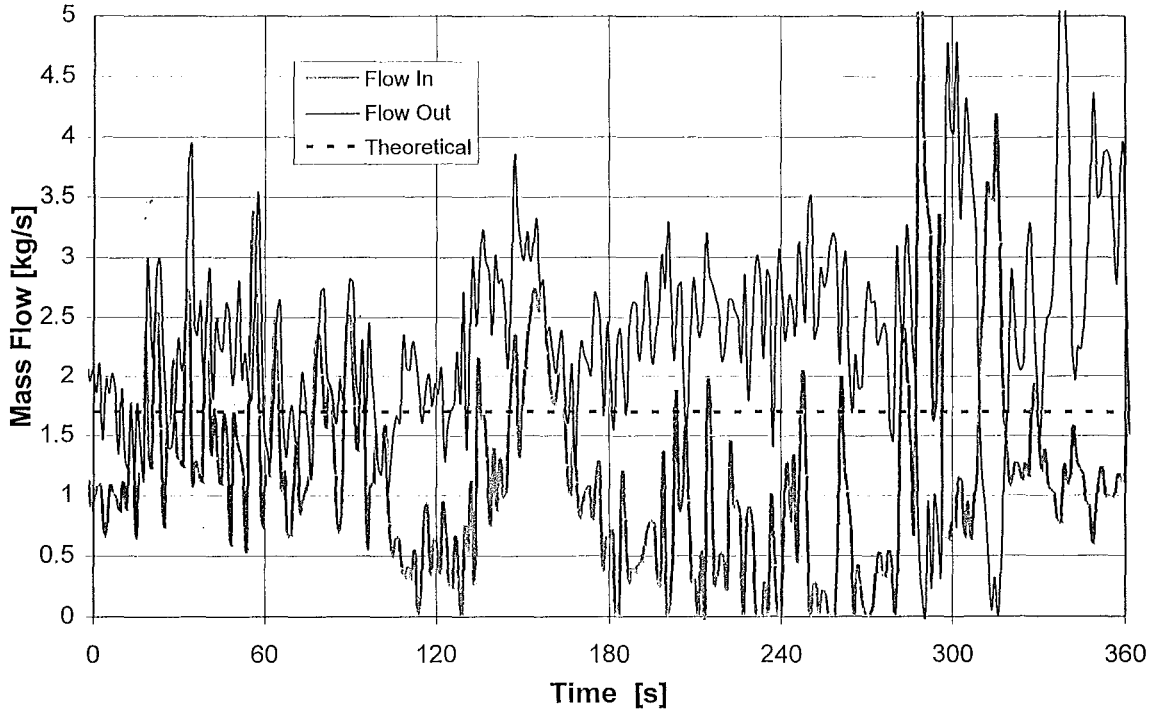

Doorway Mass Flow, Solution, 2/12/97

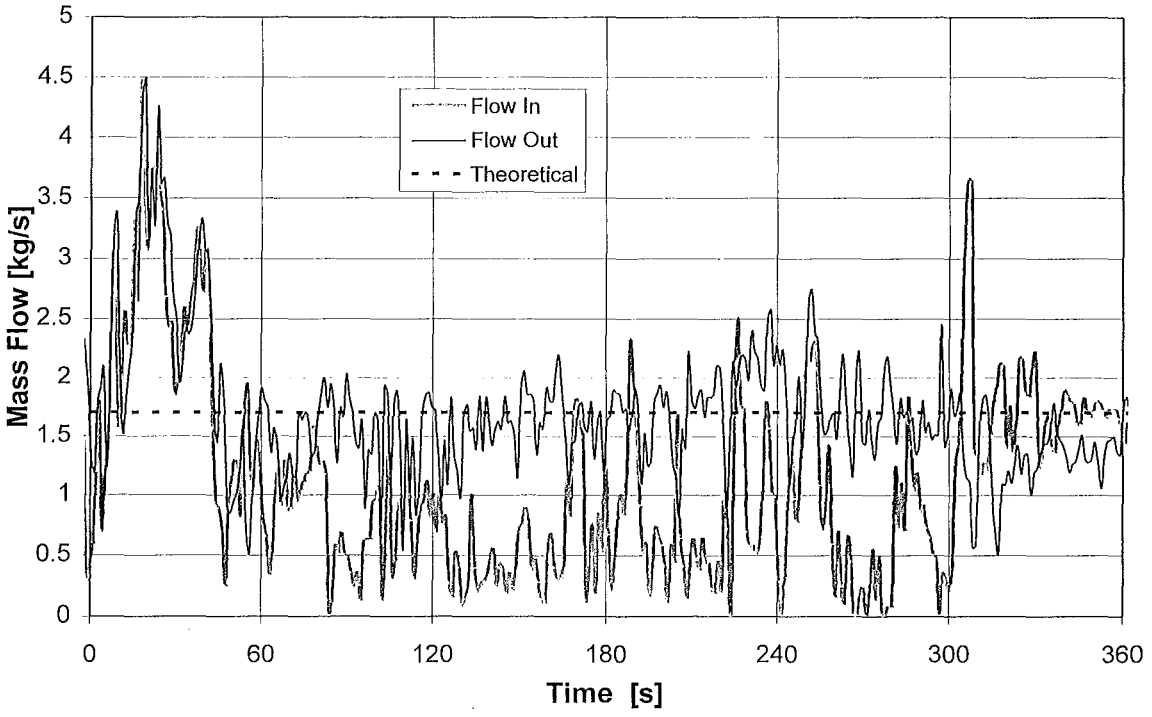

Doorway Mass Flow, Solution, 27/11/97

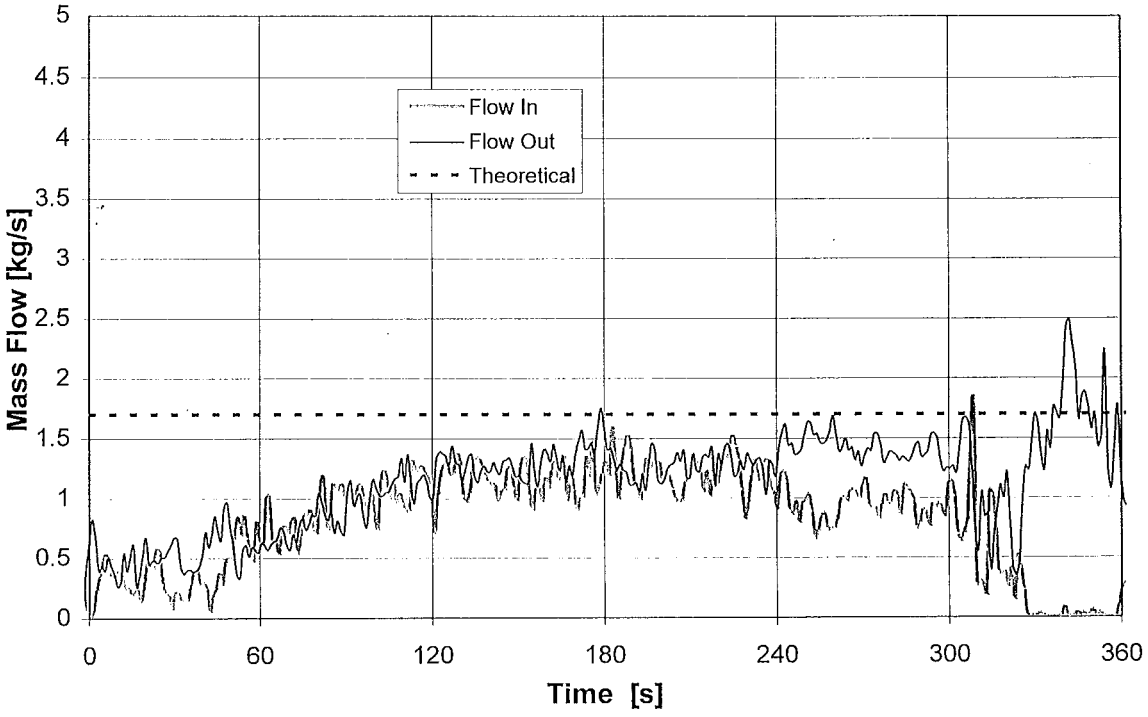

Doorway Mass Flow, Solution, 12/12/97

Appendix 7 Heat Release Rates

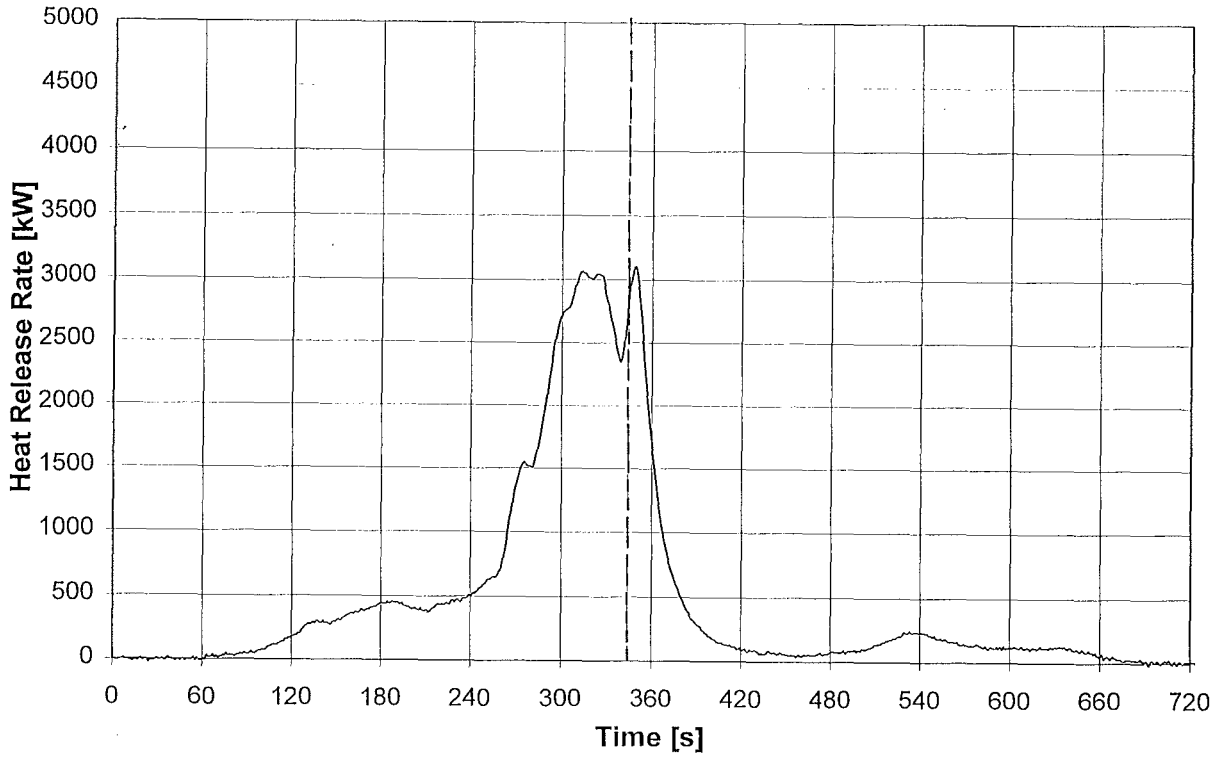

Heat Release Rate, CAFS, 27/11/97

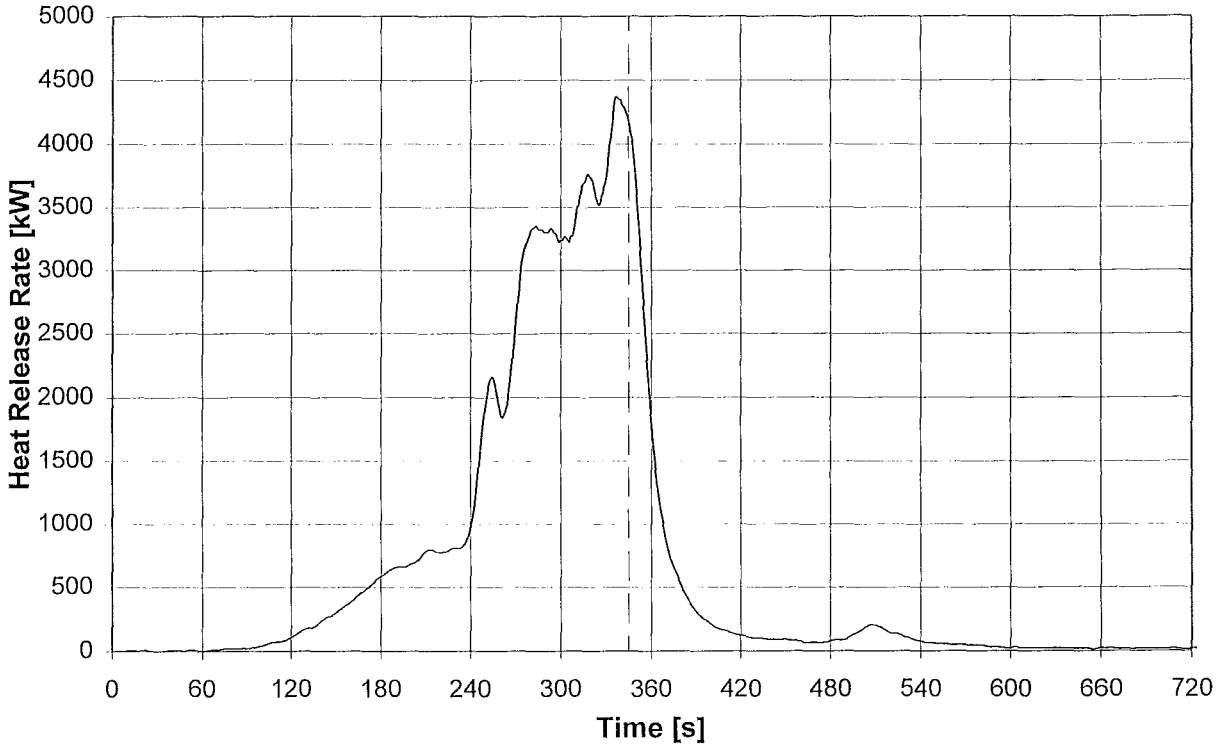

Heat Release Rate, CAFS, 2/12/97

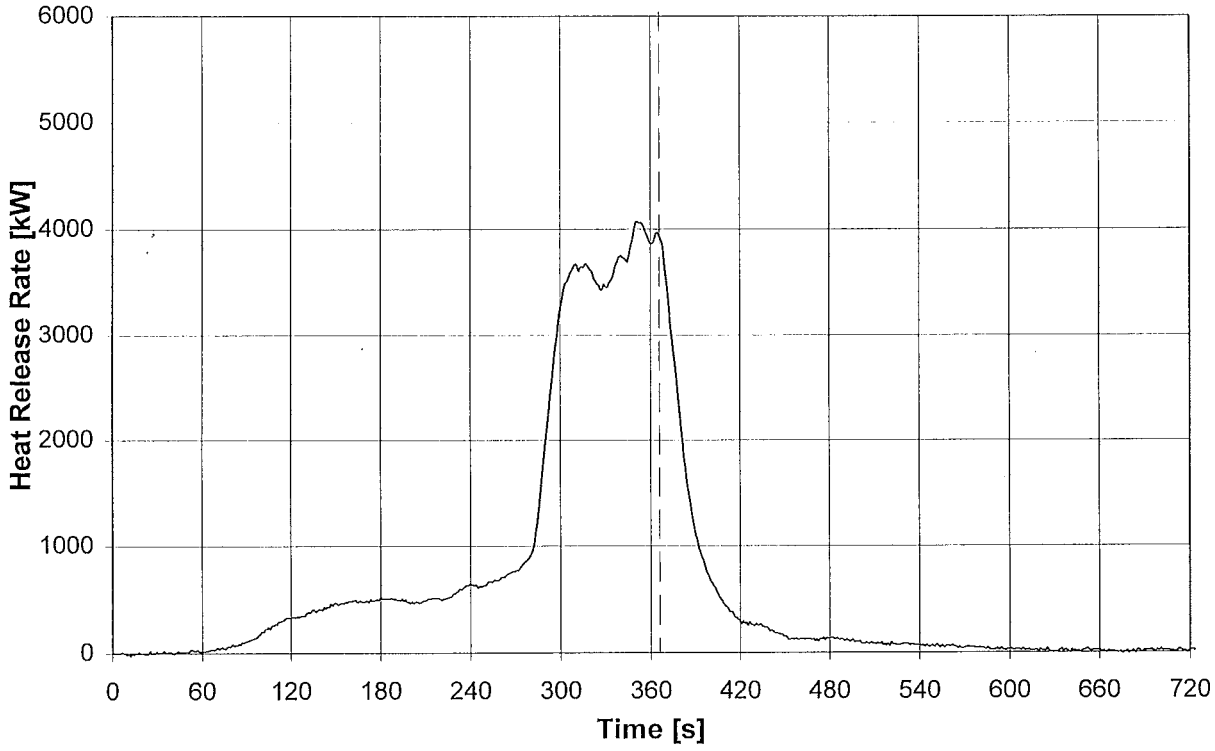

Heat Release Rate, CAFS, 12/12/97

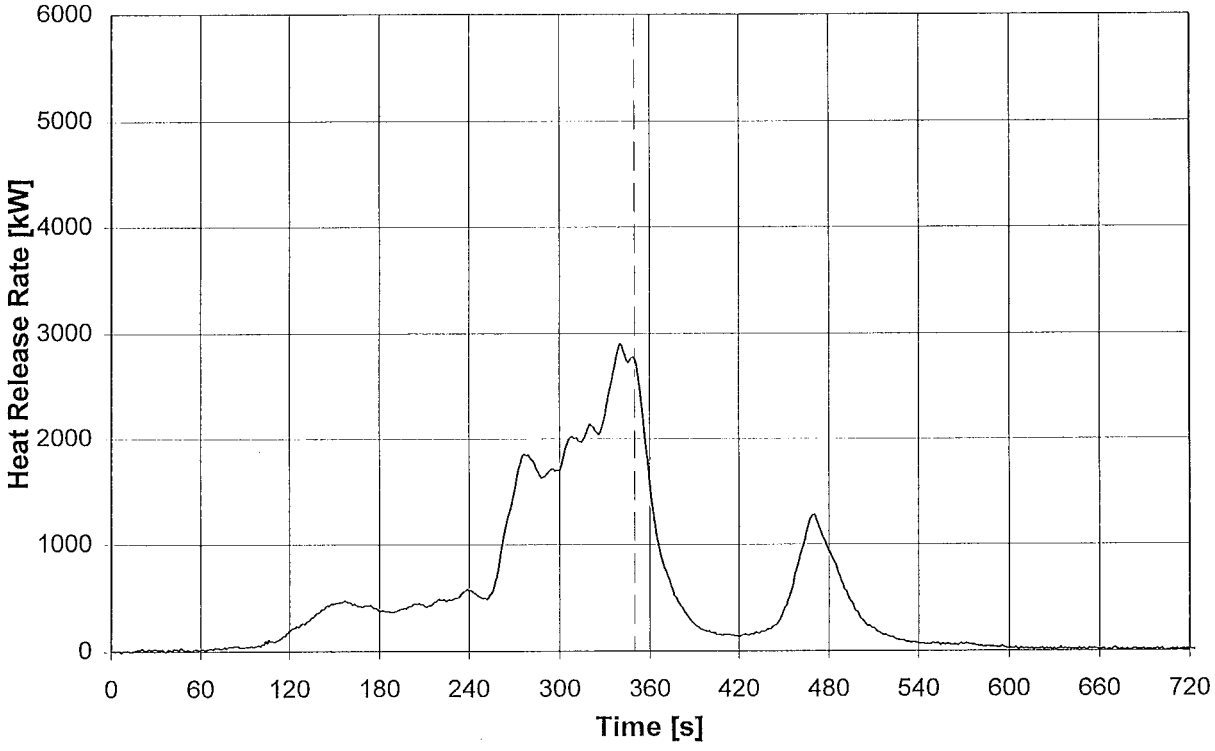

Heat Release Rate, HPD, 27/11/97

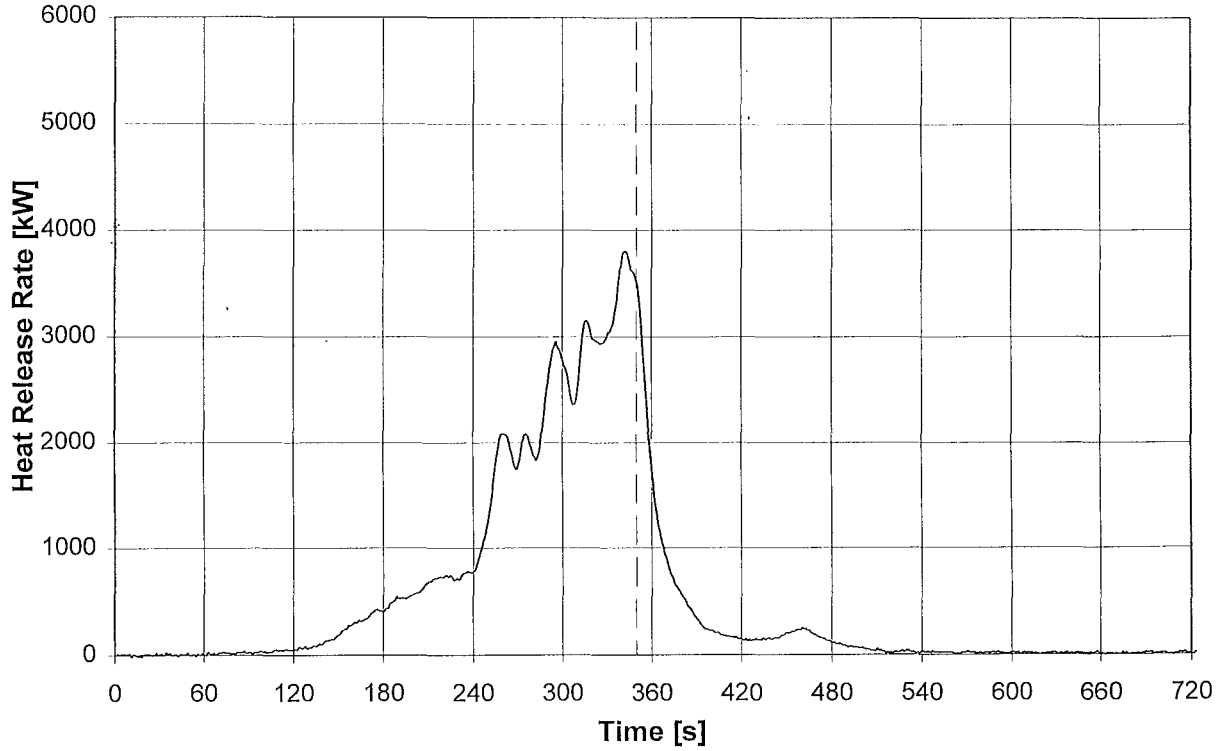

Heat Release Rate, HPD, 2/12/97

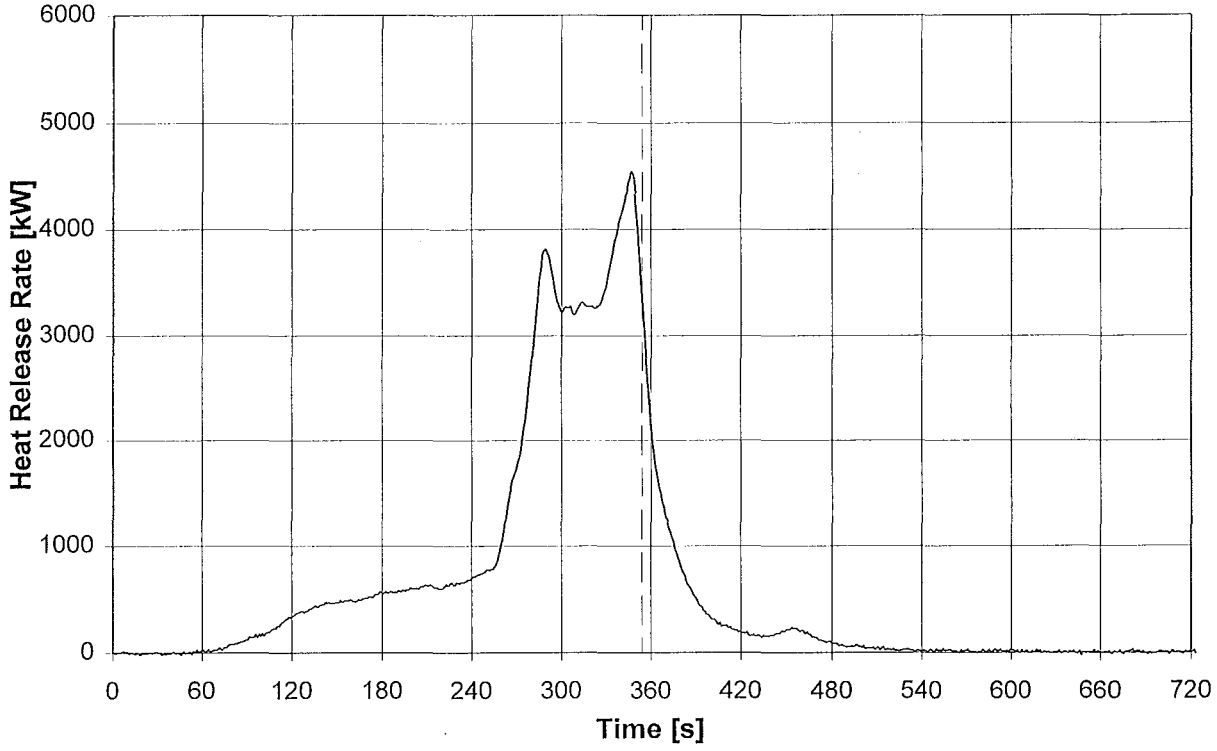

Heat Release Rate, HPD, 12/12/97

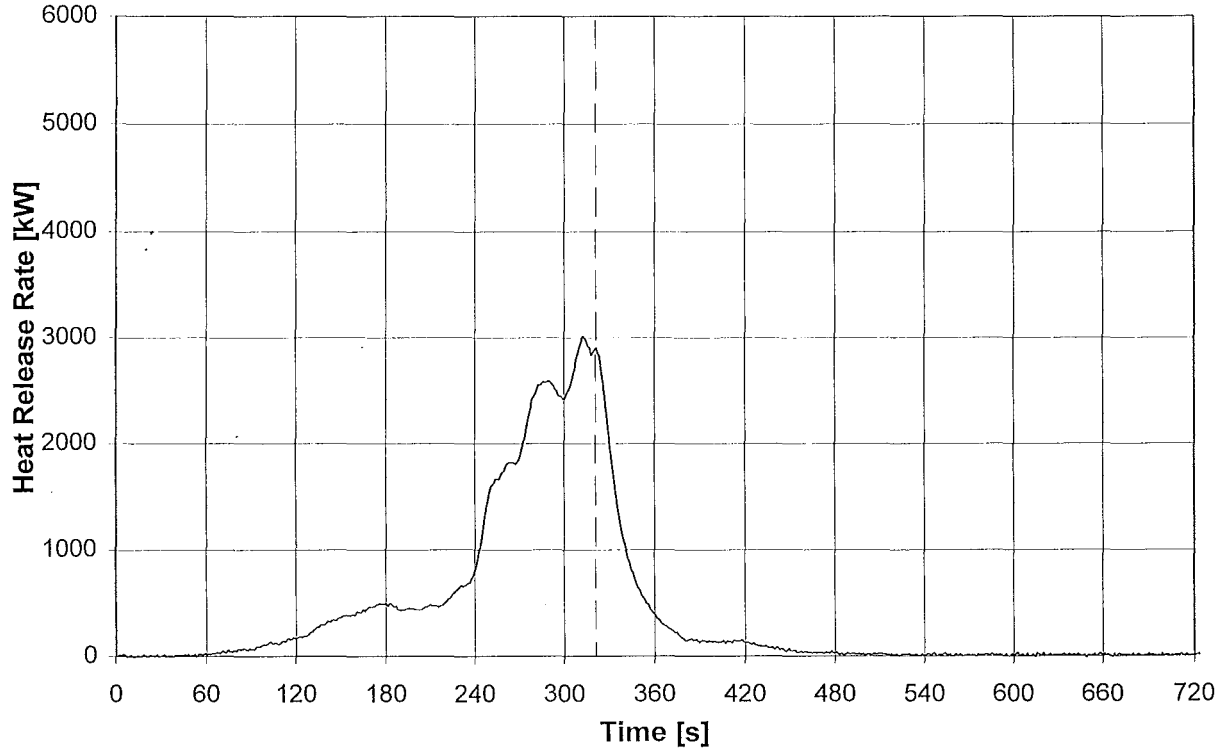

Heat Release Rate, Solution, 27/11/97

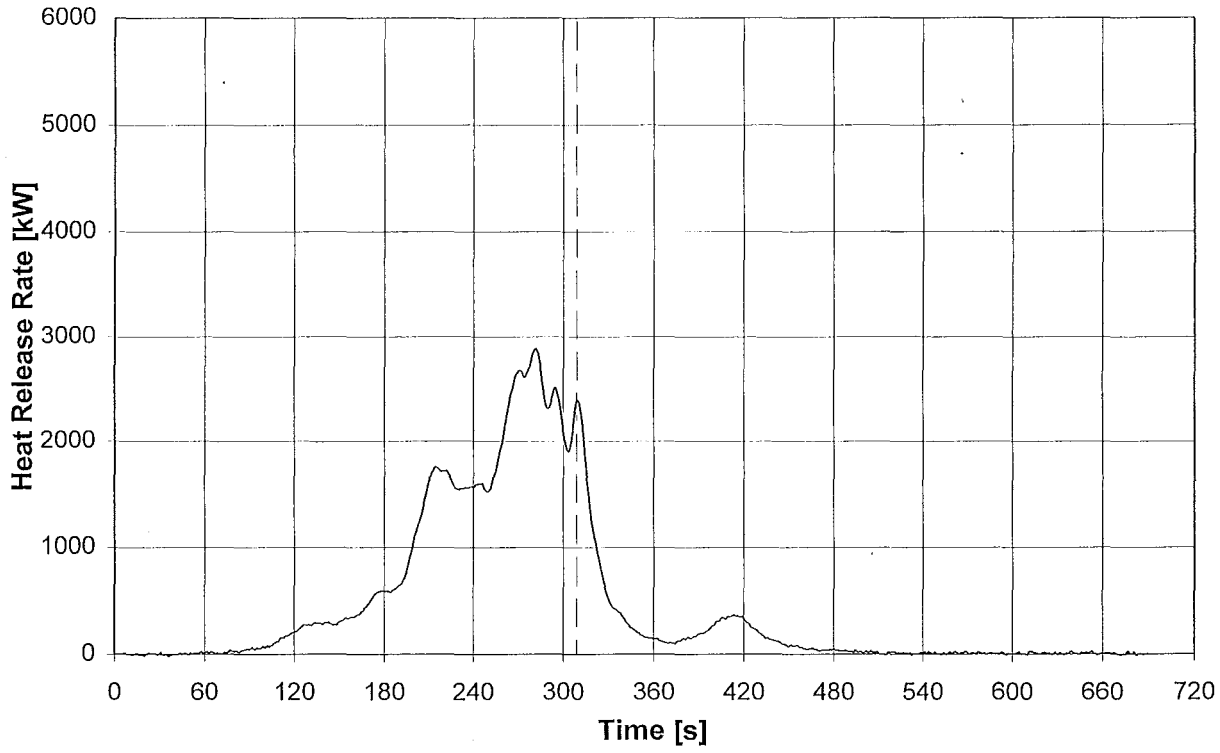

Heat Release Rate, Solution, 2/12/97

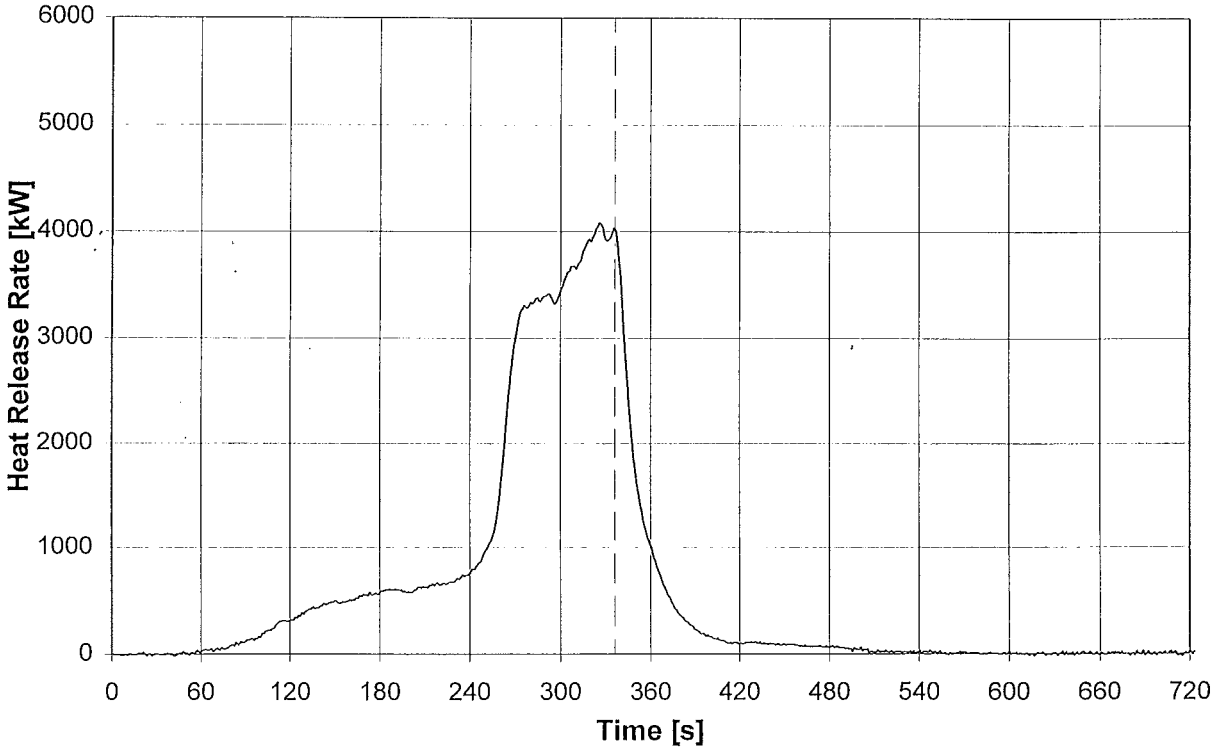

Heat Release Rate, Solution, 12/12/97

Appendix 8 Photographs of Apparatus and Experiments

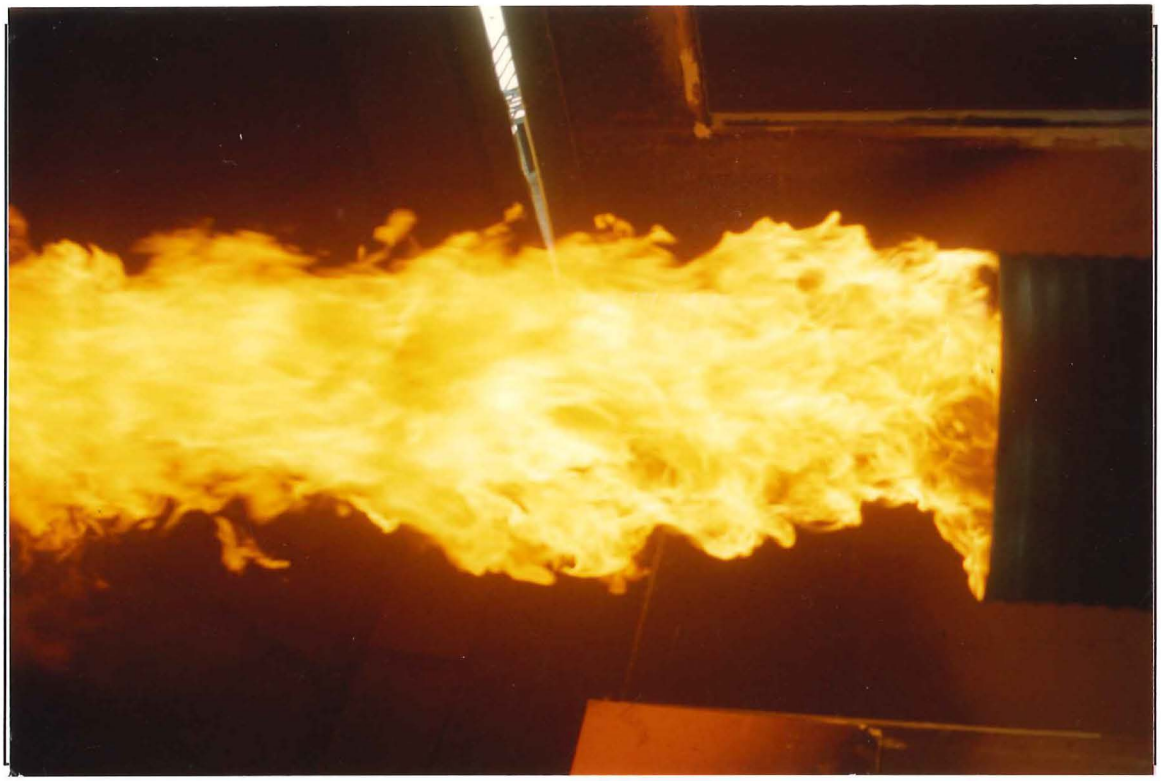

Figure A8-1: Gas Burner Calibration Run

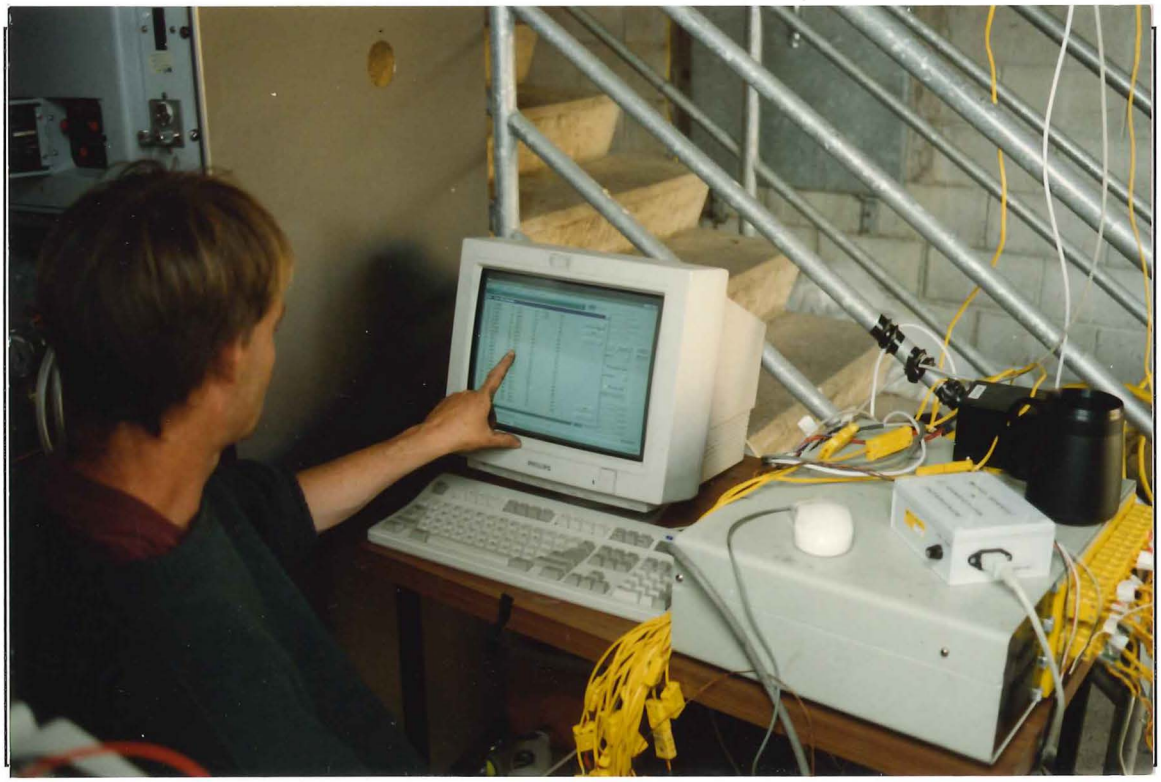

Figure A8-2: Data Acquisition System

Figure A8-3: Burning of Crib Well Established

Figure A8-4: Flames Across Ceiling

Figure A8-5: Burning Outside of Compartment Starting

Figure A8-6: Extensive Burning Outside of Compartment

Figure A8-7: Paper on Floor Ignites

Figure A8-8: Paper on Floor Burnt Off

Figure A8-9: Firefighters Ready to Attack the Fire

Figure A8-10: Start of Extinguishment Using CAFS

Appendix 9 Drawings of Equipment

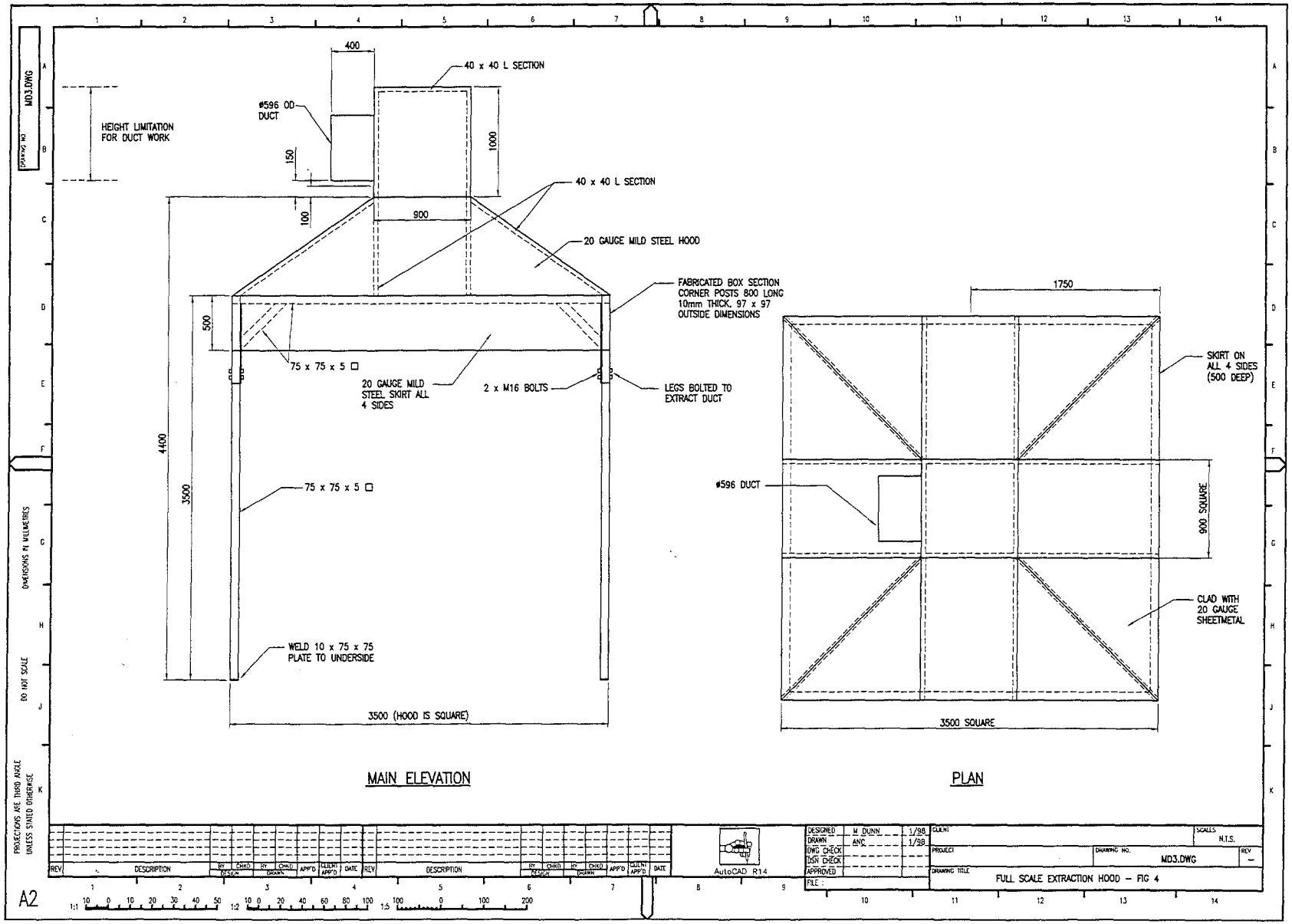

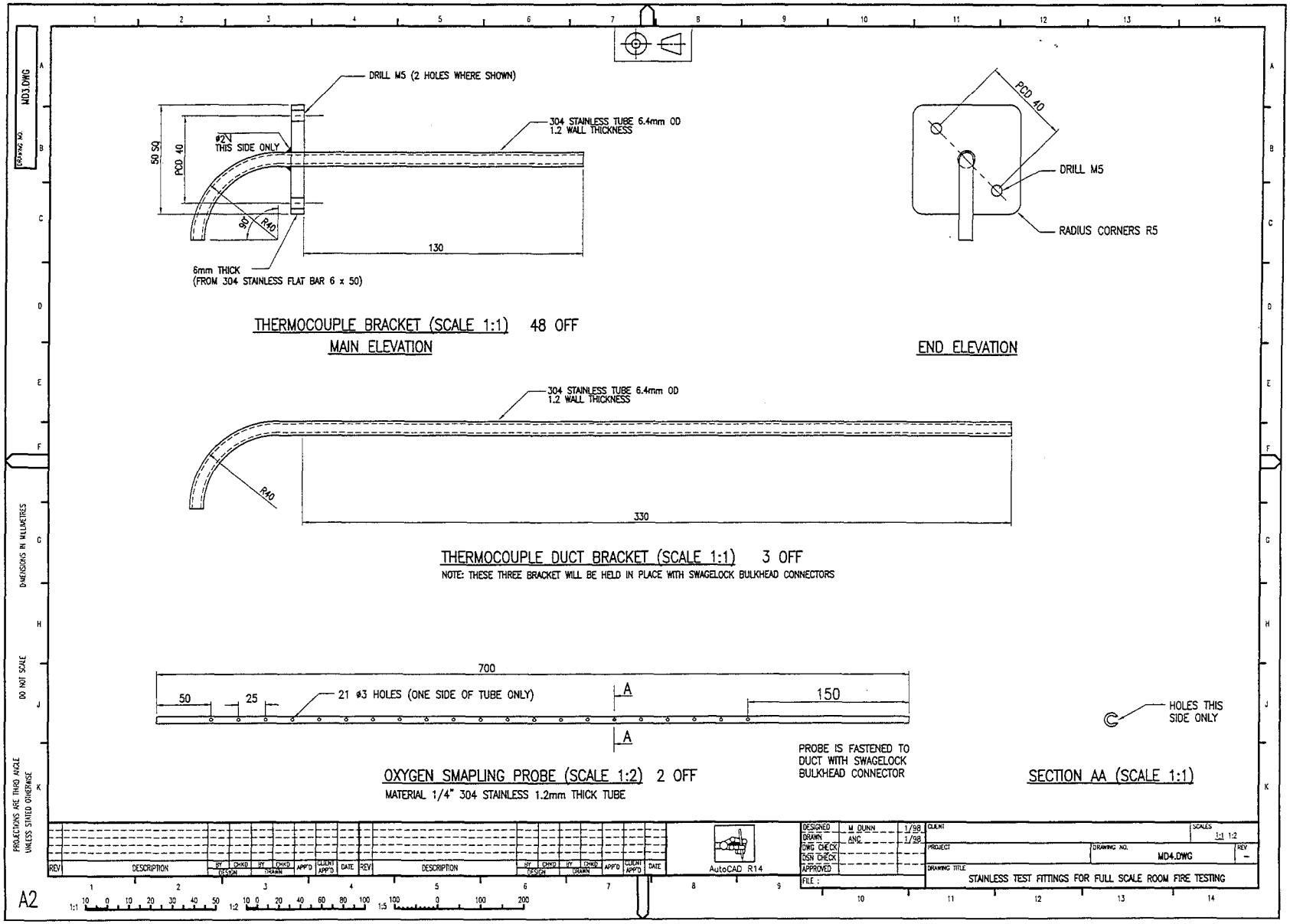
DRILL M5 (2 HOLES WHERE SHOWN)
304 STAINLESS TUBE 6.4mm OD
1.2 WALL THICKNESS
ø2
THIS SIDE ONLY
50
PCD 40
50
R40
130
6mm THICK
(FROM 304 STAINLESS FLAT BAR 6 x 50)
PCD 40
DRILL M5
RADIUS CORNERS R5
THERMOCOUPLE BRACKET (SCALE 1:1) 48 OFF
MAIN ELEVATION
END ELEVATION
304 STAINLESS TUBE 6.4mm OD
1.2 WALL THICKNESS
R40
330
THERMOCOUPLE DUCT BRACKET (SCALE 1:1) 3 OFF
NOTE: THESE THREE BRACKET WILL BE HELD IN PLACE WITH SWAGELOCK BULKHEAD CONNECTORS
700
50
25
21 ø3 HOLES (ONE SIDE OF TUBE ONLY)
A
150
A
HOLES THIS
SIDE ONLY
PROBE IS FASTENED TO
DUCT WITH SWAGELOCK
BULKHEAD CONNECTOR
OXYGEN SMAPLING PROBE (SCALE 1:2) 2 OFF
MATERIAL 1/4" 304 STAINLESS 1.2mm THICK TUBE
SECTION AA (SCALE 1:1)
MD3.DWG
DRAWING NO.
DIMENSIONS IN MILLIMETRES
DO NOT SCALE
PROJECTIONS ARE THIRD ANGLE
UNLESS STATED OTHERWISE
REV
DESCRIPTION
BY
CHKD
DESIGN
BY
CHKD
DRAWN
APP'D
CLIENT APP'D
DATE
AutoCAD R14
DESIGNED
M DUNN
1/98
DRAWN
ANC
1/98
CHK CHECK
DSN CHECK
APPROVED
FILE :
CLIENT
SCALES
1:1 1:2
PROJECT
DRAWING NO.
MD4.DWG
REV
–
DRAWING TITLE
STAINLESS TEST FITTINGS FOR FULL SCALE ROOM FIRE TESTING
A2
1:1
1:2
1:5

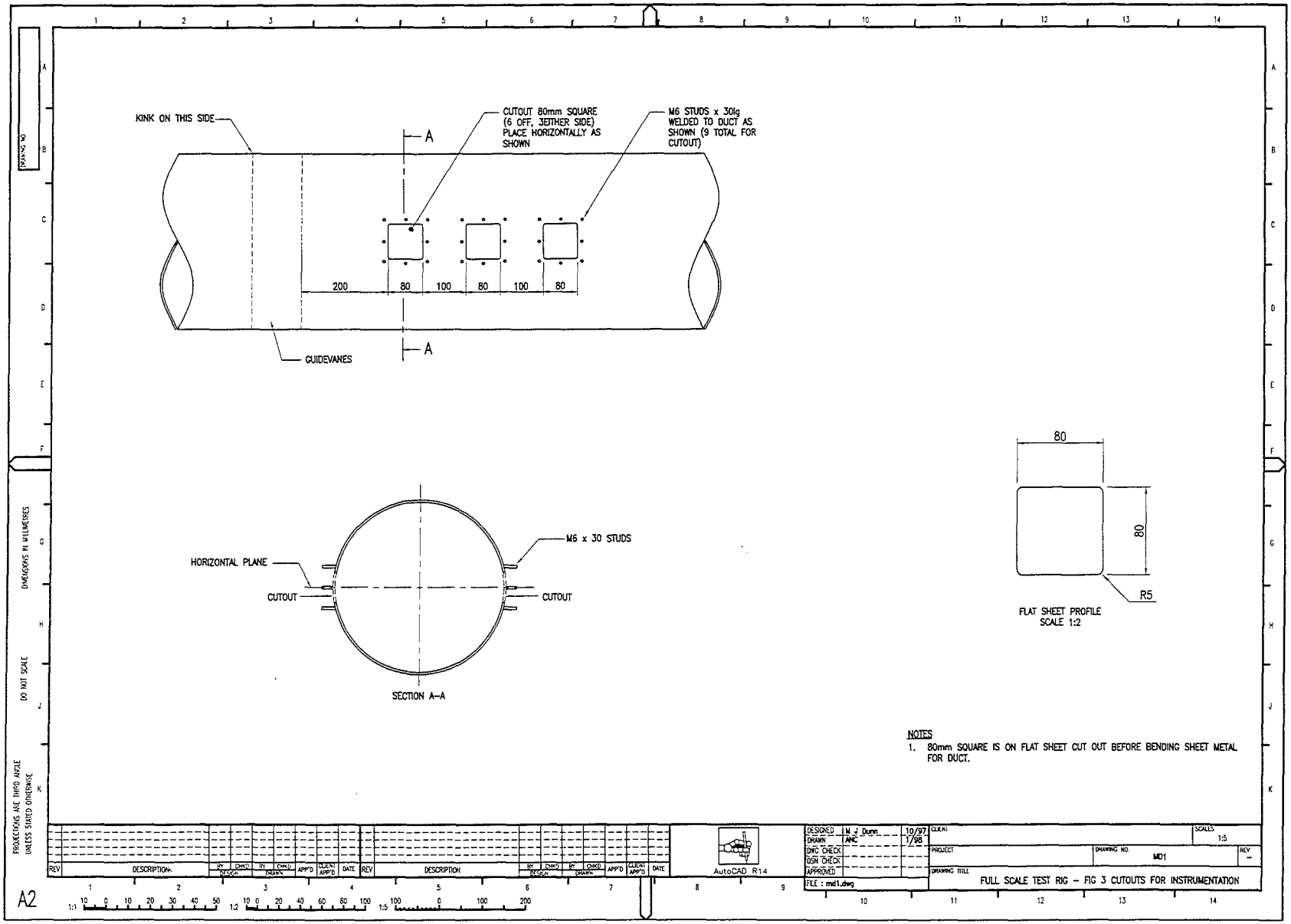
KINK ON THIS SIDE
CUTOUT 80mm SQUARE (6 OFF, 3EITHER SIDE) PLACE HORIZONTALLY AS SHOWN
M6 STUDS x 30lg WELDED TO DUCT AS SHOWN (9 TOTAL FOR CUTOUT)
A
A
200
80
100
80
100
80
GUIDEVANES
HORIZONTAL PLANE
M6 x 30 STUDS
CUTOUT
CUTOUT
SECTION A-A
80
80
R5
FLAT SHEET PROFILE
SCALE 1:2
NOTES
1. 80mm SQUARE IS ON FLAT SHEET CUT OUT BEFORE BENDING SHEET METAL FOR DUCT.
DRAWING NO
DIMENSIONS IN MILLIMETRES
DO NOT SCALE
PROJECTIONS ARE THIRD ANGLE UNLESS STATED OTHERWISE
REV
DESCRIPTION
BY DESIGN
CHK'D
BY DRAWN
CHK'D
APP'D
CLIENT APP'D
DATE
AutoCAD R14
DESIGNED M J Dunn 10/97
DRAWN ANC 1/98
DWG CHECK
DSN CHECK
APPROVED
FILE : md1.dwg
CLIENT
SCALES 1:5
PROJECT
DRAWING NO. MD1
REV -
DRAWING TITLE
FULL SCALE TEST RIG - FIG 3 CUTOUTS FOR INSTRUMENTATION
A2
1:1
1:2
1:5

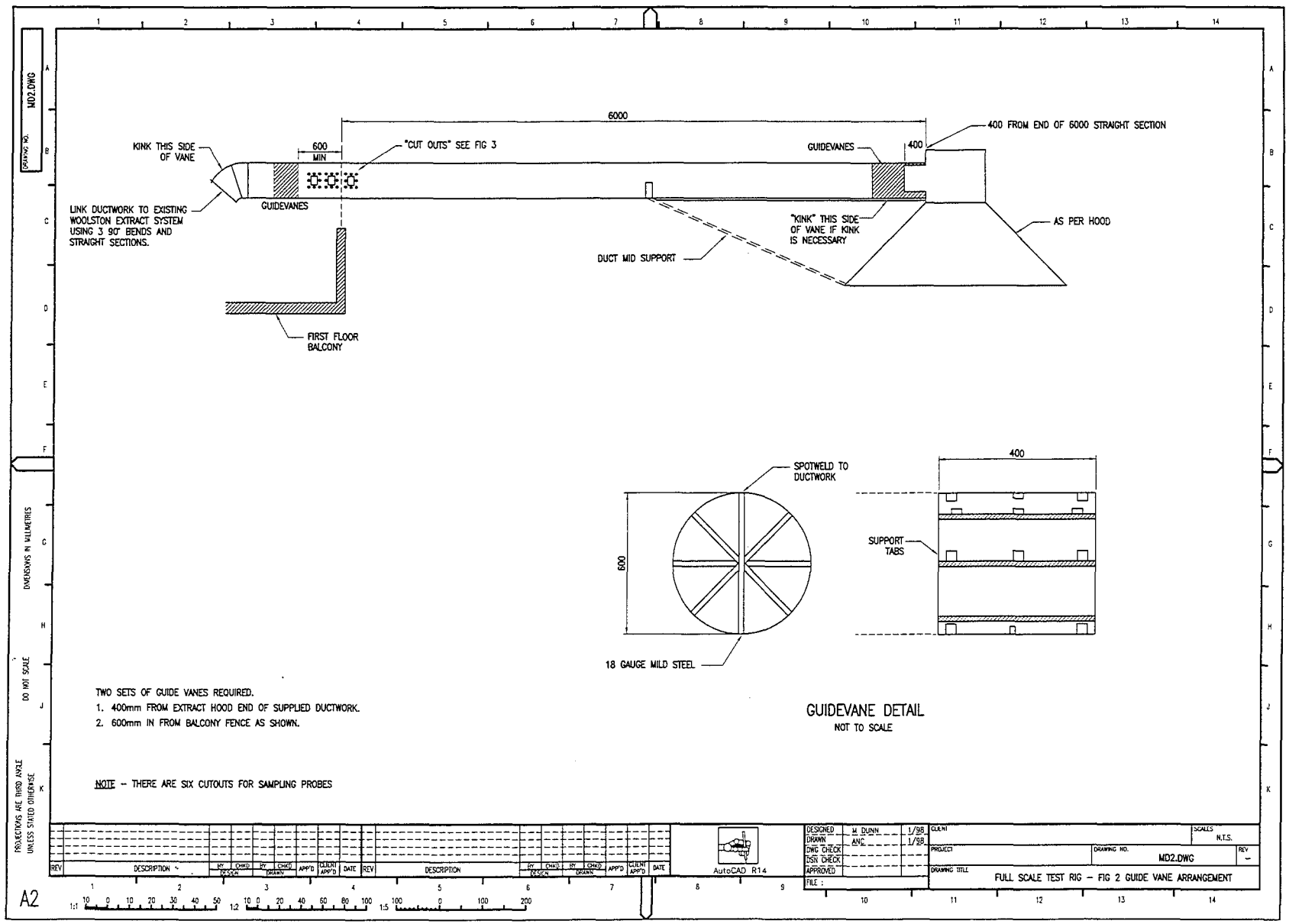
MD2.DWG
6000
400 FROM END OF 6000 STRAIGHT SECTION
KINK THIS SIDE OF VANE
600 MIN
"CUT OUTS" SEE FIG 3
GUIDEVANES
400
LINK DUCTWORK TO EXISTING WOOLSTON EXTRACT SYSTEM USING 3 90° BENDS AND STRAIGHT SECTIONS.
GUIDEVANES
"KINK" THIS SIDE OF VANE IF KINK IS NECESSARY
AS PER HOOD
DUCT MID SUPPORT
FIRST FLOOR BALCONY
SPOTWELD TO DUCTWORK
400
SUPPORT TABS
600
18 GAUGE MILD STEEL
TWO SETS OF GUIDE VANES REQUIRED.
1. 400mm FROM EXTRACT HOOD END OF SUPPLIED DUCTWORK.
2. 600mm IN FROM BALCONY FENCE AS SHOWN.
NOTE – THERE ARE SIX CUTOUTS FOR SAMPLING PROBES
GUIDEVANE DETAIL
NOT TO SCALE
DIMENSIONS IN MILLIMETRES
DO NOT SCALE
PROJECTIONS ARE THIRD ANGLE UNLESS STATED OTHERWISE
AutoCAD R14
DESIGNED M DUNN 1/98
DRAWN ANC 1/98
DWG CHECK
DSN CHECK
APPROVED
FILE :
CLIENT
SCALES N.T.S.
PROJECT
DRAWING NO. MD2.DWG
REV –
DRAWING TITLE FULL SCALE TEST RIG – FIG 2 GUIDE VANE ARRANGEMENT
A2

FIRE ENGINEERING RESEARCH REPORTS

95/1	**Full Residential Scale Backdraft**	**I B Bolliger**
95/2	**A Study of Full Scale Room Fire Experiments**	**P A Enright**
95/3	**Design of Load-bearing Light Steel Frame Walls for Fire Resistance**	**J T Gerlich**
95/4	**Full Scale Limited Ventilation Fire Experiments**	**D J Millar**
95/5	**An Analysis of Domestic Sprinkler Systems for Use in New Zealand**	**F Rahmanian**
96/1	**The Influence of Non-Uniform Electric Fields on Combustion Processes**	**M A Belsham**
96/2	**Mixing in Fire Induced Doorway Flows**	**J M Clements**
96/3	**Fire Design of Single Storey Industrial Buildings**	**B W Cosgrove**
96/4	**Modelling Smoke Flow Using Computational Fluid Dynamics**	**T N Kardos**
96/5	**Under-Ventilated Compartment Fires - A Precursor to Smoke Explosions**	**A R Parkes**
96/6	**An Investigation of the Effects of Sprinklers on Compartment Fires**	**M W Radford**
97/1	**Sprinkler Trade Off Clauses in the Approved Documents**	**G J Barnes**
97/2	**Risk Ranking of Buildings for Life Safety**	**J W Boyes**
97/3	**Improving the Waking Effectiveness of Fire Alarms in Residential Areas**	**T Grace**
97/4	**Study of Evacuation Movement through Different Building Components**	**P Holmberg**
97/5	**Domestic Fire Hazard in New Zealand**	**KDJ Irwin**
97/6	**An Appraisal of Existing Room-Corner Fire Models**	**D C Robertson**
97/7	**Fire Resistance of Light Timber Framed Walls and Floors**	**G C Thomas**
97/8	**Uncertainty Analysis of Zone Fire Models**	**A M Walker**
97/9	**New Zealand Building Regulations Five Years Later**	**T M Pastore**
98/1	**The Impact of Post-Earthquake Fire on the Built Urban Environment**	**R Botting**
98/2	**Full Scale Testing of Fire Suppression Agents on Unshielded Fires**	**M J Dunn**
98/3	**Full Scale Testing of Fire Suppression Agents on Shielded Fires**	**N Gravestock**
98/4	**Predicting Ignition Time Under Transient Heat Flux Using Results from Constant Flux Experiments**	**A Henderson**
98/5	**Comparison Studies of Zone and CFD Fire Simulations**	**A Lovatt**
98/6	**Bench Scale Testing of Light Timber Frame Walls**	**P Olsson**
98/7	**Exploratory Salt Water Experiments of Balcony Spill Plume Using Laser Induced Fluorescence Technique**	**E Y Yii**

School of Engineering
University of Canterbury
Private Bag 4800, Christchurch, New Zealand

Phone 643 364-2250
Fax 643 364-2758